NEUROTOXIC EFFECTS OF MALATHION AND LEAD ACETATE ON THE BLOOD-BRAIN BARRIER

Disruptive effects caused by different mechanisms examined with an *in vitro* blood-brain barrier system

By
PERGENTINO BALBUENA

Dissertation submitted to the faculty of the Virginia Polytechnic Institute and State University in partial fulfillment of the requirements for the degree of

DOCTOR OF PHILOSOPHY

In

Biomedical and Veterinary Sciences
(Neurotoxicology)

Marion Ehrich
Bernard S. Jortner
James B. Meldrum
Peter Eyre
Yong Woo Lee

June 14, 2010
Blacksburg, Virginia

Keywords: Malathion, Malaoxon, Lead acetate, blood-brain barrier, neurotoxicity

NEUROTOXIC EFFECTS OF MALATHION AND LEAD ACETATE ON THE BLOOD-BRAIN BARRIER

Disruptive effects caused by different mechanisms examined with an *in vitro* blood-brain barrier system

Pergentino Balbuena

ABSTRACT

Organophosphates (OP) such as malathion are organic derivatives of phosphoric acid with broad use in everyday life throughout the world, especially as insecticides. Lead particles can accumulate in soil and from there leach into our water supplies.

Interaction with the environment offers opportunities for multiple exposures to combinations of different toxicants (such as lead and malathion). Thus, it is important to assess effects that these compounds exert not only on the nervous system, but also on the blood-brain barrier (BBB). The BBB consists of specialized endothelial cells that form the vasculature of the brain; it regulates passage of nutrients, while preventing potentially damaging substances from entering the brain. The main feature of the BBB is the presence of tight junctions between cells, which provide the BBB with its low permeability.

The work presented in this dissertation tests the hypothesis that lead and malathion disrupt BBB integrity by affecting tight junctions of the BBB. The hypothesis suggests that disruptions involve changes in protein levels and gene expression as well as activation of transient receptor potential canonical channels (TRPC) that in turn increase intracellular calcium levels affecting tight junction structure. The hypothesis was tested by assessing lead-malathion interactions in an i*n vitro* BBB model. This model was constructed with rat astrocytes and rat brain endothelial cells (RBE4).

Assessments of cell toxicity in response to different concentrations of the neurotoxicants tested showed that concentrations between 10^{-5} μM and 10^{-6} μM were ideal to assess combinations of neurotoxicants. In general, protein levels of occludin, claudin 5, ZO1, and ZO2 decreased at all times, however, qPCR analysis of gene expression for all the proteins did not correlate with the assessments on protein levels. TRPC channel protein levels increased in response to neurotoxicant insult, which correlated with results for gene expression.

This study suggests that at least one of the mechanisms that neurotoxicants lead and malathion utilize to disrupt permeability of the BBB is by affecting tight junction structure. This effect could be regulated by increases in gene expression of TRPC1 and TRPC4 that are associated with increases in the number of TRPC channels on the membrane of endothelial cells of the cerebral microvasculature.

Dedication:

IN LOVING MEMORY OF

INES VENANCIO BERMEJO

THIS WORK IS DEDICATED TO MY MOTHER…

WHO PASSED AWAY DREAMING OF THE DAY THAT SHE WOULD SEE HER SON BECOME A DOCTOR…

Acknowledgments:

I would like first, to express my gratitude to the Creator of all things, God. His guidance put me on the path with many good people that helped to shape my character, my personality, and my life. Among these, my gratitude goes to my father, because from him I learned the value of hard work, honesty, respect, good morals, and love of family. He instilled in me the belief that no matter how humble your origin is, you can achieve your goals if only you dare to dream. Gracias Papá.

I would like to express my gratitude and appreciation to my main academic advisor and chairperson of my advisory committee, Dr. Marion Ehrich. Her kind supervision, her encouragement, and her high standards in the development of the research, were key factors in the development of my dissertation work and the growth and improvement of my analytical capacity. Her support of my ideas and me made this dissertation and research possible, and for that, I am forever grateful.

I would also like to express my sincere gratitude to the members of my advisory committee. Dr. Blair Meldrum, for his encouragement and support in teaching analytical chemistry, for his invaluable friendship, and because he was always available to discuss not only my research, but also any problem I encountered. Dr. Bernard Jortner, one of the finest individuals that I ever had the privilege to know, patiently and freely gave assistance that made a difference in the way I perceived not only the experimental design, but neuropathological assessment of living structures as well. Dr. Jortner, through his actions, allowed me to realize the

real value of friendship. I also thank Dr. Yong Woo Lee, for his assistance in the interpretation of the gene expression data, for his availability whenever I needed to discuss my research, for his patience and assistance, and for his ideas regarding tight junction disruption in the BBB. Dr. Peter Eyre provided help and support in the proofreading of many works presented during my research program, and recommendations regarding *in vitro* studies, always demonstrating his optimistic and humorous personality.

For their superb and warm friendship, as well as for their technical assistance and their help in all of my projects, I would like to express my sincere appreciation to Dr. Geraldine Magnin-Bissel and Mrs. Barbara Wise of the Toxicology Laboratory. Their help and expertise with the atomic absorption and gas chromatography mass-spectrometry (GC-MS) techniques made my life much easier. Thanks also to Mrs. Kristel Fuhrman from Toxicology/Biochemistry, because she was always ready to help me with any problem in the cell culture room, for her help with some of the protein determinations for my western blots, as well as for all those countless times we worked together measuring resistance. My gratitude also goes to Mr. Delbert Jones of the biochemistry laboratory, for all his help and advice with my presentations. Delbert, along with Kristel and Mrs. Xiaohua Wu, was the main engine behind my advance as a presenter/lecturer. These friends were always accessible to listen to my rehearsals for talks and presentations; their critique and evaluations of my performance helped me to become a better presenter. Thanks to Ms. Kathy Lowe from morphology, because her expertise in electron microscopy helped me a lot, and even though the part of my project involving electron microscopy did not materialized, Kathy was always there to lend a hand. Thank also to Ms.

Anjali Hirani, for her teaching of the protocol utilized in the isolation of astrocytes from rat cortices.

I would like to express my gratitude to Dr. Willard Eyestone, one of the most knowledgeable people I know in immunoblotting techniques. He was always willing to answer my questions and to solve my doubts about my western blot results, and I respect him as a researcher and as a good friend. Thanks also to Dr. William Huckle for his advice on western blotting, and for his gracious offer to use his equipment. My gratitude goes also to Dr. Wen Li, for her help and teachings about real time PCR protocols and her help with the development of primers utilized in the gene expression assessments. Dr. Li also helped me with the enzymatic separation, culture and storage of astrocytes. Thanks also to Dr. Stephen R. Werre for his help with the statistical analysis of the data presented in this work.

I would like to thank my sisters and their families for their support and love. To them goes my love and gratitude because they were always there for me when I needed them. To my nephews and nieces, because they make me feel loved and respected, to all my family, because for me, family is and always will be the greatest force behind any personal achievement. For this and more, thank you.

These acknowledgements would be undoubtedly incomplete without mentioning the person who inspired me and encouraged me to pursue this career path. He was the person who believed in me when nobody else did, the person who open a door for me and showed me that it is never too late to pursue a dream if you are willing to work hard for it. To Dr. Hassan El-Fawal,

my undergraduate college advisor, a great mentor, an awesome teacher, and a dear friend, my most sincere gratitude and thanks.

To all those whom I may not have mentioned by name or may have inadvertently overlooked, please accept my sincere apologies, forgive my unintended omission and please accept my most sincere appreciation for your help.

Declaration of work performed:

I declare that with the exception of the items indicated below, all work reported in this dissertation was performed by me.

After collecting samples from the *in vitro* systems, the GC-MS analysis was run by Dr. Geraldine Magnin-Bissel. Aside from the first set of samples run for atomic absorption that were performed by me, Mrs. Barbara Wise ran the rest of the samples in the atomic absorption analysis. Mrs. Kristel Fuhrman, Ms. Anjali Hirani, and Mrs. Xiaohua Wu helped with the extraction of the rat pups from the mother in the astrocyte isolation protocol, and Dr. Wen Li assisted with the enzymatic isolation of astrocytic cells and the following cell culture work. Mrs. Fuhrman also helped me with some of the protein determinations for the western blot analysis as well as with some of the resistance measurements.

Attributions:

The following contributors participated in the research that originated the manuscripts presented in this dissertation. Their help in the development of the methodology made this dissertation possible:

Dr. Marion Ehrich provided guidance and advice in the researching of this dissertation as well as funding for the development of the experimental design associated with this project. She also supervised the whole dissertation and the experimental design and provided her expertise in the revising of the final manuscript.

Dr. Blair Meldrum provided guidance and advice in the researching of this dissertation as well as funding for the development of the experimental design associated with the first manuscript of this project.

Dr. Geraldine Magnin-Bissel developed the protocol to assess our samples for the presence of organophosphates by gas chromatography-mass spectrometry techniques that was part of the first manuscript as well as performed the actual experiments.

Dr. Wen Li provided expertise in the molecular techniques associated with the assessments of protein levels and gene expression. She performed also some of the real time polymerase chain reactions.

TABLE OF CONTENTS

LIST OF FIGURES

Chapter 3: Results

Chapter 4: Results

LIST OF TABLES

LIST OF ABBREVIATIONS

- µ: Micro/micron
- µl: microliter
- µM: Micromolar
- ACh: Acetylcholine
- AChE: Acetylcholinesterase
- ACM: Astrocyte conditioned media
- AF-6: Afadin 6 protein
- ANOVA: Analysis of variance
- ASH-: Absent, small, or homeotic discs protein
- ASIC: Acid-sensing ion channel
- ASIP: Agouti signaling protein
- ATP: Adenosine triphosphate
- BBB: Blood-brain barrier
- BMEC: Bovine brain microvascular endothelial cells
- Ca^{++}: Calcium ion
- CaM: Calmodulin
- cDNA: complementary deoxyribonucleic acid
- CK2: Casein kinase 2
- CNS: Central nervous system
- DIgA: Drosophila disc large tumor suppressor
- DNA: Deoxyribonucleic acid

- DTNB: 5, 5’-dithiobis-(2-nitrobenzoic acid)
- E-face: Ectoplasmic fracture face
- EM: Electron multiplier
- EMP: Epithelial membrane protein
- EPA: Environmental Protection agency
- FBS: Fetal bovine serum
- GC-MS: Gas chromatography mass-spectrometry
- GFAP: Glial fibrillary acidic protein
- GK: guanylate kinase-like
- IS: Internal standard
- kDa: KiloDalton
- LDH: Lactate dehydrogenase
- LTP: Long term potentiation
- m/z: mass-over-charge ratio
- M: Molar
- MAGI-1/BAP1: Membrane-associated guanylate kinase with inverted arrangement of protein-protein interaction domain
- MAGUK: Guanylate kinase-like homologous family of proteins
- Malaoxon/malaoxon: Mx/mx
- Malathion/malathion: Mal/mal
- MDCK: Madin-Darby canine kidney
- mM: millimolar
- MMP-9: Metalloproteinase 9

- MP20: Muscle protein 20
- Na^+: Sodium ion
- NIR: Near-infrared
- NMDA: N-methyl-D-aspartate
- OP: Organophosphates
- PAR-: abnormal embryonic *PAR*artitioning of cytoplasm protein
- Pb: Lead
- PBS: Phosphate saline buffer
- PCK: Protein kinase C
- PCR: Polymerase chain reaction
- PDZ: PSD95-DIgA-ZO1 domain
- PET: Polyethylene terephthalate
- P-face: Protoplasmic fracture face
- PLC: Phospholipase C
- PMP22: Peripheral myelin protein 22
- ppb: Parts per billion
- PSD95: Postsynaptic density protein
- qPCR: Quantitative-Real time reverse transcriptase polymerase chain reaction
- RBE4: Rat brain endothelial cell line
- RNA: Ribonucleic acid
- SDS: Sodium dodecyl sulfate
- SH3: Src gene homology 3 domain
- SH-SY5Y: Neuroblastoma cell line

- SOC: Store-operated calcium entry
- SPE: Solid phase extraction
- TEER: Transendothelial electrical resistance
- TRP: Transient receptor potential channel
- TRPC: Transient receptor potential canonical channel
- TRPC: Transient receptor potential canonical channel
- TX: Triton X
- ZAK: Serine protein kinase
- ZO: Zonula occludens
- ZONAB: ZO1-associated nucleic acid binding protein
- ZU5: ZO1-uncordinatted protein 5

Statement of the Hypothesis

The proposed study consisted of analyzing organophosphate (OP) – lead interactions in two model of an i*n vitro* blood-brain barrier (BBB). These i*n vitro* systems were composed of cocultures of rat astrocytes and rat brain endothelial cells (RBE4) in one system, and rat astrocytes and bovine brain endothelial cells (BMECs) on the other. These systems helped to assist in establishing mechanisms of toxicity associated with acute combined exposures to lead and an OP, malathion.

The main hypothesis tested by this doctoral study was that *"Lead and malathion disrupt BBB integrity by affecting tight junction structural stability in the cells of the barrier. This disruption involves changes in different intracellular pathways, especially increases in membrane transient receptor potential canonical 1 and 4 channels (TRPC1/TRPC4) that in turn increase intracellular calcium levels affecting tight junction structure"*. Support for the hypothesis derives from published information stating that lead affects tight junctions by disrupting calcium related pathways necessary in tight junction and cytoskeleton maintenance (Xu *et al*., 2006). In contrast, some OPs indirectly increase the concentrations of calcium while still other OPs increase calcium-activated neutral protease (calpain), an enzyme associated with degradation of cytoskeletal elements (El-Fawal *et al*., 1990). These calcium-associated pathways may contribute to OP-induced alterations in tight junction proteins. Other studies in our laboratory (Ehrich *et al*., 2009) suggest that a direct cholinergic agonist such as carbachol increases concentrations of intracellular calcium in some cell types although carbachol itself does not cross the BBB. However, OP compounds do cross the BBB and may indirectly increase calcium concentrations in cells by first inhibiting acetylcholinesterase (AChE), thereby raising levels of acetylcholine (ACh) which then acts like carbachol (Ehrich *et al*., 2009).

Because lead and OPs may affect BBB functionality and permeability by different mechanisms, it was important to address any type of disruptive capability that these two neurotoxicants may have when models of BBB systems are exposed to both neurotoxicants at the same time. The integrity of the BBB during combined exposures to lead and malathion was assessed by changes in resistance, viability and permeability of the barrier as well as by down-regulation/up-regulation assessments of tight junction proteins after treatment with lead and malathion alone and in combination. We hypothesized that the disruptive effects of these neurotoxicants would be demonstrated, and that this BBB model would confirm the dose-response effects of lead and malathion toxicosis on membrane integrity.

There are obvious differences between the *in vitro* and *in vivo* models of the BBB, which include complex interactions of cells with cells, cells with organs, and organs with organs. What occurs in a live animal may not be fully reproducible in *in vitro* systems (Ehrich, 2003). However, despite the limitations of the *in vitro* system, it can be used for assessing lead-OP induced toxicity utilizing biochemical, pathological and morphological endpoints.

The necessity to test the present hypothesis relies on the fact that there are no prior studies that compare neurotoxicity of lead and malathion in a single experimental design. Literature shows that lead and OPs can cross the BBB when tested *in vivo* (Abou-Donia, 2003; Ehrich, 2005), and *in vitro* experiments demonstrate that lead and malathion cross the BBB (Balbuena *et al*., 2010; Meldrum *et al*., 2007; Parran *et al*., 2005). However, there is no record of performed studies assessing mechanisms associated with toxicity where lead and OPs are applied simultaneously to either *in vivo* or *in vitro* models.

In the process of testing the proposed hypothesis, experimental protocols included measurements of intracellular responses to lead/malathion toxicity. These endpoints measured

effects of the test compounds on concentrations and activity of transient receptor potential canonical channels (TRPC channels), a membrane-associated calcium channel involved in store-operated calcium entry (SOC) into the endothelial cells of the BBB, and linked to permeability regulation (Gias and Asrar, 2005). Of primary interest were the TRPC1and TRPC4 subfamilies, which are known to form heteromeric channels in endothelial cells of the BBB (Antoniotti *et al*., 2006). Endpoints also included assessments of down-regulation and/or up-regulation of transcription factors for genes of proteins involved in tight junction development and function such as occludin, claudin 5, and zona occludens proteins 1 and 2 (ZO1 and ZO2). Calcium levels vary after organophosphate treatment, and previous studies reported the ability of calcium channel blockers to modify functional deficits of organophosphate toxicosis *in vivo* (El-Fawal *et al*., 1989). At the same time, lead is known to mimic calcium-related intracellular pathways such as activation of protein kinase C among others (Toscano and Guilarte, 2005), and endothelial cell permeability through TRPC channels (Gias and Asrar, 2005). Therefore, endpoints included characterization of permeability in the endothelial cells of the BBB and the TRPC channels associated with it.

Astrocyte-conditioned medium induces BBB characteristics in brain vascular endothelial cell line RBE4 monolayers (Siddharthan *et al*., 2007); this model proved worthy in the assessment of OP-induced BBB dysfunction (Yang and Aschner 2003), as well as in the determination of ZO1 protein inhibition by chlorpyrifos in a BBB-like bilayer model of astrocytes and RBE4 cells (Parran *et al*., 2005). Although the model seems capable of supporting neurotoxicity assessments *in vitro,* assessments of such, including OPs and lead, are non-existent, and evaluations on dose combinations of both neurotoxic compounds both *in vivo* and *in vitro* are necessary.

Background & Significance

Organophosphorus compounds, also known as organophosphates, organophosphorus esters or OP compounds, are organic derivatives of phosphoric acid with broad use in everyday life throughout the world (Abou-Donia, 2003; Ehrich, 2005; EPA, 2000-2001). Although they are currently used as plasticizers, lubricants, petroleum additives, and chemical warfare agents, it is their application as insecticides in pest control of crops and households that receive most public attention. According to the Environmental Protection Agency (EPA), in 2001 105 million pounds of pure insecticides (active ingredient) were utilized in the United States alone (EPA, 2000-2001). From this total 73 million pounds, or about 70%, were OPs. This corresponds to an increase in OP compounds use of about 12% comparing it to the total use of organophosphates for the year 1980. This increase represented OP sales of about $2.5 billion of the insecticide market (EPA, 2000-200). Cases of OP poisoning are common in underdeveloped countries, but they also appear sporadically in agricultural areas of developed nations. The research literature on OPs is very extensive.

Lead poisoning worldwide, but especially in children in underdeveloped countries, still presents a big problem to society (Mañay *et al*., 2008). In some underdeveloped countries lead is still used as a chemical additive in production of tableware, and in industrialized countries it is utilized in the manufacture of ammunition and hair dye products (Goyer, 1993; Hernberg, 2000). In some rural areas, clay contaminated with lead is utilized to fabricate cooking utensils, which are then used by underprivileged families in the preparation of food. Small children are especially susceptible to lead neurotoxicosis (Pocock *et al*., 1994). Environmental lead poisoning was epidemic in the 19th century during the period of early industrialization; then, in the 1920's lead caused a resurgence of ecological pollution when tetraethyl lead began to be added to gasoline (Hernberg, 2000). Although lead poisoning is among the most preventable diseases in

young children, cases of lead poisoning still appear, not only worldwide but also in economically underprivileged regions of industrialized countries (Filippelli and Laidlaw, 2009; Mañay *et al*., 2008). Lead is a stable heavy metal that stays in the environment for long periods. Because of these characteristics, lead particles in the environment can accumulate in soil, and from there leach into the water that supplies our drinking reserves (Filippelli and Laidlaw, 2009; Toscano and Guilarte, 2005). At the same time, old lead pipes in water systems in municipalities that cannot afford to change their water lines, also present a serious problem (Schock et al., 2008).

Interaction with the environment offers opportunities for exposure not only to one specific toxicant, but also to multiple combinations of different toxicants. Therefore, assessment of combinations of different toxicants that are known to be present in the environment is a priority. The presence of lead and OPs in the environment is well documented, and therefore, it is of great importance to assess effects that both compounds exert not only on the nervous system, but also on the barrier that regulates the transport of nutrients and other molecules in and out of the nervous system, that is, the BBB.

Cell culture systems have been used for many years to test lead toxicity and are being increasingly utilized to study the effects of OPs in an attempt to replicate historical data from whole animal studies (Nostrandt and Ehrich, 1992; Ehrich and Veronesi, 1999). The clinical extrapolation of data from both *in vitro* and *in vivo* studies, however, causes concern among scientists. This is due to the inability of most *in vitro* systems to incorporate a reasonable representation of the normal pharmacokinetic pathways of toxic compounds, including lead and OPs, that occur following *in vivo* exposures (absorption, distribution, biotransformation and excretion) (Ehrich and Veronesi, 1999). Nevertheless, *in vitro* systems have considerable value in the investigation of mechanisms associated with exposure and induction of perturbations in

cellular and molecular targets that are similar to those found in the intact animal, especially since studies can be conducted with cells originating from susceptible species, including humans (Rowles *et al*., 1995).

The blood brain barrier (BBB) consists of specialized endothelial cells and astrocytes that line the vasculature of the brain. The BBB allows passage of essential nutrients and other molecules, while preventing potential damaging substances from entering the brain. Toxic effects and the crossing through the blood brain barrier of lead and organophosphates by themselves are well documented (Balbuena *et al*., 2010; Ehrich, 2003; Meldrum *et al*., 2007; Shi and Zheng, 2007). However, neurotoxic effects on the BBB induced by exposures to lead and malathion combined, either *in vivo* or *in vitro*, are not well understood. Earlier studies used either *in vivo* or *in vitro* models to characterize neurotoxic damage caused by either lead or OPs in separate assessments, including changes in BBB functionality. Our laboratory has established an effective *in vitro* model that can measure organophosphate and lead toxicity endpoints along with other toxicant effects (Balbuena *et al*., 2008). This system may be effective in establishing parameters of toxicity for *in vitro* systems, but has yet to be correlated with whole animal toxicity in similar experimental designs.

Specific Aims & Justification

1. To evaluate the viability of cells utilized in the construction of the *in vitro* barrier following exposure to different concentrations of lead and malathion in order to find non-lethal concentration ranges for further permeability and neurotoxicant transport studies. Cytotoxicity studies were performed to test the viability of the cells used in the construction of the BBB model. Our analysis focused on concentrations of these neurotoxicants that ranged from 0.001 micromolar (μM) to 1 millimolar (mM). The final ranges were between 1 and 10 μM for both compounds since these concentrations did not reduce cell viability significantly and their cytotoxicity was not biologically relevant. Assessment of viability for all the cell types utilized in the construction of the BBB models was determined by quantification of adenosine triphosphate (ATP), an indicator of the presence of metabolically-active cells. This assay was selected over other tests of viability such as the MTT assay (which measure reduction by enzymes of 3-(4,5-Dimethylthiazol-2-yl)-2,5-diphenyltetrazolium bromide), because of its sensitivity. Quantification of ATP can be measured in cells at numbers below the detection limits of standard fluorometric and colorimetric assays such as the MTT.

2. To assess BBB integrity after acute lead and malathion exposure. Assessment of BBB integrity was needed since both lead and OPs cross the BBB and OPs disrupt transendothelial electrical resistance (TEER) (Balbuena *et al*., 2010; Meldrum *et al*., 2007; Parran *et al*., 2005). Electrical resistance, tight junction proteins, and acetylcholinesterase activity in cells under the BBB after OP exposure are indicators of BBB integrity. Compared with endothelial cells in other locations, the main characteristic of the BBB endothelium is the presence of tight junctions between cells. These tight

junctions confer on the endothelial cells of the barrier their characteristic properties: high TEER and low permeability to most molecules. Among the molecules identified as main contributors of tight junction structure in the BBB are transmembrane proteins occludin and claudin 5 (Abbott *et al*., 2006). The carboxy (c)-terminal domain of occludin localized in the cytosol is capable of linking with zonula occludens protein 1 (ZO1). ZO1 in turn, can associate with zonula occludens 2 (ZO2) in addition to the cytoskeleton structure (Abbott *et al*., 2006; Banerjee and Bhat, 2007).

These proteins are important in forming the tight junctions of the BBB. Any disruption of these proteins could disturb BBB integrity, and because of that, assessments of tight junctions in response to lead/OP acute toxicosis were performed. To test membrane integrity *in vitro*, protein immunoblot analysis and real-time PCR (qPCR) were performed to assess the presence and alterations in the levels of occludin, claudin 5, ZO1, and ZO2 at the protein and gene levels before and after treatment with lead and OPs in the endothelial cells of the barrier model. To assess variations over time, measurements were taken at 2, 4, 8, 16, and 24 hour periods. Electrical resistance in the *in vitro* system was assessed following exposure to lead/malathion concentrations in order to evaluate any dose-time response present. Assessments of the integrity of the barrier also included measurements of malathion and lead in the medium on the abluminal side of our system, since the compounds were added on the luminal side, any amount found in the abluminal side would have to pass through the BBB barrier system. For lead, atomic absorption techniques were utilized to assess concentrations of the metal in abluminal medium.

Organophosphate concentrations in the abluminal medium were assessed by gas chromatography-mass spectrometry (GC-MS). However, despite the specificity of the technique, the remaining concentrations of the labile organophosphorus esters used for these experiments were so minimal that they could not be detected directly by GC-MS (Figures 1 and 2), so an indirect method for assessment was needed. Since OP compounds irreversibly inhibit the enzyme acetylcholinesterase (AChE) in exposed cells, assessments of inhibition of this enzyme in a layer of neuroblastoma cells (SH-SY5Y) cultured on the abluminal side of the BBB system allowed us to infer the passage of the OP through the barrier model. Since lead seems to increase the capacity of malathion to inhibit acetylcholinesterase (Balbuena *et al*., 2008), measurements of enzyme inhibition for both neurotoxicants alone and in combination were performed.

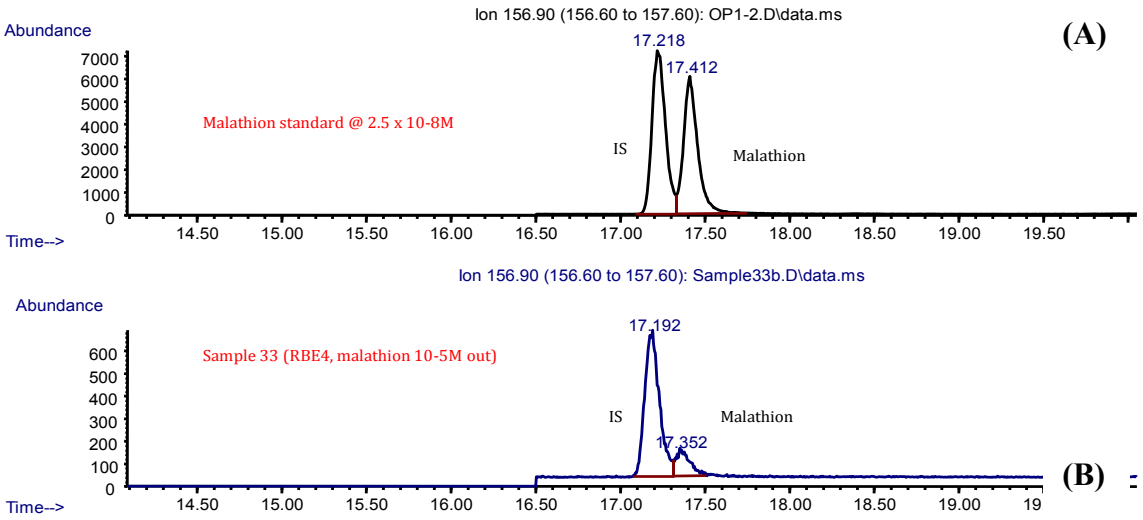

FIGURE 1 Chromatograms of a malathion standard at 10^{-8}M (A), and a sample from the BBB-transfer experiments with a concentration of 10^{-5}M (B). The Y-axes represent the abundance of ion of component while the X-axes express the retention time in minutes. The peaks to the left of both chromatograms represent the malathion derivative or internal standard (IS) whereas the peaks to the right indicate the samples assessed.

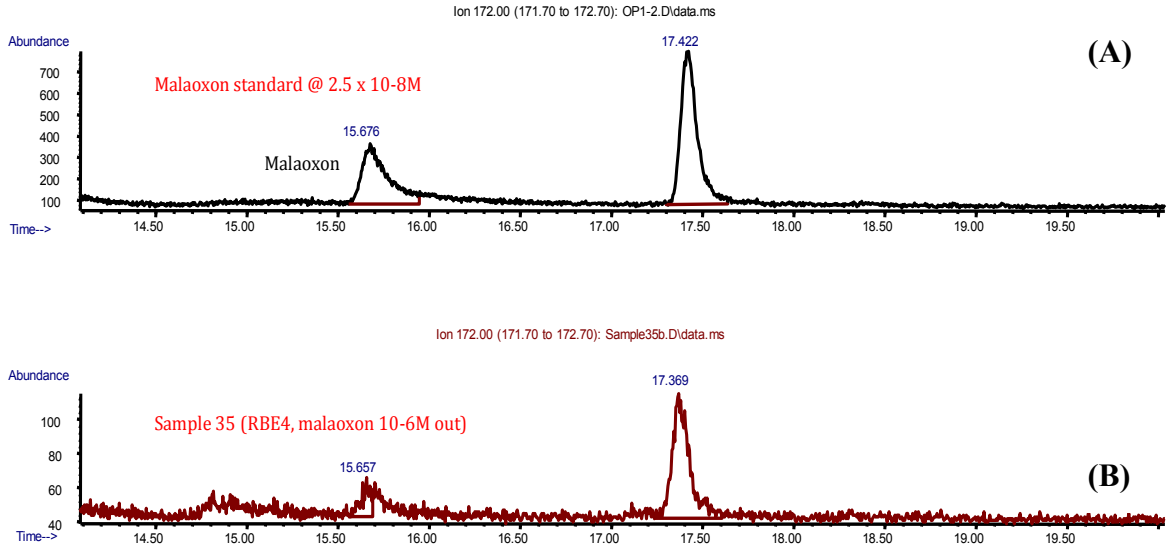

FIGURE 2 Chromatograms of a malaoxon standard at 10^{-8}M (A), and a sample from the BBB-transfer experiments with a concentration of 10^{-6}M (B). The y-axes represent the abundance of ion of component while the x-axes express the retention time in minutes. The peaks on the right of both chromatograms represent the malaoxon derivative or internal standard (IS) whereas the peaks on the left denote the samples assessed. The minimal abundance of the recovered sample ion (B) in comparison to the standard (A) cannot be distinguished from the background.

3. To assess transient receptor potential canonical channels (TRPC) as a mechanism to induce tight junction protein damage in response to lead-OP BBB exposure. Alterations in intracellular calcium and in calcium-membrane transport channels may be a mechanism responsible for changes in BBB permeability during lead and OP exposures. In endothelial cells of the blood vessels, cytosolic calcium transitions, which are induced by several mechanisms including store-operated calcium depletion and entry, act on multiple effectors to collectively disrupt adherens junctions, reorganize focal adhesions,

realign actin filaments into centrally radiating stress fibers, and increase inwardly directed tension in response to inflammatory mediators (Tiruppathi *et al*., 2006). This could cause the induction of gaps between adjacent endothelial cells, thus affecting permeability. Therefore, we hypothesized that BBB permeability is altered in lead and OP toxicosis by means of a similar mechanism utilized by some pro-inflammatory molecules in vascular endothelial cells; that is, the store-operated calcium (SOC) entry pathway (Cioffi and Stevens, 2006; Tiruppathi *et al*., 2006).

Transient receptor potential (TRP) channels and specifically the canonical subfamily of TRP proteins, TRPC channels, are associated with the store-operated calcium entry pathway (Montell, 2005; Pedersen *et al*., 2005; Tiruppathi *et al*., 2006; Zhu *et al*., 1996). TRPC1 and TRPC4 can form subunits of a channel that selectively conducts calcium. Depletion of endoplasmic reticulum calcium in response to inflammatory mediators activates the TRPC1/TRPC4 complex (Cioffi and Stevens, 2006). Entry of calcium through this channel triggers cytoskeletal reorganization that disrupts tight and adherens junctions in the endothelial cells of the BBB, thus increasing permeability. In order to test OP induction of BBB permeability by activating this specific calcium-activated channel, specific TRPC1 antibodies were utilized to assess changes in protein expression in response to neurotoxicant insult associated with BBB increases in permeability. Since the hypothesis assumes that TRPC channels play a role in calcium related increased permeability in the endothelial cells of the barrier, the first step was to establish the presence of such channels in our BBB system. This information was obtained utilizing qPCR to assess down/up regulation of the genes that encode the protein, and western blots to localize the presence of the protein in the cellular

components of the BBB. Once the presence of these calcium channels was confirmed, measurements of variations in concentrations of protein levels in the RBE4 cells in response to malathion-lead treatment were performed.

Chapter 1:
Literature Review

Blood-brain barrier.

The blood-brain barrier (BBB) is a diffusion selective barrier established by the endothelial cells that line cerebral microvessels. This barrier is essential for the normal function of the central nervous system (CNS) because it regulates molecular transport from the blood vessels into the brain (Abbott *et al*., 2006; Ballabh *et al*., 2004). The main characteristics of the cerebral endothelial cells are the absence of fenestrations, the relatively low number of pinocytotic vesicles, a high mitochondrial content, and many specific transport systems in both the luminal and abluminal sides (Yang and Aschner, 2003). The BBB has several roles. It allows the passing of molecules that supply the brain with essential nutrients, and mediates the release of waste products from the brain into the circulatory system (Abbott *et al*., 2006). It also regulates ionic and fluid movement between the blood and the brain, thus maintaining the homeostasis of the CNS.

After decades of researching its complex structural characteristics, scientists now have a more detailed knowledge of the composition and specific features, whether physical or chemical, of the endothelial cells constituting the barrier and the unique properties they confer to the BBB. The endothelial cells of the BBB differ from endothelial cells of other parts of the vasculature in that they form specific structures on the membranes of adjacent endothelial cells called tight junctions (Abbott *et al*., 2006). The tight junctions strictly regulate the permeability of the BBB and contribute to its elevated transendothelial electrical resistance (TEER) (Abbott *et al*., 2006). Tight junctions of the brain microvascular endothelial cells regulate the paracellular flux of molecules across the BBB (Ballabh *et al*., 2004). Various mechanisms of transport through the BBB are utilized in order to achieve the ionic homeostasis necessary for the normal function of

the CNS. These include fluid-mediated transport, receptor-mediated transport, adsorptive-mediated transport, and carrier-mediated transport (Abbott *et al*., 2006; de Boer *et al*., 2003). Adsorptive-mediated transport is dependent on the charge (negative) of the membrane of the cells, and because of this non-specificity, is more suited for positively charged molecules. Carrier-mediated transport is conducted by membrane-fixed structures that transport small size molecules. Receptor-mediated transport, on the other hand, consists of receptors that are internalized with their own ligands and therefore, can internalize larger particles. Fluid-phase mediated transport is a non-saturable, non-specific transport. The quantity of particles or compounds that can be transported by the fluid-phase mediated transport depends upon their extracellular concentrations (Ballabh *et al*., 2004; de Boer *et al*., 2003).

Small lipophilic molecules such as oxygen and carbon dioxide diffuse freely across the cell membrane along their concentration gradients. On the abluminal side of the endothelial cells and attached to it at irregular intervals is another type of cell that is just beginning to be studied: the pericyte. Pericytes and endothelial cells are sheathed in a 30-40 nm thick membrane composed of collagen type IV, heparin sulfate proteoglycans, laminin, fibronectin, and other extracellular matrix proteins called the basal lamina (Hawkins and Davis, 2005). The basal lamina is delineated by the astrocyte processes (end-feet); these in turn ensheathe the cerebral capillaries (Hawkins and Davis, 2005; Lai and Kuo, 2005). The role that neuroglia and even neurons may have in inducing the main characteristics of the endothelial cells of the BBB has been the subject of continuous research in recent years.

Neurons may play a role in regulation of astroglial morphology, differentiation and proliferation. Pericytes may be involved in the induction and maintenance of barrier properties in a manner similar to glia; however, this possibility is still being studied (Hawkins and Davis,

2005; Lai and Kuo, 2005; Yang and Aschner, 2003). Astrocytes on the other hand contribute directly or indirectly to the induction and maintenance of the BBB properties of the cerebral endothelial cells (Abbott 2002; Holash et al., 1993; Isobe et al., 1996). Along with BBB maturation, astroglial differentiation can be morphologically recognized as the astrocytic capability of generation and distribution of excitatory chemical signals (Lee *et al*., 2009; Volterra and Meldosi, 2005). This "gliotransmission" of astrocytes implies structural and molecular heterogeneity of specific domains in its membranes. However, in areas where the processes or end-feet contact the superficial or perivascular basal lamina, the cytosolic domain of the astrocyte membrane is studded with arrays (square or orthogonal) of intramembranous particles that suggest a close interaction and communication between astrocytes, pericytes and endothelial cells (Wolburg *et al*., 2009). In areas where the contact between basal lamina and astrocyte processes is lost (anatomical bending of cellular membrane), the density of these intramembranous particles is dramatically reduced (Holash et al., 1993; Wolburg *et al*., 2009). It is suggested that the mature attained astrocytic gliotransmission property is dependent on the extracellular matrix of the basal lamina. Some other molecules such as the metalloproteinases family of proteins may also be associated with BBB function.

BBB *IN VIVO*:

Empirical evidence of a permeability barrier *in vivo* was first described by Paul Ehrlich in 1885 when he noted that a water-soluble dye injected into the circulatory system would stain all the organs except the spinal cord and the brain (Ehrlich, 1904). Ehrlich, however, attributed his

observation to a low affinity of nervous tissue for the dye he utilized (Ehrlich, 1904). Edwin Goldmann demonstrated in 1913 the presence of a physiological barrier in the central nervous system by injecting the dye directly into the cerebrospinal fluid of the brain and recording that the dye stained all cell types in the brain, but failed to stain any tissue of the periphery (Goldmann, 1913). The elucidation of the transport mechanisms, cell-signaling interactions, biochemical pathways, molecular composition, and intracellular structural interactions of the BBB is an ongoing process with many questions still unanswered. Nevertheless, a vast array of information came about from the second half of the last century to present. The incidence of CNS disorders such as Alzheimer's disease, Parkinson's disease, stroke, and the increased occurrence of neurotoxicosis caused by compounds that cross the BBB are among the reasons research on the barrier functionality is so extensive. Since the BBB restricts the entry of most pharmaceuticals into the brain, knowledge of the mechanisms utilized by molecules that can cross the BBB would be a great asset in the development of drugs to treat neurological pathologies (Patel *et al*., 2009).

Crossing of a molecule through the BBB is dependent upon its physicochemical properties, such as lipophilicity and solubility, and its pharmacokinetic profile in plasma. This profile, in turn, depends upon how the compound is absorbed, distributed, metabolized, and excreted (Alavijeh *et al*., 2005). Neurotoxic effects of compounds that cross the BBB have been studied extensively. Studies include those on OPs done in our laboratory and by other groups. These studies contributed to a more comprehensible knowledge of the mechanisms involved in OP neurotoxicosis (Ehrich and Gross, 1983; El-Fawal *et al*., 1990; Harel *et al*., 2000; Jortner and Ehrich, 1987; Petroianu *et al*., 2007). Nevertheless, the transport mechanism utilized by these compounds as they cross the BBB is still to be elucidated. Biochemical mechanisms contributing

to lead-induced changes in neuronal function have been reported (Toscano and Guilarte, 2005; Wang *et al*., 2006), but the mechanism or mechanisms by which lead crosses the BBB are yet to be established.

BBB *IN VITRO*:

Experimental models of *in vitro* BBB systems began to be used in the 1980's after techniques to isolate endothelial cells from brain microvessels were developed (Bowman *et al*., 1981; Diglio *et al*., 1982). These techniques allow the isolated endothelial cells to be cultured *in vitro* while retaining their primary histochemical and morphological properties. Audus and Borchardt (1986a) cultured a monolayer of endothelial cells on a porous membrane, which enabled the description of transport profiles and the assessment of factors that influenced drug transport across the endothelial monolayer. These authors went on to establish that the cerebrovascular endothelial monolayer conferred a certain "barrier" function toward polar substances (Audus and Borchardt, 1986a; Audus and Borchardt, 1986b), and also noticed that the carrier systems present in the *in vivo* BBB appeared to be present in the *in vitro* model as well (Audus and Borchardt, 1986b).

Another group constructed a monolayer barrier utilizing freshly isolated cerebrovascular endothelial cells from bovine brains, seeded in collagen-fibronectin coated cellulose "discs" (van Bree *et al.*, 1988). The authors utilized this BBB *in vitro* model to assess permeability, lipophilicity and effects of molecular size in solute transport across the barrier for different concentrations of atenolol, metoprolol, pindolol, propranolol, acetaminophen, antipyrine,

phenacetin and fluorescein conjugated dextrans. By assessing permeability and transport mechanisms in their *in vitro* system, they concluded that the bovine brain vascular endothelial cells cultured on cellulose discs retained the ability to develop tight junctions (van Bree *et al.*, 1988). Many advances of our knowledge of the BBB were elucidated by studying the properties and function of cerebral endothelial cells in *in vitro* models. These include transport processes, cell-to-cell interactions, biochemical properties, and physiological characteristics. *In vitro* systems have also been utilized in drug research to expand our knowledge of the BBB (Joo, 1992). Because *in vitro* studies allow culturing of most cell types, existing protocols include even isolation and studying of human brain microvascular endothelial cells (Biegel et al., 1995). As good as these studies and assessments were in helping to elucidate biological, physical, chemical, and physiological mechanisms, they still presented protocols and studies that assessed a bi-dimensional structure, meaning a single monolayer of endothelial cells cultured on a cellulose membrane coated with one or several extracellular matrix proteins. Although the model was functional, it lacked most of the multi-dimensional interactions that endothelial cells maintain with the cells in their surroundings *in vivo*.

In the 1990's scientists started to utilize co-culture systems that included not only microvascular endothelial cells, but also another component of the BBB *in vivo*, i.e., the astrocyte (Isobe *et al*., 1996). Astrocytes affect the permeability of endothelial cells by inducing phenotypes characteristic of the BBB *in vivo*; however, co-cultures of astrocytes and brain microvascular endothelial cells are a relatively new model when assessments are performed *in vitro.* Reinhart and Gloor (1997) reviewed pharmacological and toxicological research describing several different approaches for BBB co-culture *in vitro* model assessments. The models described in this review include purified bovine, porcine, rat and human brain

microvascular endothelial cells as well as several immortalized cell lines co-cultured with astrocytes of various species (Reinhart and Gloor, 1997). The co-culture BBB models enhance the principal characteristics of the barrier and allow the systems to be employed as a great tool in BBB assessments. The broad use of BBB co-culture *in vitro* models in the last few years has increased our knowledge of the biochemical, physical, and molecular mechanisms of the BBB. Nonetheless, many of these assessments include co-culture models constructed with cells from different animal species. These models include bovine endothelial cells with rat astrocytes, rat astrocytes with human endothelial cells and canine endothelial cells with rat astrocytes (Joo, 1992; Reinhart and Gloor, 1997, Coisne *et al*., 2005). Since these assessments include cellular components of at least two different species, one may hypothesize that species differences could influence the outcome of the assessments measured by such studies. This is very important because, *in vitro* mixed species co-culture models provide results that cannot be validated by *in vivo* testing.

In neurotoxicology assessments of OP compounds and lead in our laboratory, both *in vitro* and *in vivo* evaluations demonstrate the passing of both neurotoxicants through the barrier (Balbuena *et al*., 2008; Balbuena *et al*., 2010; Dyer et al., 1992; Ehrich et al., 2004; Jortner et al., 2005; Meldrum *et al*., 2007; Parran *et al*., 2005). However, assessments of two different *in vitro* co-culture systems, one constructed with bovine brain microvascular endothelial cells and rat astrocytes, and the other constructed with rat brain endothelial cells and rat astrocytes, showed differences in TEER, diffusion, and metabolism of neurotoxicants (Balbuena *et al*., 2008; Balbuena *et al*., 2010; Meldrum *et al*., 2007). In light of these results, it is advisable to avoid when possible construction of *in vitro* systems than contain more than one species cell types. For the assessments on the second part of this dissertation, a co-culture system totally obtained from

rats was used. It utilized astrocytes from neonatal rat brains and a rat endothelial cell line that our laboratory is familiar with: the RBE4 line. This line is derived from immortalized rat brain microvascular endothelial cells. The preliminary work performed in our laboratory suggested that this model would be appropriate for testing the hypothesis of this dissertation (Balbuena *et al*., 2008; Balbuena *et al*., 2010; Meldrum *et al*., 2007).

Tight Junction Proteins.

Homeostasis of the microenvironment in the neuronal parenchyma is essential for normal function of the brain. Since the BBB is responsible for this characteristic, the endothelial cells forming this barrier protect the parenchymal environment against variations in the composition of blood, the breakdown of concentration gradients, and especially against neurotoxic compounds (Kniesel and Wolburg, 2000). The structures that confer the endothelial cells with these barrier properties are the tight junctions. The first assessments of permeability efficiency in endothelial cells of the BBB include experiments performed with electron microscopy (Reese and Karnovsky, 1967) and the use of freeze-fracture to show that the endothelial cell tight junctions were, in fact, the most complex junctions in the cardiovascular system and responsible for the barrier capabilities (Nagy *et al*., 1984).

Tight junctions form pentalaminar layers, which result from the fusion of the external leaflets of partner cell membranes at their contact points. Tight junctions can appear, depending on the orientation of the section, as a chain of fusion points or “kissing points”, or as a domain of one occluded intercellular cleft of variable length (Brightman and Reese, 1969; Wolburg and

Lippoldt, 2002). Utilizing the freeze-fracture technique, the microarchitecture of tight junctions in the plane of the membrane can be assessed. Tight junctions express variability in their fracture properties in terms of their association with either one of the membrane leaflets forming the junction (Kniesel and Wolburg, 2000; Liebner et al., 2000; Wolburg and Lippoldt, 2002). BBB tight junctions of mammalian species are characterized by their high complexity; in freeze-fracture technique images they are associated predominantly with the protoplasmic fracture face or P-face, which forms a network of strands and leaves grooves at the ectoplasmic fracture face or E-face occupied by very few particles (Kniesel and Wolburg, 2000; Liebner et al., 2000; Nagy *et al*., 1984). When particles occur at the E-face, tight junction structures are arranged in chains, whereas when occurring at the P-face, structures are frequently formed as continuous cylindrical profiles (Kniesel and Wolburg, 2000). The altered particle distribution in brain microvessel tight junctions may be indicative of a strong tight junction-cytoskeleton interaction.

Several tight junction-associated protein components have been identified in the last two decades. Forming the intercellular structure of the tight junction are at least two transmembrane proteins, occludin (Ando-Akatsuka et al., 1996; Furuse *et al*., 1993) and the claudin family (Furuse et al., 1998; Tsukita and Furuse, 2000). These are the most important membranous components of the tight junction that have been identified. A group of cytosolic membrane proteins called the *zonula occludens* form the scaffolding complex holding this membranous structure together. This family of proteins includes ZO1 (Stevenson *et al*., 1986), ZO2 (Jesaitis and Goodenough, 1994), and ZO3 (Balda and Anderson, 1993; Haskins et al., 1998). Both occludin and claudins contain four transmembrane domains and two extracellular loops. In the generally accepted model of a tight junction, the loops of protein from one membrane intercalate with the loops of protein from the adjacent membrane, effectively sealing the intercellular cleft

between the two cells. However, another line of thought challenges the notion that this structural arrangement of peptide chains would be responsible for the extremely high transcellular electrical resistance of tight junctions (Wolburg *et al.*, 2006). The supporters of this line of thought suggest, instead, that there is a continuation of outer membrane leaflets between two adjacent junction connected cells. These leaflets form lipid structures such as inverse micelles that in turn stabilize the membrane proteins and these structures form the tight junction (Grebenkämper and Galla, 1994; Hein *et al*., 1992; Wolburg et al., 2003). According to this model, the hydrophilic domain between transmembrane domain two and three could be located within the micelle instead of the cytoplasm. In both models, however, the extracellular loops have free access to the intercellular cleft. At present, whether the conventional protein model or the lipid-protein model better represents the final structure of the tight junctions is a subject of considerable research. Nevertheless, the presence of protein structures in the tight junctions is an undeniable reality.

ZONULA OCCLUDENS FAMILY (ZO1, ZO2, ZO3)

The zonula occludens family of proteins (ZO proteins) included the first tight junction-specific molecules to be identified around the mid 1980's. ZO1 specifically is a 220-225 kDa protein that was initially isolated as tight junction-specific epitope for antibodies raised against a crude tight junction fraction isolated from rat liver (Fanning, 2006; Itoh *et al*., 1999a; Stevenson *et al*., 1986). ZO proteins belong to a group of membrane-associated guanylate kinase-like homologues (MAGUKs), which are involved in creating and maintaining specialized membrane

domains in various types of cells (Fanning, 2006). These molecular structures contain several common structural domains of about 80-90 amino acids called PDZ, one 50-70 long SH3 domain that binds to guanylate kinase-like (GK) modules or to ligands at least seven residues in length that contain a PXXP sequence, and one guanylate kinase-like domain. PDZ stands for a combination of the first letters of three proteins, postsynaptic density protein (PSD95), drosophila disc large tumor suppressor (DlgA), and zonula occludens 1 protein (ZO1). These three proteins attach to the PDZ domain, which in turn, helps anchor these transmembrane proteins to the cytoskeleton, holding together the signaling complexes (Fanning, 2006; Itoh *et al*., 1999a). ZO proteins just like other MAGUKs are highly conserved throughout phylogeny and are thus presumed to be components of conserved cellular function. In addition to the core domains of PDZ, SH3 and GUK, ZO proteins also contain an additional two PDZ domains within the amino terminal half of the protein, and an acidic domain adjacent to the GUK domain whose function is not known (Itoh *et al*., 1993; Willott *et al*., 1993).

ZO proteins contain a large proline-rich C-terminal domain; the C-terminus of ZO1 also contains a conserved domain known as ZU5 of unknown function. Furthermore, both the N- and the C- terminal halves of the ZO proteins display complex splicing patterns (Fanning, 2006). Most of the tight junction proteins that are associated with the ZO family bind to domains within the N-terminal half of the protein structure, whereas the C-terminal half of the molecular structure associates with cytoskeletal molecules. This suggests that at least one of the functions of ZO proteins is to connect the paracellular seal formed by the tight junction with the actin cytoskeleton (Fanning, 2006; Itoh *et al*., 1999a). There are two isoforms of ZO1, ZO1α+ and ZO1 α-; they differ by an internal 80-residue domain termed domain α (Citi, 2001). Most epithelial cells express both isoforms, but endothelial cells express exclusively the α- isoform. It

appears that the α- isoform is restricted to cells with a higher degree of junctional plasticity (Balda and Anderson, 1993; Giepmans and Moolenaar, 1998; Kurihara *et al*., 1992). ZO1 associates with a number of junctional and cytoskeletal proteins. For example, its PDZ1 domain interacts with claudins (Itoh *et al*., 1999a), with protein conexin-43 or Cx-43 through the PDZ2 domain (Giepmans and Moolenaar, 1998) and with other ZO-2 and ZO-3 molecules through the PDZ2 domain (Fanning *et al*., 1998; Itoh *et al*., 1999a; Itoh *et al*., 1999b).

The SH3 domain interacts with a serine protein kinase (ZAK) and with the nucleic acid-binding protein ZONAB (Balda *et al*., 1996; 1 Balda *et al*., 2000). The GUK domain associates with occludin (Fanning *et al*., 1998); however, it remains to be determined whether ZO1 interacts with G-protein-binding proteins. The proline-rich region of ZO1 interacts with F-actin (Fanning *et al*., 1998; Itoh *et al*., 1997). ZO1 interactions, expression, and subcellular localization indicate a vital function in tight junction structures. The N-terminal half of ZO1 cluster transmembrane junctional proteins and other PDZ-containing proteins at sites of cell-to-cell contacts (Balda *et al*., 1996; Citi, 2001; Fanning *et al*., 1998; Giepmans and Moolenaar, 1998). This creates a submembrane network that is anchored to the cytoskeleton through the C-terminal half of the protein.

ZO2 was identified as a 160-kDa polypeptide that co-immunoprecipitates with ZO1 but has a distinct antibody reactivity, peptide map, and turnover rate (Citi, 2001; Gumbiner *et al*., 1999) The protein contains 3 PDZ domains, 1 SH3, and one GUK domain (Jesaitis and Goodenough, 1994). It has about 51% sequence identity with ZO1 and it encloses a 36-residue alternatively splicing region (β) at the C-terminal end (Beatch *et al*., 1996; Citi, 2001). The C-terminal proline-rich region of ZO2 shares only about 25% amino acid homology with the same region in ZO1 (Citi, 2001). ZO2 interacts with occludin and α-catenin through an N-terminal fragment

(Itoh *et al*., 1999b) while a fragment of the C-terminal associates with actin microfilaments, suggesting that the proline-rich region of ZO2 interacts with actin in the cytoplasm (Citi, 2001; Itoh *et al*., 1999b). Just like ZO1, ZO2 has been detected in many types of cells, however, in non-epithelial or non-endothelial cells it associates with cadherins (Jesaitis and Goodenough, 1994). Although ZO2 shares similarities with ZO1 such as domain organization, protein interactions, and subcellular localization, whether both proteins perform similar or completely different roles in tight junction induction, function, and structural modification remains a subject of intense research.

ZO3 protein was first identified in ZO1 precipitates as a phosphorylated 130-kDa polypeptide (Balda *et al*., 1993; Citi, 2001). ZO3 has an amino acid homology of about 47% with ZO1 and ZO2 although the amino acid sequence linking PDZ2 and PDZ3 domains in ZO3 is a unique proline-rich motif (Citi, 2001; Haskins *et al*., 1998). ZO3 associates with ZO1 but not with ZO2 in *in vitro* experiments, suggesting that ZO1 forms independent protein complexes with both ZO2 and ZO3 (Citi, 2001; Haskins *et al*., 1998; Wittchen *et al*., 1999). Whereas ZO3 interacts with the cytosolic skeleton through F-actin associations, it also interacts with the cytoplasmic domain of claudin-1 through connections at the PDZ1 site (Wittchen *et al*., 1999), and with ZO1 and ZO2 through the PDZ2 motifs (Citi, 2001; Itoh *et al*., 1999b; Wittchen *et al*., 1999).

The scaffold complex attaching the tight junction proteins to the cytoskeleton structure in cell-to-cell interactions includes several additional proteins. These include membrane-associated guanylate kinase with an inverted arrangement of protein-protein interaction domains or MAGI-1/BAP1 (Ide *et al*., 1999), AF-6 protein (Takai *et al*., 2003; Yamamoto *et al*., 1997), the atypical protein kinase C specific interacting protein or ASIP/PAR-3 (Ebnet *et al*., 2003; Hirose *et al*.,

2002) and the PAR-6 (Gao *et al*., 2002). The scaffold may also interact with some other non-PDZ tight junction plaque proteins like cingulin (Citi *et al*., 1988; Citi *et al*., 1989), symplekin (Citi, 2001; Fanning, 2006), and human ASH1 (Citi, 2001; Fanning, 2006); however, these proteins were localized mainly in endothelial cell junctions of the general (i. e. non-cerebral) vasculature. Localization of these proteins in tight junctions of the endothelial cells in the BBB has not been reported.

OCCLUDIN

Occludin is a 65-kDa integral plasma membrane protein localized specifically at tight junctions. It was first isolated in the 1990's (Tsukita and Furuse , 2003). Based on its amino acid sequence, occludin was predicted to be a polytopic membrane protein. The protein includes four transmembrane domains, two extracellular loops of similar size enriched in tyrosines and glycines, and three cytoplasmic domains: one intracellular short turn, a small amino terminal domain, and a long carboxyl terminal region (Gonzalez-Mariscal *et al*., 2003). The ends of both the C- and N- terminals of the protein are localized in the cytosol where the C- terminal cytoplasmic domain interacts with ZO1, ZO2, ZO3, and cingulin as well as with actin filaments, (Balda and Matter, 1998a; Balda and Matter, 1998b; Balda and Matter, 2000). Occludin migrates as a tight cluster of 62-82 kDa bands on SDS gels as a result of phosphorylation on serine, threonine and tyrosine residues (Balda and Matter, 1998a; Sakakibara *et al*., 1997; Wong, 1997; Wong and Gumbiner, 1997).

These phosphorylations are regulated by protein kinase C (Andreeva *et al*., 2001), casein kinase 2 (CK2) (Chen *et al*., 2002; Cordenonsi *et al*., 1999), $p34^{cdc2}$/cyclin B complex (Andreeva *et al*., 2001), and the non-receptor tyrosine kinase c-Yes (Chen *et al*., 2002). Occludin appears to have several functions. In epithelial cells, highly phosphorylated occludin localizes in the cytoplasm (Andreeva *et al*., 2001), however, in endothelial cells, shear stress significantly reduces occludin content and increases its tyrosine phosphorylation with an associated increase in hydraulic conductivity (DeMaio *et al*., 2001; Gonzalez-Mariscal *et al*., 2003). Hydraulic conductivity is described as the membrane transport property that describes the relationship between the water flux in the vasculature and both the force driving water and solutes out of the circulation, and the resorptive force opposing the former (DeMaio *et al*., 2001). In *Xenopus* embryos, occludin dephosphorylation correlates with *de novo* assembly of tight junctions (Cordenonsi *et al*., 1997). Therefore, occludin phosphorylation may play different roles in distinct biological systems or, alternatively, phosphorylation of different residues may have dissimilar consequences. The last 150 amino acids of the cytosolic C-terminal structure of occludin are highly conserved among species and have been proposed to form a typical α–helical structure. This structure interacts directly with F-actin (Wittchen *et al*., 1999), giving the protein a unique characteristic among tight junction proteins, since most of them require the mediation of scaffold proteins to associate with the actin cytoskeleton. The carboxyl segment of occludin is also responsible for the binding to the MAGUK proteins ZO1, ZO2, and ZO3 (Furuse *et al*., 1994; Haskins *et al*., 1998; Itoh *et al*., 1999b; Wittchen *et al*., 1999).

Some other observations, however, suggest that occludin is not the only integral membrane protein involved in the structural composition of tight junctions. Balda *et al.* (Balda *et al*., 1996) introduced occludin with truncated COOH-terminals into Madin-Darby canine kidney (MDCK)

cells causing the re-concentration of endogenous occludin along the cell border in a dot-like manner, but the continuous network of tight junction strands was not affected. Endothelial cells in non-neuronal tissue and Sertoli cells in some species generate tight junctions but express little occludin (Hirase *et al*., 1997). In transgenic mice carrying a null mutation in the occludin gene, occludin -/- offspring mice were born with no gross phenotype in the expected Mendelial ratios; however, they showed significant postnatal growth retardation (Saitou *et al*., 2000).

Tight junctions did not appear to be affected morphologically, and the barrier function of intestinal epithelium was normal. However, histological abnormalities of various tissues including calcification of the brain were present in the offspring (Saitou *et al*., 2000). Although these assessments support the existence of a tight junction with at least another tight junction-specific integral membrane protein, one can conclude at present, that occludin is indispensable. In order to better understand the molecular mechanisms behind the complex phenotypes of occludin, and its importance in tight junction formation, further study of functional and structural parameters at the cellular and molecular levels is required.

CLAUDIN FAMILY

Since there are have been studies that demonstrated formation of tight junctions in at least some cellular structures without occludin, an alternative scenario is possible, which suggests that other molecules can form strand structures and form an effective barrier without occludin. The initial biochemical assessments to identify other tight junction molecules were reported by the Tsukita research group (Furuse *et al*., 1998). They examined potential candidates from tight

junction fractions in chicken liver. Protein isolation, purification, and peptide sequencing resulted in the cloning of two full-length c-DNAs encoding related proteins of 211 and 230 residues of approximately 22-27 kDa each, which were named claudins (Furuse *et al*., 1998; Turksen and Troy, 2006). Claudins are integral membrane proteins with four hydrophobic membrane-spanning regions, two extracellular and one intracellular loop with both the C-terminal and the N-terminal localized in the cytoplasmic region of the cellular membrane (Furuse *et al*., 1998; Furuse and Tsukita, 2006). The first of the two extracellular loops is larger than the second, but both appear to be involved in the homophilic and /or heterophilic interactions implicated in tight junction formation (Turksen and Troy, 2006). The WWCC motif, W-X(17-22)-W-X(2)-C-X-(8-10)-C within the first loop is conserved among members of the claudin family (Furuse *et al*., 1998; Turksen and Troy, 2006). This motif is also found in some non-claudin molecules such as PMP22, EMP, MP20 and the γ5-subunit of the voltage-gated calcium channels (Furuse and Tsukita, 2006). At their C-terminus, claudins contain a PDZ-binding motif that connects to the PDZ domain of peripheral membrane proteins such as the ZO family members (Furuse *et al*., 1998; Furuse and Tsukita, 2006; Turksen and Troy, 2006). Claudins form a multigene family of about 24 members and the expression pattern of each claudin species varies considerable among different tissues (Morita et al., 1999; Rahner et al., 2001; Wilcox *et al*., 2001). Claudins 3, 7, 1, 2, 10, 11, 16, 4, 8 and 15 mRNA is detected in large amounts in the kidney (Kiuchi-Saishin *et al*. 2002; Li *et al*., 2004; Reyes *et al*., 2002; Yu *et al*., 2003). Claudin 4, claudin 7, and claudin 8 are expressed primarily in the lung and kidney (Turksen and Troy, 2006). Claudin 6 is expressed in large amounts in embryos but not in adult tissues (Moriwaki *et al*., 2007; Turksen and Troy, 2001); claudin 5 is expressed specifically in endothelial cells of blood vessels, suggesting a role in the regulation of blood vessel permeability (Morita *et al*.,

1999; Nitta *et al*., 2003). The tight junctions of the BBB formed by endothelial cells are well developed and indispensable in the regulation of paracellular transport. And claudin 5 is as a major constituent of the tight junctions of the BBB, responsible for this transport regulation (Morita *et al*., 1999). Claudin 5 deficient mice are born alive; however, they die within one day of birth (Nitta *et al*., 2003). Although these mice present no morphological abnormalities in the brain as shown by light and electron microscope assessments, tracer perfusion experiments revealed that the BBB formed by endothelial cells of claudin 5 deficient mice was severely disrupted and permeable (Nitta *et al*., 2003). Because tight junction structures are fundamental in the regulation and function of BBB permeability and transport, the assessment of tight junction components in neurotoxicity assessment of compounds known to cross the barrier is an imperative step in the elucidation of BBB pathology.

Transient Receptor Potential Canonical Channels (TRPC calcium channels).

The transient receptor potential (TRP) superfamily, to which the TRPC group belong, is distinct from other groups of ion channels in that they display an overwhelming diversity in ion selectivity and modes of activation, in addition to several physiological functions (Alexander *et al*., 2008; Gaudet, 2008; Montell, 2005). Some are involved in sensory perception and are directly activated by temperature and mechanical or osmotic stress (Montell, 2005); others are activated downstream of receptor stimulation through a phospholipase C (PLC)-dependent pathway (Gaudet, 2008). In some other cases, a given response is the result of the integration of

several signals of a different nature (chemical or physical) and/or different sources (intra or extracellular stimulation) (Alexander *et al*., 2008; Gaudet, 2008). In mammals, the TRP superfamily contains about 30 members distributed into six families according to genetic sequence and function. Within each TRP subfamily, there is a high level of primary amino acid sequence similarity; nevertheless, this similarity is limited primarily to the transmembrane segments and a small region COOH-terminal of the sixth transmembrane domain (Montell, 2001).

The most prominent members of the TRP superfamily are the transient receptor potential canonical channels group (TRPC) that seems to be involved in the regulation of endothelial cell permeability (Tiruppathi *et al*., 2006). TRPC channels are very large tetramers (about 700 to 1000 amino acids) composed of six putative transmembrane 70-250 kDa subunits or domains. Each channel is made up of different subunits from a total of seven isoforms, TRPC1 to TRPC7 (Nilius and Droogmans, 2001; Pedersen *et al*., 2005), which can assemble both as homomeric and heteromeric complexes (Pedersen *et al*., 2005). TRPCs show similarity to voltage-gated calcium channels in the region called S3 through S6, which includes the S5-S6 linker that forms the ion selective pore (Montell and Rubin, 1989; Zhu *et al*., 1996). The only exception is localized in the fourth transmembrane segment S4, where TRPCs lack the complete set of positively charged residues that confer voltage sensitivity (voltage sensor) to most of voltage-gated ion channels (Catterall, 2000; Montell and Rubin, 1989).

TRPC proteins contain three to four ankryin repeats and are PLC-operated nonselective cation channels (Montell, 2001) that demonstrate variable Ca^{2+}/ Na^{+} permeability ratios ranging from 1 to 9 (Montell, 2001). Given the complex set of molecular responses elicited by TRPC activation, it seems that TRPCs play pivotal roles in a wide variety of cellular and tissue

functions. The objective of this proposal is, however, to assess the relationship between TRPC1 channels and endothelial cells of the BBB regarding permeability and their functional response to neurotoxic agents such as OP compounds and lead. One of the functions of endothelial cells is to maintain the barrier functions of blood vessels in the BBB. Increases in endothelial intracellular calcium increase the BBB permeability by inducing fissure formation between endothelial cells (Tiruppathi *et al*., 2003). Increases of the cytoplasmic Ca^{2+} concentration of cells occurs in two ways: release from intracellular stores through the store-operated calcium (SOC) entry pathway or by direct Ca^{2+} influx into the cell through the cell membrane (Cioffi and Stevens, 2006; Parekh and Putney Jr., 2005; Tiruppathi *et al*., 2006). TRPCs in endothelial cells have been implicated in the response from store-operated calcium pathways that deplete calcium in the intracellular space (Tiruppathi *et al*., 2003) by PLC-catalyzed formation of inositol 1, 4, 5-triphosphate or IP3 (Montell *et al*., 2002). Since lead and OP are associated with variations in intracellular calcium concentrations in different cell systems (El-Fawal *et al*., 1990; Goldstein, 1993; Long *et al*., 1994; Marcovac and Goldstein, 1988; Schanne *et al*., 1997; Schuh *et al*., 2002), the TRPC channels are good candidates to explain the rising of intracellular calcium induced by lead-OP neurotoxicity.

Neurotoxic Compounds.

NEUROTOXICITY OF ORGANOPHOSPHATES

Organophosphorus (OP) compounds are derivatives of phosphorus, phosphoric, phosphinic, and phosphonic acids containing both a carbon and a pentavalent phosphorus atom. The phosphorus atom motif is usually bivalently connected to an oxygen atom (Abou-Donia, 2003; Aldridge, 1996; Marrs and Ballantyne, 2004). The electrophilicity or positive charge of the phosphorus atom confers the OP compounds with their phosphorylating properties, which in turn, delineate the specific biological function of these compounds, that is, the inhibition of the cholinesterase enzyme acetylcholinesterase (Aldridge, 1996; Marrs and Ballantyne, 2004).

Acetylcholinesterase (AChE) enzyme functions to terminate the neuronal impulse that occurs when acetylcholine (ACh) is released into the synaptic cleft of neural and neuromuscular junctions (Abou-Donia, 2003; Aldridge, 1996; Massiah *et al*., 2001). As an important means of regulating the depolarization of post-synaptic cells, AChE removes ACh from the cleft by increasing the hydrolysis of ACh to acetate and choline (Abou-Donia, 2003; Massiah *et al*., 2001; Silman and Sussman, 2005). There are three functional regions in the tridimensional structure of AChE; the first is a catalytic triad that operates the active site mechanism, the second is a gorge that connects the active site region to the protein structural surface, and the third is a peripheral anionic site at the surface of the protein (Abou-Donia, 2003; Massiah *et al*., 2001).

The active center of the enzyme includes several subunits. The first is the catalytic triad, formed by Ser-200, His-440, and Glu-327 (Casida and Quistad, 2005; Greenblatt *et al*., 2003; Harel *et al*., 2000; Silman and Sussman, 2005; Silman and Sussman, 2008). There is also an acyl pocket formed by Phe-295 and Phe-297, which is responsible for the acetyl ester specificity of AChE (Marrs and Ballantyne, 2004). The center also includes a choline subunit formed by Trp-86, Glu-202, and Tyr-337 (Casida and Quistad, 2005; Harel *et al*., 2000; Silman and Sussman, 2008). Finally, it also includes the peripheral site, which is composed of Trp-286, Tyr-72, Tyr-

124, and Asp-74 (Abou-Donia, 2003; Casida and Quistad, 2005; Greenblatt *et al*., 2003; Silman and Sussman, 2005; Silman and Sussman, 2005). Next to the active site cluster is an oxyanion hole created by main-chain N-H groups contributed by Gly-118, Gly-119, and Ala-201 (Harel *et al*., 2000; Massiah *et al*., 2001). These hydrogen bond donors stabilize complexes of the enzyme with the transition state of ACh and with covalent and transition state analog inhibitors such as the OP compounds (Greenblatt *et al*., 2003; Harel *et al*., 2000; Massiah *et al*., 2001; Silman and Sussman, 2008).

OP inhibition of AChE is achieved by phosphorylating the serine hydroxyl group at the catalytic triad site (Abou-Donia, 2003; Aldridge, 1996). The acidic ester formed with the enzyme is extremely stable and its hydrolysis occurs very slowly (Abou-Donia, 2003; Marrs *et al*., 2004). When the enzyme contains methyl or ethyl groups in its structure, hydrolysis will regenerate it within hours; however, if inhibitors contain isopropyl groups, restoration of AChE levels will depend upon synthesis of new enzyme molecules (Marrs *et al*., 2004). AChE that is phosphorylated by OP compounds is likely to lose alkyl groups, a process called aging and that results in a negatively charged monoalkyl enzyme unable to be hydrolyzed with the resulting accumulation of acetylcholine at the cholinergic (muscarinic and nicotinic) receptors of the CNS (Casida and Quistad, 2005; Silman and Sussman, 2008). Over-excitation of cholinergic receptors induced by OP toxicosis incites muscarinic reactions such as salivation, lacrimation, miosis, accommodative spasm, bronchoconstriction, bradycardia, and intestinal cramps (Ecobichon, 2001; Ehrich, 2005; Kamanyire and Karalliedde, 2004). Nicotinic reactions include depolarizing neuromuscular blockade and muscle paralysis (Abou-Donia, 2003; Ecobichon, 2001; Ehrich, 2005; Kamanyire and Karalliedde, 2004). Cholinergic over-activation of CNS receptors results in seizures, respiratory depression and coma (Ecobichon, 2001; Ehrich, 2005; Kamanyire and

Karalliedde, 2004). OPs cross the BBB due in part to their lipophilicity, although the exact mechanisms employed in the barrier crossing are not yet elucidated. It is proposed in this dissertation that OP compounds disturb BBB function by disrupting tight junction formation.

NEUROTOXICITY OF LEAD

Lead (Pb) is a ubiquitous toxic metal detectable in practically all phases of the inactivate environment and in all biological systems (Goyer and Clarkson, 2001; Hernberg, 2000; Shi and Zheng, 2007). Pb exists in both organic and inorganic forms. The organic from of Pb is more toxic than the inorganic form because its degradation coefficient is lower than that of inorganic Pb, however, only a small proportion of population exposures is related to organic Pb (Goyer and Clarkson, 2001; Hernberg, 2000; Bondy, 1988).

Pb toxicity, which remains a major public health issue (Hernberg, 2000), has been associated with altered liver, kidney, lung, cardiovascular, immune, bone, and CNS functions (Boulding *et al*., 1975; Bressler *et al*., 1999; Goldstein *et al*., 1974; Goldstein, 1990; Marchetti, 2003; Silbergeld, 1992; Toscano and Guilarte, 2005; White *et al*., 2007; Zheng, 2001; Zheng *et al*., 2003). At high concentrations, Pb also disrupts the cerebral capillary endothelial cells forming the BBB, causing extensive cerebral hemorrhage and the extra-vascular distribution of albumin (Goldstein *et al*., 1974; Kerper and Hinkle, 1997b; Shi and Zheng, 2007). Albumin is a large molecular weight protein found in the systemic circulation, which is normally excluded from the brain parenchyma (Goldstein *et al*., 1974). Pb toxicity is accompanied by damage to many

membranes; it crosses the BBB and causes breakdown of active transport systems in cerebral capillaries (Shi and Zheng, 2007; US Department of Human Services, 2006).

Lead exists predominantly bound to proteins in soft tissues such as the kidney, liver and brain. Pb is a divalent cation that binds strongly to sulfhydryl, amine, phosphate, and carboxyl groups of these proteins. The highest affinity of Pb is with the sulfhydryl fraction of the protein, inferring that lead may interfere with the activity of zinc metalloenzymes because zinc binds to the sulfhydryl group at the active site of the enzyme (US Department of Human Services, 2006). Pb also binds to metallothionein, a cysteine-rich protein synthesized in kidney and liver that is involved in regulation of physiological metals. However, lead does not displace cadmium or zinc, the endogenous substrates of the protein (Eaton *et al.*, 1980; Walkes and Klaassen, 1985), although it increases the concentration of the protein in kidney (Wang *et al*., 2008). Pb is capable of entering cells through voltage-gated L-type Ca^{2+} channels in bovine adrenal medullary cells (Legare *et al*., 1998), through store-operated Ca^{2+} channels in bovine brain capillary endothelial cells (Kerper and Hinkle, 1997a; Kerper and Hinkle, 1997b), and through calcium-permeable acid-sensing ion channels or ASICs (Wang *et al*., 2006).

Although Pb affects molecular mechanisms in cardiovascular, renal, hematological, skeletal and CNS systems, the scope of this dissertational review focuses on the effects of this neurotoxicant on the brain parenchyma and specifically on the BBB since that is the extent of the hypothesis. Lead affects the CNS by means of multiple mechanisms (for review, see Toscano *et al*., 2005). The most important mechanisms affected by Pb in the brain are calcium related pathways. Lead mimics calcium action and/or disrupts calcium homeostasis in the cell (Bressler *et al*., 1999; Calderon-Salinas *et al*., 1999; Fullmer *et al*., 1985; Goldstein, 1993; He *et al*., 2000; Kerper and Hinkle, 1997a; Kerper and Hinkle, 1997b; Sun and Suszkiw, Platt and Busselberg,

1994; 1995; Wang *et al*., 2006; Watts *et al*., 1995). Calcium is involved as a cofactor in many cellular processes (Mellström *et al*. 2008); therefore, many intracellular and extracellular signaling pathways can be affected by Pb exposure.

One of the most studied processes related to Pb-calcium interactions is the activation of protein kinase C (PKC) (Kohout *et al*., 2002; Mosior and Epand, 1997; Nalefski and Newton, 2001; Xu *et al*., 2005; Xu *et al*., 2006). The PKC family consists of 12 isoforms distributed in different tissues with different enzymatic cofactor requirements (Shirai and Saito, 2002; Steinber, 2008). γ-PKC is one of several calcium-dependent forms of the enzyme and therefore a target for lead neurotoxicity (Kohout *et al*., 2002; Nalefski and Newton, 2001). This γ-isoform is neuron-specific and it is involved in long-term potentiation, spatial learning, and memory processes (Clark t al., 1991; Nihei *et al*., 2001; Xu *et al*., 2005). Pb has the capacity not only to activate, but also to inhibit PKCs. Micromolar concentrations of Pb can activate PKC-dependant phosphorylation (Nihei *et al*., 2001), however, in *in vitro* preparations only picomolar concentrations are needed to achieve activation of the enzyme (Avazeri *et al*., 2006). PKC also induces the formation of the activation protein 1 (AP-1) transcriptional regulatory complex (Macian *et al*., 2001), which regulates the expression of the glial fibrillary acidic protein (GFAP); this protein is induced during periods of reactive gliosis in astrocytes (Eng and Ghirnikar, 1994, Eng *et al*., 2000). A deregulation of GFAP gene expression may alter astrocytic function in the BBB. Premature activation of PKC by Pb in immature brains impairs microvascular formation and function, and in high concentrations, it accounts for gross defects in the BBB that contribute to acute lead encephalopathy (US Department of Human Services, 2006).

Calcium modulated protein or Calmodulin (CaM), a major intracellular receptor for calcium, is another protein affected by Pb. Calcium induces a conformational change in the structure of CaM, converting the protein to its active form (Colomer and Means, 2007; Wayman *et al*., 2008). Because Pb can substitute for calcium in many biological processes, the metal is capable of abnormally activating CaM protein (Habermann *t al*., 1983; Kursula and Majava, 2007). Lead activation of CaM can also affect proper functioning of cAMP messenger pathways (Heo *et al*., 1998). Lead also affects many neurotransmitter pathways in the brain including the glutaminergic, dopaminergic, and cholinergic pathways (Jason and Kellogg, 1981; Kidd *et al*., 2007; Lasley and Gilbert, 2000; Suzkiw, 2004).

Hippocampal long-term potentiation (LTP) is a cellular model of learning and memory characterized by a constant increase in synaptic efficacy in response to high frequency stimulation (Bevilagua *et al*., 2005; Manabí, 2008; Pelletier and Lacaille, 2008). Pb disrupts LTP, which is associated with the learning process and the storing of information, by increasing the threshold for induction, by reducing the magnitude of potentiation, and by accelerating the rate of decay of LTP (Gilbert and Mack, 1996; Gilbert and Mack, 1998; Lasley and Gilbert, 2000). Pb achieves these disruptions by disturbing glutamate release (presynaptic effects) and the N-methyl-aspartate (NMDA) receptor function (Gilbert and Lasley, 2007; Lasley and Gilbert, 2000). LTP is more readily affected by Pb during early development, however, exposure after weaning also affects synaptic plasticity (Gilbert and Mack, 1996; Gilbert and Mack, 1998).

Lead is also associated with impairment of the induction of pair-pulse facilitation in the dentate gyrus that is normally induced by glutamate release. The exact mechanism for the inhibition of glutamate release is not known, but it may involve the prevention of activation of PKC (Avazeri *et al*., 2006; Mosior and Epand *et al*., 1997; Nalefski and Newton, 2001; Nihei *et*

al., 2001). Studies have shown that continuous exposures of rats to Pb from gestation to adulthood resulted in increases in binding of non-competitive antagonists such as MK-801 to NMDA receptors in cortical areas, hippocampus, and forebrain. This suggests that alterations of ligand binding to NMDA receptors in the hippocampal formations and cortical areas may play a role in lead induced neurotoxicity (Ma *et al*., 1998). Neurotoxicity assessments suggest that Pb may impair regulation of dopamine synthesis and release, although some other studies report opposing effects of Pb on nigrostriatal and mesolimbic systems regarding receptor binding, dopamine synthesis, and turnover and uptake of neurotransmitter (Lasley and Lane, 1995).

The cholinergic system plays a role in learning and memory processes, and exposure to Pb induces numerous changes in cholinergic functions (Jett and Guilarte, 1995; Si and Lee, 2003). Pb may reduce ACh release into the synaptic cleft by blocking calcium entry into the terminal of the presynaptic neuron (Manalis *et al*., 1984). Pb can also modulate nicotinic receptor activation *in vitro* (Oortgiesen et al., 1997; Si and Lee, 2003), although no studies *in vivo* can corroborate if Pb alters the expression of nicotinic receptors in the developing brain. Finally, chronic exposure of rats to Pb affects the muscarinic modulation of glutaminergic synaptic transmission in the hippocampus (Wang et al., 2007), indicating yet another mechanism by which Pb can modulate essential biochemical pathways in cell function.

Chapter 2: Experimental Design & Methods

CONSTRUCTION OF THE BLOOD-BRAIN BARRIER

The studies included in this dissertation tested the hypothesis that a combination of two neurotoxicants, lead (a toxic metal) and malathion (an organophosphate insecticide), might be capable of disrupting blood brain barrier (BBB) function. Studies were designed to test this hypothesis by measuring changes in transendothelial electrical resistance (TEER), disruption of tight junction complexes in the endothelial layer of the barrier, and changes of calcium related pathways mechanisms affecting barrier function. Two different models were constructed, one with rat astrocytes and a rat endothelial cell line (RBE4), and the other with rat astrocytes and bovine brain endothelial cells (BMEC). A layer of neuronal cells (SH-SY5Y) was cultured under the models to mimic parenchyma. The RBE4, a rat brain endothelial cell line from the laboratory of Dr. Michael Aschner (Vanderbilt University), rat astrocytes obtained from neonatal rat brains, and the SH-SY5Y cells were cultured in 75 cm flasks (VWR International Inc, Bridgeport NJ) with special media designed to support cell proliferation.

RBE4 cultures (Figure 3) were kept in 44.5% minimum essential medium (MEM), 44.5% Ham's F10 with glycine or glutamine, 10% fetal bovine serum (FBS), and 1% of a penicillin/streptomycin/amphotericin B solution, with non-essential amino acid solution to ensure proper proliferation of cells. BMECs (Figure 4) were cultured with 80% Dulbecco's modified eagle's medium, 15% heat-inactivated horse serum, 4% fetal bovine serum, 1% penicillin/streptomycin/amphotericin B solution, and heparin 1.5 nM. SH-SY5Y media included 88% Ham's F12, 10% fetal bovine serum, 1% of a penicillin/streptomycin/amphotericin B solution, and 1% non-essential amino acid solution. Astrocytes (Figure 5) were cultured in 75 cm flasks with 89% MEM, 10% horse serum, and 1% of a penicillin/streptomycin/amphotericin B

solution. All the cell culture media and reagents were obtained from Mediatech Inc. (Manassas VA).

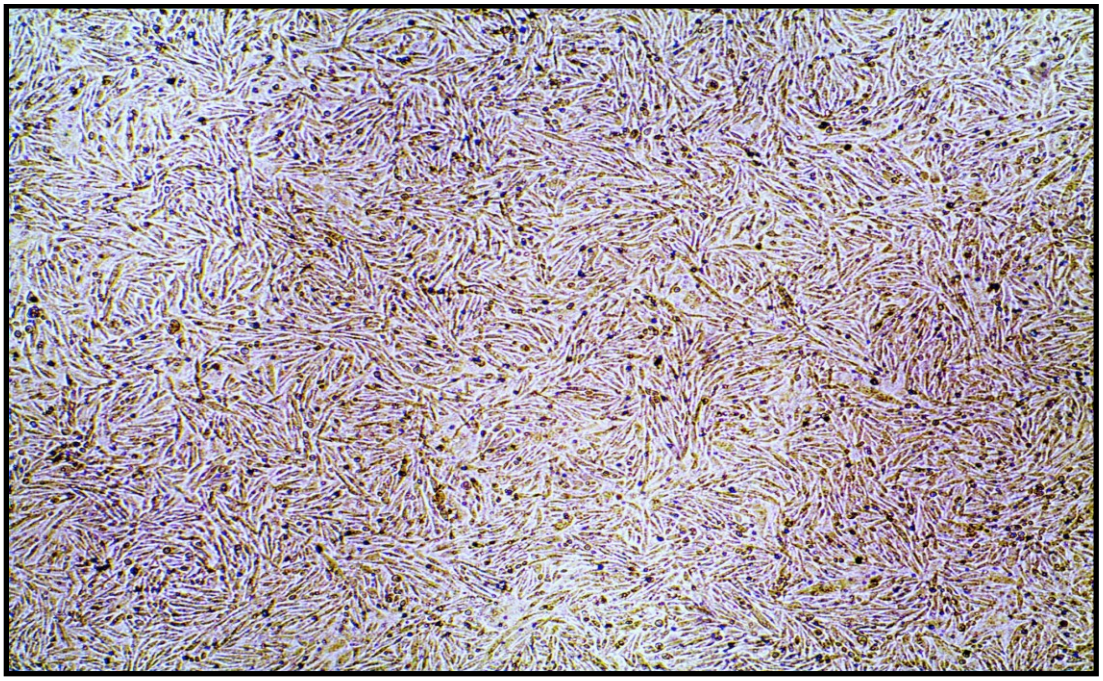

Figure 3 100% Confluent RBE4 cells observed at 4X magnification

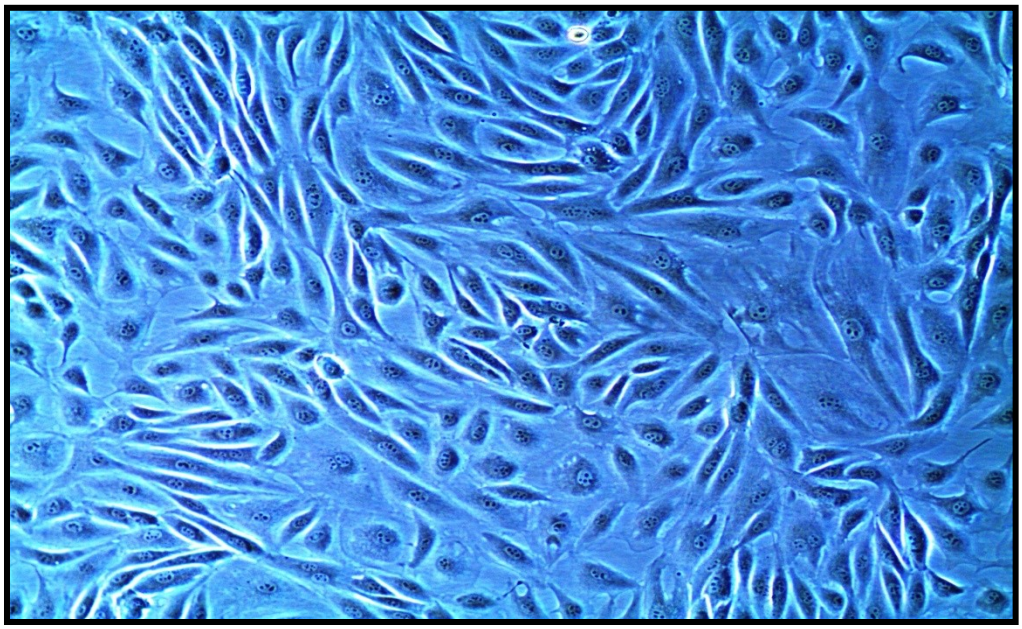

Figure 4 BMECs at confluency observed at 10X magnification

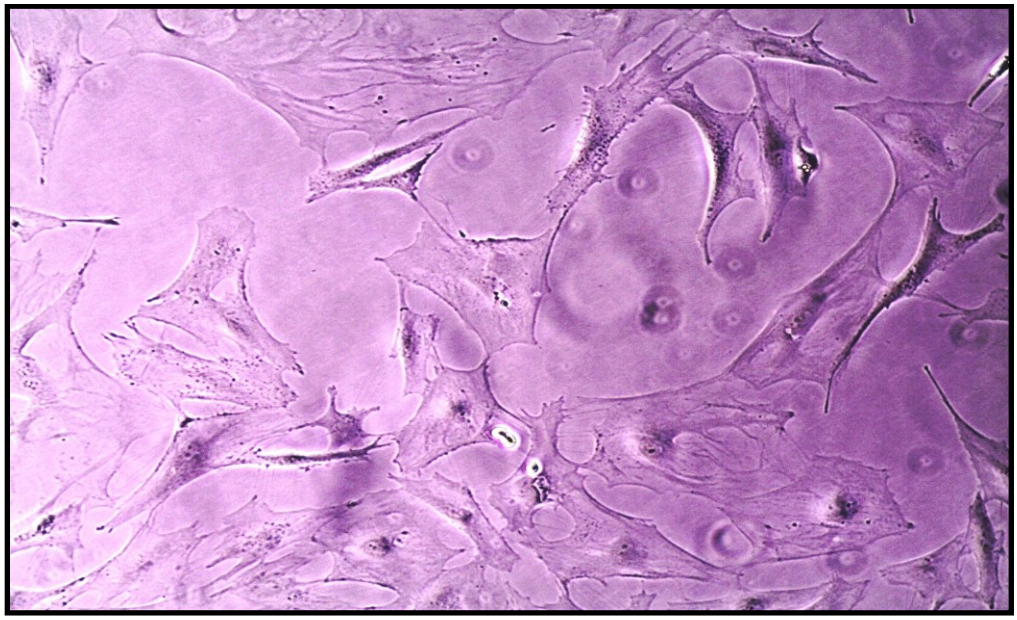

Figure 5 Astrocytes growing on a flask observed with a 10X magnification objective

Once the cells reached confluency, the barrier was constructed by plating astrocytes on the abluminal side and endothelial cells on the luminal side of BIOCOAT® polyethylene terephthalate (PET) porous membranes or inserts (VWR International Inc). Astrocytes were seeded on the abluminal side of these 0.45 micron pore-size collagen coated inserts at a concentration of 1.6 x10^6 cells per insert and were incubated for 8 hr at 38°C to allow attachment of the astrocytes to the porous membrane (Figure 6).

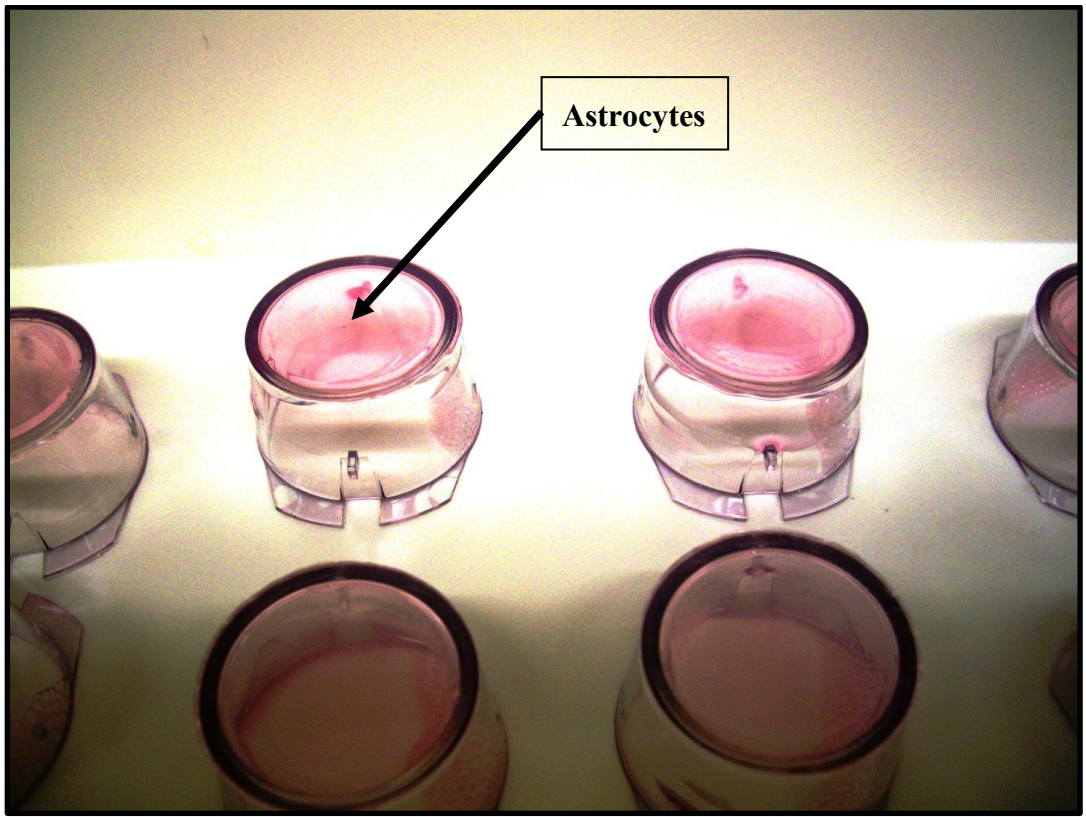

Figure 6 Astrocytes were placed on the abluminal side (bottom) of 0.45-micron pore-size collagen coated BIOCOAT® polyethylene terephthalate (PET) porous membranes. They were incubated for 8 hr to allow attachment of the cells to the membrane.

After the astrocytes reached 100% confluency on the membranes, RBE4 cells or BMECs at concentrations of 1 x 10^5 were seeded on the luminal side of these inserts and cultured for an additional 4 days. The inserts were then placed in six-well plates (VWR International Inc) as shown in Figure 7 to mimic the separation between the microvascular circulatory lumen and the parenchymal space. To replicate the parenchyma in the brain, the neuronal-type cell line SH-SY5Y was cultured on the bottom of the well to mimic the neuronal component of the BBB-neurovascular unit. Once all of the cells on the models reached confluency, the systems were ready for neurotoxicant transfer assessments. The schematics of the model are showed in Figure 8.

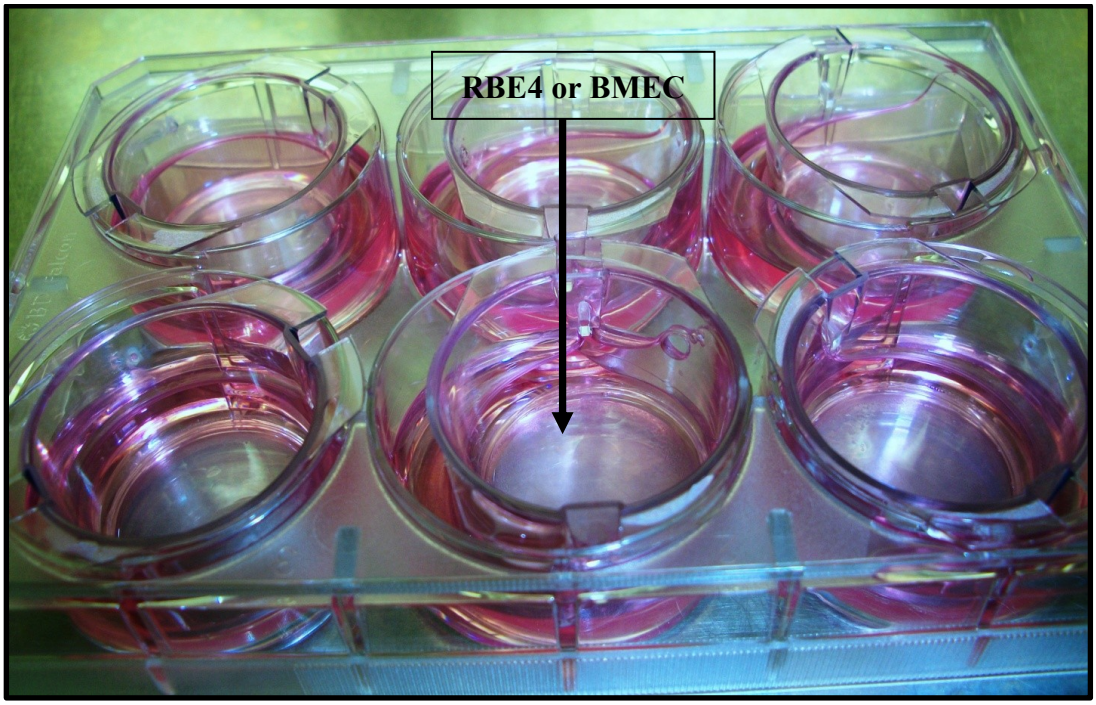

Figure 7 The *in vitro* BBB model. After astrocytes reached 100%confluency on the bottom (abluminal side) of inserts, RBE4 or BMECs were seeded on the top (luminal side) of the membranes to allow for contact between both types of cells and astrocytes in order to induce BBB properties.

Assessments of activity or variation in concentrations of the malathion crossing the BBB in the liquid medium below the insert (abluminal side) were not possible at the low concentrations proposed for use; therefore, an indirect method for assessment of malathion activity was necessary. Malathion is metabolized by cells into its toxic oxidized product malaoxon, which inhibits the activity of acetylcholinesterase, the enzyme that degrades acetylcholine. Since acetylcholinesterase is inhibited by activated malathion, increases in concentrations of the OP in the abluminal side of the model decreases acetylcholinesterase concentrations in the neuronal cells at the bottom of the well giving us an indirect method of assessing malathion concentrations passing through the barrier.

For the assessment of acetylcholinesterase inhibition by malathion in the BBB *in vitro* model, the SH-SY5Ycells were cultured in the bottom of the wells at a starting concentration of 1×10^5 cells per well (Figure 6). SH-SY5Y cells are known to develop neuronal physiological profiles in presence of retinoic acid (Nostrandt and Ehrich, 1992), and have been demonstrated in our laboratory to be a valuable model in the assessment of OP-induced neurotoxic effects (Carlson and Ehrich, 2000; Ehrich and Correll, 1998; Nostrandt and Ehrich, 1992; Pope *et al*., 1995; Rowles *et al*., 1995; Veronesi *et al*., 1997).

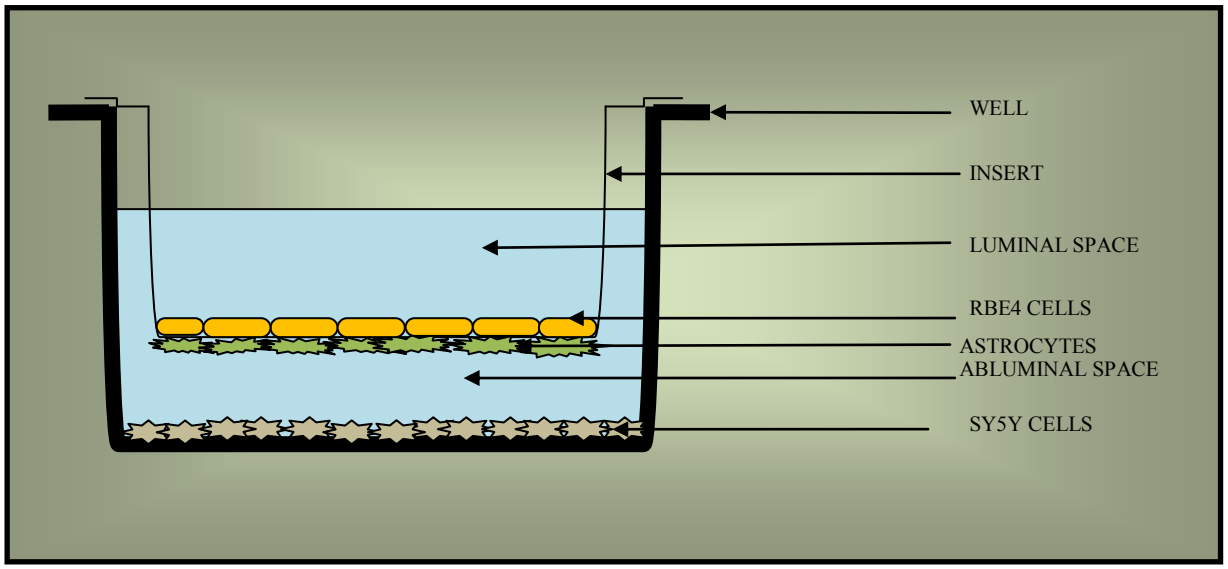

Figure 8 Schematic of an *in vitro* model of the BBB with endothelial (RBE4) cells on the luminal side, astrocytes on the abluminal side, and SY5Y neuroblastoma cells on the bottom of the well mimicking parenchyma.

TREATMENTS

Lead acetate and malathion treatments were assessed. Lead acetate dissolves in water more readily than other inorganic lead salts such as lead chloride or lead nitrate, so this characteristic makes it a better choice for utilizing high concentrations in small volumes. Once the cells of the BBB model were fully confluent, the luminal sides of the inserts were treated with lead concentrations of 1 µM and 10 µM, and malathion (mal) concentrations of 10 µM. A malaoxon (mx) concentration of 1 µM was also assessed to evaluate the capacity of the model to metabolize malathion into its far more toxic metabolite malaoxon. Malathion is converted to its metabolite malaoxon by cytochrome P450 enzymes (Buratti *et al*., 2005). Malaoxon then induces the neurotoxic increases in ACh, therefore, it is reasonable to include measurements of the metabolite in our design as a positive control. These concentrations were chosen because

preliminary data (Balbuena *et al*., 2008; Balbuena *et al*., 2010; Meldrum *et al*., 2007) suggested that these concentrations induce a response in the model without provoking any cytotoxic response. The following combinations were assessed: Pb 1µM, Pb 10µM, mal 10µM, mx 1µM, Pb 1µM + mal 10µM, Pb 1µM + mx 1µM, Pb 10µM + mal 10µM, and Pb 10µM + mx 1µM. A non-treated control was included for comparison (Figure 9).

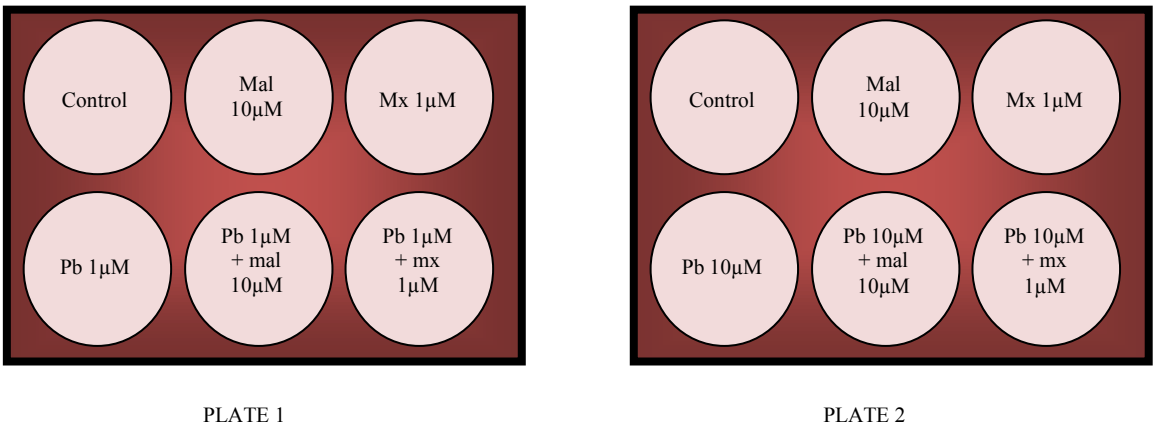

Figure 9 Concentrations of both malathion and lead to be tested using inserts in six-well plates.

Malathion and malaoxon were applied to the luminal side of the inserts. This was followed by incubation at 37°C and 5% CO_2 with 90-95% humidity for 10 hr. After the 10 hr incubation period, lead acetate was applied and inserts were incubated for an additional period of 14 hr. Previous work in our laboratory demonstrated that this period of time was well suited to cause adverse effects on barrier permeability and resistance (Balbuena *et al*., 2008; Balbuena *et al*., 2010; Meldrum *et al*., 2007).

Specific Aim 1: To Evaluate Viability Variations on Cells of the BBB.

VIABILITY OF BBB CELLULAR COMPONENTS USING ADENOSINE 5'-TRIPHOSPHATE (ATP) BIOLUMINESCENT ANALYSIS

For viability assessments of the different types of cells utilized in the construction of the BBB, bioluminescent assessments were performed. These assessments utilized a homogenous method of determining the number of viable cells in culture based on quantitation of the ATP present in these cells. Since only fully metabolically functional cells produce ATP, this method ensures an easy and accurate count of cell viability. The assessment of such an endpoint allowed for the choice of a non-lethal test compound concentration to be used for further experiments. The assessments were performed utilizing the CellTiter-Glo® viability assay, which relies on the properties of a thermostable luciferase that generates a stable luminescent signal and involves the addition of a single reagent (CellTiter-Glo® reagent) directly to cells cultured in serum-supplemented medium. This homogenous "add-mix-measure" format results in cell lysis and generation of a luminescent signal proportional to the amount of ATP present in accordance with the following scheme:

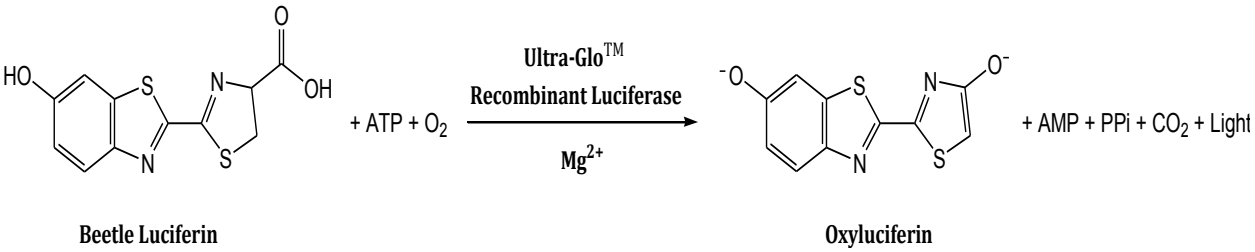

Beetle Luciferin Oxyluciferin

Here, the luciferin is mono-oxygenated by the catalyzation of the Ultra-Glo™ luciferase in the presence of Mg^{2+}, ATP and molecular oxygen. The products of this reaction are oxyluciferin, adenosine monophosphate, carbon dioxide, a pyrophosphate anion, and light. The light generated in this manner is then measured in a spectrophotometer.

For the assay, cells were incubated with treatments for a 24 hr period (as noted in the treatments section), and then samples were tested in 96-well plates according to the protocol provided with the kit. Three controls were prepared in each experiment setup in order to accurately calculate percent cytotoxicity. This included a background control, which provided information about the luminescence of the cell medium alone. There was also a measurement of cells in medium with no treatment, which provided information about ATP production by untreated normal cells (negative control). Finally, a positive control provided information about 100% cell death luminescence; this positive control group was treated with 10% Triton X (TX). Triplicates of treated samples and controls were incubated for 24 hr with 90 µl of medium and 10 µl of treatment compounds or PBS for the controls (Table 1). On the next day, plates were equilibrated to room temperature. Transferring eukaryotic cells from a 37°C incubator to room temperature has little effect on the ATP content (Lundin *et al*., 1986), and the kit recommends cultured cells be allowed to equilibrate to 22°C for up to 2 hr. Our samples were standardized to a one-hour period at room temperature. Each control and treatment group was then mixed with the CellTiter-Glo® reagent mixture from the kit in a 1:1 ratio (Table 1). Plates loaded in accord with Table 2 were placed on an orbital shaker for two minutes to induce cell lysis. After this, plates were incubated at room temperature for and additional ten minutes. After incubation, the luminescence of the samples was measured at 490 nm in a spectrophotometer. To determinate the percentage viability, the averages of the absorbance values of the sample triplicates were

calculated. The average absorbance values of the background control were then subtracted from the sample values by the plate reader operating system software . The resultant number was divided by the negative control values. The final number was then multiplied by 100 according to the following formula to establish percentage viability:

$$\text{Viability (\%)} = \frac{\text{sample value}}{\text{Negative control}} \times 100$$

Contents of the well	Blank (no cells)	Cells Alone	Positive control	Cells with treatments
Medium	90 µl	90 µl	90 µl	90 µl
10% Triton X			10 µl	
PBS	10 µl	10 µl		
Treatments				10 µl
Reaction Mixture	100 µl	100 µl	100 µl	100 µl
Total volume in well	200 µl	200 µl	200 µl	200 µl

Table 1 Well contents of the plate set up for the assessment of luminescence with the total volumes for treatment groups and controls.

	1	2	3	4	5	6	7	8	9	10	11	12
A	$Ma10^{-3}$	$Ma10^{-3}$	$Ma10^{-3}$	$Ma10^{-3}$	Medium	Medium	Medium	Medium	$Pb10^{-3}$	$Pb10^{-3}$	$Pb10^{-3}$	$Pb10^{-3}$
B	$Ma10^{-4}$	$Ma10^{-4}$	$Ma10^{-4}$	$Ma10^{-4}$	$Mx10^{-3}$	$Mx10^{-3}$	$Mx10^{-3}$	$Mx10^{-3}$	$Pb10^{-4}$	$Pb10^{-4}$	$Pb10^{-4}$	$Pb10^{-4}$
C	$Ma10^{-5}$	$Ma10^{-5}$	$Ma10^{-5}$	$Ma10^{-5}$	$Mx10^{-4}$	$Mx10^{-4}$	$Mx10^{-4}$	$Mx10^{-4}$	$Pb10^{-5}$	$Pb10^{-5}$	$Pb10^{-5}$	$Pb10^{-5}$
D	$Ma10^{-6}$	$Ma10^{-6}$	$Ma10^{-6}$	$Ma10^{-6}$	$Mx10^{-5}$	$Mx10^{-5}$	$Mx10^{-5}$	$Mx10^{-5}$	$Pb10^{-6}$	$Pb10^{-6}$	$Pb10^{-6}$	$Pb10^{-6}$
E	$Ma10^{-7}$	$Ma10^{-7}$	$Ma10^{-7}$	$Ma10^{-7}$	$Mx10^{-6}$	$Mx10^{-6}$	$Mx10^{-6}$	$Mx10^{-6}$	$Pb10^{-7}$	$Pb10^{-7}$	$Pb10^{-7}$	$Pb10^{-7}$
F	$Ma10^{-8}$	$Ma10^{-8}$	$Ma10^{-8}$	$Ma10^{-8}$	$Mx10^{-7}$	$Mx10^{-7}$	$Mx10^{-7}$	$Mx10^{-7}$	$Pb10^{-8}$	$Pb10^{-8}$	$Pb10^{-8}$	$Pb10^{-8}$
G	Medium	Medium	Medium	Medium	$Mx10^{-8}$	$Mx10^{-8}$	$Mx10^{-8}$	$Mx10^{-8}$	Medium	Medium	Medium	Medium
H	PosCont	PosCont	PosCont	PosCont	Blank	Blank	Blank	Blank	PosCont	PosCont	PosCont	PosCont

Table 2 96-well plate set up for the ATP Bioluminescent assay for RBE4, astrocytes, and SH-SY5Y cells with the different concentrations of neurotoxicants plus the controls for each cell type. The concentrations of malaoxon, malathion and lead acetate are provided. Medium=cell media with cells, Blank=cell media with no cells, PosCont=medium with 10% Triton X, Mx=malaoxon, Ma=malathion, Pb=lead acetate

Specific Aim 2: To Assess Passage of Neurotoxicant and BBB Integrity After Exposures.

BBB *IN VITRO* MODEL TRANSENDOTHELIAL ELECTRICAL RESISTANCE (TEER)

For the assessment of integrity variations in our *in vitro* BBB models, lead acetate and malathion were tested at the appropriate concentrations established from viability determinations. The first indication of disruption of integrity in the barrier is a reduction in TEER, and therefore, we measured TEER in our BBB *in vitro* models. After treatment, both

sides of the inserts were washed with 2 ml sterilized phosphate buffered saline (PBS) at 37°C and then maintained in 2 ml of this solution until resistance measurements were performed. The measurements took place within 15 minutes, since longer periods negatively affect the resistance of the model. In order to evaluate accurately the TEER of our bilayer co-cultures, the TEER value of a clean insert containing no cells was subtracted from each measurement of the inserts with cell bilayers. The co-culture inserts and the control (clean insert) were placed in the chamber of a tissue resistance measurement volt-ohm-meter (79-ENDOHM-24snap apparatus, World Precision Instruments Inc., Sarasota, FL). Six different measurements were taken from each insert, and the average of these numbers utilized in the final determination of TEER. The device gives the results in ohms, and the resistance is calculated with the following formula:

$$R\ (\Omega cm^2) = (SA - IA) \times K$$

R is the TEER given in ohms per centimeter square (Ωcm^2), SA is the average ohm measurements of the samples, IA is the average ohm measurement of the insert alone and K is a constant representing the physical surface area of the insert that is available for cell culturing. For the inserts utilized in this experiment, the constant (K) was 7.065. To assess concentration-time response effects in TEER, resistance was assessed for all the concentrations after an incubation period of 24 hr. This incubation period was appropriate for our experiments since

prior assessments of organophosphates in our laboratory showed that the 24 hr period induced a response in cell cultures without inducing cell death (Parran *et al*., 2005). In order to provide statistical validation, measurements of three different insert preparations were recorded as in Table 3.

TREATMENT	24 HR		
Pb 1µM			
Pb 10µM			
mal 10µM			
mx 1µM			
Pb 1µM + mal 10µM			
Pb 1µM + mx 1µM			
Pb 10µM + mal 10µM			
Pb 10µM + mx 1µM			
Control			

Table 3 Measurements of TEER for our inserts with different concentrations of neurotoxicants. After a 24 hr incubation period TEER was assessed three times and recorded. Pb = lead, mal = malathion, mx = malaoxon.

ASSESSMENTS OF PASSAGE OF LEAD THROUGH BBB SYSTEMS

Passage of lead acetate through the two different BBB models was determined by graphite furnace atomic absorption, utilizing a Spectra AA 220FS spectrophotometer (Varian Inc., Walnut Creek, CA). A standard curve was constructed using five different concentrations between 50 and 600 μg/l, with 50 μg/l (50 ppb) recognized as the limit of detection. The linearity of the standard curve was demonstrated by correlation coefficients (r^2) of 0.9936 for the samples collected for assays done with RBE4 cells ($y = 0.0014x + 0.0481$) and 0.9886 for assays done with samples collected from incubations with BMECs ($y = 0.0015x + 0.0756$). Duplicate samples variation was established to be less than 3 percent. For the atomic absorption determinations, lead was applied to the luminal side of the inserts, with measurements on media taken from both the luminal and abluminal sides 14 hr after application of the compounds to the systems. Comparisons were made with lead concentrations on media taken from the luminal and abluminal sides of the inserts right after application of treatments (time of application 0, T =0).

ASSESSMENTS OF PASSAGE OF MALATHION/OXON THROUGH BBB SYSTEMS

Gas Chromatography-Mass Spectrometry (GC-MS) was the method used in an attempt to measure concentrations of malathion and malaoxon on either side of the in vitro BBB after 14 hr and 24 hr incubation periods. For these analyses, malathion, malaoxon, and malathion-d_{10} (internal standard) were purchased from Chem Services Inc (West Chester PA). All the solvents used for sample preparation were GC-MS grade (low-residue concentration). Stock solutions

(0.1 M) were prepared in acetonitrile, with standard solutions of malathion and malaoxon (2.5 x 10^{-8} M to 10^{-6} M) prepared in acetone; each contained 10^{-7} M of the internal standard. Standards and experimental samples were purified and concentrated using solid phase extraction (SPE). The SPE cartridge (Waters Oasis HLB, 1 cc, 30 mg; Waters Corp., Milford, MA) was conditioned successively with 1 ml of methanol and 1 ml of water.

Following loading of the samples, the cartridge was washed twice with 1 ml of water and then the OP compounds were eluted with 1.5 ml of ethyl acetate. The ethyl acetate extract was transferred to a 1-dram glass vial and the solvent evaporated under a stream of nitrogen at 25°C with a Pierce Reacti-Therm III unit (Pierce Biotechnology Inc., Rockford, IL). The residue was reconstituted in 100 µl of ethyl acetate and analyzed by GC-MS. An Agilent Technologies 6890 gas chromatograph and a 5973 inert mass spectrometer (Agilent Technologies, Wilmington, DE) were used to carry out the analyses. A capillary column HP5-MS (5% phenyl methyl siloxane) with a length of 30 m, an internal diameter of 0.25 mm, and a film thickness of 0.25 µm was used. The split/splitless injection port was used in splitless mode at 220°C. The oven initial temperature was held for 2 min at 60°C, ramped at 3°C/min up to 200°C, and then ramped at 15°C/min up to 300°C, the temperature being held at 300°C for 3 min. The carrier gas was helium at a constant flow rate of 1.2 ml/min, the transfer line temperature was 250°C, and the injection volume was 2 µl. The spectrometer was used in negative chemical ionization mode.

The source and the quadrupole had a temperature of 150°C and an electron multiplier (EM) voltage of 1624 V was used. The gain factor set at 10 provided a resulting EM voltage of 2176 V. The solvent delay was 14 min, and the acquisition was done in single-ion monitoring mode with low resolution, the dwell time being set at 100 milliseconds. Malathion, malaoxon, and malathion-d_{10} had respective retention times of 17.4, 15.7, and 17.2 min, respectively. At

each concentration, the abundance of the ions m/z 156.9 (mass-over-charge ratio) and m/z 172.0 were added for malathion and the abundance of the ions at m/z 141.0 and m/z 172.0 were added for malaoxon. For malathion-d_{10} (internal standard), the abundance of the ion at m/z 156.9 was measured. The calibration curve was calculated by plotting the ratio of the abundance of the analyte (malathion or malaoxon) over the abundance of the internal standard at each concentration. The calibration curves for malathion and malaoxon provided a correlation coefficient of 0.9994 and a detection limit of 0.05 picomoles with a signal over noise ratio of 5. Coefficients of variation ranged from 11% at the highest concentration of standard to 52% at the lowest concentration of standard after injecting three different standard preparations. The recoveries of the sample extractions ranged from 64 to 110%.

Because the remaining concentrations of the labile OP esters used for these experiments were so minimal that they could not be detected directly by GCMS after the incubation periods, an indirect method for assessment was needed. Since OP compounds irreversibly inhibit the enzyme AChE in exposed cells, assessments of inhibition of this enzyme in a layer of neuroblastoma cells (SH-SY5Y) below the BBB system allowed us to infer the passage of the organophosphates through the BBB models.

ACETYLCHOLINESTERASE DETERMINATION IN SH-SY5Y CELLS

Acetylcholinesterase assessments were performed to assess not only passage of the OP compounds through the *in vitro* barrier systems, but also to determine resistance variations in response to neurotoxicant treatments. Malathion is associated with decreases in TEER and

therefore increases permeability in a BBB *in vitro* model (Balbuena *et al*., 2008; Balbuena *et al*., 2010; Meldrum *et al*., 2007; Parran *et al*., 2005). OP compounds decrease levels of acetylcholinesterase enzyme *in vitro* (Ehrich and Correll, 1998; Gallo and Lawryk, 1991; Nostrandt and Ehrich, 1992; Pope *et al.*, 1995; Rowles *et al*., 1995; Veronesi *et al*., 1997) and *in vivo* (Ehrich *et al*., 1995; Ehrich *et al*., 2004; Jortner *et al*., 2005; Nostrandt *et al*., 1992). These decreases are associated with permeability increases and TEER reductions. This fact combined with the impossibility of measuring OP compound concentrations in the medium available to our BBB system, justified the assessments of acetylcholinesterase inhibition in SH-SY5Y cells under our BBB models in response to lead and malathion treatments.

Cells were collected and resuspended in PBS at a cell concentration of 1×10^7/ml. Acetylcholinesterase assays were performed according to a standard protocol developed by our laboratory (Ehrich *et al*., 1995). This is a spectrophotometric microplate assay for acetylcholinesterase activity with acetylthiocholine as substrate. Hydrolysis of the thiocholine substrate in the presence of enzyme and 5, 5'-dithiobis-(2-nitrobenzoic acid) or DTNB was determined after 30 min, and the production of the characteristic yellow product was assessed at 412 nm wavelength in a spectrophotometer. Accuracy in the measurements over the time-period (30 min) is of importance, since color development is proportional to the time passed. Changes in times of assessments diminish the accuracy of the assay, therefore, all measurements were performed exactly 30 minutes after initiation of the thiocholine substrate hydrolysis.

TIGHT JUNCTION AND SCAFFOLD PROTEIN WESTERN BLOT ANALYSES

As noted in the literature review, high TEER characteristics are the result of induction of tight junctions in the BBB, and any decrease in TEER from treatments with both lead acetate and malathion may be associated with a change in tight junction proteins expression. Endothelial cells respond to induction by astrocytes and some other glial cells creating the structural scaffold that supports tight junction formation. Astrocytes also induce endothelial cells to express the actual proteins that constitute such junction. Therefore, variations in concentration and expression of tight junction proteins and scaffold proteins in the RBE4 cells were assessed.

RBE4 cells were cultured in 100 x 20 mm petri dishes (Becton Dickinson and Company; Franklin Lakes, NJ) from an original concentration of $1x10^5$. Cells were maintained in incubation at 37°C with 5% CO_2 and 90-95% humidity until confluence was reached. Since astrocytes are responsible for inducing tight junction structures in the paracellular space of adjacent endothelial cells, RBE4s were treated with astrocyte-conditioned media for an additional two days to allow the cell monolayer to assemble tight junctions in the paracellular space between cells. After treatment, cells were washed with PBS at 37°C and lysed for five minutes, then the lysed cell solute was collected and centrifugated at 600xg for 10 minutes. The supernatant was collected and the pellet frozen for further re-suspension.

The supernatant containing the denaturized proteins was utilized to perform western blots for tight junction proteins ZO1, ZO2, occludin, and claudin-5 utilizing a method modified from that used in the Prion Biology laboratory of Dr. Willard Eyestone at the Virginia-Maryland Regional College of Veterinary Medicine (Peralta and Eyestone, 2009). Briefly, samples were diluted with Laemmli buffer (Bio-Rad Laboratories, Philadelphia PA), heated at 95°C, and

plated in Criterion® pre-cast gels (Bio-Rad Laboratories). The samples were then run in a Criterion® electrophoresis cell chamber (Bio-Rad Laboratories) for one hour at 200V.

After electrophoresis, the gel was transferred to a cellulose membrane (Bio-Rad Laboratories) in a transfer "sandwich" packet; it was then blotted in a Criterion® blotter tank (Bio-Rad Laboratories) for one hour at 100V. After this, the membrane was blocked and incubated with primary antibodies for the proteins of interest for an additional hour, washed with PBS and incubated again, this time with a secondary antibody for anohter hour. Then, the samples were washed again in PBS before the membrane was read in an Odyssey® Infrared Imaging System (LI-COR® Biosciences, Lincoln, NE). Table 4 gives a schematic representation of the experimental set up for this part of the research.

PROCEDURE	1ST STEP	2ND STEP	3RD STEP	4TH STEP	5TH STEP	6TH STEP
Gel loading	Samples are prepared	Gel is placed in the electrophoresis cell chamber	Chamber is filled with running buffer	Samples and markers are loaded in the gel		
Electrophoresis	The electrophoresis chamber is run for 1 hr at 200V					
Gel wash	Gel is removed from clamping frame	Gel is washed with blotting buffer for 30 min				
Electroblotting (Transfer of protein)	Blotter tank is filled with blotting buffer	Insert cartridge is prepared with sponges and filter paper	Membrane is placed on cartridge	Gel is placed in cartridge	Insert cartridge is placed blotter tank	Blotter tank is run for 1 hr at 100V
Membrane blocking	Membrane is then treated with blocking buffer for 30 min					
Primary Antibody	Membrane is incubated with primary antibody for 1 hr at room temperature					
Membrane wash	Membrane is washed for 5 min	Solution is discarded and membrane washed again for 5 min	Solution is discarded and membrane washed again for 5 min	Solution is discarded and membrane washed again for 5 min		
Secondary Antibody	Membrane is incubated with secondary antibody for 30 min at room temperature					
Membrane wash	Membrane is washed for 5 min	Solution is discarded and membrane washed again for 5 min	Solution is discarded and membrane washed again for 5 min	Solution is discarded and membrane washed again for 5 min	Final membrane wash with PBS	
Membrane Reading	Membrane is scanned to Odyssey imaging system	Image is analyzed and data recorded				

Table 4 Arrangement for the immunoblot gel electrophoresis analysis of tight junction and scaffold proteins for aim 2 of this dissertation research.

REAL-TIME REVERSE TRANSCRIPTION-POLYMERASE CHAIN REACTION ANALYSES FOR EXPRESSION OF TIGHT JUNCTION AND SCAFFOLD PROTEINS GENES

In order to substantiate the results obtained from the western blot analysis, real time reverse transcriptase-polymerase chain reaction (qPCR) analyses of the tight junction proteins cited above were performed. For the treatments, RBE4 cells were grown to confluence from an original concentration of $1x10^5$ in 100 mm x 20 mm cell culture dishes (Sigma-Aldrich). Cells were maintained at 37°C and 5% CO_2 with 90-95% humidity until confluence was reached and then treated with astrocyte-conditioned media for an additional two days. Cells were then treated with malathion for 10 hr before lead was added for an additional 14 hr. After treatments, cells were collected for qPCR as follows:

Total RNA extraction and reverse transcription/cDNA synthesis: Total RNA was extracted utilizing the Total RNA purification RNeasy kit from Qiagen (Valencia, CA). Briefly, cells were lysed with lysis buffer applied directly on the cell culture dishes after washing them with ice-cold PBS; lysates were then homogenized with 70% ethanol utilizing a blunt 20-gauge needle (0.9 mm diameter), and pipetted into RNeasy spin columns and centrifugated. Samples were treated with DNase I in order to digest any genomic DNA that may have been present in the samples and then washed again in the columns. RNA was then eluted directly from the columns with 30 µl of RNase-free water. Concentrations of total RNA were determined for samples with an eppendorf UV/Vis bioPhotometer analysis system (Hamburg, Germany), and then RNAs were stored at -80°C. Reverse transcription synthesis was carried out utilizing the reverse

transcription system from Promega (Madison, WI), processing 1 µg of total RNA per reaction. Briefly, total RNA was incubated at 70°C for 10 minutes and placed on ice.

Reactions were prepared at the following concentrations: 50 ng/µl of total RNA, 50 mM $MgCl_2$, 10X reverse transcription buffer (100 mM Tris-HCl[pH 9.0 at 25°C]; 500 mM KCl; 1% Triton®X-100), 1 mM each dNTP mixture, 1u/µl recombinant RNasin® ribonuclease inhibitor, 50u/µg AMV reverse transcriptase (high concentration), and 0.5 µg of random primers per microgram RNA with Nuclease-free water to a total volume of 20 µl per reaction. Reactions were incubated at room temperature for 10 minutes and then at 42°C for 15 minutes before they were heated at 95°C for 5 minutes. After cooling off, cDNA reactions were stored at -20°C until used.

Quantitative real time polymerase chain reaction: Rattus norvegicus real time oligonucleotide primers for occludin, accession number BC062037, sense 5'-GCCTTTTGCTTCATCGCTTCC-3', antisense 5'-AACAATGATTAAAGCAAAAG-3'; claudin 5, accession number BC082073, sense 5'-GCAGAGGCACCAGAACAG-3', antisense 5'-CAGACACAGCACCAGACC-3'; ZO1, accession number NM_001166266, sense 5'-CTGAAGAGGATGAAGAGTATTACC-3', antisense 5'-TGAGAATGGACTGGCTTGG-3'; ZO 2, accession number BC103479, sense 5'-TGGAGGGGATGGATGATGAC-3', antisense 5'-CGCCGTCCGTATCTTCAAAG-3', and β-actin (as an internal normalizing control) accession number NM_053558, sense 5'-TATCGGCAATGAGCGGTTCC-3', antisense 5'-GTGTTGGCATAGAGGTCTTTACG-3'; were designed with the Beacon Designer™ 7.6 software (Premier Biosoft International, Palo Alto, CA).

Primers were designed to be compatible with the SYBR® Green PCR assays avoiding significant cross homologies and preventing secondary structures that can interfere with SYBR® Green primer extension. Primers were synthesized by Invitrogen and then concentrations of each primer were standardized to 30 µM concentrations. Quantitative real time PCR (qPCR) amplifications were carried out utilizing an iCycler iQ™ optical system (Bio-Rad). The PCR reaction mix was generated by adding 12.5 µl of SYBR® Green Supermix® (Bio-Rad) with 0.25 µl of each primer (forward/reverse), 1 µl of cDNA template, and RNA-free water to a total of 25 µl per reaction. The relative quantification of gene expression was attained utilizing the comparative C_T method (Livak and Schmittgen, 2001).

Specific Aim 3: To Assess TRPC Channel Activity In Response to Neurotoxicity.

TRPC PROTEINS WESTERN BLOT ANALYSES

The first step was to establish the presence of TRPC channels in the membrane of the RBE4 cells and any variations in both TRPC1 and TRPC4 protein in response to neurotoxic assault. Both TRPC1 and TRPC4 subunits are involved in the formation of the TRPC store-operated calcium channels in endothelial cells of the BBB. For this purpose, RBE4 cells were cultured in 100 x 20 mm petri dishes (Becton Dickinson and Company; Franklin Lakes, NJ). Cells were maintained at 37°C and 5% CO_2 with 90-95% humidity until they reached 100%

confluency. RBE4s were treated with astrocyte-conditioned media for an additional two days to allow the cell monolayer to assemble tight junctions in the paracellular space between cells. After treatment, cells were washed with PBS at 37°C and lysed for five minutes, then the lysed cell solute was collected and centrifugated at 600xg for 10 minutes. The supernatant was collected and utilized in the protein determinations of TRPC1 and TRPC4. RBE4 cells protein supernatants were analyzed as described previously for tight junction protein determinations (page 63) and following the set- up provided in Table 4.

REAL-TIME REVERSE TRANSCRIPTION-POLYMERASE CHAIN REACTION ANALYSES FOR EXPRESSION OF TRPC1 AND TRPC4 GENES

qPCR was performed to substantiate the results obtained from the protein blots and to assess any fluctuation in protein expression induced by a neurotoxic response to the compounds tested. qPCR assessments of both TRPC1 and TRPC4 subunits of the TRPC channel family were performed utilizing TRPC1 primer (GeneBank accession number NM_053558), sense 5'-AGGTGAAGGAGGAGAACACCTTG-3', antisense 5'-CCATAAGTTTCTGACAACCGTAGTCC-3'; and TRPC-4 primer (GeneBank accession number AF421364), sense 5'-AATTACTCGTCAACAGGCGGC-3', antisense 5'-CACCACCACCTTCTCCGACTT-3'; and occludin accession number BC062037, sense 5'-GCCTTTTGCTTCATCGCTTCC-3', antisense 5'-AACAATGATTAAAGCAAAAG-3' as a normalizing control. Primers were designed with the Beacon Designer™ 7.6 software (Premier Biosoft International, Palo Alto, CA) and were compatible with the SYBR® Green PCR assays

avoiding significant cross homologies and preventing secondary structures that can interfere with SYBR® Green primer extension.

Total RNA extraction and reverse transcription/cDNA synthesis were performed as described in the methods section for the scaffold and tight junction gene expressions (page 66). For the qPCR amplifications were carried out utilizing an iCycler iQ™ optical system (Bio-Rad). The PCR reaction mix was generated by adding 12.5 µl of SYBR® Green Supermix® (Bio-Rad) with 0.25 µl of each primer (forward/reverse), 1 µl of cDNA template, and RNA-free water to a total of 25 µl per reaction. The relative quantification of gene expression was attained utilizing the comparative C_T method. This method is similar to the standard curve method, except it uses arithmetic formulas to achieve the same result for relative quantitation. The amount of target (sample gene), normalized to an endogenous reference (endogenous gene) and relative to a calibrator (constant), is given by $2^{-\Delta\Delta C}{}_T$, and $\Delta\Delta C_T = \Delta C_{Tq} - \Delta C_{Te}$. In this equations, $\Delta\Delta C_T$ represents the difference between the threshold cycle (C_T) of a target gene amplification (ΔC_{Tq}), and the threshold cycle of the endogenous (reference) gene amplification (ΔC_{Te}) (Livak and Schmittgen, 2001).

STATISTICAL ANALYSES

Regarding measurements of viability, differences in ATP activity for the different treatments was assessed using analysis of variance of balanced repeated measurements with each six-well plate as an experimental unit. Measurements of TEER in our inserts and

acetylcholinesterase inhibition were analyzed utilizing analysis of variance. Balanced repetitions of TEER measurements were utilized.

For immunoblot gel electrophoresis, multiway ANOVA analysis of repetitive samples was utilized with the petri dish containing confluent cells considered the experimental unit. In the case of q-PCR, a logistical calculation analysis was performed from the data obtained from the samples with the same experimental unit utilized for the immunoblotting. ANOVA analyses for all the experiments were followed by a Dunnett's test to identify means of treatments that were significantly different from the mean of the control groups. Differences where the p value was less than 0.05 were considered significant.

Preliminary Findings

Abstract of the poster presented at the 46th Society of Toxicology annual meeting and ToxExpo™ Charlotte, NC. March 2007

TRANSFER OF LEAD ACETATE THROUGH AN IN VITRO BLOOD-BRAIN-BARRIER SYSTEM

B. Meldrum, P. Balbuena, K. Fuhrman, B. Wise, A. Hirani, Y. Lee, M. Ehrich.

Virginia-Maryland Regional College of Veterinary Medicine, Virginia Tech, Blacksburg, VA, USA

Lead –induced neurotoxicity remains a problem for humans and animals. Effects of this heavy metal are dependent on its ability to reach the brain. Transport of lead acetate was examined in an *in vitro* blood-brain barrier (BBB) system consisting of rat endothelial (RBE4) cells and astrocytes. These cells were cultured in minimal essential medium (MEM) with 10% fetal bovine serum and in MEM with 10% heat-inactivated horse serum and placed on the upper and lower sides, respectively, of 0.45 micron pore size inserts coated with collagen type I and placed in six-well plates. Lead acetate in concentrations of 0.1, 1, 10, and 100 micromolar were placed inside the insert, on the endothelial cells. After 14 hours of exposure, electrical resistance of the BBB and lead concentrations in cell culture medium under the barrier were determined. A concentration-related decrease in resistance from the control value 210-390 ohms. cm^2 was seen, with 118-130 ohm.cm^2 measured at the highest lead concentration. Lead (215 ppb) was detected in the medium under the insert of cells exposed to 100 micromolar lead. Separate experiments indicated that RBE4 cells exposed to concentrations as high as 100 micromolar lead still had greater than 90% viability, as indicated by lack of uptake of trypan blue dye. Microscopic visualization of the co-cultures suggested that endothelial cells directly exposed to the lead sustained more damage (indicated by morphological change) as the concentration of lead increased. These experiments indicate that this *in vitro* system has a potential value in studies examining lead transport into the nervous system.

Abstract of the poster presented at the 47th Society of Toxicology annual meeting and ToxExpo™ Seattle WA., March 2008

TRANSFER OF NEUROTOXICANTS (MALATHION AND LEAD ACETATE) IN COMBINATION THROUGH IN VITRO BLOOD-BRAIN BARRIER SYSTEMS

P. Balbuena, B. Meldrum, K. Fuhrman, B. Wise, M. Ehrich
Virginia-Maryland Regional College of Veterinary Medicine, Virginia Tech, Blacksburg, VA

Organophosphate (OP) and lead-induced toxicities remain a problem for humans and animals and combined exposures are a possibility. We previously noted that OP insecticides such as malathion and chlorpyrifos could disturb the integrity of in vitro blood-brain barrier (BBB) systems (Neurotoxicol 26,277; SOT 2007 Abstract 707). The present study examined the possibility that OP exposure could alter the transfer of lead through the BBB. Transport of malathion (10 μM), malaoxon (1 μM) and lead acetate (1 and 10 μM) were examined in systems using rat astrocytes co-cultured with rat endothelial (RBE4) cells or bovine endothelial cells on lower and upper sides, respectively, of 0.45 micron collagen-coated inserts in 6-well plates. The lead was applied above the insert 10 hr after malathion or malaoxon and 14 hr later passages of the OP compounds and lead through the BBB were determined below the insert by esterase inhibition in underlying neuroblastoma cells or by atomic absorption, respectively. Results indicated that the dual treatment could decrease resistance of the BBB containing bovine cells by 7-24% over that noted following treatments with the OP compounds or lead alone. The ratio of lead under the insert compared to that applied to the BBB was higher for the rat endothelial cell-astrocyte co-culture than for the bovine endothelial cell-astrocyte co-culture (>30% and <10%, respectively). Effects of malaoxon on AChE inhibition in neuroblastoma cells under the BBB were greater than those of protoxicant malathion, suggesting limited capability for toxicant biotransformation in these BBB model systems. They do appear to have, however, potential for examining the influence of one neurotoxicant on the transport of another.

Abstract of the poster presented at the 48th Society of Toxicology annual meeting and ToxExpo™ Baltimore, MD. March 2009

A COMBINATION OF NEUROTOXICANTS (MALATHION AND LEAD ACETATE) DISRUPT BLOOD BRAIN BARRIER (BBB) FUNCTION BY REDUCING TIGHT JUNCTION PROTEINS

Pergentino Balbuena, Wen Li and Marion Ehrich

Virginia-Maryland Regional College of Veterinary Medicine,
Virginia Tech, Blacksburg, VA

Induction of neurotoxicity by organophosphorus (OP) compounds and lead remains a problem for both humans and animals because combined exposures in environmental settings occur. We previously noted that OP compounds such as malathion and chlorpyrifos could disrupt BBB integrity using In vitro models (Neurotoxicol 26, 277; SOT 2007 abstract 707), and that a combination of malathion and lead enhanced such disruption (SOT 2008 abstract 2277). The present study examined the possibility that both neurotoxicants alone and in combination disturbed BBB integrity by disrupting tight junction proteins. Rat brain endothelial cells (RBE4s) passages 12-14 were cultured in petri dishes and induced to form tight junctions with astrocyte-conditioned media after confluence. Cells were then exposed to malathion 10 μM, malaoxon 1μM, and lead acetate 1μM and 10 μM alone and in combination for a 24 hr period. OP compounds were applied first, lead was added 10 hr later, and cultures incubated for an additional 14 hr. Then, cells were lysed, collected and centrifugated before western blots were performed to determine total protein expression. Positive controls for tight junction proteins occludin, claudin 1, and zona occludens 1 (ZO1) were included. The results were analyzed utilizing the Odyssey infrared imaging system. Results indicated that occludin was reduced by up to 75% and 80% by 1μM and 10 μM lead acetate respectively, about 60% by malathion 10 μM, and about 84% by malaoxon 1μM. Combinations of both neurotoxicants decreased occludin from70% to 90%. ZO1 was decreased by lead acetate by about 40% and by OP compounds by about 30%; together they decreased ZO1 by about 60%. Claudin 1 was reduced by neurotoxicant

mixtures in about 30%, and by lead alone in about 40%, but not significantly by OP compounds. Results suggest a direct relationship between induction of damage to BBB integrity and a decrease of proteins that form the tight junction in rat brain endothelial cells. In RBE4s, therefore, at least one of the mechanisms that OP compounds and lead utilize to disrupt BBB integrity is by decreasing occludin, claudin 1, and ZO1 tight junction proteins in the barrier.

Key words: blood-brain barrier, *in vitro*, organophosphorus compounds, lead acetate.

Chapter 3: Results

COMPARISON OF TWO BLOOD-BRAIN BARRIER *IN VITRO* SYSTEMS: CYTOTOXICITY AND TRANSFER ASSESSMENTS OF MALATHION/OXON AND LEAD ACETATE

P. Balbuena[1], B. Meldrum[1], W. Li[1], Geraldine Magnin-Bissel[1], and M. Ehrich[1]

[1]Virginia-Maryland Regional College of Veterinary Medicine, Virginia Tech, Blacksburg, VA,

Corresponding author: M Ehrich, Virginia-Maryland Regional College of Veterinary Medicine

1 Duck Pond Drive, Virginia Tech, Blacksburg VA 24061.

Telephone (540) 231-6033; e-mail marion@vt.edu

Abbreviated Title: Transfer of neurotoxicants through *in vitro* BBB systems

*Paper published in Toxicological Sciences 114 (2), 260-271, 2010. Reprinted with permission of the publisher

ABSTRACT

Toxicity and integrity disruption in response to transport through the blood-brain barrier (BBB) of the organophosphates malathion and malaoxon and heavy metal lead acetate were assessed in two in vitro barrier systems. One system was constructed using bovine brain microvascular endothelial cells (BMEC), while the other system was constructed with rat brain microvascular endothelial cells (RBE4); both were cocultured with rat astrocytes. We hypothesized that these models would respond differently to neurotoxic compounds. Concentrations of malathion, malaoxon, and lead acetate between 0.01mM and 1mM were assessed for their capacity to cause cytotoxicity to the astrocytes and endothelial cells utilized to construct the BBB systems, with the least cytotoxic concentrations chosen for transfer assessments of neurotoxicants through the barrier systems. Concentrations of malathion at 10mM, malaoxon at 1mM, and lead acetate at 1 and 10mM were selected. Lead concentrations were measured in media of the abluminal and luminal sides of both systems using graphite furnace atomic absorption at the beginning of the treatment (T0) and 14 h later (T14). Passage of organophosphate compounds was determined utilizing inhibition of acetylcholinesterase enzyme in a neuroblastoma cell line (SH-SY5Y) located below the barrier system. Transendothelial electrical resistance was assessed as a measurement of integrity of the barrier systems, with baseline values higher with the RBE4-astrocyte system than with the BMEC-astrocyte system. Metabolic capability, as measured by esterase activity, was higher in BMECs, which were more likely to retain lead than RBE4 cells. Results suggest that differences in endothelial cell source can affect the outcome of studies on toxicant transfer through in vitro BBB systems.

Key Words: BBB, malathion, malaoxon, lead acetate, endothelial cells, astrocytes, TEER

INTRODUCTION

The blood-brain barrier (BBB) is a selective diffusion barrier formed by specialized endothelial cells lining the cerebral microvessels (Abbott *et al*., 2006; Hawkins and Davis, 2005). The unique interactions of these endothelial cells with cellular components of the central nervous system (CNS), such as astrocytes, pericytes, and neuronal processes, confer upon the barrier its distinctive restrictive properties, characterized by an electrical resistance around 2000 Ωcm^2 *in vivo* and 700 Ωcm^2 *in vitro* and an extremely low permeability to even small ions (Risau and Wolfburg, 1990; Risau *et al*., 1998; Yang and Aschner, 2003). This allows for tight ionic transport regulation through specific transporters and channels, which provide an optimal environment for neuronal function (Abbott *et al*., 2006). Disruptions of BBB permeability are associated with pathological conditions in the CNS, such as ischemic stroke (Brouns and De Deyn, 2009; Kidwell *et al*., 2008; Takenaga *et al*., 2009), traumatic brain injury (Ballabh *et al*., 2004; Lotocki *et al.*, 2009), multiple sclerosis (Hawkins and Davis, 2005; Kirk *et al*., 2003; McQuaid *et al*., 2009), and Alzheimer's disease (Starr *et al*., 2009).

Lead is a recognized neurotoxicant that can disrupt the cerebral capillary endothelial cells forming the BBB, resulting in cerebral hemorrhage and the leakage of proteins (Goldstein *et al*., 1974; Kerper and Hinkle, 1997b; Shi and Zheng, 2007). Lead is capable of entering cells through voltage-gated L-type calcium channels (Legare *et al*., 1998; Sanders *et al*., 2009), through store-operated calcium channels (Kerper and Hinkle, 1997a, b), and through calcium-permeable acid-sensing ion channels (Wang *et al*., 2006). Lead is known to cross the BBB under in vivo conditions (Bradbury and Deane, 1993), but at present, there are no studies that assess lead permeability through an in vitro BBB of endothelial cells cocultured with astrocytes.

The present study examined the effects of two neurotoxic substances, a heavy metal (lead) and an organophosphorus (OP) compound (malathion), on an in vitro BBB. Malathion is a widely used insecticide in agriculture for both crops and animals (Environmental Protection Agency, 2000-2001; Eskenazi *et al*., 1999). Likewise, it is used as an insecticidal spray in many homes around the world, and its presence in environmental settings is well documented (Ehrich, 2005; Gao *et al*., 2009; Hoffman *et al*., 2004). Lead is also ubiquitous as an environmental pollutant (Liu *et al*., 2008) from sources such as lead mining and refining operations (Hernberg, 2000),remodeling older homes containing lead based paints and ingestion of flaking lead paint from decaying homes (Dixon *et al*., 2009; Jacobs *et al*., 2002), automobile exhaust from the use of leaded gasoline for many years (Needleman, 1997), and contaminated water supplies from old plumbing using lead pipes or lead soldering or from grease and oils used on agricultural machinery (Schock *et al*., 2008). Hence, the potential exists for a significant number of individuals to be exposed simultaneously to both these neurotoxicants in a variety of ways. Thus, it was important to use these in vitro models to examine whether there are any potential synergistic or antagonistic effects of these neurotoxicants on one another in crossing the BBB.

OP compounds were chosen for study because at least one OP compound, chlorpyrifos, has been associated with disruptions of BBB permeability in vitro. Parran *et al*. (2005) used a BBB model consisting of bovine brain microvascular endothelial cells (BMEC) and rat astrocytes to assess changes in transendothelial electrical resistance (TEER) in response to chlorpyrifos. Another group utilized rat brain microvascular endothelial cells (RBE4) treated with rat astrocyte-conditioned medium to assess transendothelial permeability in response to

chlorpyrifos treatments (Yang *et al*., 2001). Neither group, however, described the mechanism or mechanisms by which OP compounds disrupt BBB permeability. The efficacy of OP compounds as insecticides resides in their capability to inhibit acetylcholinesterase (AChE), which is involved in the degradation of the neurotransmitter acetylcholine. The importance of capability to inhibit esterases has not been examined as a contributing mechanism to OP-induced disruption of the BBB, which is why both malathion, a protoxicant, and malaoxon, the active esterase inhibitor, were included among the test compounds.

BBB in vitro models have been constructed in the last few years to assess different parameters of molecular transport (Cecchelli *et al*., 2007). These models include endothelial cells from different species, placed in cocultures mostly with rat astrocytes (Hayashi *et al*., 1997; Parran *et al*., 2005) or in monolayers of endothelial cells induced to present BBB characteristics (Perrière *et al.*, 2007; Roux and Couraud, 2005; van Bree *et al*., 1988). Although human brain vascular endothelial cell monolayer models have been created (Cucullo *et al*., 2007; Ishihara *et al*., 2008), the majority of models involve mixed cells of bovine, rat, and porcine origin (Roux and Couraud, 2005), although some research groups have created BBB systems with cells from the same animal species (Nakagawa *et al*., 2009; Perrière *et al*., 2007).

Two techniques are well-established in the construction of in vitro BBB models: The first consists in the seeding of endothelial cell monolayers on a coated membrane. The cells are then induced to develop BBB characteristics such as high TEER and low permeability by feeding them with astrocyte or glial conditioned media (Omidi *et al*., 2008) or by seeding astrocytes or glial cells on a well below the insert (Omidi *et al*., 2008; Perrière *et al*., 2007; Smith *et al*., 2007). The second technique consists of culturing endothelial cells and astrocytes or glial cells on separate sides of a porous membrane allowing them to interact with each other and develop BBB

characteristics (Hayashi *et al*., 1997; Parran *et al*., 2005; Roux and Couraud, 2005). The second technique demonstrates better results in terms of TEER measurements and molecular transport across the barrier (Cecchelli *et al*., 2007; Roux and Couraud, 2005). Gaillard *et al*. (2001) constructed a bilayer BBB model with rat astrocytes and calf endothelial cells on opposite sides of a porous membrane and found that it displayed many characteristics of the BBB, including expression of endothelial cell markers, presence of tight junction proteins, high TEER, and decreased paracellular transport. Later, Parran *et al*. (2005) were able to use a similar model to assess alterations in integrity of the BBB in response to organophosphate treatment. Most recently, Malina *et al.* (2009) were able to assess differences between monolayers, noncontact cocultures, and bilayers on porous artificial membranes utilizing porcine brain endothelial cells and rat astrocytes.

Despite the abundance of BBB models, alterations of the BBB resulting from lead, malathion, and mixtures of these neurotoxicants with the barrier while they are passing through, as well as any disrupting effects they may induce on the permeability of the actual barrier structure, have not been described. These alterations are best studied using in vitro systems, such as the models cited above. In vitro studies are valuable because, in addition to reducing the use of animals, they provide systems by which mechanisms associated with toxicant transfer can be determined.

The purpose of this study was to assess two different models of an in vitro BBB system and the feasibility of measuring permeability changes in the BBB in response to combinations of lead and malathion treatments. One model consisted of rat astrocytes and BMECs on the abluminal and luminal sides, respectively, of a porous collagen-coated membrane. The other model was constructed in a similar manner but utilized a RBE4 instead of the bovine brain

microendothelial cells. We hypothesized that the species differences in endothelial cells would contribute to differences in response after application of the neurotoxicants lead and malathion alone and in combination. Malaoxon, the active metabolite of malathion, was included in order to assess metabolic activity of the different cell types. Most studies of neurotoxicants focus only on one compound. However, under natural conditions, multiple exposures often occur since the two compounds studied here are both commonly present in our environment (Costa, 2008a, b)

MATERIALS AND METHODS

Chemicals. Malaoxon 98.2% pure, malathion standard, malathion-d_{10} standard, chlorpyrifos-oxon 98% pure, and chlorpyrifos 98.2% pure were obtained from Chem Services Inc. (West Chester, PA). Malathion of 94% purity was donated by the American Cyanamid Company, agricultural division (Princeton, NJ). Lead acetate was purchased from Sigma Chemical Company (St Louis, MO).

Animals and cell lines. A Sprague-Dawley pregnant rat (Harlan laboratories, Dublin, VA) was obtained at day 13 of pregnancy and housed in quarantine for 7 days with a 12-h light-dark cycle and free access to water and standard rat chow. At day 21 of pregnancy, the rat was anesthetized and the neonatal pups were surgically removed by Cesarean section. The brains of pups were isolated, meninges were removed, and brain cortices were collected. Astrocytes were isolated from the neonatal cortices utilizing the isolation protocol of Allen et al. (2000) modified to do a wet dissection of the brain cortices. The RBE4 was a gift from the

laboratory of Dr Michael Aschner, Vanderbilt University. The bovine endothelial primary cell culture (BMECs) was obtained from Cell Applications Laboratories (San Diego, CA). SH-SY5Y human neuroblastoma cells were obtained from ATCC Bioresource Center (Manassas, VA).

Viability assay. The cells were seeded at concentrations of 5000 cells per well in 96-well opaque plates overnight and treated with 0.01, 0.1, 1, 10, and100 μM, and 1mM concentrations of malathion, malaoxon, or lead acetate for 24 h. Cells were then assessed for viability with the CellTiter-Glo Luminescent Cell Viability Assay Kit (Promega Corp., Madison, WI). Concentrations chosen for later studies were those providing > 78% viability in all cell types (Table 1).

Construction of the barrier system. RBE4 cells, BMEC, SH-SY5Y cells, and rat astrocytes were cultured in75-cm flasks (VWR International Inc., Bridgeport, NJ) with special media designed to support cell proliferation. RBE4 cultures were kept in 44.5% minimum essential medium (MEM), 44.5% Ham's F10 with glycine or glutamine, 10% fetal bovine serum (FBS), and 1% of a penicillin/streptomycin/amphotericin. B solution, with nonessential amino acid solution to ensure proper proliferation of cells. BMECs were cultured with 80% Dulbecco's modified Eagle's medium, 15% heat-inactivated horse serum, 4% FBS, 1% penicillin/streptomycin/amphotericin B solution, and heparin 1.5nM. SH SY5Y cells were kept in 84% Ham's F12 medium, 14% FBS, 1%- penicillin/streptomycin/amphotericin B solution, and 1% nonessential amino acids solution. Astrocytes were cultured in 75-cm flasks with 89% MEM, 10% horse serum, and 1% of a penicillin/streptomycin/amphotericin B solution. All the cell culture media and reagents were obtained from Mediatech Inc.

(Manassas, VA).

Once the cells reached confluency, the barrier was constructed by plating astrocytes on the abluminal side and endothelial cells on the luminal side of BIOCOAT polyethylene terephthalate(PET) porous membranes or inserts(VWR International Inc.). These inserts have impermeable walls that are higher than the walls of the wells in the plate, so any transfer of materials from inside the insert into the well needs to go through the porous membrane at the bottom of the insert.

Astrocytes were seeded on the abluminal side of these 0.45-μm pore-size collagen-coated inserts at a concentration of 1.6×10^6 cells per insert and were cultured for 7 days on the membranes. After the astrocytes reached confluency, RBE4 cells or BMECs at concentrations of 1.3×10^5 were seeded on the luminal side of these inserts and cultured for an additional 4 days. To replicate the microvascular and parenchymal spaces of the BBB, the inserts were placed in six-well plates (VWR International Inc.) and the neuronal-type cell line SH- SY5Y was cultured on the bottom of the well to mimic neuronal parenchyma. Once all of the cells on the models reached confluency (Fig. 1), the systems were ready for neurotoxicant transfer assessments. Test substances were added to the well of the insert (luminal surface); sampling was done by collecting medium both above and below the insert.

TEER measurements. TEER of both BBB models was assessed with the Millicell-ERS (electrical resistance system) with an EndOhm-6 chamber attachment (Bedford, MA). The results were expressed as Ωcm^2 of cell surface. For the experiments in which neurotoxicants were applied separately, measurements of TEER on the BBB models in response to treatments of lead, malaoxon, and malathion were performed after a 14-h incubation period with the neurotoxicants.

For the experiments in which combinations of the neurotoxicants were applied, the malathion and malaoxon were applied first and the inserts incubated for 10 h before lead acetate was applied and the inserts then were incubated for an additional 14-h period. OP compound exposure caused a time-dependent decrease in electrical resistance in our previous study; the times chosen here are within the relatively stable period of OP-altered resistance demonstrated previously (Parran et al., 2005).

Lead measurements. Passage of lead acetate through the systems was determined by graphite furnace atomic absorption utilizing a Spectra AA 220FS model spectrometer (Varian Inc., Walnut Creek, CA). A standard curve was constructed using five different concentrations between 50 and 600 μg/l, with 50 μg/l (50 ppb) recognized as the limit of detection. The linearity of the standard curve was demonstrated by correlation coefficients (r^2) of 0.9936 for samples collected for assays done with RBE4 cells ($y = 0.0014x + 0.0481$) and 0.9886 for assays done with samples collected from incubations with BMECs ($y = 0.0015x + 0.0756$). Duplicate samples varied < 3%. For these determinations, lead was applied to the luminal side of the inserts, with measurements on media taken from both the luminal and the abluminal side 14 h later. Comparisons were made with lead concentrations on the luminal and abluminal sides of the insert at time of application ($T = 0$).

Measurements of OP passage through the BBB. Gas Chromatography-Mass Spectrometry (GC-MS) was the method used in an attempt to measure concentrations of malathion and malaoxon on either side of the in vitro BBB after a 14- to 24-h incubation period. For these analyses, malathion, malaoxon, and malathion-d_{10} (internal standard) were purchased from Chem Services

Inc. All the solvents used for sample preparation were GC-MS grade (low-residue concentration). Stock solutions (0.1M) were prepared in acetonitrile, with standard solutions of malathion and malaoxon (2.5 x 10^{-8} to 10^{-6}M) prepared in acetone; each contained 10^{-7}M of the internal standard. Standards and experimental samples were purified and concentrated using solid phase extraction (SPE). The SPE cartridge (Waters Oasis HLB, 1 cc, 30 mg; Waters Corp., Milford, MA) was conditioned successively with 1 ml of methanol and 1 ml of water. Following loading of the samples, the cartridge was washed twice with 1 ml of water and then the OP compounds were eluted with 1.5 ml of ethyl acetate. The ethyl acetate extract was transferred to a 1-dram glass vial and the solvent evaporated under a stream of nitrogen at 25°C with a Pierce Reacti-Therm III unit (Pierce Biotechnology Inc., Rockford, IL). The residue was reconstituted in 100 µl of ethyl acetate and analyzed by GC-MS. An Agilent Technologies 6890 gas chromatograph and a 5973 inert mass spectrometer (Agilent Technologies, Wilmington, DE) were used to carry out the analyses. A capillary column HP5-MS (5% phenyl methyl siloxane) with a length of 30 m, a diameter of 0.25 mm, and a film thickness of 0.25 µm was used. The split/splitless injection port was used in splitless mode at 220°C.The oven initial temperature was held 2 min at 60°C, ramped at 3°C/min up to 200°C, and then ramped at 15°C/min up to 300°C, the temperature being held at 300°C for 3 min. The carrier gas was helium at a constant flow rate of 1.2 ml/min, the transfer line temperature was 250°C, and the injection volume was 2 µl. The spectrometer was used in negative chemical ionization mode. The source and the quadrupole had a temperature of 150°C and an electron multiplier (EM) voltage of 1624 V was used. The gain factor set at 10 provided a resulting EM voltage of 2176 V. The solvent delay was 14 min, and the acquisition was done in single-ion monitoring mode with low resolution, the dwell time being set at 100 ms. Malathion, malaoxon, and malathion-d_{10} had respective retention times of

17.4, 15.7, and 17.2 min, respectively. At each concentration, the abundance of the ions m/z 156.9 (mass-over-charge ratio) and m/z 172.0 were added for malathion and the abundance of the ions at m/z 141.0 and m/z 172.0 were added for malaoxon. For malathion-d_{10} (internal standard), the abundance of the ion at m/z 156.9 was measured. The calibration curve was calculated by plotting the ratio of the abundance of the analyte (malathion or malaoxon) over the abundance of the internal standard at each concentration. The calibration curves for malathion and malaoxon provided a correlation coefficient of 0.9994 and a detection limit of 0.05 pmole with a signal over noise ratio of 5. Coefficients of variation ranged from 11% at the highest concentration of standard to 52% at the lowest concentration of standard after injecting three different standard preparations. The recoveries of the sample extractions ranged from 64 to 110%.

Because the remaining concentrations of the labile OP esters used for these experiments were so minimal that they could not be detected directly by GC- MS after the 14- to 24-h incubation period, an indirect method for assessment was needed. Since OP compounds irreversibly inhibit the enzyme AChE in exposed cells, assessments of inhibition of this enzyme in a layer of neuroblastoma cells (SH-SY5Y) below the BBB system allowed us to infer the passage of the organophosphates through the BBB models. A similar system has been used for evaluation of cytotoxicity after toxicant transport through the BBB (Hallier-Vanuxeem et al., 2009). For the experiments where compounds were tested separately, effects of malathion and malaoxon were measured after a 14-h incubation period. When OP compounds and lead were both applied, measurements were performed after a 24-h incubation period. A standard curve that plotted five different malaoxon concentrations against AChE inhibition in SH-SY5Y cells demonstrated linear inhibition between 10^{-10} and

10^{-6}M. This curve matched malaoxon-induced inhibition of AChE in this cell line reported earlier ($r^2 = 0.96$, y = 0.03679-6.175; Ehrich et al., 1997). The ability of endothelial cells to have their esterases inhibited during the passage of OP compounds was assessed by a procedure routinely used in our laboratory (Correll and Ehrich, 1991; Rowles et al., 1995). For these experiments, the ability of both the RBE4 and BMEC to convert the protoxicant chlorpyrifos to the active esterase inhibitor chlorpyrifos-oxon was determined by esterase activity 14 h after exposure. Results were expressed in nanomoles per minute per milligram of enzyme protein and comparisons made utilizing two-way ANOVA.

Statistical analyses. All results are expressed as mean ± SD of three or more individual assays. Data were analyzed utilizing one-way ANOVA, followed by Dunnett's test. Esterase assessments were analyzed by two-way ANOVA, followed by a Bonfferoni posttest. *p* values less than 0.05 were considered to be significant.

RESULTS

Assessment of cytotoxicity for all the cells involved in the construction of the BBB models showed different patterns of toxic effects depending not only on the concentrations of the neurotoxicants but also on the type of cell tested (Table 1). Astrocytes were sensitive to lead but were not notably affected by malathion or malaoxon, although the 92% viability of malaoxon at 10^{-3}M was statistically less than control. BMECs were more sensitive to malathion and malaoxon, with the highest concentration of malaoxon reducing viability almost 100%.

However, lead did not affect BMEC viability at any tested concentration. RBE4 cells were more sensitive to malathion than to malaoxon. Lead reduced RBE4 viability by approximately 10% at the highest concentrations of 10^{-3} and 10^{-4}M. For the neuroblastoma cells (SH-SY5Y), malaoxon was considerably toxic, with the highest concentration of 10^{-3}M reducing cell viability by 97%. Cytotoxic responses of the SH-SY5Y cells to malathion and lead were considerably less than the response to malaoxon. Viability results allowed the selection of feasible nonlethal neurotoxicant concentrations to be tested on our BBB models.

Figure 2 shows the effects that malathion and malaoxon had on BBB resistance. The model with RBE4 cells (Fig. 2A) exhibits a higher baseline TEER when compared to the BMECs (Fig. 2B). Nevertheless, both models demonstrated a concentration-related response to malathion. The passage of malathion through the BBB models was measured using AChE enzyme activity in SH-SY5Y cells at the bottom of the well below the BBB models (Figs. 3A and 3B). Enzyme inhibition in response to malathion in both models demonstrated a relatively similar concentration-response effect. Since malathion is not capable of inhibiting AChE of SH-SY5Y cells at the low concentrations used for these experiments (Barber *et al*., 1999), it can be assumed that conversion of malathion to AChE-inhibiting malaoxon took place in the endothelial cells. When malaoxon was added to the luminal side of the insert, the concentration capable of inhibiting the AChE of the neuroblastoma cells was 20-40% of the original concentration placed above the inserts for both in vitro BBB systems.

Lead also decreased TEER of both models in a concentration- related manner. TEER decreased in response to lead in both the RBE4-astrocyte model (Fig. 4A) and the BMEC-astrocyte model (Fig. 4B). Analysis of lead presence in the abluminal space of both models indicated that both allowed the passage of the metal through the artificial barrier; however, the

RBE4- astrocyte model allowed for a greater quantity of lead to pass when compared with the BMEC-astrocyte model (Fig. 5). After exposure to 10^{-4}M, the lead concentrations in the abluminal fluid of the RBE4 and BMEC in vitro BBB models were 2.5 and 0.9% of the lead loaded, suggesting considerable uptake by the RBE4 + astrocyte and the BMEC + astrocyte cells of the insert over the 14-h incubation period.

Whether one neurotoxicant could affect the passage of another through the BBB systems was examined using malathion 10μM, malaoxon 1μlM, and lead 10 and 1μM. Figure 6 illustrates the differences in passage of lead acetate in both models. The amount of total lead in the luminal side of the barrier at the beginning of the experiments (T = 0) for both models was 1280 ± 342 ppb for the 10μM concentration and 155 ± 11 ppb for the 1μM concentration (Fig. 6A). After the 14-h incubation period, the lead remaining in the luminal side of the RBE4-astrocyte model was 47% less (606 ppb) when 10^{-5}M was applied and 60% less (95 ppb) when the 10^{-6}M concentration was applied (Fig. 6B). Measurements of lead concentrations on the abluminal side of the RBE4-astrocyte model are shown in Figure 6C; about 30% (380 ppb) of the total lead crossed this BBB when10^{-5}M was applied. The total lead crossing the barrier when 10^{-6}M lead was applied was approximately 24% (37 ppb).

In the case of the BMEC-astrocyte BBB model, after the 14-h period, the lead remaining in the luminal side was about 78% less (280 ppb) than at T = 0 after application of 10^{-5}M lead and 53% less (73 ppb) after application of the 10^{-6}M lead. (Fig. 6D). Measurements of lead in media of the abluminal side of this BMEC-astrocyte model indicated that from the total lead at T = 0, only 5% (70 ppb) and 20% (31 ppb) crossed the barrier when 10^{-5} or 10^{-6}M lead were applied, respectively (Fig. 6E). From this, we can infer that both the RBE4 and the BMEC BBB models allowed for the transfer of both neurotoxicants. However, for lead at 10^{-5}M, the BMEC

BBB model retained significantly more lead in the cells forming the system than the RBE4 BBB model, 73 versus 18% of total lead applied, respectively. For lead at 10^{-6}M, both BBB models retained about the same amount of lead in the cells forming the system (about 34%).

Both BBB models registered significant decreases in TEER in response to treatments of combined neurotoxicants, although, in contrast to the treatments with the compounds alone, the response did not follow a concentration response (Fig. 7). With the RBE4-astrocyte system (Fig. 7A), all the combinations decreased the TEER when compared to the control. The combination of 10^{-5}M lead and 10^{-5}M malathion decreased the TEER by about 30%, which was less than seen with separate treatments. As expected, malaoxon reduced TEER the most; however, the combination with lead at 10^{-6}M did not reduce TEER more than it did with the separate treatments. With the BMEC-astrocyte model (Fig. 7B), treatments decreased the TEER, but only malaoxon 10^{-6}M had effects greater than the others.

Passage of the malathion and malaoxon through the barrier is represented in Figure 8 by showing inhibition of AChE enzyme in SH-SY5Y cells underneath the BBB models. Inhibition of AChE in the RBE4-astrocyte BBB model was present when OP compounds were given alone and in combinations with lead (Fig. 8A), but the differences among treatments were not statistically significant. The effects were less notable in the BBB model utilizing BMECs and astrocytes (Fig. 8B), although malathion and malaoxon exhibited 40 and 80% enzyme inhibition, respectively. These results suggested a difference in capacity of the endothelial cells utilized to construct these BBB models in their ability to metabolize malathion into malaoxon.

The capability of the RBE4 and BMEC cells to oxidize OP compounds to active esterase inhibitors was examined by assessing activity of two esterases found in nonneuronal cells, carboxylesterase (CBX) and neuropathy target esterase (NTE). These were measured in control cells

and in cells treated with the OP compound chlorpyrifos and its active esterase-inhibitory analog chlorpyrifos-oxon, as these particular OP compounds inhibit both these enzymes (Richardson, 1995). The RBE4 cells (Fig. 9A) had less CBX and NTE enzymatic activity when compared to the BMEC (Fig. 9B). The CBX present in the RBE4 cells is only about 25% of the amount of CBX present in the BMEC. The NTE present in the RBE4 is about 20% of that present in the BMEC. Chlorpyrifos-oxon reduced both the CBX and the NTE levels significantly in RBE4 cells; chlorpyrifos was successfully converted into its oxygen analog by the RBE4 cells as confirmed by its inhibition of both CBX and NTE to levels comparable to those of chlorpyrifos-oxon (Fig. 9A). This suggests sufficient monooxygenase enzymes to metabolize the compound. There is inhibition of both esterases in the BMEC in response to chlorpyrifos-oxon (Fig. 9B); however, this inhibition is statistically significant only for the highest concentrations tested. BMECs were not able to metabolize chlorpyrifos into chlorpyrifos-oxon as the inhibition of CBX and NTE was not statistically significant when compared to the control values (Fig. 9B).

DISCUSSION

Although the in vitro models of the BBB represent viable systems for molecular transport and TEER measurements, most of them are constructed with cells from different animals. Since *in vitro* BBB models have value in pharmacological and toxicological assessments (de Boer *et al*., 2003), there is a need to establish any differences that may exist in these models when responding to treatments with neurotoxicants. This study provides a comparison of neurotoxicant transport in BBB models using cocultures of endothelial cells and astrocytes from similar and different species.

Furthermore, effects on sequential exposure to two neurotoxicants were compared.

It is important to determine concentrations of test agents that cause cell toxicity because an increase in barrier permeability will occur when endothelial cells die. However, BBB disruption can also occur at nonlethal concentrations of test agents. In our initial studies, viability of the cell types utilized in our BBB models depended on the neurotoxicants and their concentrations. Differences noted included the sensitivity of both BMEC and SH-SY5Y cells to malaoxon, which may be related to the activities of esterases in these cells. The BMECs were also the only cells not affected by lead at any concentration tested, suggesting the presence of mechanisms within the cell to reduce the negative effects of lead on cellular function. Alternatively, these cells may lack enzyme systems that are sensitive to lead and therefore appear to be more resistant to the metal (Goyer and Clarkson, 2001). The RBE4 endothelial cells, on the other hand, were affected by lead in all but the lowest concentration tested. As expected from the literature, astrocytes used in the BBB model were especially sensitive to lead (Lindahl *et al*., 1999; Tiffany-Castiglione *et al*., 1989; White *et al*., 2007).

Endothelial cells perform similar functions as part of the tridimensional structures to which they belong. Indeed, when isolated from these biological structures, they maintain their unique morphological characteristics. Nevertheless, if they have different origins, they may react differently in vitro. Both endothelial cell types in this experiment, the RBE4 cells and the BMECs, responded differently to cytotoxic insults from lead, malathion, and malaoxon. BBB models constructed with these cells, therefore, were expected to respond differently when BBB integrity and transfer of compounds through the barrier were assessed. This was, indeed, noted.

When the BBB models were exposed to the lead and malathion-oxon treatments, both

decreased TEER measurements in a concentration-related manner. However, differences in basal TEER, transport of lead, and capability to activate OP compounds to esterase inhibitory analogs were noted. The model constructed with RBE4 cells had higher TEER measurements than the system constructed with BMEC, which is somewhat unusual because higher TEER has been reported when primary BMECs are used (Deli *et al*., 2005; Reinhardt and Gloor, 1997). That both the RBE4 cells and the astrocytes were of rat origin may have contributed to the results seen.

In the present experiments, OP compounds were transported similarly but lead transport differed through the two BBB systems. The RBE4 model allowed more lead alone to pass through than the BMEC model, and the BMEC model tolerated higher concentrations while retaining more of the metal. Reasons for these differences are unclear at present. When the BBB models were exposed to both OP compounds and lead, concentrations of lead in the abluminal side of the RBE4 model were more than five times that of the lead found in the abluminal side of the BMECs model. Lead in the luminal side of the RBE4 cells was twice as much that of the lead found in the luminal side of the BMECs model. The RBE4 model therefore allowed more lead to pass through the barrier while at the same time retaining more of the metal in the luminal space. This suggests sequestering of lead in the BMEC model. This lead retention by the system, however, did not protect the model from changes in TEER. The retention of lead by BMECs is of special interest because lead retention is associated in vivo with interactions of the metal with calcium-dependent signaling pathways that contribute to alterations in vascular resistance, hypertension, and cellular inflammation (Navas-Acien *et al*., 2007; Vaziri, 2008).

Although comparison of in vitro and in vivo results can only be done with utmost caution, it is worth noting that the passage of lead through the in vitro BBB barriers (2.5 and 0.09% for

RBE4 and BMEC systems, respectively, after 10^{-4}M application) compares with the plateau of uptake of ^{203}Pb into the cerebral spinal fluid (0.05 ml/g or 5%) reported by Bradbury and Deane (1993) after its continuous iv administration to anesthetized rats.

We noted that levels of inhibition of AChE by OP compounds alone and in combination with lead were higher in the RBE4 model than in the BMEC model, suggesting a higher capacity of the rat endothelial cells to metabolize malathion into malaoxon. We also noted differences in basal activity of two other esterases, CBX and NTE. This may be indicative of either a higher amount of monooxygenases or a lesser quantity of carboxylesterase enzymes in the RBE4 cells. Historically, xenobiotic biotransformation is more likely to occur in primary cells than in cell lines because cell lines generally lose capability to biotransform such compounds (Donato *et al*., 2008). Nevertheless, the RBE4 line has been known to maintain higher levels of xenobiotic metabolic activity when compared to rat cerebrovascular endothelial cell primary cultures, even after 20 passages (Chat *et al*., 1998).

The results provided in these experiments demonstrate that even though brain microvessel endothelial cells of the BBB from different species shared many characteristics at the molecular and cellular level (Deli *et al*., 2005), they respond differently when associated with rat astrocytes. Both our models were capable of producing measurable responses in the presence of neurotoxicants alone and in combination. However, metabolic activities, quantities of neurotoxicants transferred, and sensitivity to test compounds differed between BMEC and RBE4 cells. Nevertheless, the models have utility for assessments of TEER. More research is needed, however, in order to elucidate specific mechanisms associated with the differences between endothelial cells and the contribution this makes to the passage of OP compounds and lead

through the BBB

FUNDING

Virginia-Maryland Regional College of Veterinary Medicine

ACKNOWLEDGMENTS

The authors thank technicians Kristel Furhman and Barbara Wise for their help and technical support and Anjali Hirani and Xiaohua Wu for assistance with astrocyte isolations.

REFERENCES

Abbott, N. J., Ronnback, L., and Hansson, E. (2006). Astrocyte-endothelial interactions at the blood- brain barrier. *Nature Reviews, Neuroscience*. **7,** 41-53.

Allen, J. W., Mutkus, L. A., and Aschner, M. (2000). Isolation of neonatal rat cortical astrocytes for primary cultures. In Current Protocols in Toxicology volume 2 (M. D. Maines, L. G. Costa, E. Hodgson, D. J. Reed, and I. G. Sipes, Eds.), pp. 12.4.1-12.4.15. John Wiley & Sons, Inc., New Jersey.

Ballabh, P., Braun, A., and Nedergaard, M. (2004).The blood-brain barrier: An overview structure, regulation, and clinical implications. *Neurobiology of Disease*. **16,** 1-13.

Barber, D., Correll, L., and Ehrich, M. (1999). Comparative effectiveness of organophosphorus protoxicant activating systems in neuroblastoma cells and brain homogenates. J. *Toxicol. Environ. Health.* 57, 63-74.

Bradbury, M. W. B., and Deane, R. (1993). Permeability of the blood-brain barrier to lead. *Neurotoxicology* 14, 131-136.

Brouns, R., and De Deyn, P. P. (2009). The complexicity of neurobiological processes in acute ischemic stroke. *Clinical Neurology and Neurosurgery*. **111,** 482-495.

Cecchelli, R., Berezowski, V., Lundquist, S., Culot, M., Renftel, M., Dehouck, M. P., and Fenart, L. (2007). Modeling of the blood-brain barrier in drug discovery and development. *Nature Reviews: Drug Discovery*. **6,** 650-661.

Chat, M., Bayol-Denizot, C., Suleman, G., Roux, F., and Minn, A. (1998). Drug metabolizing enzyme activities and superoxide formation in immortalized rat brain endothelial cells. *Life Sciences*. **62,** 151-163.

Correll, L., and Ehrich, M. (1991). A microassay method for neurotoxic esterase determinations. *Fundamental and Applied Toxicology.* **16,** 110-116.

Costa, D. L. (2008). Air pollution. In Casarett and Doull's Toxicology, The Basic Science of Poisons (C. D. Klaassen, Ed.), 7th ed., pp. 1119-1156. McGraw-Hill, New York.

Costa, L. G. (2008). Toxic effects of pesticides. In Casarett and Doull's Toxicology, The Basic Science of Poisons (C. D. Klaassen, Ed.), 7th ed., pp. 883-930. McGraw-Hill, New York.

Cucullo, L., Hossain, M., Rapp, E., Manders, T., Marchi, N., and Janigro, D. (2007). Development of a humanized *in vitro* blood-brain barrier model to screen for brain penetration of antiepileptic drugs. *Epilepsia*. **48,** 505-516.

de Boer, A. G., van der Sandt, I. C. G., and Gaillard, P. J. (2003). The role of drug transporters at the blood-brain barrier. *Annual Review of Pharmacology and Toxicology*. **43,** 629–656.

Deli, M. A., Abraham, C. S., Kataoka, Y., and Niwa, M. (2005). Permeability studies on *in vitro* blood-brain barrier models: Physiology, pathology, and pharmacology. *Cellular and Molecular Neurobiology*. **25,** 59-127.

Dixon, S. L., Gaitens, J. M., Jacobs, D. E., Strauss, W., Nagaraja, J., Pivetz, T., Wilson, J. W., and Ashley, P. (2009). Exposure of U.S. children to residential dust lead, 1999-2004: II. The contribution of lead- contaminated dust to children's blood lead levels. Environ. *Health Perspect*. 111, 468-474.

Donato, M.T., Lahoz, A., Castell, J. V., and Gomez-Lechon, M. J. (2008). Cell lines: A tool for *in vitro* metabolism studies. *Current Drug Metabolism*. **8,** 1-11.

Ehrich, M. (2005). Organophosphates. In: Encyclopedia of Toxicology volume 2 (P. Wexler, ed.), pp. 308-311. Academic Press, San Diego.

Ehrich, M., Correll, L., and Veronesi, B. (1997). Acetylcholinesterase and neuropathy target esterase inhibitions in neuroblastoma cells to distinguish organophosphorus compounds causing acute and delayed neurotoxicity. *Fundam. Appl. Toxicol*. 38, 55-63.

Environmental Protection Agency. (2000-2001). Pesticide Market Estimates. Pesticide Industry Sales webpage. Available at: http://www.epa.gov/oppbead1/pestsales/01pestsales/table_of_contents2001_2.htm. Accessed August 10, 2009.

Eskenazi, B., Bradman, A., and Castorina, R. (1999). Exposure of children to organophosphate pesticides and their potential adverse health effects. Environ. Health Perspect. 107, 409-419.

Gaillard, P. J., Voorwinden, L. H., Nielsen, J. L., Ivanov, A., Atsumi, R., Engman, H., Ringbom, C., de Boer, A.G., and Breimer, D.D. (2001). Establishment and functional characterization of an *in vitro* model of the blood-brain barrier, comprising a co-culture of brain capillary endothelial cells and astrocytes. *European Journal of Pharmaceutical Sciences*. **12,** 215-222.

Gao, J., Liu, L., Liu, X., Zhou, H., Lu, J., Huang, S., and Wang, Z. (2009). The occurrence and spatial distribution of organophosphorus pesticides in Chinese surface water. *Bull. Environ. Contam. Toxicol*. 82, 223-229.

Goldstein, G.W., Asbury, A. K., and Diamond, I. (1974). Pathogenesis of lead encephalopathy: Uptake of lead and reaction of brain capillaries. *Archives of Neurology.* **31,** 382-383.

Goyer, R. A., and Clarkson, T. W. (2001). Toxic effects of metals. In Casarett and Doull's Toxicology, The Basic Science of Poisons (C. D. Klaassen, Ed.), 6th ed., pp. 811-867. McGraw-Hill, New York.

Hallier-Vanuxeem, D., Prieto, P., Culot, M., Diallo, H., Landry, C., Tahti, H., and Cecchelli, R. (2009). New strategy for alerting central nervous system toxicity: integration of blood-brain barrier toxicity and permeability in neujrotoxicity assessment. *Toxicol. in Vitro*. 23, 447-453.

Hawkins, B. T., and Davis, T. P. (2005). The blood-brain barrier/neurovascular unit in health and disease. *Pharmacological Reviews*. **57,** 173-185.

Hayashi, Y., Nomura, M., Yamagishi, S., Harada, S., Yamashita, J., and Yamamoto, H. (1997). Induction of various blood-brain barrier properties in non-neuronal endothelial cells by close apposition to co-cultured astrocytes. *Glia*. **19,** 13-26.

Hernberg, S. (2000). Lead poisoning in a historical perspective. Am. J. Ind. Med. 38, 244-254.

Hoffman, R. S., Capel, P. D., and Larson, S. J. (2004). Comparison of pesticides in eight U.S. urban streams. Environ. Toxicol.Chem. 19, 2249-2258.

Ishihara, H., Kubota, H., Lindberg, R. L., Leppert, D., Gloor, S. M., Errede, M., Virgintino, D., Fontana, A., Yonekawa, Y., and Frei, K. (2008). Endothelial cell barrier impairment induced by glioblastomas and transforming growth factor β2 involves matrix metalloproteinases and tight junction proteins. *Journal of Neuropathology and Experimental Neurology*. **67,** 435-448.

Jacobs, D. E., Clickner, R. P., Zhou, J. Y., Viet, S. M., Marker, D. A., Rogers, J. W., Zeldin, D. C., Broene, P., and Friedman, W. (2002). The prevalence of lead-based hazards in U.S. housing. *Environ. Health Perspect*. 110, A599-A606.

Kerper, L. E., and Hinkle, P. M. (1997a). Lead uptake in brain capillary endothelial cells: Activation by calcium store depletion. *Toxicology and Applied Pharmacology.* **146,** 127-133.

Kerper, L. E., and Hinkle, P. M. (1997b). Cellular uptake of lead is activated by depletion of intracellular calcium stores. *The Journal of Biological Chemistry.* **272,** 8346-8352.

Kidwell, C. S., Latour, L., Saver, J. L., Alger, J. R., Starkman, S., Duckwiler, G., Jahan R., Vinuela, F., Kang, D. W., and Warach, S. (2008). Thrombolytic toxicity: Blood-brain barrier disruption in human ischemic stroke. *Cerebrovascular Diseases*. **25,** 338-343.

Kirk, J., Plumb, J., Mirakhur, M., and McQuaid, S. (2003). Tight junctional abnormality in multiple sclerosis white matter affects all calibres of vessel and is associated with blood-brain barrier leakage and active demyelination. *The Journal of Pathology*. **201,** 319-327.

Legare, M. E., Barhoumi, R., Hebert, E., Bratton, G. R., Burghardt, R. C., and Tiffany-Castiglioni, E. (1998). Analysis of Pb^{2+} entry into cultured astroglia. *Toxicological Sciences.* **46,** 90-100.

Lindahl, L. S., Bird, L., Legare, M. E., Mikeska, G., Bratton, G. R., and Tiffany-Castiglione, E. (1999). Differential ability of astroglia and neuronal cells to accumulate lead: Dependence on cell type and on degree of differentiation. *Toxicological Sciences.* **50,** 236-243.

Liu, J., Goyer, R. A., and Waalkes, M. P. (2008). Toxic effects of metals. In Casarett and Doull's Toxicology, The Basic Science of Poisons (C. D. Klaassen, Ed.), 7th ed., pp. 931-979. McGraw-Hill, New York.

Lotocki, G., Vaccari, J. P. de R., Perez, E. R., Sanchez-Molano, J., Furones-Alonso, O., Bramlett, H. M., and Dietrich, W. D. (2009). Alterations in blood-brain barrier permeability to large molecules and leukocyte accumulation after traumatic brain injury: Effects of post-traumatic hypothermia. *Journal of Neurotrauma*. **26,** 1123-1134.

Malina, K. C., Cooper, I., and Teichberg, V. I. (2009). Closing the gap between the *in vivo* and *in vitro* blood-brain barrier tightness. *Brain Research*. **1284,** 12-21.

McQuaid, S., Cunnea, P., McMahon, J., and Fitzgerald, U. (2009). The effects of blood-brain barrier on glial cell function in multiple sclerosis. *Biochemical Society Transactions*. **37,** 329-331.

Nakagawa, S., Deli, M. A., Kawaguchi, H., Shimizudani, T., Shimono, T., Kittel, A., Tanaka, K., and Niwa, M. (2009). A new blood-brain barrier model using primary rat brain endothelial cells, pericytes and astrocytes. *Neurochemistry International.* **54,** 253-263.

Navas-Acien, A., Guallar, E., Silbergeld, E. K., and Rothenberg, S. J. (2007). Lead exposure and cardiovascular disease: A systematic review. *Environmental Health Perspectives.* **115,** 472-482.

Needleman, H. L. (1997). Clamped in a straitjacket: the insertion of lead into gasoline. Environ. Res. 74, 95-103.

Omidi, Y., Barar, J., Ahmadian, S., Heidari, H. R., and Gumbleton, M. (2008). Characterization and astrocytic modulation of system L transporters in brain microvasculature endothelial cells. *Cell Biochemistry and Function*. **26,** 281-391.

Parran, D. K., Magnin, G., Li, W., Jortner, B. S., and Ehrich, M. (2005). Chlorpyrifos alters functional integrity and structure of an *in vitro* BBB model: Co-cultures of bovine endothelial cells and neonatal rat astrocytes. *Neurotoxicology.* **26,** 77-88, 291.

Perrière, N., Yousif, S., Cazaubon, S., Chaverot, N., Bourasset, F., Cisternino, S., Declèves, X., Hori, S., Terasaki, T., Deli, M., Scherrmann, J. M., Temsamani, J., Roux, F., and Couraud, P. O. (2007). A functional *in vitro* model of rat blood-brain barrier for molecular analysis of efflux transporters. *Brain Research*. **1150,** 1-13.

Reinhardt, C. A., and Gloor, S. M. (1997). Co-culture blood-brain barrier models and their use for pharmacotoxicological screening. *Toxicology in Vitro*. **11,** 513-518.

Richardson, R. J. (1995). Assessment of the neurotoxic potential of chlorpyrifos relative to other organophosphorus compounds: A critical review of the literature. *Journal of Toxicology and Environmental Health*. **44,** 135-165.

Risau, W., Esser, S., and Engelhardt, B. (1998). Differentiation of blood-brain barrier endothelial cells. *Pathologie-biologie*. **46,** 171-175.

Risau, W., and Wolfburg, H. (1990). Development of the blood-brain barrier. *Trends in Neurosciences*. **13,** 174-178.

Roux, F., and Couraud, P. O. (2005). Rat brain endothelial cell lines for the study of blood-brain barrier permeability and transport functions. *Cellular and Molecular Neurobiology*. **25,** 41-58.

Rowles, T., Song, X., and Ehrich, M. (1995). Identification of endpoints affected by exposure of human neuroblastoma cells to neurotoxicants at concentrations below those that affect cell viability. *In Vitro Toxicology*. **8,** 3-13.

Sanders, T., Liu, Y., Buchner, V., and Tchounwou, P. B. (2009). Neurotoxic effects and biomarkers of lead exposure: A review. *Reviews on Environmental Health*. **24,** 15-45.

Schock, M. R., Hyland, R. N., and Welch, M. M. (2008). Occurrence of contaminant accumulation in lead pipe scales from domestic drinking-water distribution systems. *Environ. Sci. Technol.* 42, 4285-4291.

Shi, L. Z., and Zheng, W. (2007). Early lead exposure increases the leakage of the blood-cerebrospinal fluid barrier *in vitro*. *Human & Experimental Toxicology.* **26,** 159-167.

Smith, M., Omidi, Y., and Gumbleton, M. (2007). Primary porcine brain microvacular endothelial cells: Biochemical and functional characterization as a model for drug transport and targeting. *Journal of Drug Targeting*. **15,** 253-258.

Starr, J. M., Farrall, A. J., Armitage, P., McGurn, B., and Wardlaw, J. (2009). Blood-brain barrier permeability in Alzheimer's disease: A case-control MRI study. *Psychiatry Research: Neuroimaging.* **171,** 232-241.

Takenaga, Y., Takagi, N., Murotoni, K., Tanonaka, K., and Takeo, S. (2009). Inhibition of Src activity decreases tyrosine phosphorylation of occludin in brain capillaries and attenuates increase in permeability at the blood-brain barrier after transient focal cerebral ischemia. *Journal of Cerebral Flow and Metabolism*. **29,** 1099-1108.

Tiffany-Castiglione, E., Sierra, E. M., Wu, J. N., and Rowles, T. K. (1989). Lead toxicity in neuroglia. *Neurotoxicology.* **10,** 417-443.

Van Bree, J. B., Audus, K. L., and Borchardt, R. T. (1988). Carrier-mediated transport of baclofen across monolayers of bovine brain endothelial cells in primary culture. *Pharmaceutical Research.* **5,** 369-371.

Vaziri, N. D. (2008). Mechanisms of lead-induced hypertension and cardiovascular disease. *American Journal of Physiology, Hearth and Circulatory Physiology.* **295,** H454-H465.

Wang, W., Duan, B., Xu, H., Xu, L., and Xu, T. (2006). Calcium-permeable acid-sending ion channel is a molecular target of the neurotoxic metal ion lead. *The Journal of Biological Chemistry*. **281,** 2497-2505.

Wang, W., Duan, B., Xu, H., Xu, L., and Xu, T. (2006). Calcium-permeable acid-sending ion channel is a molecular target of the neurotoxic metal ion lead. *J. Biol. Chem*. 281, 2497-2505.

White, L. D., Cory-Slechta, D. A., Gilbert, M. E., Tiffany-Castiglione, E., Zawia, N. H., Virgolini, M., Rossi-George, A., Lasley, S. M., Qian, Y. C., and Basha, M. R. (2007). New and evolving concepts in the neurotoxicology of lead. *Toxicology and Applied Pharmacology.* **25,** 1-27.

Yang, J., and Aschner, M. (2003). Developmental aspects of blood-brain barrier (BBB) and rat brain endothelial (RBE4) cells as *in vitro* models for studies on chlorpyrifos transport. *Neurotoxicology.* **24,** 741-745.

Yang, J., Mutkus, L. A., Summer, D., Stevens, J. T., Eldridge, J. C., Strandhoy, J. W., and Aschner, M. (2001). Transendothelial permeability of chlorpyrifos in RBE4 monolayers is modulated by astrocyte-conditioned medium. *Molecular Brain Research*. **97,** 43-50.

TABLES AND FIGURES

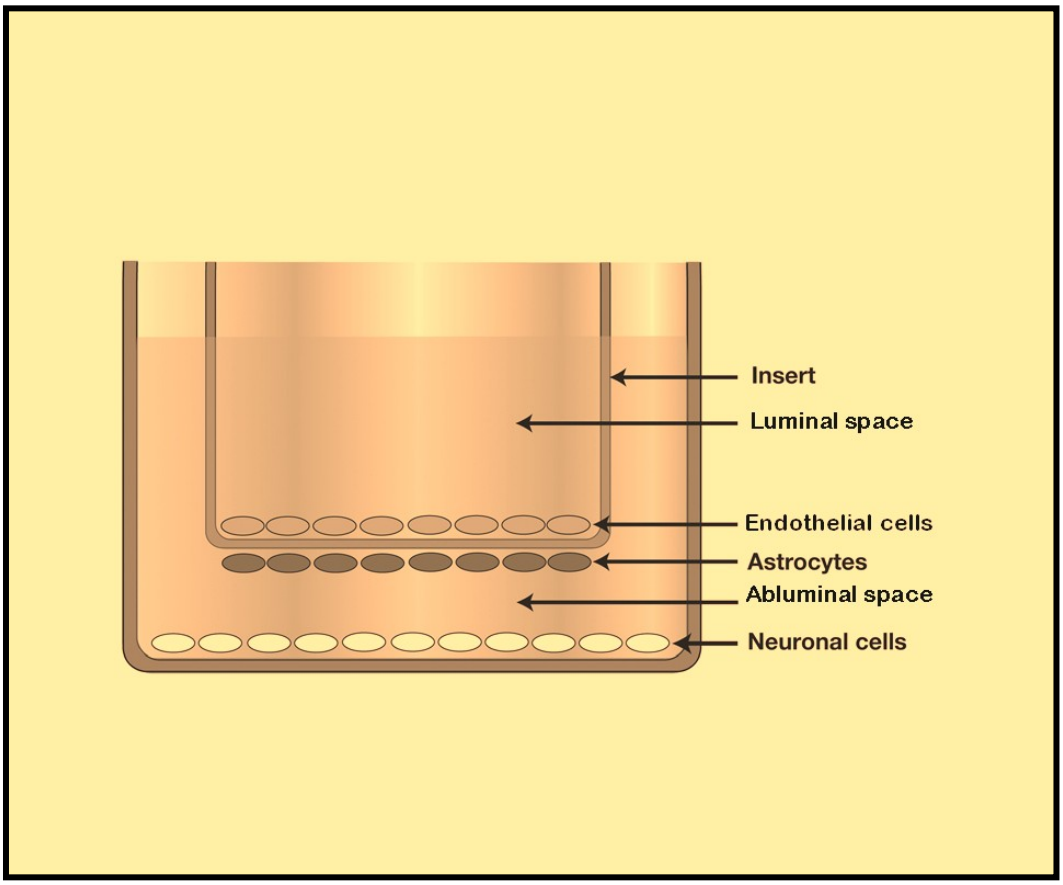

Figure 1 Schematic of the *in vitro* model of the BBB. Endothelial (RBE4 or BMEC) cells were plated on the luminal side and astrocytes on the abluminal side of a polyethylene terephthalate (PET) porous membrane coated with collagen I. SH-SY5Y neuroblastoma cells were seeded at the bottom of the well to mimic parenchyma. Astrocytes were plated first and left to attach to the membrane for 7 days, before endothelial cells were seeded on the luminal side of the membrane.

Table 1. Assessment of cytotoxicity in cells of the blood-brain barrier *in vitro* models.

	10^{-3} M	10^{-4} M	10^{-5} M	10^{-6} M	10^{-7} M	10^{-8} M	Control
ASTROCYTES							
Malathion	13648±369 (93%)*	14839±748 (100%)	14689±534 (100%)	14523±462 (100%)	14426±754 (100%)	14988±477 (100%)	14699±856
Malaoxon	13602±1201 (92%)*	14359±372 (100%)	15262±1883 (100%)	14323±594 (100%)	14747±1104 (100%)	15257±573 (100%)	14699±856
Lead	10602±405 (72%)**	10570±478 (72%)**	12295±356 (84%)*	11790±234 (80%)*	11351±326 (80%)*	13038±626 (89%)*	14699±856
BMECs							
	10^{-3} M	10^{-4} M	10^{-5} M	10^{-6} M	10^{-7} M	10^{-8} M	Control
Malathion	46518±3158 (55%)**	55428±2401 (65%)**	66520±2023 (78%)*	75629±2079 (88%)*	76707±2548 (90%)*	87338±2170 (100%)	85288±6702
Malaoxon	563±159 (0.7%)**	64932±2874 (76%)**	75458±4644 (88%)*	84313±2344 (99%)	84432±1795 (99%)	88567±6799 (100%)	85288±6702
Lead	84125±2909 (98%)	84881±3952 (99%)	81079±6616 (95%)*	89605±2730 (100%)	91522±3830 (100%)	84930±3523 (99%)	85288±6702
RBE4s							
	10^{-3} M	10^{-4} M	10^{-5} M	10^{-6} M	10^{-7} M	10^{-8} M	Control
Malathion	63745±3168 (72%)**	64945±2258 (73%)**	73629±2411 (83%)*	74300±2362 (84%)*	75419±3522 (85%)*	83040±3581 (94%)*	88621±4366
Malaoxon	83031±1646 94%)*	81267±5771 (91%)*	86411±4686 (97%)	89230±8264 (100%)	85406±2147 (96%)*	85483±5817 (96%)*	88621±4366
Lead	77267±2219 (87%)*	83015±2708 (94%)*	86775±2418 (98%)	82322±2000 (93%)*	85757±6778 (97%)	89444±2290 (100%)	88621±4366
SH-SY5Ys							
	10^{-3} M	10^{-4} M	10^{-5} M	10^{-6} M	10^{-7} M	10^{-8} M	Control
Malathion	84725±4829 (84%)*	89433±1813 (89%)*	91304±2540 (90%)*	91138±3599 (90%)*	91075±1432 (90%)*	95561±2822 (95%)*	101062±3579
Malaoxon	3369±5177 (3%)**	64526±4213 (64%)**	73890±3326 (73%)**	88069±3107 (87%)*	94267±4642 (93%)*	102859±2983 (100%)	101062±3579
Lead	81257±1869 (80%)*	84703±1589 (84%)*	89942±2870 (89%)*	95272±3744 (95%)*	102811±2075 (100%)	100302±1613 (99%)	101062±3579

Cytotoxicity of neurotoxicants for cell types was determined by quantification of adenosine triphosphate (ATP), an indicator of the presence of metabolically active cells. The numbers represent relative luminescence units (RLU) expressed as the mean ± SD of three separate experiments (N=3), each done with triplicate samples for each concentration tested. Numbers in parenthesis represent percentages of cell viability when compared to controls. Asterisks indicate statistically significant declines in viability (*), and biologically relevant decreases for these specific experiments (**); concentrations providing less than 78% viability in all cell types were not utilized in subsequent studies.

FIGURE 2

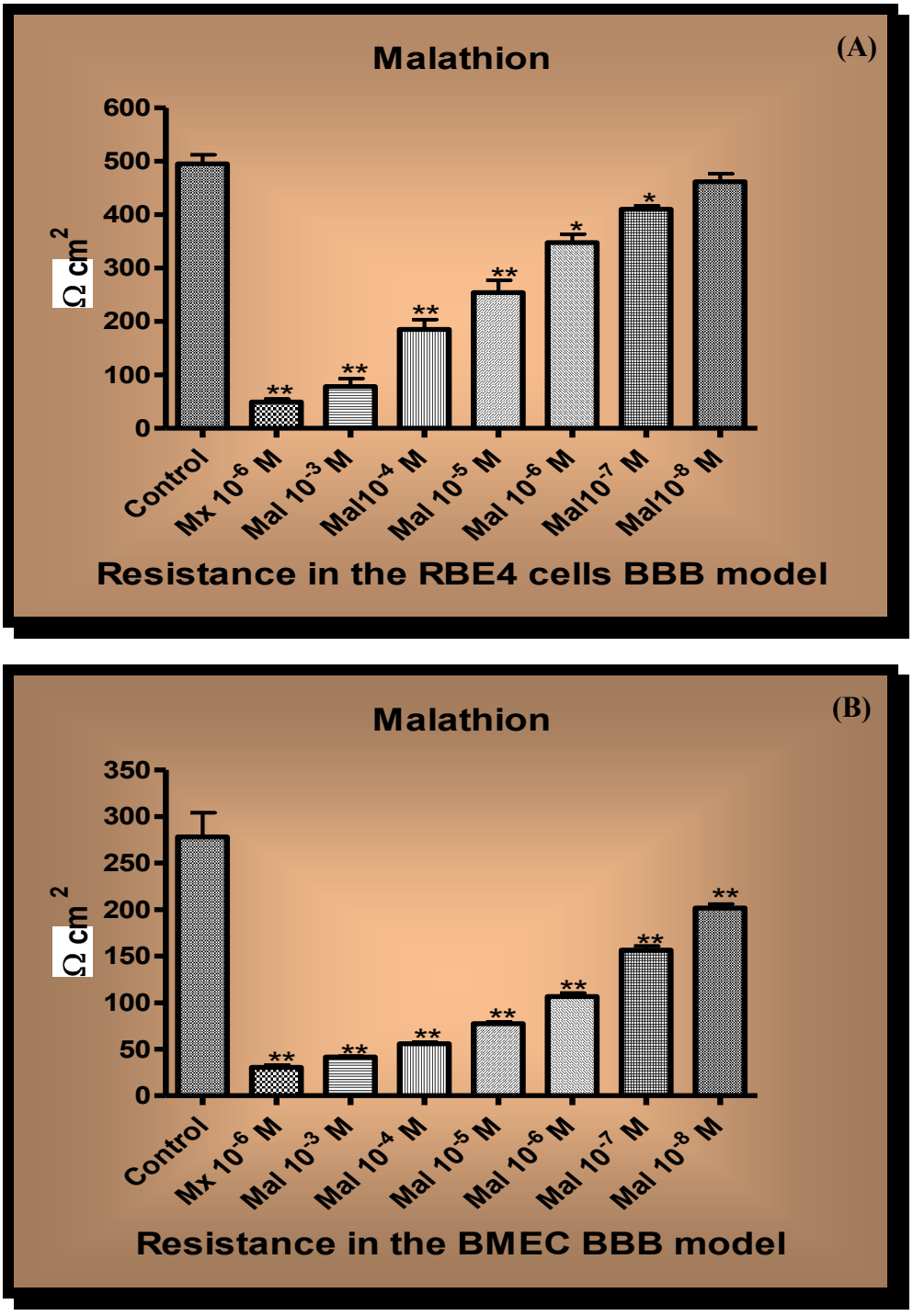

Figure 2. TEER assessments at different concentrations of malathion (Mal) in both BBB models. There is a concentration response in both models of BBB with significant differences in decreases of resistance for both models, (*) $p < 0.05$ and (**) $p < 0.01$. However, the system constructed with RBE4 cells (A) shows a higher resistance when compared to the system constructed with BMECs (B). The malathion's oxygen analog malaoxon (Mx) was included as a positive control. Resistance is expressed in ohms per square centimeter (Ω cm^2). Columns represent the mean ± SD of three separate experiments (n=3), using three means of triplicate samples. If the SD is small, it may appear too close to be distinguished from the mean.

FIGURE 3

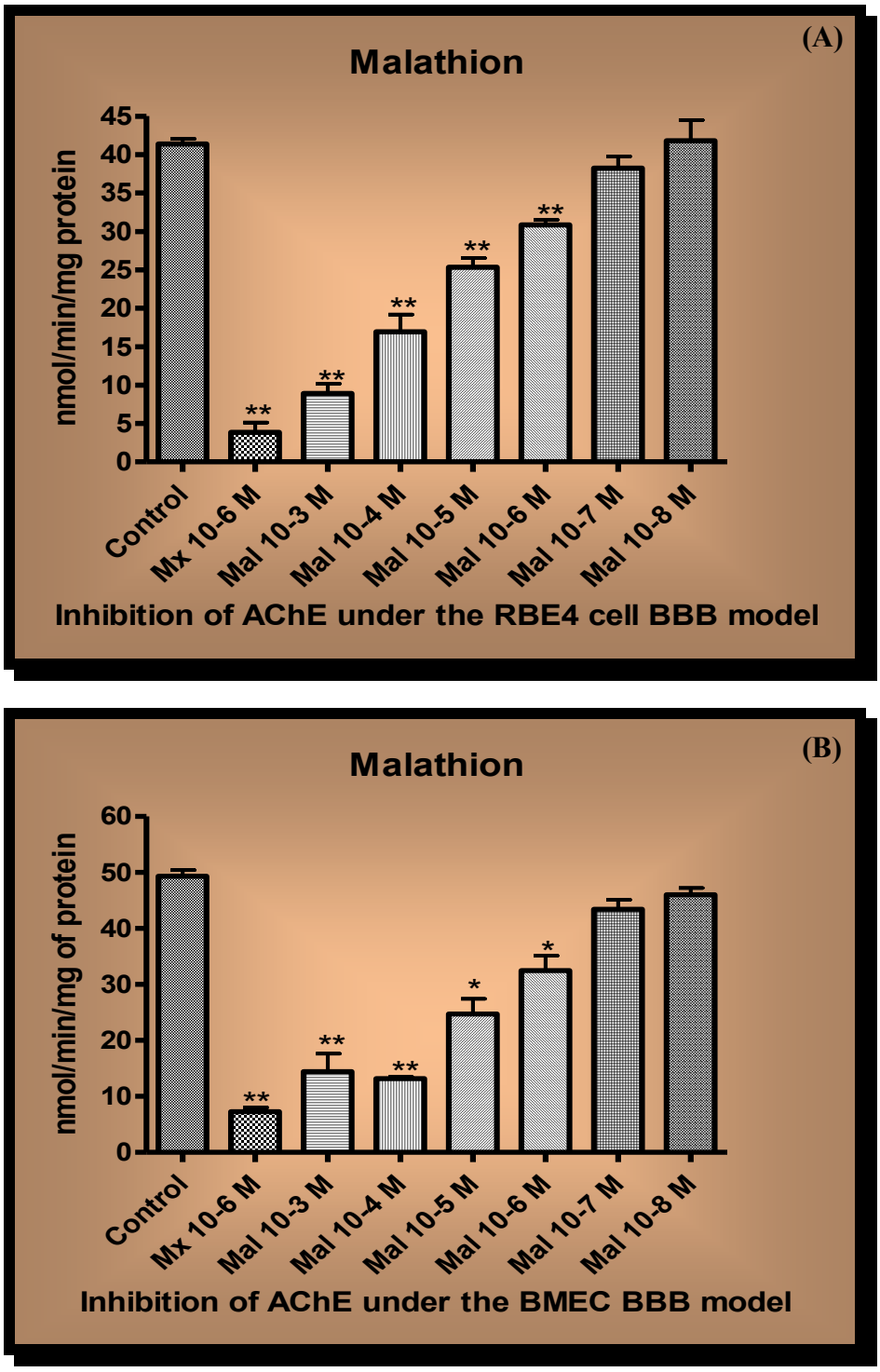

Figure 3 Passing of malathion (Mal) and malaoxon (Mx) through the barrier. Leakage was assessed by measuring the inhibition of AChE enzyme in SH-SY5Y cells cultured below the barrier systems. Both the RBE4 cells model (A) and the BMEC model (B) presented a similar concentration response to the OP compounds. Baseline AChE activities, based on protein concentrations, were similar. Results are expressed in nanomoles per minute per milligram of protein. Columns represent the mean ± SD of three separate experiments, each done with triplicate samples. Asterisks denote significant differences from control (* = $p < 0.05$; ** = $p < 0.01$).

FIGURE 4

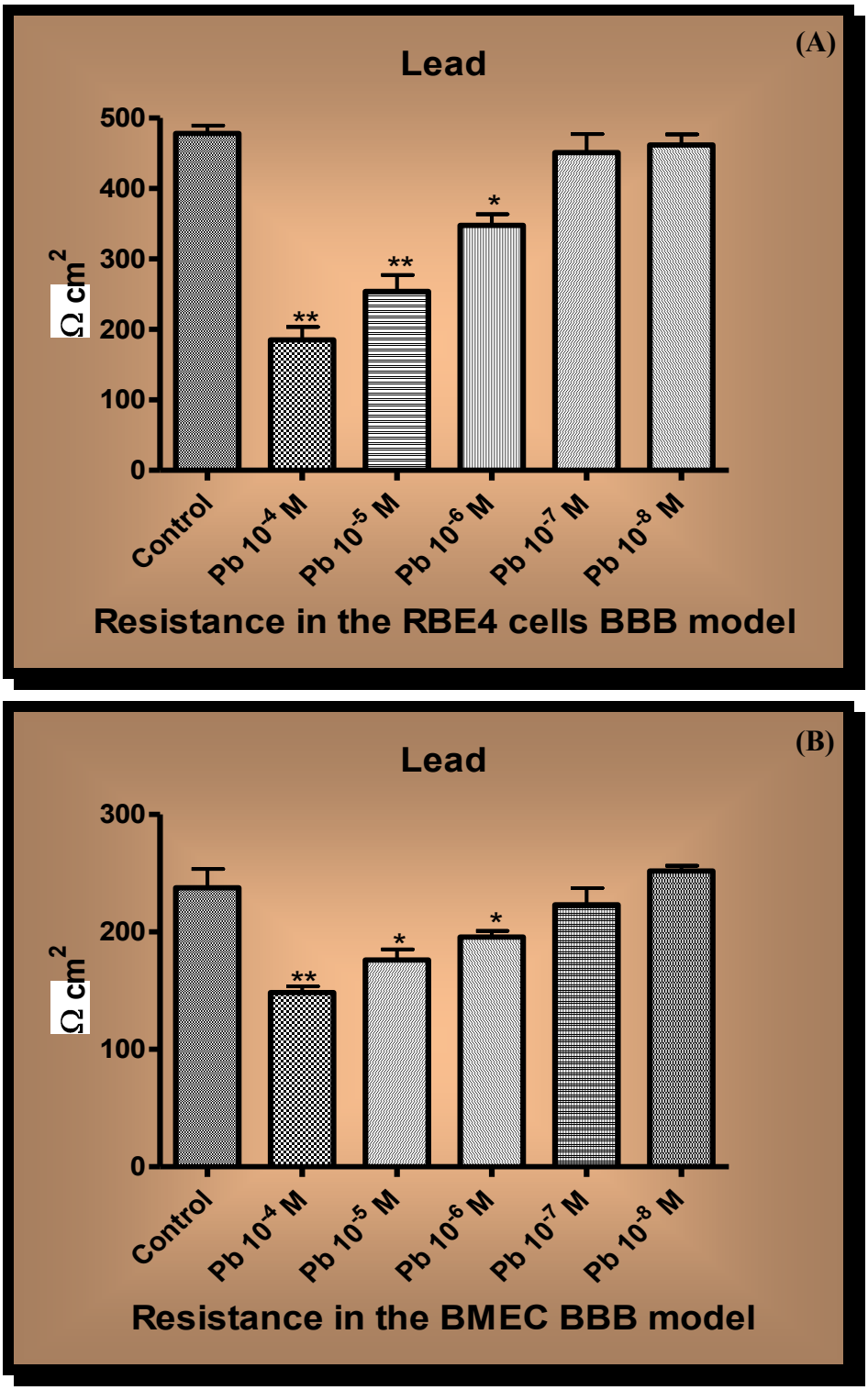

Figure 4 TEER after exposure to lead acetate in both BBB models. Both the RBE4 model (A) and the BMEC model (B) demonstrated decreases in resistance in response to lead (Pb), but effects were greater in the RBE4 cells model. Lead concentrations of 10^{-7}M and 10^{-8}M did not reduce TEER in either model. Significant differences from control are indicated by * ($p < 0.05$) and ** ($p < 0.01$). Bars represent the mean ± SD of three separate experiments, each done with triplicate samples.

FIGURE 5

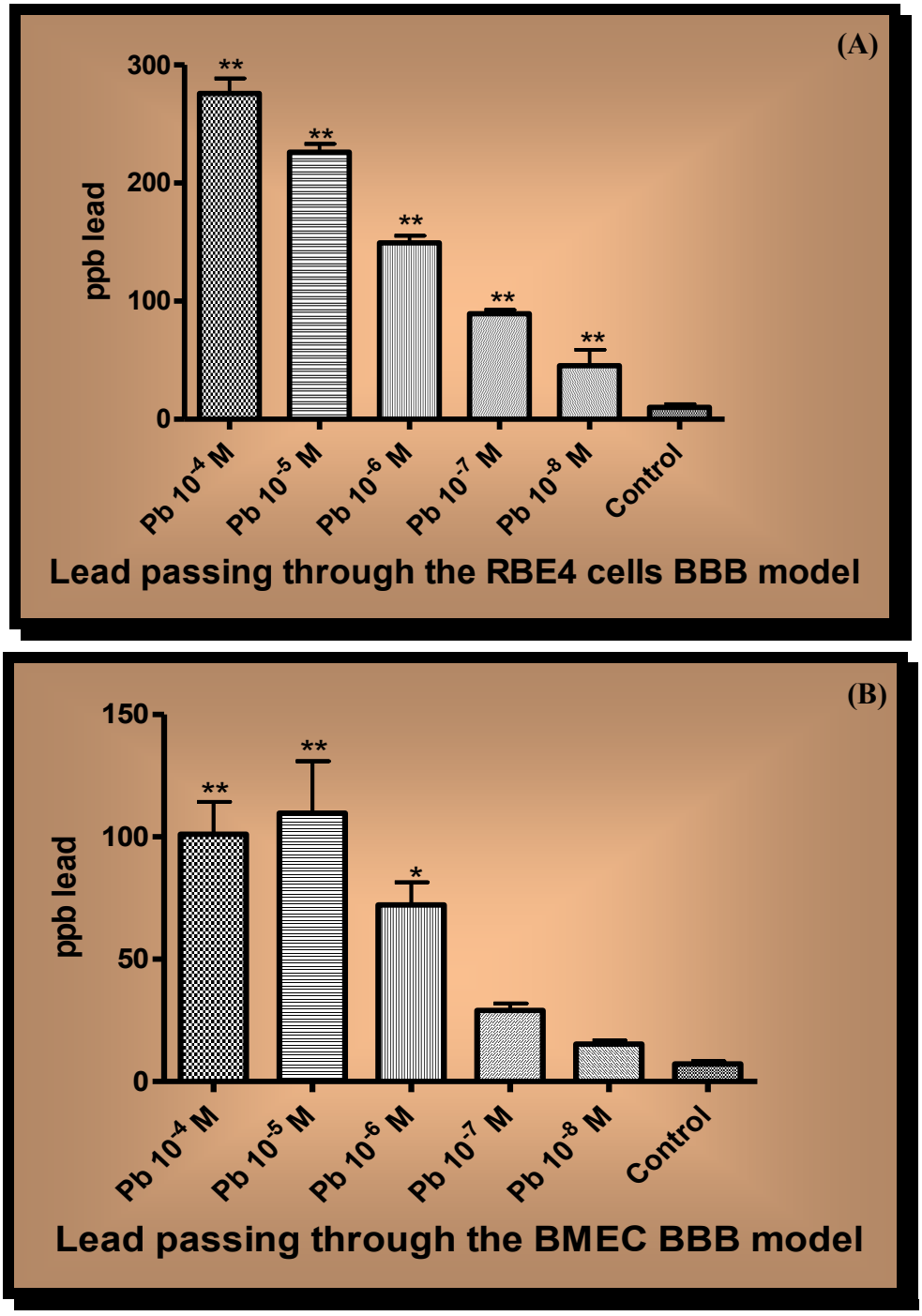

Figure 5 The amount of lead collected on the abluminal side of both BBB models was directly proportional to the concentrations of the metal applied to the luminal side of the cell bilayer. Samples were analyzed by atomic absorption and results represent parts per billion (ppb) of lead (Pb) expressed as means ± SD of three separate experiments, each done with triplicate samples. For the RBE4 cells model (A), increases in lead measurements in media collected below the membranes corresponded with increases in concentrations of the metal in the luminal side, these increases were significant, $p < 0.01$ (**) for all the concentrations when compared to the control. For the BMEC BBB model (B), significant variations occur only for the highest concentrations, 10^{-4}M and 10^{-5}M $p < 0.01$ (**), and 10^{-6}M $p < 0.05$ (*).

FIGURE 6

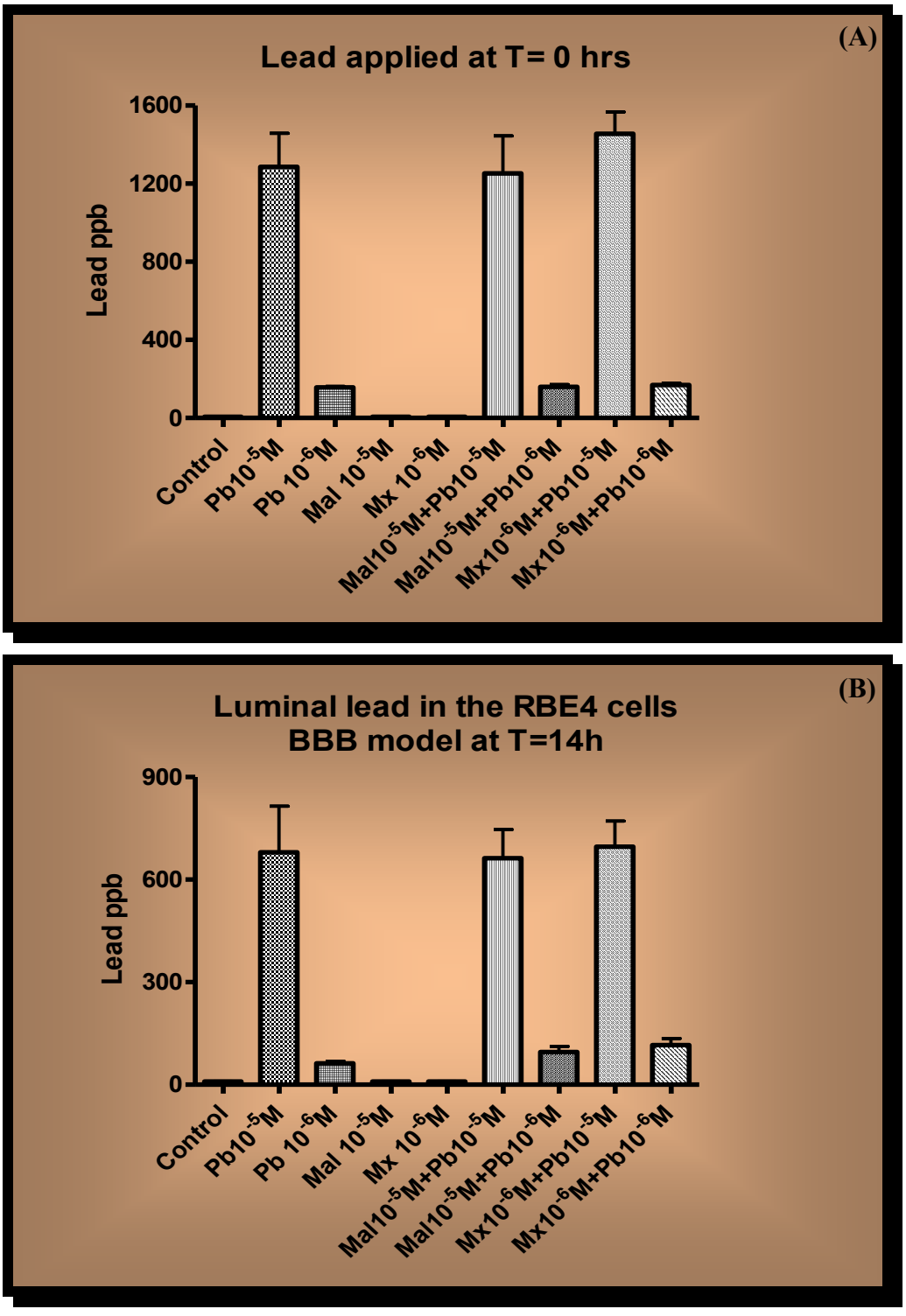
(A)
Lead applied at T= 0 hrs
Lead ppb
1600
1200
800
400
0
Control
Pb10-5M
Pb 10-6M
Mal 10-5M
Mx 10-6M
Mal10-5M+Pb10-5M
Mal10-5M+Pb10-6M
Mx10-6M+Pb10-5M
Mx10-6M+Pb10-6M
(B)
Luminal lead in the RBE4 cells
BBB model at T=14h
Lead ppb
900
600
300
0
Control
Pb10-5M
Pb 10-6M
Mal 10-5M
Mx 10-6M
Mal10-5M+Pb10-5M
Mal10-5M+Pb10-6M
Mx10-6M+Pb10-5M
Mx10-6M+Pb10-6M

(C)

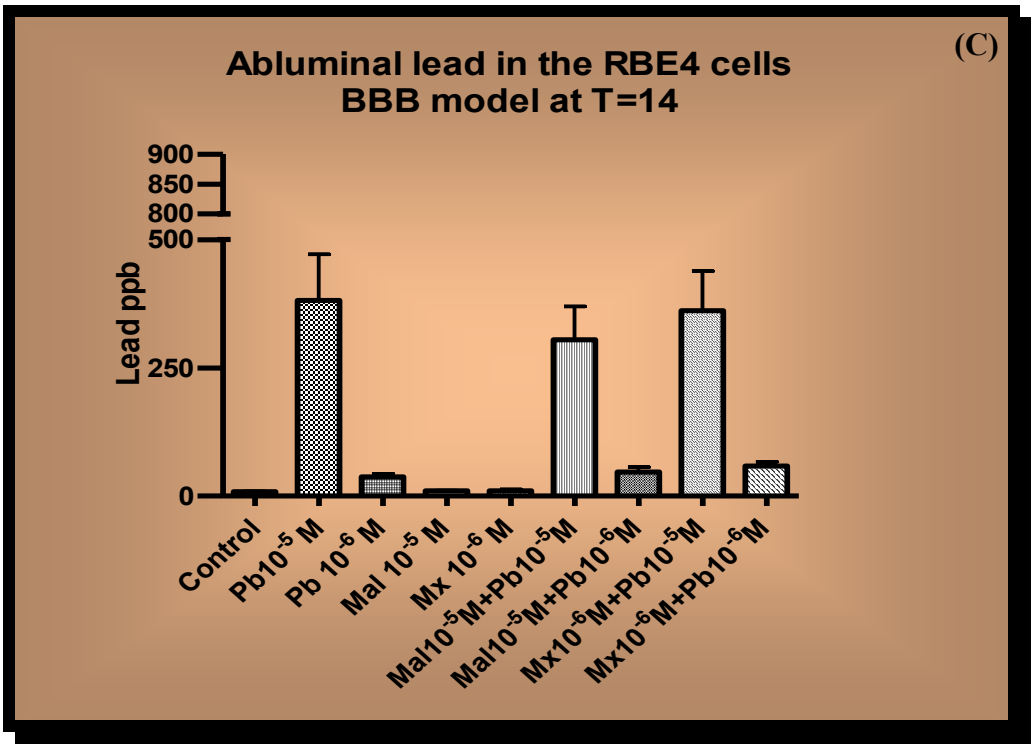
(C)
Abluminal lead in the RBE4 cells
BBB model at T=14
Lead ppb
900
850
800
500
250
0
Control
Pb10-5 M
Pb 10-6 M
Mal 10-5 M
Mx 10-6 M
Mal10-5M+Pb10-5M
Mal10-5M+Pb10-6M
Mx10-6M+Pb10-5M
Mx10-6M+Pb10-6M

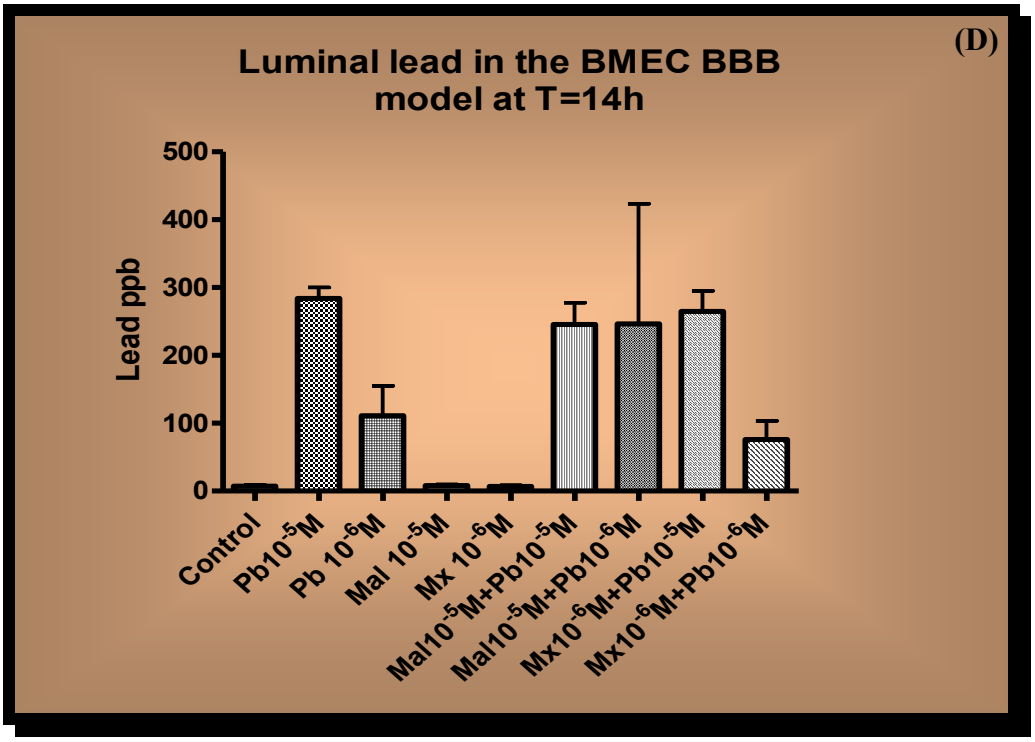
(D)
Luminal lead in the BMEC BBB
model at T=14h
Lead ppb
500
400
300
200
100
0
Control
Pb10-5M
Pb 10-6M
Mal 10-5M
Mx 10-6M
Mal10-5M+Pb10-5M
Mal10-5M+Pb10-6M
Mx10-6M+Pb10-5M
Mx10-6M+Pb10-6M

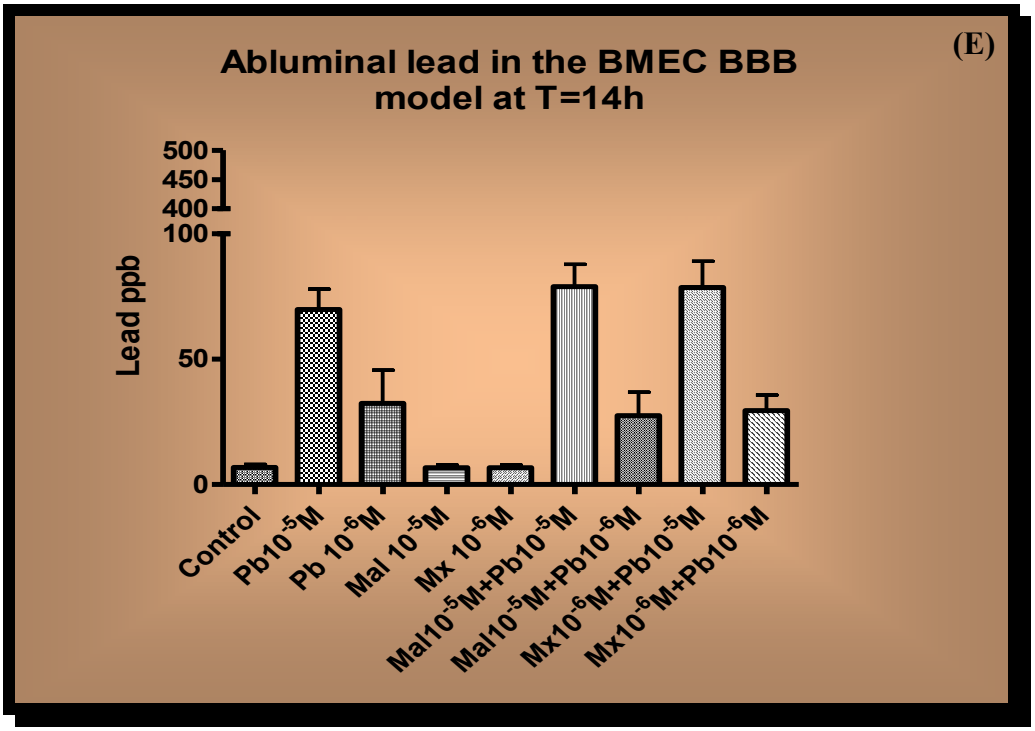

Figure 6 Comparison of combinations of malathion (Mal) and malaoxon (Mx) with lead (Pb) passing through both BBB models. Samples were collected from the luminal and abluminal sides of the BBB models at the beginning of the experiment (T=0) and after a 14 hr incubation period (T=14). Samples were then analyzed for lead by atomic absorption. Results are expressed in parts per billion (ppb) with columns representing the mean ± SD of three separate experiments, each done with triplicate samples. Since lead measurements for both models at T=0 were similar, we combined them to construct a single graph for T=0 (A), therefore, for statistical analysis of this set of data n=6. Luminal measurements of lead in the RBE4 model at T=14 (B) were around 50% for 10^{-5}M and 39% for 10^{-6}M compared to total Pb concentrations at T=0; combinations with malathion and malaoxon did not alter the amounts of lead remaining in the luminal side of the barrier. Lead recovered in the abluminal side of the RBE4 BBB model at T=14 (C) was about 30% for 10^{-5}M and 24% for 10^{-6}M of the total lead applied in the luminal side at T=0. This was true regardless of whether the lead was applied alone or in combination with the organophosphates. For the BMEC BBB model, luminal lead was about 22% for 10^{-5}M and about 50% for 10^{-6}M of the amount of lead applied on the luminal side at T=0 (D). Amounts of lead on the abluminal side of the BMEC barrier for 10^{-5}M and 10^{-6}M were about 5% and 20% respectively, of the lead applied on the luminal side at T=0 (E). Combination of lead with malathion and malaoxon did not significantly change these percentages.

FIGURE 7

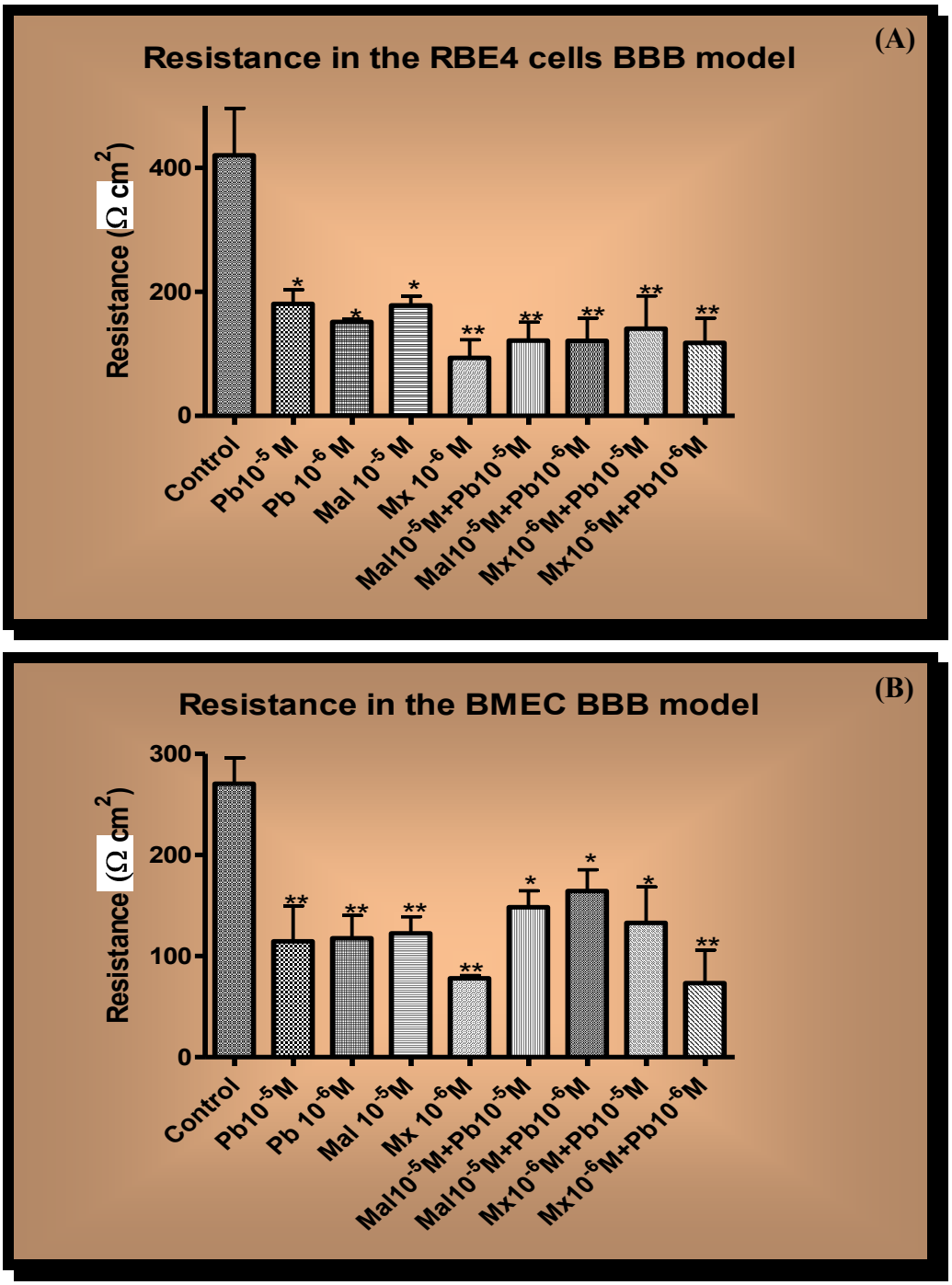

Figure 7 Assessment of resistance for the combinations of lead (Pb) with malathion (Mal) and malaoxon (Mx) in both BBB models. TEER was significantly reduced by treatments. For the RBE4 model (A), treatments with neurotoxicants alone and in combination decreased resistance significantly with $p < 0.01$(**). For the BMEC model (B), compounds alone reduced TEER significantly with $p < 0.01$ (**), and combinations also significantly reduced resistance, with $p < 0.05$ (*). However, neurotoxicant combinations did not significantly decrease the resistance when compared to compounds alone.

FIGURE 8

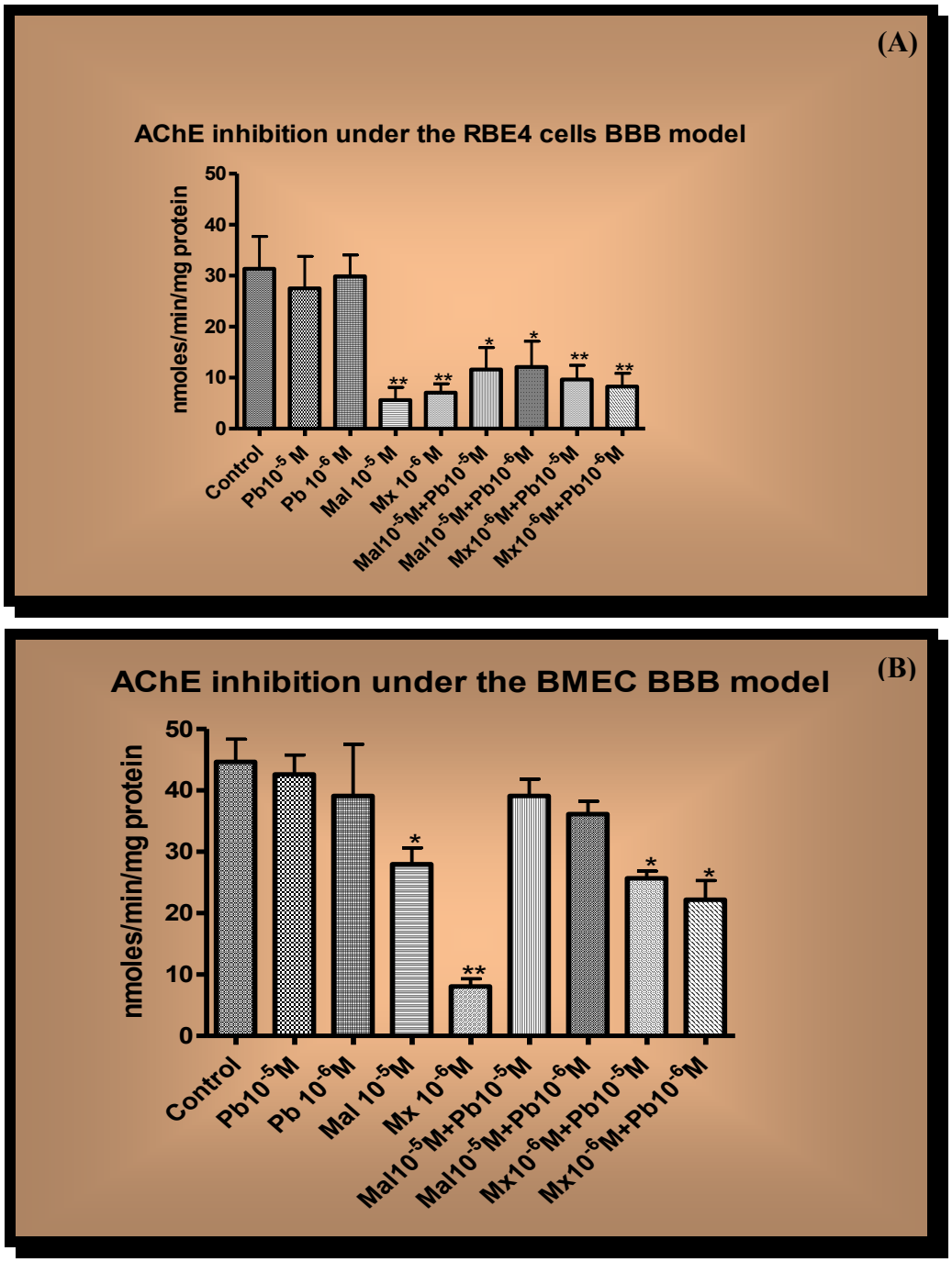

Figure 8 Inhibition of AChE enzyme in SH-SY5Y cells under the inserts of both BBB models in response to lead-malathion combinations. Results are given as mean ± SD of three separate experiments, each done with triplicate samples, and expressed in nanomoles per minute per milligram of protein (nmoles/min/mg). In the RBE4 BBB model (A), malathion (Mal) and malaoxon (Mx) significantly reduced AChE activity when compared with the control, $p < 0.01$ (**); malathion inhibited the enzyme as much as malaoxon suggesting activation by the RBE4 cells. For the BMEC BBB model (B), both malathion and malaoxon inhibited AChE activity. P values for malathion inhibition were $p < 0.05$ (*), and for malaoxon $p < 0.01$ (**). Although malathion significantly inhibits AChE when compared to the control, a comparison with malaoxon suggested a limited capability of the BMEC to metabolize OPs to their oxidized AChE-inhibiting analogs.

FIGURE 9

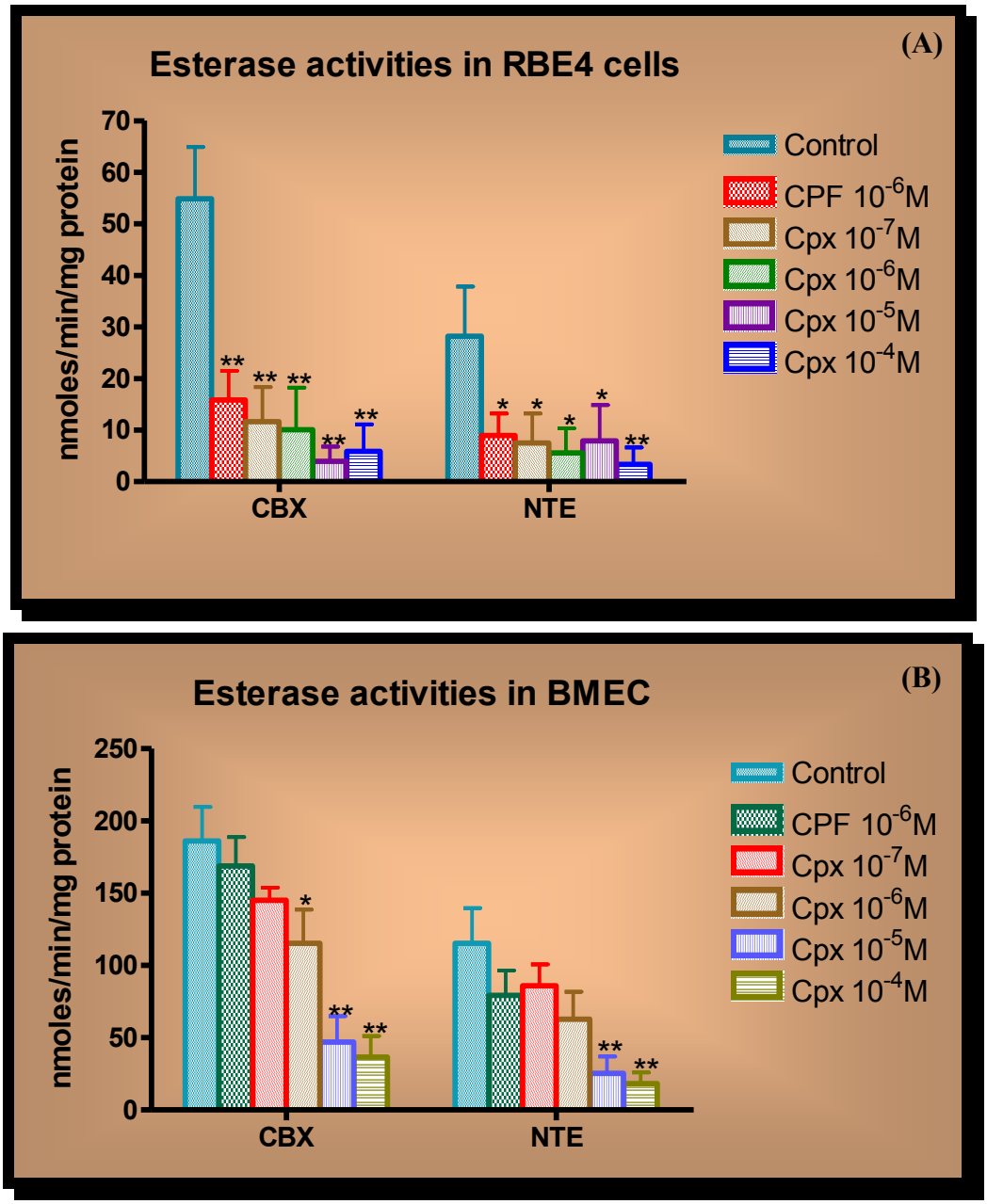

Figure 9 OP-induced inhibition of esterases in RBE4 and BMEC endothelial cells. Enzymatic levels of two different types of non-neuronal esterases, carboxylesterase (CBX) and neuropathy target esterase (NTE) were examined in response to treatment with chlorpyrifos (CPF) and its esterase-inhibitory analog chlorpyrifos-oxon (Cpx). Units are nanomoles of phenyl valerate hydrolyzed per minute per milligram of protein. Results are given as mean ± SD of three separate experiments, each done with triplicate samples. In the RBE4 BBB model (A), chlorpyrifos-oxon inhibited both CBX and NTE significantly at all concentrations with P values of $p < 0.01$ (**) when compared to the controls. The activation of chlorpyrifos to chlorpyrifos-oxon by the RBE4 cells was demonstrated by the similar levels of inhibition by the OP and its activated analog. For the BMEC BBB model (B), both CBX and NTE were inhibited by chlorpyrifos-oxon, although only the highest concentrations inhibited the esterases significantly. Chlorpyrifos alone on the other hand, did not inhibit either esterase, suggesting a limited capability of the BMEC to metabolize the OP into its esterase-inhibiting analog, (*) = $p < 0.05$; (**) = $p < 0.01$.

Chapter 4:

ASSESSMENTS OF TIGHT JUNCTION PROTEINS OCCLUDIN, CLAUDIN 5 AND SCAFFOLD PROTEINS ZO1 AND ZO2 IN ENDOTHELIAL CELLS OF THE RAT BLOOD-BRAIN BARRIER: CELLULAR RESPONSES TO NEUROTOXICANTS MALATHION AND LEAD ACETATE

Pergentino Balbuena[1], Wen Li[1], and Marion Ehrich[1]

[1]Virginia-Maryland Regional College of Veterinary Medicine, Virginia Tech, Blacksburg, VA,

Corresponding author: Marion Ehrich, Virginia-Maryland Regional College of Veterinary Medicine, 1 Duck Pond Drive, Virginia Tech, Blacksburg VA 24061.

Telephone (540) 231-6033; e-mail marion@vt.edu

Prepared FOR SUBMISSION to Neurotoxicology.

ABSTRACT:

The blood-brain barrier (BBB) is essential for central nervous system (CNS) normal function. It is formed by endothelial cells with special characteristics, which confer the BBB with low permeability and high transendothelial electrical resistance (TEER). We previously demonstrated that malathion and lead, two neurotoxicants widely present in the environment, decrease TEER and increase permeability in *in vitro* models of the BBB. In this study we assessed tight junction disruption at the protein and gene expression levels using a rat brain microvascular endothelial cell line (RBE4s) exposed to lead acetate at 10^{-5} M and 10^{-6} M, malathion at 10^{-5} M, malaoxon at 10^{-6} M, and their combinations. Cells were incubated with treatments for 2 hr, 4 hr, 8 hr, 16 hr, and 24 hr periods. Immunoblotting assessments demonstrated that protein levels of tight junction proteins occludin and claudin 5, and scaffold proteins ZO1 and ZO2 were decreased after treatments. Gene expression determinations did not correlate with the decreases in protein, suggesting that a different mechanism is responsible for tight junction and scaffold protein decreases in the BBB.

Key words: BBB, tight junctions, malathion, lead acetate, endothelial cells.

INTRODUCTION:

The blood-brain barrier (BBB) in mammals is established by the endothelial cells that make up the cerebral microvessels, forming a diffusion selective barrier between the circulatory system and the brain parenchyma. This physical barrier is essential for the normal function of the central nervous system (CNS) because it regulates cerebral blood flow and paracellular and intracellular molecular transport (Abbott *et al*., 2006; Ballabh *et al*., 2004). The main characteristics of the cerebral endothelium are the absence of fenestrations, the relatively low number of pinocytotic vesicles, increased mitochondrial content, and very specific transport systems (Abbott *et al*., 2006; Yang and Aschner, 2003). The endothelial cells of the BBB differ from endothelial cells of other parts of the vasculature in that they form specific structures on the membranes of adjacent endothelial cells called tight junctions (Abbott *et al*., 2006). These tight junctions form pentalaminar layers as a result of the fusion of the external leaflets of adjacent cell membranes in the brain microvascular endothelia (Brightman and Reese, 1969; Farquhar and Palade, 1963; Kniesel and Wolburg, 2000). The tight junctions not only strictly regulate the permeability of the BBB and contribute to its elevated transendothelial electrical resistance (TEER), they also regulate the paracellular flux of molecules across the BBB (Abbott *et al*., 2006; Ballabh *et al*., 2004; Wolburg and Lippoldt, 2002; Wolburg *et al*., 2002; 2006).

The crossing of a molecule through the healthy BBB is dependent upon its physicochemical properties, such as lipophilicity and solubility, and its pharmacokinetic profile in plasma. This profile in turn, depends upon how the compound is absorbed, distributed, metabolized, and excreted (Alavijeh *et al*. 2005). Some neurotoxicants that cross the BBB, such as heavy metals and organophosphates, are associated with increases in BBB permeability *in vitro* (Balbuena *et*

al., 2010; Parran *et al*., 2005; Yang and Aschner, 2003; Shi and Zheng, 2007), but mechanistic aspects of such disruption have not been completely elucidated.

Malathion [S-(1, 2-dicarbethoxy) ethyl O, O-dimethyl-phosphorodithioate] crosses the BBB. It is an organophosphate (OP) insecticide widely used around the world and in the United States (Abou-Donia, 2003; Ehrich, 2005; EPA, 2000-2001). Malathion is a common cause of poisoning in underdeveloped countries and sporadically in agricultural areas of developed nations (Eddleston *et al*., 2008; Gunnell *et al*., 2007). Organophosphate neurotoxicity studies are extensive in the literature and include those done in our laboratory and by other groups (Ehrich and Gross, 1983; El-Fawal *et al*., 1990; Harel *et al*., 2000; Jortner and Ehrich, 1987; Petroianu *et al*., 2007; Balbuena *et al*, 2010).

Another neurotoxicant that crosses the BBB is lead, which is a stable heavy metal that stays in the environment for long periods. Because of this characteristic, lead particles in the environment can accumulate in soil and from there leach into the water that supplies our drinking reserves (Filippelli and Laidlaw, 2009; Toscano and Guilarte, 2005). Lead poisoning remains a problem, especially in underdeveloped countries (Mañay et al., 2008). Biochemical mechanisms contributing to lead-induced changes in neuronal functionality have been reported (Gilbert and Mack, 1998; Gilbert et al., 1996; Toscano and Guilarte, 2005; Wang 2006). Lead exposure has also been associated with leakage of the BBB *in vitro* (Balbuena *et al*., 2010; Shi and Zheng, 2007) and *in vivo* (Bouldin *et al*., 1975; Goldstein *et al*., 1974). We previously reported that lead, alone and in combination with malathion, disrupted the BBB (Balbuena *et al*., 2010). Nevertheless, the mechanisms associated with such disruption of the BBB are yet to be established.

In this study, we evaluated transmembrane proteins forming the intercellular structure of the tight junction because their alteration could contribute to BBB disruption induced by malathion and lead. There are at least two transmembrane proteins associated with formation of the BBB, occludin (Ando-Akatsuka *et al*., 1996; Furuse *et al*., 1993) and the claudin family (Furuse *et al*., 1998; Tsukita and Furuse, 2000). Claudin 5 is expressed specifically in endothelial cells of blood vessels, suggesting a role of this protein in the regulation of blood vessel permeability (Morita *et al*., 1999a; 1999b; Nitta *et al*., 2003). Occludin and the claudin family are the most important membranous components of the BBB tight junctions that have been identified. Both contain four transmembrane domains and two extracellular loops (Ando-Akatsuka *et al*., 1996; Furuse *et al*., 1993; Furuse *et al*., 1998; Tsukita and Furuse, 2000). There is association between tight junction morphology and the expression of tight junction proteins in endothelial cells of the BBB (Liebner *et al*., 2000), and between the expression of these proteins and the manifestation of the specific characteristics (low permeability and high TEER) of the barrier in cerebral microvasculature (Balda and Matter, 1998; Wolburg and Lippoldt, 2002; Hawkins and Davis, 2005).

The BBB also has a scaffold protein complex holding this paracellular membranous structure together. This is formed by a group of cytosolic membrane proteins called the *zonula occludens* (ZO) protein family, which includes ZO1 (Stevenson et al., 1986), ZO2 (Jesaitis and Goodenough, 1994), and ZO3 (Balda and Anderson, 1993; Haskins *et al*., 1998). This complex attaches the tight junction proteins to the cytoskeleton structure in cell-to-cell interactions (Itoh *et al*., 1999; Fanning, 2007). ZO proteins belong to a group of membrane-associated guanylate kinase-like homologues or MAGUKs, which are involved in creating and maintaining specialized membrane domains in various types of cells (Fanning, 2007). ZO1 has been

associated with oxidant-induced barrier disruption because it serves as an important linker between perijunctional actin and the tight junction proteins occludin and claudins (Musch *et al*., 2005). At present, no studies describing changes on these proteins associated with neurotoxic effects caused by organophosphates or heavy metals have been reported, but such changes could contribute to the disruption of the BBB induced by malathion and lead. Therefore, we hypothesized that the loss of these proteins could be associated with disruption of the BBB induced by these neurotoxicants.

The present study first assessed changes in the levels of protein of tight junction proteins occludin and claudin 5, as well as the scaffold proteins ZO1 and ZO2 in response to combinations of neurotoxicants malathion/oxon and lead acetate. We then examined effects of these neurotoxicants on gene expression of these proteins for a possible mechanism for neurotoxicant-induced protein effect. Since increases in permeability are associated with BBB damage, and both compounds increase permeability of the barrier (Balbuena *et al*., 2010), it is important to establish if the effects of these neurotoxicants are a post-translational effect at the protein level, or a pre-translational effect involving changes in gene expression.

MATERIALS AND METHODS

Chemicals: Malathion of 94% purity was donated by the American Cyanamid Company, agricultural division (Princeton, NJ). Malaoxon 98.2% pure was obtained from Chem Services Inc. (West Chester, PA); it was included in experiments as an active esterase inhibitor in order to determine the contribution of esterase inhibition to changes in levels of tight junction and scaffold proteins. Lead acetate, Na_2HPO_4, KH_2PO_4, NaCl, trizma base, triton X-100, glycine,

SDS, tween-20, and deoxycholate were purchased from Sigma-Aldrich, Inc. (St. Louis, MO). Blocking buffer was purchased from LI-COR Biotechnology (Lincoln, Nebraska).

Cell culture: The rat brain microvascular endothelial cell line RBE4 was donated by the laboratory of Dr. M. Aschner, Vanderbilt University. Cells were cultured in 100 mm x 20 mm polystyrene tissue-culture treated dishes (Sigma-Aldrich) at a concentration of 1.5 X 10^5 cells per culture dish and were left to reach 100% confluency. RBE4 cultures were cultured in 44.5% minimum essential medium (MEM), 44.5% Ham's F10 with glycine, 10% fetal bovine serum (FBS), and 1% of a penicillin/streptomycin/amphotericin B solution and kept at 37°C with a mixture of air and 5% CO_2. All the cell culture media and reagents utilized in cell culture procedures were obtained from Mediatech Inc. (Manassas, VA), unless otherwise noted. After 3-4 days cells were incubated for an additional 2 days with astrocyte conditioned medium (ACM) in order to induce the presence of tight junctions on the endothelial cells. ACM has been associated with induction of blood-brain barrier specific characteristics such as tight junctions in several cell lines (Abbott, 2002; Omidi et al., 2008). After the incubation with the ACM, cells were treated with neurotoxicants malathion/oxon and lead acetate.

Treatments: Cells were treated with compounds alone and in combinations at different times and concentrations. Treatments groups include lead acetate at 10^{-5} M ($Pb10^{-5}$ M) and 10^{-6} M, malathion 10^{-5} M ($Mal10^{-5}$ M), malaoxon 10^{-6} M ($Mx10^{-6}$ M), and combinations of both neurotoxicants ($Pb10^{-5}$ M+$Mal10^{-5}$ M, $Pb10^{-5}$ M+$Mx10^{-6}$ M, $Pb10^{-6}$ M+$Mal10^{-5}$ M, and $Pb10^{-6}$ M+$Mx10^{-5}$ M). Cells were incubated with treatments for 2 hr, 4 hr, 8 hr, 16 hr, and 24 hr periods.

Previous results indicated that cell viability was maintained after exposure to these concentrations of test compounds for this period of time.

Western blot assessment: RBE4 cells were washed in 5 ml ice-cold phosphate buffered saline (PBS) pH 7.4 and then lysed for 10 minutes with an ice-cold lysis buffer solution containing 150 mM NaCl, 10 mM trizma base, 0.5% v/v triton X-100, and 0.5% w/v deoxycholate. Lysates were centrifugated at 16,000g for 5 minutes and resuspended in 700 µl of ice-cold PBS. Lysates were processed immediately for protein determination; sample concentrations were adjusted to 1 mg/ml and stored at -20°C. Proteins were separated by electrophoresis in 4%-15% Tris-HCl 1.0 mm pre-casted gels (Bio-Rad Laboratories, Hercules CA), and then transferred to a 0.45 µm pure nitrocellulose membrane by electroblotting. Membranes were blocked for 1 hr at room temperature with Odyssey blocking buffer (LI-COR Biotechnology) and then incubated for one hour with polyclonal antibodies (Santa Cruz Biotechnology, Santa Cruz, CA) anti-claudin 5, anti-occludin, anti-ZO1, anti-ZO2, and anti-β-actin (as a normalizing control) at 1:200 dilutions. Membranes were washed 5 times (5 minutes each) with a solution of PBS pH 7.4 and 0.1 % Tween-20 and then incubated for one hour with IRDye™ 700DX conjugated affinity purified anti-rabbit IgG (donkey) and IRDye™ 800CW conjugated affinity purified anti-goat IgG (donkey) secondary antibodies (Rockland, Gilbertsville PA) at 1:5000 dilutions. Membranes were washed and then analyzed by near-infrared (NIR) fluorescence detection methods with the Odyssey® Infrared Imaging System. Results were expressed as relative band fluorescence in pixels.

Total RNA extraction and reverse transcription/cDNA synthesis: Total RNA was extracted utilizing the Total RNA purification RNeasy kit from Qiagen (Valencia, CA). Briefly, cells were lysed with lysis buffer applied directly on the cell culture dishes after washing them with PBS at 4°C; lysates were then homogenized with 70% ethanol utilizing a blunt 20-gauge needle (0.9 mm diameter), and pipetted into RNeasy spin columns and centrifugated. Samples were treated with DNase I in order to digest any genomic DNA that may have been present in the samples and then washed again in the columns. RNA was then eluted directly from the columns with 30 µl of RNase-free water. Concentrations of total RNA were determined for samples with an eppendorf UV/Vis bioPhotometer analysis system (Hamburg, Germany), and then RNAs were stored at -80°C. Reverse transcription synthesis was carried out utilizing the reverse transcription system from Promega (Madison, WI) processing 1 µg of total RNA per reaction. Briefly, total RNA was incubated at 70°C for 10 minutes and placed on ice. Reactions were prepared at the following concentrations: 50 ng/µl of total RNA, 50 mM $MgCl_2$, 10X reverse transcription buffer (100 mM Tris-HCl[pH 9.0 at 25°C]; 500 mM KCl; 1% Triton®X-100), 1 mM each dNTP mixture, 1u/µl recombinant RNasin® ribonuclease inhibitor, 50u/µg AMV reverse transcriptase (high concentration), and 0.5 µg of random primers per microgram RNA with Nuclease-free water to a total volume of 20 µl per reaction. Reactions were incubated at room temperature for 10 minutes and then at 42°C for 15 minutes before they were heated at 95°C for 5 minutes. After cooling off, cDNA reactions were stored at -20°C until used.

Quantitative real time polymerase chain reaction: Rattus norvegicus oligonucleotide primers for occludin, claudin 5, ZO1, ZO 2, and β-actin (as an internal normalizing control) were designed with the Beacon Designer™ 7.6 software (Premier Biosoft International, Palo Alto, CA) as shown

in Table 1. Primers were designed to be compatible with the SYBR® Green PCR assays avoiding significant cross homologies and preventing secondary structures that can interfere with SYBR® Green primer extension. Primers were synthesized by Invitrogen and then concentrations of each primer were standardized to 30 µM concentrations. Quantitative real time PCR (qPCR) amplifications were carried out utilizing an iCycler iQ™ optical system (Bio-Rad). The PCR reaction mix was generated by adding 12.5 µl of SYBR® Green Supermix® (Bio-Rad) with 0.25 µl of each primer (forward/reverse), 1 µl of cDNA template, and RNA-free water to a total of 25 µl per reaction. The relative quantification of gene expression was attained utilizing the comparative C_T method as described by Livak and Schmittgen (2001).

Statistical analysis: All results are expressed as means ± SEM of three or more individual assays. Multiple comparisons were performed by utilizing one-way analysis of variance (ANOVA), followed by Dunnett's test. Data were analyzed by GraphPad Prism 4 (GraphPad software, San Diego, CA); *p* values less than 0.05 were considered to be significant.

RESULTS

Protein levels were analyzed over time for all treatments and responses were assessed in terms of overall changes of levels of protein over a period of 24 hr. Measurements were performed at 2 hr, 4 hr, 8 hr, 16 hr, and 24 hr. Immunoblotting protein determination of occludin demonstrated decreased quantities at 2 hr after exposure to Pb at both concentrations tested (Fig 1). Protein was still decreased at 4 hr after Pb exposure. In fact, all treatments significantly decreased occludin at all times after exposure. This was especially notable for combinations of lead with malathion (Pb 10^{-6} M+Mal10^{-5} M) and combinations of lead with malaoxon (Pb 10^{-6}

M+Mx10^{-6} M) at 24 hr ($p< 0.001$). Like occludin, claudin 5 protein levels were significantly decreased at all times after exposures to neurotoxicants alone and in combination, when compared to controls, with the exception of malaoxon (Mx 10^{-6} M) at 4 hr (Fig 2).

Scaffold protein ZO1 levels decreased in response to all treatments (Fig 3). The decrease caused by Pb 10^{-6} M+Mal10^{-5} M was significant at 24 hr when compared to the other time periods ($p<0.05$).

Protein levels for scaffold protein ZO2 exhibited a pattern similar to ZO1, with significant decreases of protein levels at all times for all treatments, but there were no significant differences among protein decreases of compounds alone *vs.* combinations (Fig 4).

Since decreases in protein levels for both the tight junction and the scaffold proteins were observed, assessments on gene expression were investigated as a potential mechanism for the reduction of occludin, claudin 5, ZO1, and ZO2. Expression of the gene for occludin increased at least 2 fold ($p< 0.05$) after cells were exposed to lead (Pb10^{-5} M) and malathion (Mal 10^{-5} M) at 2 hr and 4 hr respectively (Fig 5a). The combination of Pb 10^{-5} M+Mal10^{-5} M also increased gene expression at 2 hr ($p< 0.05$) (Fig 5b).

Claudin 5 gene expression, on the other hand, was downregulated by the neurotoxicants alone and in combination at 2 hr and 4 hr (Fig 6a and Fig 6b) which is associated with the protein decreases seen with the western blots. However, both concentrations of lead increased gene expression at the 24 hr period (Fig 6a) while the protein levels observed with western blots remained decreased (Fig 2).

qPCR assessments for ZO1 gene expression demonstrated significant increases greater than 2-fold ($p<0.05$) for lead (Pb10^{-5} M) at 2 hr. A more dramatic increase occurred with malaoxon (Mx 10^{-6} M) which showed about 3.5-fold ($p<0.001$) increase at the 4 hr period (Fig

7a). Neurotoxicants in combination blunted the early effects seen with lead and malaoxon alone, but resulted in significant increases in ZO1 gene expression at 24 hr ($p<0.001$) (Fig 7b).

Gene expression levels of the ZO2 gene in response to neurotoxicants alone were similar to those observed with ZO1, with malaoxon ($Mx10^{-6}$ M) causing a dramatic 4-fold increase ($p<0.001$) and lead ($Pb10^{-5}$ M) causing at least a 3-fold increase in gene expression at the 4 hr period ($p<0.001$) (Fig 8a). The effects of combinations of lead plus malathion/oxon on gene expression are provided in Fig 8b. Increases with $Pb10^{-6}$ M+$Mal10^{-5}$ M were greater at 4 hr and were still increased at 24 hr ($p<0.05$).

It appears that with lead and malathion/oxon treatments, gene expression in the RBE4 for the tight junction proteins occludin and claudin 5, as well as gene expression of scaffold proteins ZO1 and ZO2, did not correlate with levels of these proteins assessed in RBE4 cells.

DISCUSSION

Previous work with concentrations of lead and malathion similar to those utilized in these experiments caused decreases in transendothelial electrical resistance (TEER) of the BBB *in vitro* systems (Balbuena *et al*., 2010). TEER decreases are associated with increases in permeability and disruption of the BBB (Ballabh *et al*., 2004), and these increases in permeability are usually associated with tight junction disruption (Kniesel and Wolburg, 2000; Nitta et al., 2003). The results presented here demonstrated that lead and malathion in concentrations that affect BBB permeability in the model cited above affected tight junction proteins and scaffold proteins. Both neurotoxicants alone and in combinations reduced occludin protein at all the time points measured. Gene expression assessments however, did not appear to correlate with levels of proteins, indicating that the effects inducing the reduction in tight

junction protein and scaffold protein levels were not connected to changes in gene expression. This suggests that other mechanisms could be responsible for the decreased protein levels in response to the neurotoxicants lead and malathion.

Although not determined in these studies, BBB increases in permeability due to changes in occludin levels have been associated with cellular oxidative stress in response to hypoxia followed by reoxygenation in the brain (McCaffrey *et al*., 2009; Lochhead *et al*., 2010). Lead did not decrease occludin protein levels or gene expression in epithelial cells of the blood-cerebrospinal fluid barrier in a previous *in vitro* study (Shi and Zheng, 2007), but it has previously been reported to increase BBB permeability *in vivo* (Goldstein *et al*., 1974; Bouldin *et al*., 1975). The present experiments demonstrated changes in levels of protein in endothelial cells of our *in vitro* BBB model. This may be due to different responses from different cell types.

Decreases in occludin protein levels observed here in response to neurotoxicant insult, did not correlate with occludin gene expression analysis. However, qPCR results indicated an early increase in gene expression, suggesting that the upregulation of the gene was the result of the decrease in protein levels rather than a neurotoxic effect on the expression of its gene. It is possible that the reduction of protein levels may be explained by a posttranslational effect of both neurotoxicants. Other mechanisms may also be involved. Occludin proteolysis in endothelial cells has been associated with increases in permeability (Wachtel *et al*., 1999), and this suggests the activation of otherwise inactive proteases in the paracellular space between endothelial cells of the BBB. Extracellular matrix metalloproteinases mediate many different proteolytic reactions involving cellular surfaces elements, including adhesion molecules, receptors, and intercellular junction proteins, and at least one (MMP-9), has been associated with disruption of occludin and claudin 5 in brain endothelial cells *in vitro* (Chen *et al*., 2009;

Fujimura *et al*., 1999). Calcium influx has been associated with activation of metalloproteinases (Barbosa *et al*., 2006; Kohn *et al*., 1994), and lead exposure is associated with activation of calcium-associated pathways (Schanne *et al*., 1997, Goldstein, 1993). Therefore, further assessments are necessary in order to elucidate if activation of metalloproteinases by these neurotoxicants using mechanisms associated with intracellular calcium increases is responsible for the changes in occludin levels in BBB endothelial cells.

Claudin 5 gene expression was downregulated by both neurotoxicants and their combinations, and the protein levels assessed by western blots demonstrated a pattern of protein levels concurrent with the gene expression. However, even when the gene was over-expressed (24 hr), protein levels were still below those of the controls suggesting the presence of additional mechanisms contributing to reducing protein levels. Like occludin, claudin 5 decreases have been associated with MMP-9 activation and permeability of endothelial cells (Chen *et al*., 2009; Fujimura *et al*., 1999), but further studies are necessary to elucidate if this activation is the result of neurotoxicant insult by lead and malathion.

Gene expression of scaffold proteins ZO1and ZO2 was upregulated, but protein levels were decreased for all the neurotoxicants treatments. Even at 24 hr when the gene expression was dramatically increased, there was still a decrease in protein levels in response to neurotoxicant insult. It, therefore, appears that protein decreases in response to neurotoxicant insult were disconnected from gene expression. ZO1 is an intracellular protein, and cannot be affected by metalloproteinases activation. However, lead and organophosphates have been associated with increases in intracellular calcium levels (Goldstein, 1993; Long *et al.*, 1994; Schanne *et al.*, 1997; Marcovac and Goldstein, 1998; Schuh *et al.*, 2002; Tiruppathi *et al.*, 2003; Wang *et al.*, 2006), and increases in intracellular calcium levels are associated with increases in

barrier permeability (Kerper and Hinkle, 1997; Brown and Davis, 2002; Tiruppathi *et al.*, 2003; Wang et al., 2006) mostly due to re-adjustment of scaffold proteins and their actin cytoskeleton support. It is possible, therefore, that calcium activation contributes to ZO1 and ZO2 protein decreases in RBE4 endothelial cells after lead and malathion exposure.

The results suggest that both malathion and its esterase-inhibiting metabolite malaoxon, can induce decreases in protein levels and changes in gene expression. The results of the present study also suggest that lead has a greater effect on tight junction proteins compared to organophosphates, whereas organophosphates seem to have a greater impact on scaffold proteins. This is notable because it may contribute to changes in damaging effects when exposures to combinations of these neurotoxicants occur.

Permeability of the BBB is associated with many pathological conditions and disruption of the tight junction proteins and scaffold proteins that form and support this structure are one of the main causes of such permeability. We show in this work with rat RBE4 cells that disruption and decreases in levels of tight junction proteins occludin and claudin 5, and scaffold proteins ZO1 and ZO2, does not correlate with upregulation or downregulation of gene expression, and therefore new approaches are necessary to elucidate the mechanism or mechanisms involved in the decreases of protein levels induced by lead and malathion treatments in RBE4 cells.

This study does note, however, that these neurotoxicants decrease the proteins associated with tight junction formation, and that this loss probably contributes to neurotoxicant transfer across the BBB. The decreases in occludin, claudin 5, ZO1, and ZO2 protein levels demonstrated in this work confirms a relationship between neurotoxicant insults and increase in permeability due to tight junction and scaffold protein damage.

REFERENCES

Abbott N J, Ronnback L, Hansson E. Astrocyte-endothelial interactions at the blood- brain barrier. Nat Rev Neurosci 2006; 7:41-53.

Abbott NJ. Astrocyte-endothelial interactions and blood-brain barrier permeability. J Anat 2002; 200:629-638.

Abou-Donia MB. Organophosphorus ester-induced chronic neurotoxicity. Arch Environ Health 2003; 58:484-498.

Alavijeh MS, Chishty M, Qaiser MZ, Palmer AM. Drug metabolism and pharmacokinetics, the blood-brain-barrier, and central nervous system drug discovery. NeuroRx 2005; 2:554-571.

Ando-Akatsuka Y, Saitou M, Hirase T, Kishi M, Sakaqkibara A, Itoh M, Yonemura S, Furuse M, Tsukita S. Interspecies diversity of the occludin sequence: cDNA cloning of human, mouse, dog, and rat-kangaroo homologues. J Cell Biol 1996; 133:43–48.

Balbuena P, Li W, Magnin-Bissel G, Meldrum B, Ehrich M. Comparison of two blood-brain barrier *in vitro* systems: Cytotoxicity and transfer assessments of malathion/oxon and lead acetate. Toxicol Sci 2010, 114:260-271.

Balda MS, Anderson JM. Two classes of tight junctions are revealed by ZO1 isoforms. Am J Physiol 1993; 264:C918–C924.

Balda SM, Matter K. Tight junctions. J Cell Sci 1998; 111:541-547.

Ballabh P, Braun A, Nedergaard M. The blood-brain barrier: An overview of structure, regulation, and clinical implications. Neurobiol Dis 2004; 16:1-13.

Barbosa F, Gerlach RF, Tanus-Santos JE. Matrix metalloproteinase-9 activity in plasma correlates with plasma and whole blood lead concentrations. Basic Clin Pharmacol Toxicol 2006; 98:559-564.

Bouldin TW, Mushak P, O'tuama LA, Krigman MR. Blood-brain barrier dysfunction in acute lead encephalopathy: a reappraisal. Env Health Perspect 1975; 12:81-88.

Brightman MW, Reese TS. Junctions between intimately apposed cell membranes in the vertebrate brain. J Cell Biol 1969; 40:648-677.

Brown RC, Davis TP. Calcium modulation of adherens and tight junction function: a potential mechanism for blood-brain barrier disruption after stroke. Stroke 2002; 33:1706-17011.

Chen F, Ohashi N, Li W, Eckman C, Nguyen JH. Disruption of occludin and claudin-5 in brain endothelial cells in vitro and in brains of mice with acute liver failure. Hepatology 2009; 50:1914-1923.

Citi S. The cytoplasm plaque protein of the tight junction. In: Cereijido M, Anderson J, editors. Tight Junctions 2nd Edition. Florida: CRC Press LLC; 2001. p. 231-264.

Eddleston M, Buckley NA, Eyer P, Dawson AH. Management of acute organophosphorus pesticide poisoning. Lancet 2008; 3781:597-607.

Ehrich M, Gross WB. Modification of TOTP toxicity in chickens by stress. Toxicol Appl Pharmacol 1983; 70:249-254.

Ehrich M. Organophosphates. In: Wexler P, editor. Encyclopedia of Toxicology Vol. 2, San Diego: Academic Press; 2005. pp 308-311.

El-Fawal HAN, Correll L, Gay L, Ehrich M. Protease activity in brain, nerve, and muscle of hens given neuropathy-inducing organophosphates and a calcium channel blocker. Toxicol App Pharmacol 1990; 103:132-142.

Environmental Protection Agency. (2000-2001). Pesticide market estimates. Pesticide industry sales webpage. Retrieved August 10, 2009, from http://www.epa.gov/oppbead1/pestsales/01pestsales/usage2001_3.htm#3_8

Fanning AS, Little BP, Rahner C, Utepbergenov D, Walther Z, Anderson JM. The unique -5 and -6 motifs of ZO1 regulate tight junction strand localization and scaffold properties. Mol Biol Cell 2007; 18:721-731.

Farquhar MG, Palade GE. Junctional complexes in various epithelia. J Cell Biol 2004; 17:375-412.

Filippelli GM, Laidlaw MA. The elephant in the playground: confronting lead-contaminated soils as an important source of lead burdens to urban populations. Perspect Biol Med 2009; 53:31-45.

Fujimura M, Gasche Y, Morita-Fujimura Y, Massengale J, Kawase M, Chan PH. Early appearance of activated matrix metalloproteinase-9 and blood-brain barrier disruption in mice after cerebral ischemia and reperfusion. Brain Res 1999; 842:92-100.

Furuse M, Fujita K, Hiragi T, Fujimoto K, Tsukita S. Claudin-1 and -2: novel integral membrane proteins localizing at tight junctions with no sequence similarity to occludin. J Cell Biol 1998; 141:1539–1550.

Furuse M, Hirase T, Itoh M, Nagafuchi A, Yonemura S, Tsukita S. Occludin: a novel integral membrane protein localizing at tight junctions. J Cell Biol 1993; 123:1777–1788.

Giepmans BN, Moolenaar WH. The gap junction protein conexin-43 interacts with the second PDZ domain of the zona occludens-1 protein. Curr Biol 1998; 8:931-934.

Gilbert ME, Mack CM, Lasley SM. Chronic developmental lead exposure increases the threshold for long term potentiation in rat dentate gyrus *in vivo*. Brain Res 1996; 736:118-124.

Gilbert ME, Mack CM. Chronic lead exposure accelerates decay of long term potentiation in rat dentate gyrus *in vivo*. Brain Res 1998; 789:139-149.

Goldstein GW, Asbury AK, Diamond I. Pathogenesis of lead encephalopathy: uptake of lead and reaction of brain capillaries. Arch Neurol 1974; 31:382-389.

Goldstein GW. Evidence that lead acts as a calcium substitute in second messenger metabolism. Neurotoxicol 1993; 14:97-101.

Grebenkämper K, Galla HJ. Translational diffusion measurements of a fluorescent phospholipid between MDCK-1 cells support the lipid model of the tight junctions. Chem Phys Lipid 1994; 71:133-143.

Gunnell D, Eddleston M, Phillips MR, and Konradsen F. The global distribution of fatal pesticide self-poisoning: systematic review. BMC Public Health 2007; 7:357-372.

Harel M, Kryger G, Rosenberry TL, Mallender WD, Lewis T, Fletcher RJ, Guss JM, Silman I, Sussman JL. Three-dimentional structures of *Drosophila melanogater* acetylcholinesterase and of its complexes with two potent inhibitors. Protein Sci 2000; 9:1063-1072.

Haskins J, Gu L, Wittchen ES, Hibbard J, Stevenson BR. ZO-3, a novel member of the MAGUK protein family found at the tight junction, interacts with ZO1 and occludin. J Cell Biol 1998; 141:199–208.

Hawkins BT, Davis TP. The blood-brain barrier/neurovascular unit in health and disease. Pharmacol Rev 2005; 57:173-185.

Hein M, Madefessel C, Haag B, Teichmann K, Post A, Galla HJ. Implications of a non-lamellar lipid phase for the tight junction stability. part II: reversible modulation of transepithelial resistance in high and low resistance MDCK-cells by basic amino acids, Ca+, protoamine and protons. Chem Phys Lipid 1992; 63:223-233.

Itoh M, Furose M, Morita K, Kubota K, Saitou M, Tsukita S. Direct binding of three tight junction-associated MAGUKs, ZO1, ZO-2, and ZO-3 with the COOH termini of claudins. J Cell Biol 1999; 147:1351-1363.

Jesaitis LA, Goodenough DA. Molecular characterization and tissue distribution of ZO-2, a tight junction protein homologous to ZO1 and the Drosophila discs-large tumor suppressor protein. J Cell Biol 1994; 124:949–962.

Jortner B, Ehrich M. Neurophatological effects of phenyl saligenin phosphate in chickens. Neurotoxicol 1987; 8:97-108.

Kerper LE, Hinkle PM. Lead uptake in brain capillary endothelial cells: activation by calcium store depletion. Toxicol App Pharmacol 1997; 146:127-133.

Kniesel U, Wolburg H. Tight junctions of the blood-brain barrier. Cell Mol Neurobiol 2000; 20:57-76.

Kohn EC, Jacobs W, Kim YS, Alessandro R, Stetler-Stevenson WG, Liotta LA. Calcium influx modulates expression of matrix metalloproteinase-2 (72-kDa type IV collagenase, gelatinase A). J Biol Chem 1994; 269:21505-21511.

Kurihara H, Anderson JM, Farquhar MG. Diversity among tight junctions in rat kidney: glomerular slit diaphragms and endothelial junctions express only one isoform of the tight junction protein ZO1. Proc Natl Acad Sci 1992; 89:7075-7079.

Liebner S, Kniesel U, Kalbacher H, Wolburg H. Correlation of tight junction morphology with the expression of tight junction proteins in blood-brain barrier endothelial cells. Eur J Cell Biol 2000; 79:707-717.

Livak KJ, Schmittgen TD. Analysis of relative gene expression data using real-time quantitative PCR and the C_T method. Methods. 25: 402-408, 2001.

Lochhead JJ, McCaffrey G, Quigley CE, Finch J, Demarco KM, Nametz N, Davis TP. Oxidative stress increases blood-brain barrier permeability and induces alterations in occludin during hypoxia-reoxygenation. J Cereb Blood Flow Metab. Epub ahead of print, doi:10.1038/jcbfm.2010.29.

Long GJ, Rosen JF, Schanne FAX. Lead activation of protein kinase C from rat brain. J Biol Chem 1994; 14:834-837.

Marcovac J, Goldstein GW. Picomolar concentrations of lead stimulate brain protein kinase C. Nature 1988; 334:71-73.

McCaffrey G, Willis CL, Staatz WD, Nametz N, Quigley CA, Hom S, Lochhead JJ, Davis TP. Occludin oligomeric assemblies at tight junctions of the blood-brain barrier are altered by hypoxia and reoxygenation stress. J Neurochem 2009; 110:58-71.

Morita K, Furuse M, Fujimoto K, Tsukita S. Claudin multigene family encoding four transmembrane domain protein components of tight junction strands. Proc Natl Acad Sci 1999a; 96:511-516.

Morita K, Sasaki H, Furose M, Tsukita S. Endothelial claudin: claudin-5/TMVCF constitutes tight junction strands in endothelial cells. J Cell Biol 1999b; 147:185-194.

Musch MW, Walsh-Reitz MM, Chang EB. Roles of ZO1, occludin, and actin in oxidant-induced barrier disruption. Am J Physiol Gastrointest Liver Physiol 2006; 290: 222-231.

Nitta T, Hata M, Gotoh S, Seo Y, Sasaki H, Hashimoto N, Furuse M, Tsukita S. Size-selective loosening of the blood-brain barrier in claudin-5-deficient mice. J Cell Biol 2003; 161:653-660.

Omidi Y, Barar J, Ahmadian S, Heidari HR, Gumbleton M. Characterization and astrocytic modulation of system L transporters in brain microvasculature endothelial cells. Cell Biochem Funct 2008; 26:381-391.

Parran DK, Magnin G, Li W, Jortner BS, Ehrich M. Chlorpyrifos alters functional integrity and structure of an *in vitro* model: co-cultures of bovine endothelial cells and neonatal rat astrocytes. Neurotoxicol 2005; 26:77-88, 291.

Petroianu GA, Lorke DE, Hasa MY, Adem A, Sheen R, Nurulain SM, Kalasz H. Paraoxon has a minimal effect on pralidoxime brain concentration in rats. J Appl Toxicol 2007; 27:350-357.

Schanne FAX, Long GJ, Rosen JF. Lead-induced rise in intracellular free calcium is mediated trough activation of protein kinase C in osteoblastic bone cells. Biochim Biophys Acta 1997; 1360:247-254.

Schuh RA, Lein PJ, Beckles RA, Jett DA. Non-cholinesterase mechanisms of chlorpyrifos neurotoxicity: altered phosphorylation of CA^{2+}/ cAMP response element binding protein in cultured neurons. Toxicol Appl Pharmacol 2002; 182:176-185.

Shi LZ, Zheng W. Early lead exposure increases the leakage of the blood-cerebrospinal fluid barrier *in vitro*. Hum Exp Toxicol 2007; 26:159-167.

Stevenson BR, Siliciano JD, Mooseker MS, Goodenough DA. Identification of ZO1: a higher molecular weight polypeptide associated with the tight junction (zonula occludens) in a variety of epithelia. J Cell Biol 1986; 103:755–766.

Tiruppathi C, Minshall RD, Paria BC, Vogel SM, Malik AB. Role of Ca2+ signaling in the regulation of endothelial permeability. Vascul Pharmacol 2003; 39:173-185.

Toscano CD, Guilarte T. Lead neurotoxicity: from exposure to molecular effects. Brain Res Rev 2005; 49:529 – 554.

Tsukita S, Furose M. Pores in the wall: claudins constitute tight junction strands containing aqueous pores. J Cell Biol 2000; 149:13-16.

Wachtel M, Frei K, Ehler E, Fontana A, Winterhalter K, Gloor SM. Occludin proteolysis and increased permeability in endothelial cells through tyrosine phosphatase inhibition. J Cell Sci 1999; 112:4347-4356.

Wang W, Duan B, Xu H, Xu L, Xu T. Calcium-permeable acid-sending ion channel is a molecular target of the neurotoxic metal ion lead. J Biol Chem 2006; 281:2497-2505.

Wolburg H, Liebner S, Lippoldt A. Freeze-fracture studies of Cerebral endothelial tight junctions. Meth Mol Med 2003; 89:51-66.

Wolburg H, Lippoldt A, Ebnet K. Tight junctions and the blood-brain barrier. In: Gonzalez-Mariscal L, editor. Tight Junctions. New York: Springer Science+Business Media, 2006. pp 175-195.

Wolburg H, Lippoldt A. Tight junctions of the blood-brain barrier: development, composition and regulation. Vascul Pharmacol 2002; 38:323-337.

Yang J, Aschner M. Developmental aspects of blood-brain barrier (BBB) and rat brain endothelial (RBE4) cells as *in vitro* models for studies on chlorpyrifos transport. Neurotoxicol 2003; 24:741-745.

Tables and figures:

Gene	Accession Number	Primer/Forward	Primer/Reverse	Product Length (bp)
Occludin	BC062037	5'-GCCTTTTGCTTCATCGCTTCC-3'	5'-AACAATGATTAAAGCAAAAG-3'	186
Claudin 5	BC082073	5'-GCAGAGGCACCAGAACAG-3'	5'-CAGACACAGCACCAGACC-3'	162
ZO1	NM_001166266	5'-CTGAAGAGGATGAAGAGTATTACC-3'	5'-TGAGAATGGACTGGCTTGG-3'	220
ZO2	BC103479	5'-TGGAGGGGATGGATGATGAC-3'	5'-CGCCGTCCGTATCTTCAAAG-3'	195
B-actin	NM_053558	5'-TATCGGCAATGAGCGGTTCC-3'	5'-GTGTTGGCATAGAGGTCTTTACG-3'	144

Table 1 *Rattus norvegicus* oligonucleotide primer sequences used in the real time PCR assessments. All the primers were synthesized by Invitrogen (Carlsbad, CA).

FIGURE 1

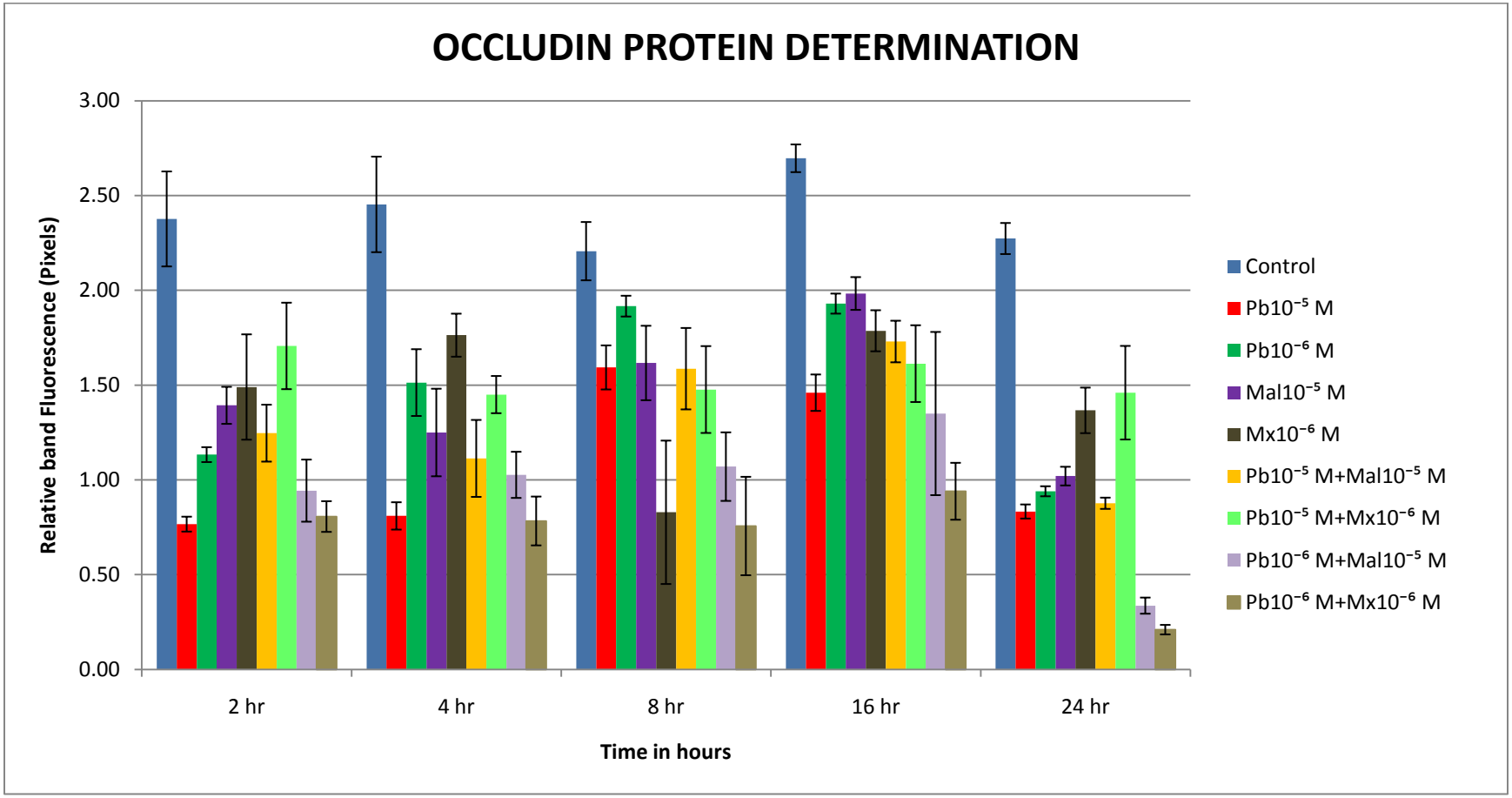

Figure 1. Western blot determination of occludin protein in RBE4 cells following the treatment with neurotoxicants at 5 different time periods. All treatments reduced occludin at all times (p<0.05). However, when compounds alone were compared to combinations, no statistical significances were noted. Bars represent means±SEM of at least three separate experiments (n=3) using three means of triplicate samples. Pb= lead, Mal= malathion, and Mx= malaoxon.

FIGURE 2

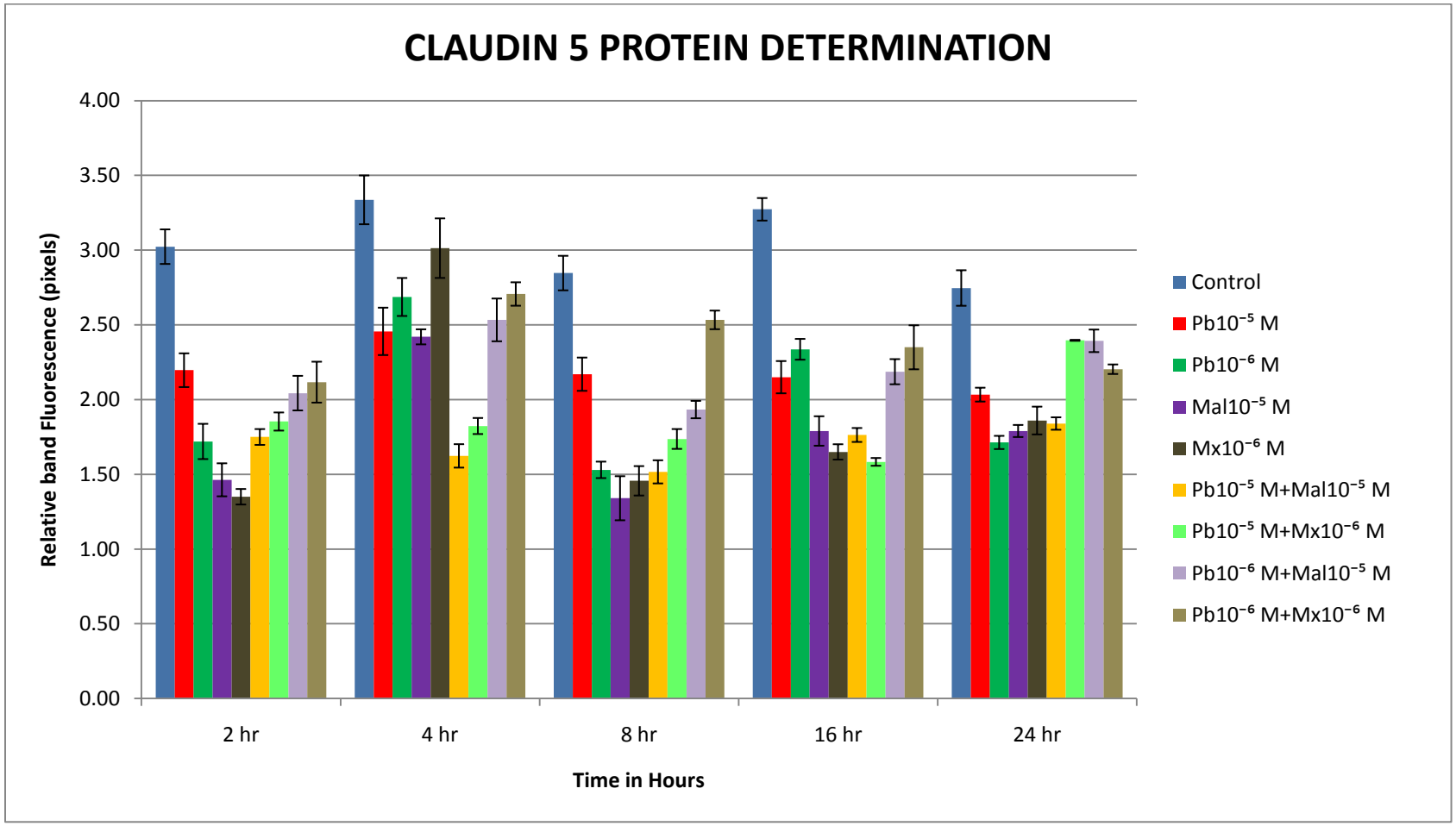

Figure 2. Western blot determinations of membrane bound claudin 5 protein in RBE4 cells following treatment with neurotoxicants at 5 different time periods. Claudin 5 protein was affected at all times by neurotoxicants ($p<0.05$), except by malaoxon (Mx) at 4 hr. However, combinations of the compounds did not increase the reduction of the protein when compared to the treatments of compounds alone. Pb= lead, Mal= malathion, and Mx= malaoxon.

FIGURE 3

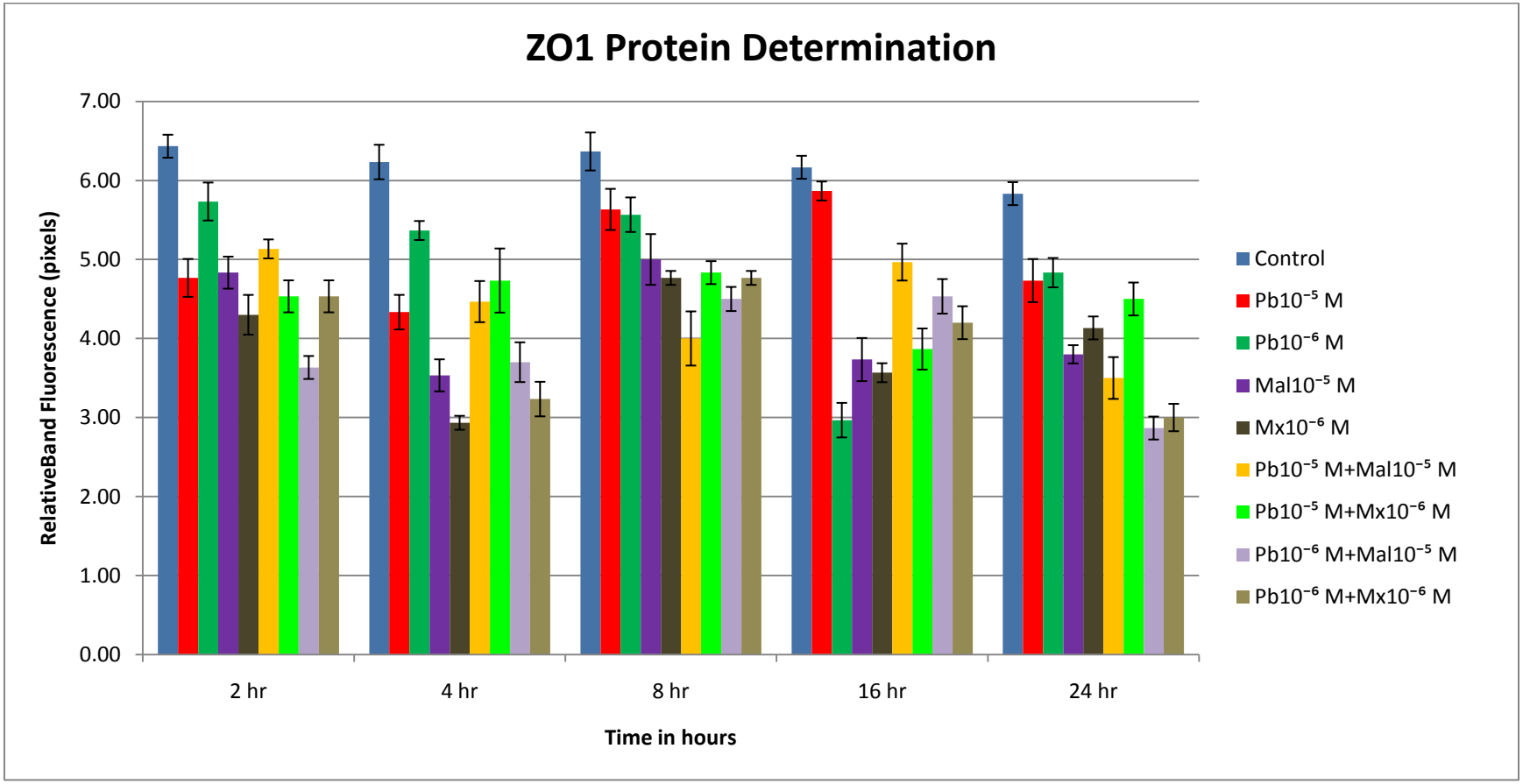

Figure 3. Western blot determinations of ZO1 protein in RBE4 cells following treatment with neurotoxicants at 5 different time periods. Neurotoxicants alone and in combination decreased protein at all time points ($p<0.05$), but in general, there was not a greater effect associated with combinations of the compounds. Pb= lead, Mal= malathion, and Mx= malaoxon.

FIGURE 4

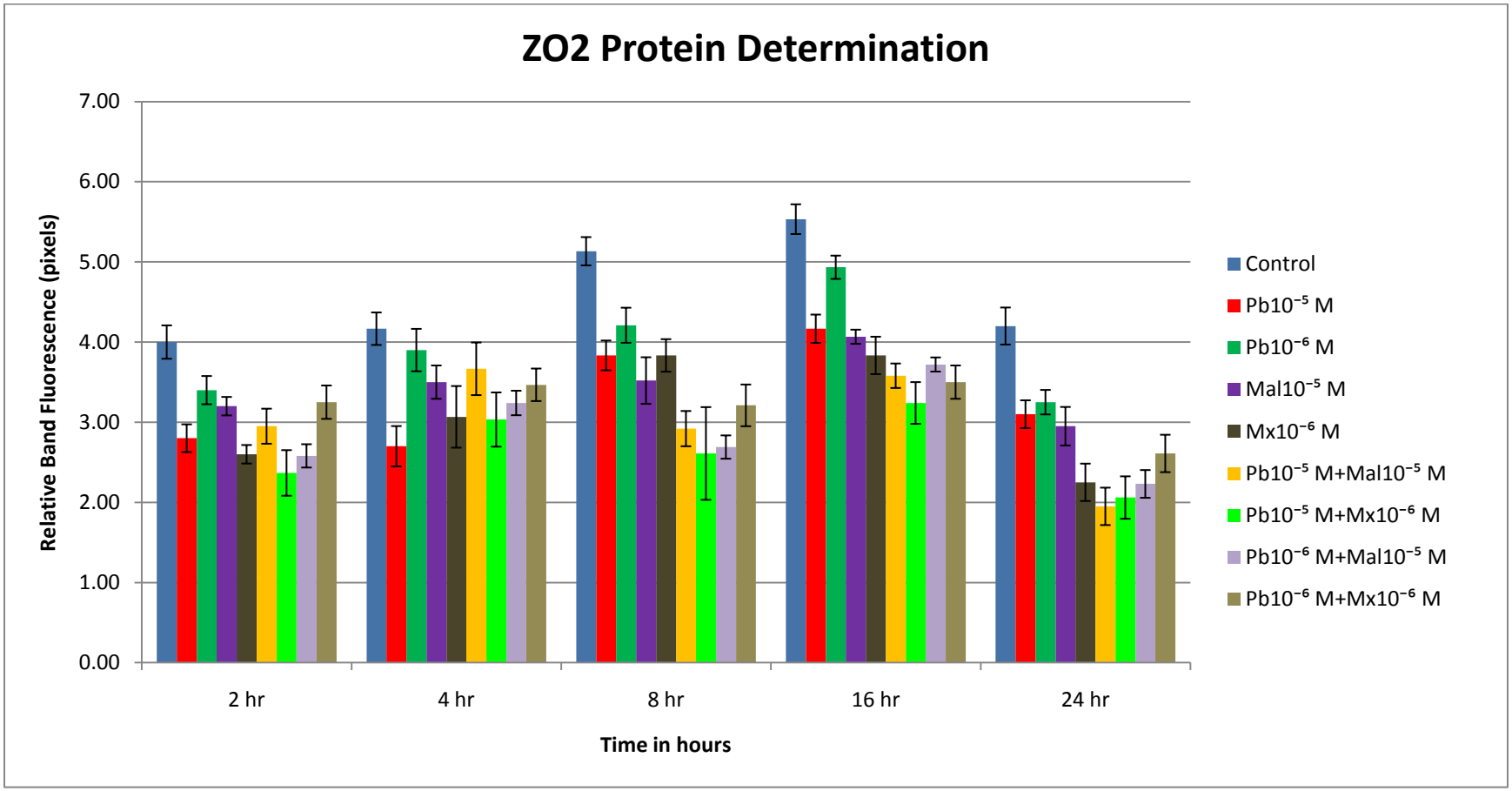

Figure 4. Western blot determinations of ZO2 protein in RBE4 cells following treatment with neurotoxicants at 5 different time periods. A significant decrease in protein levels was observed for all treatments when compared with control ($p<0.05$), except for the 4 hr period. Combinations of neurotoxicants in general increased damage. Bars represent means±SEM of at least three separate experiments. Pb= lead, Mal= malathion, and Mx= malaoxon.

FIGURE 5

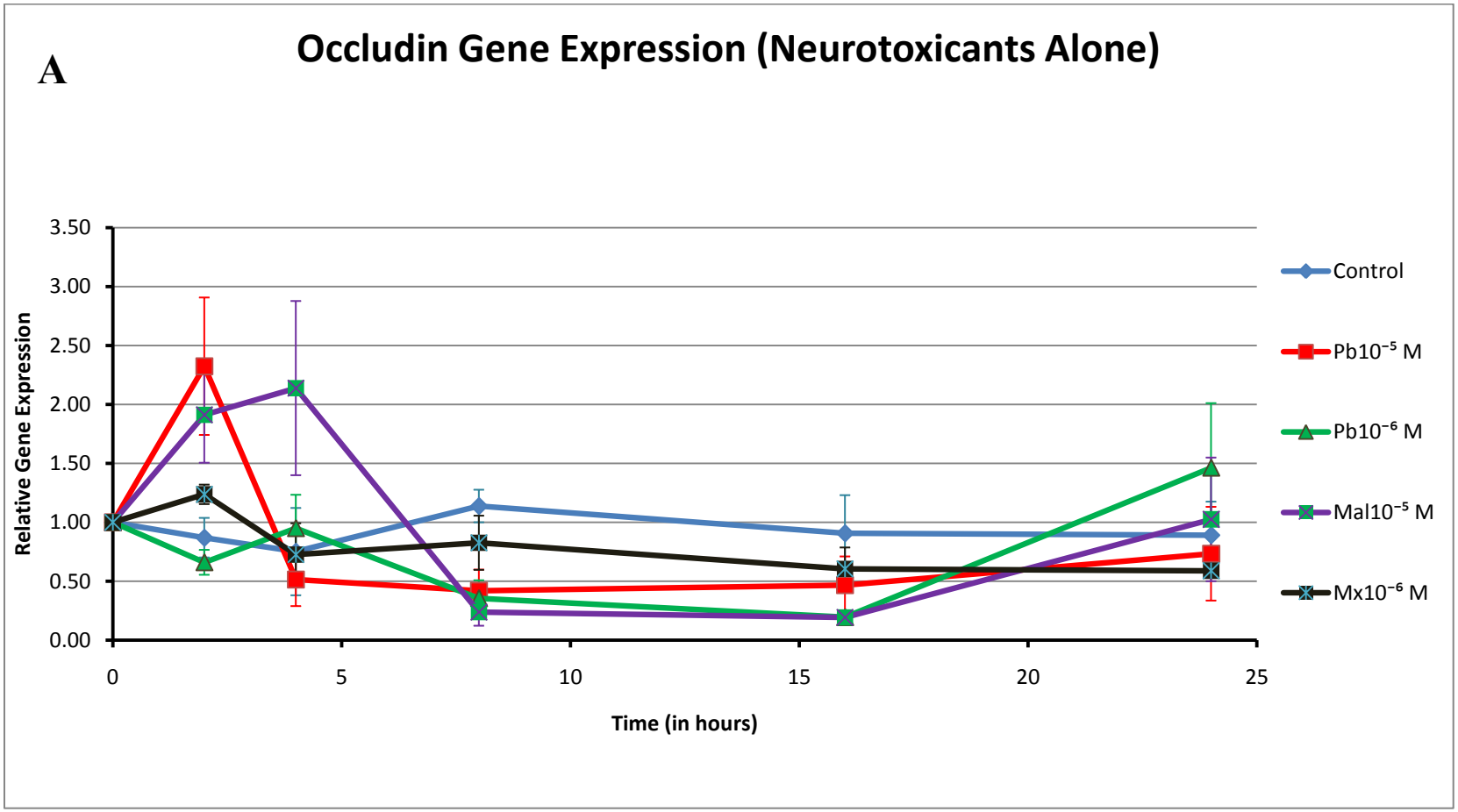

Figure 5a. Occludin gene expression in RBE4 cells after treatments with neurotoxicants alone. Gene expression was measured at 2hr, 4 hr, 8, hr, 16 hr, and 24 hr after exposure to lead (Pb), malathion (Mal), and malaoxon (Mx). Although it appears that lead 10^{-5} M and Mal 10^{-5} M upregulated gene expression at 2 hr and 4 hr respectively, especially since increases were greater than 2-fold, these increases were not statistically significant. Points represent means±SEM of at least three separate experiments (n=3) using three means of triplicate samples.

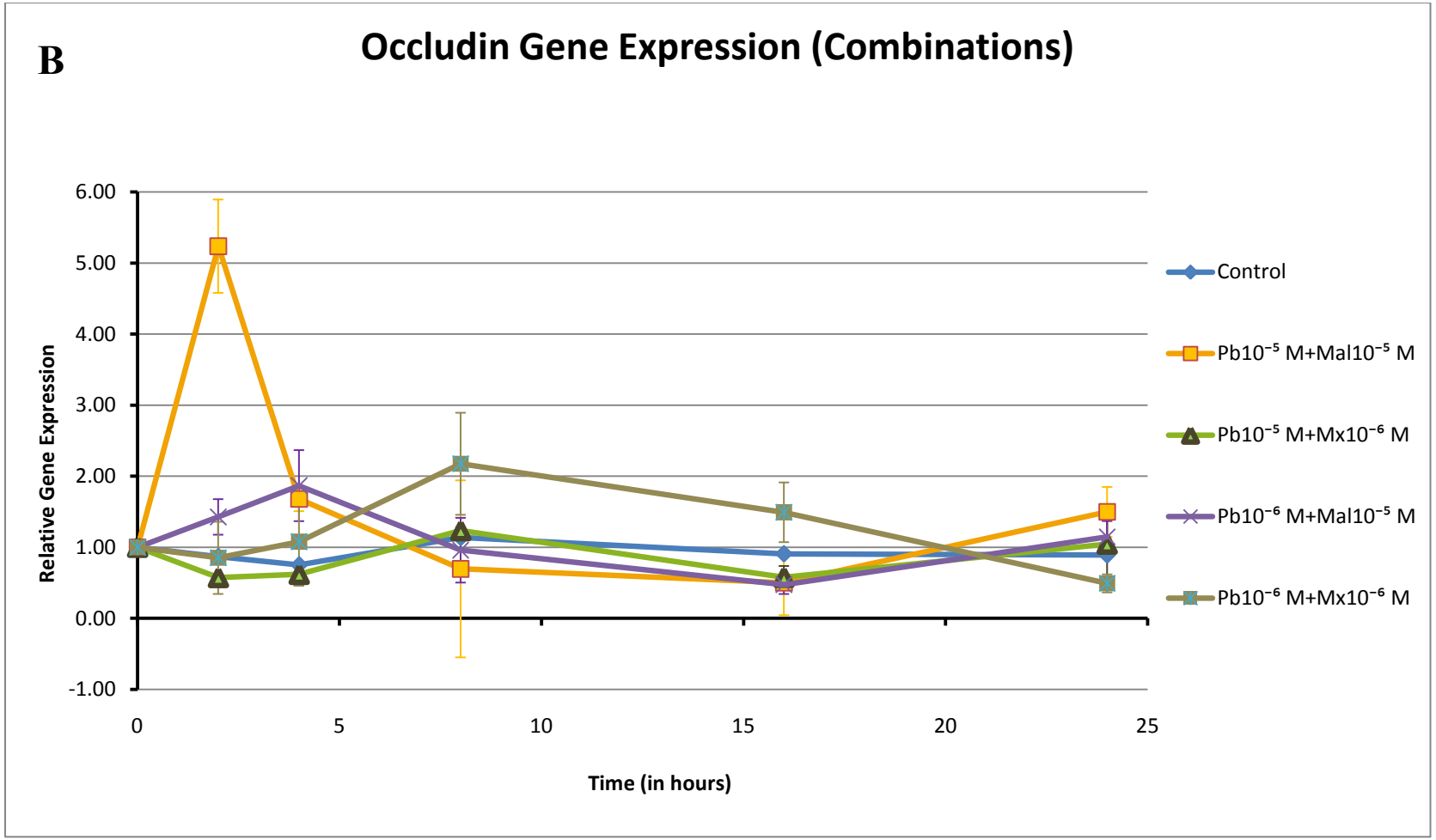

Figure 5b. RBE4 cells response in occludin gene expression to the combinations of the neurotoxicants. Only the combination of lead 10^{-5} M with Mal 10^{-5} M at 2 hr significantly increases gene expression. This combination increased the gene expression of occludin 5-fold (p<0.001) when compared to controls.

FIGURE 6

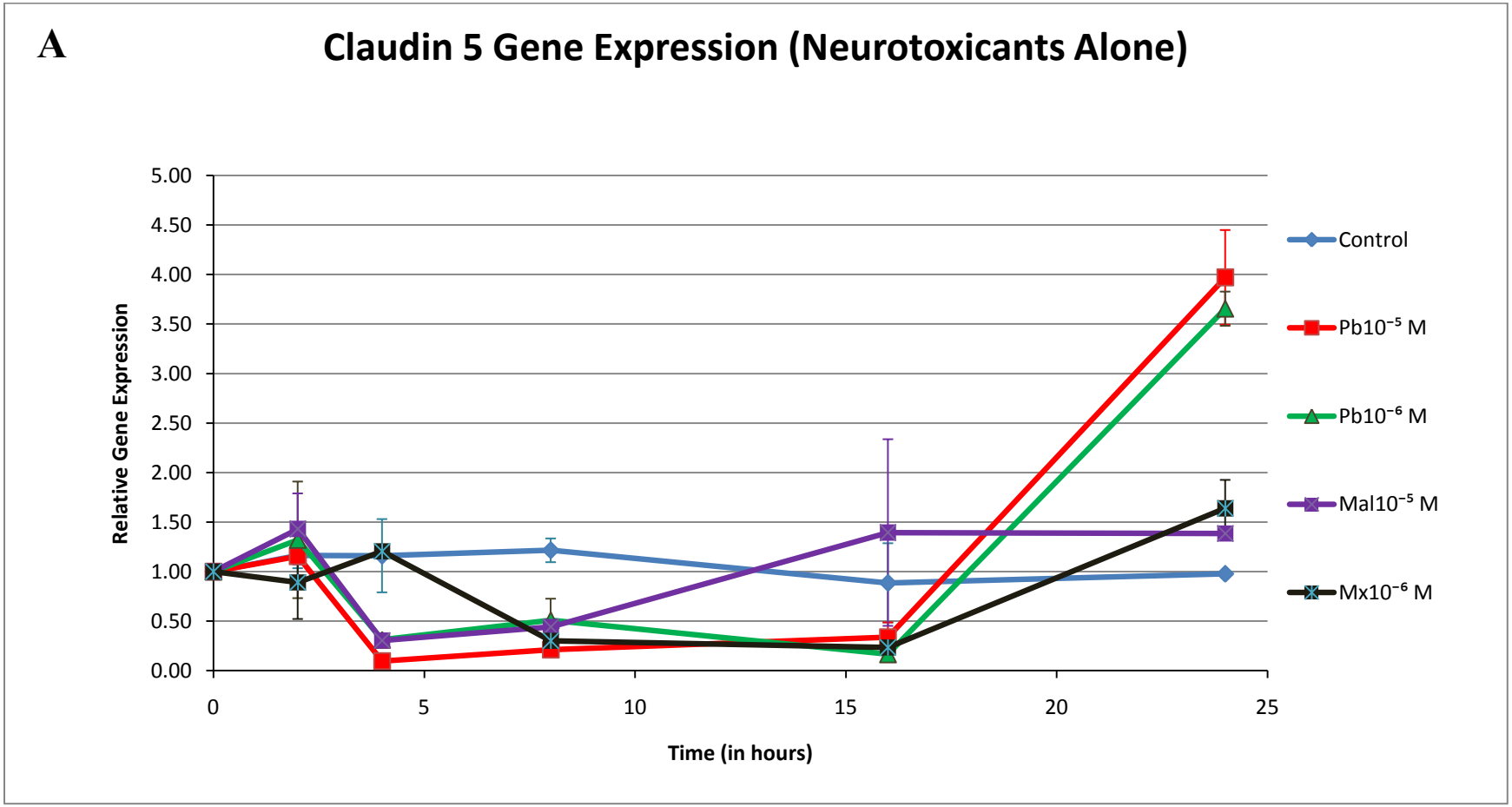

Figure 6a. RBE4 cells claudin 5 gene expression responses to treatments with neurotoxicants alone. Pb= lead, Mal= malathion, and Mx= malaoxon. All concentrations decreased Claudin 5 expression at 4 hr when compared to control ($p<0.05$), with the exception of Mx 10^{-6} M. In contrast, both concentrations of lead increased the gene expression at 24 hr by almost 4-fold ($p<0.001$). Organophosphates did not significantly increase the expression of the gene at 24 hr.

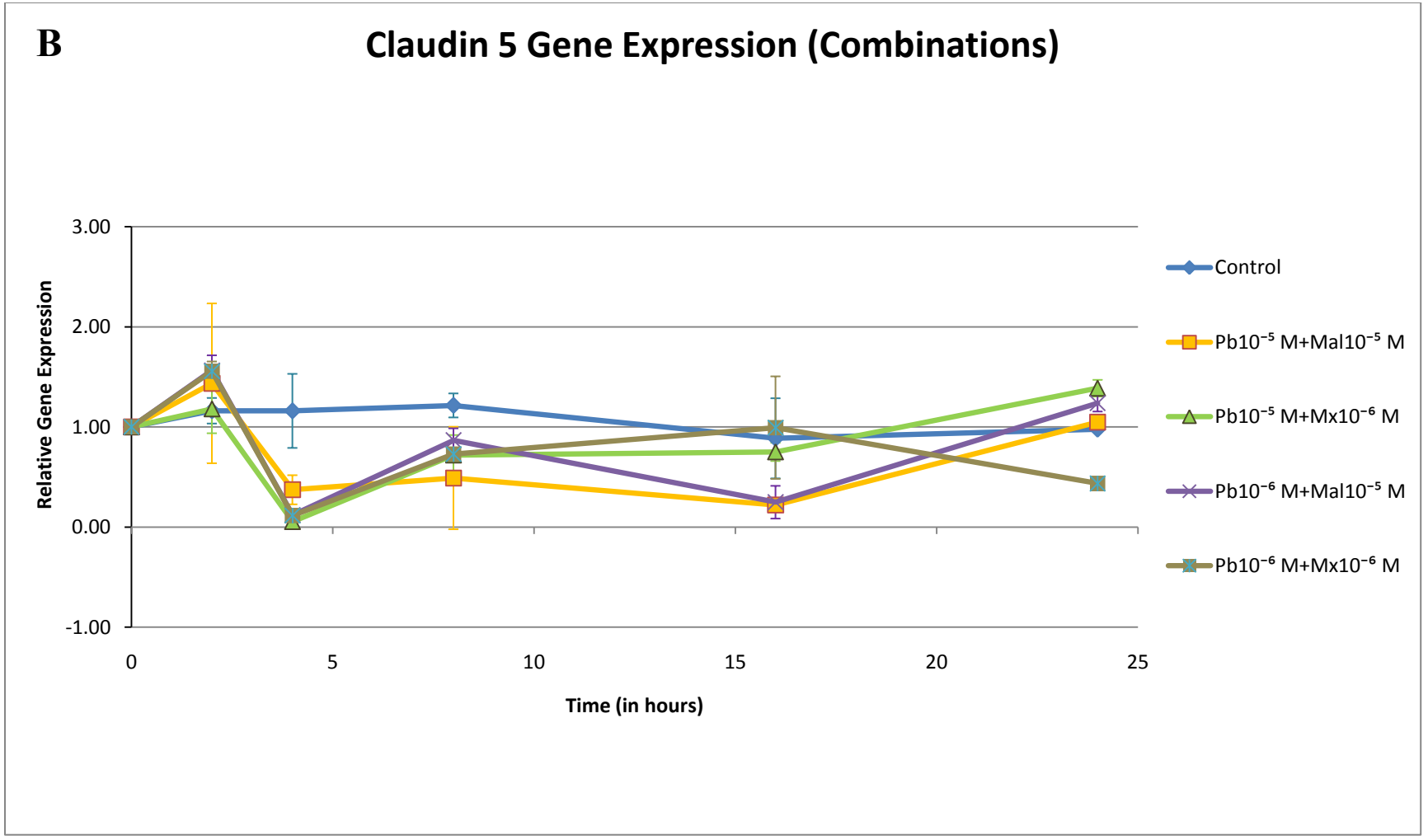

Figure 6b. RBE4 cells response in claudin 5 gene expression to treatments with combinations of the neurotoxicants. All combinations decreased claudin 5 expression at 4 hr (p<0.05). At 16 hr however, only the combinations of lead (Pb) with malathion (Mal) resulted in gene downregulation (p<0.05). At 24 hr, only the combination of lead ($Pb10^{-6}$ M) with malaoxon ($Mx10^{-6}$ M) was decreasing gene expression (p<0.05).

FIGURE 7

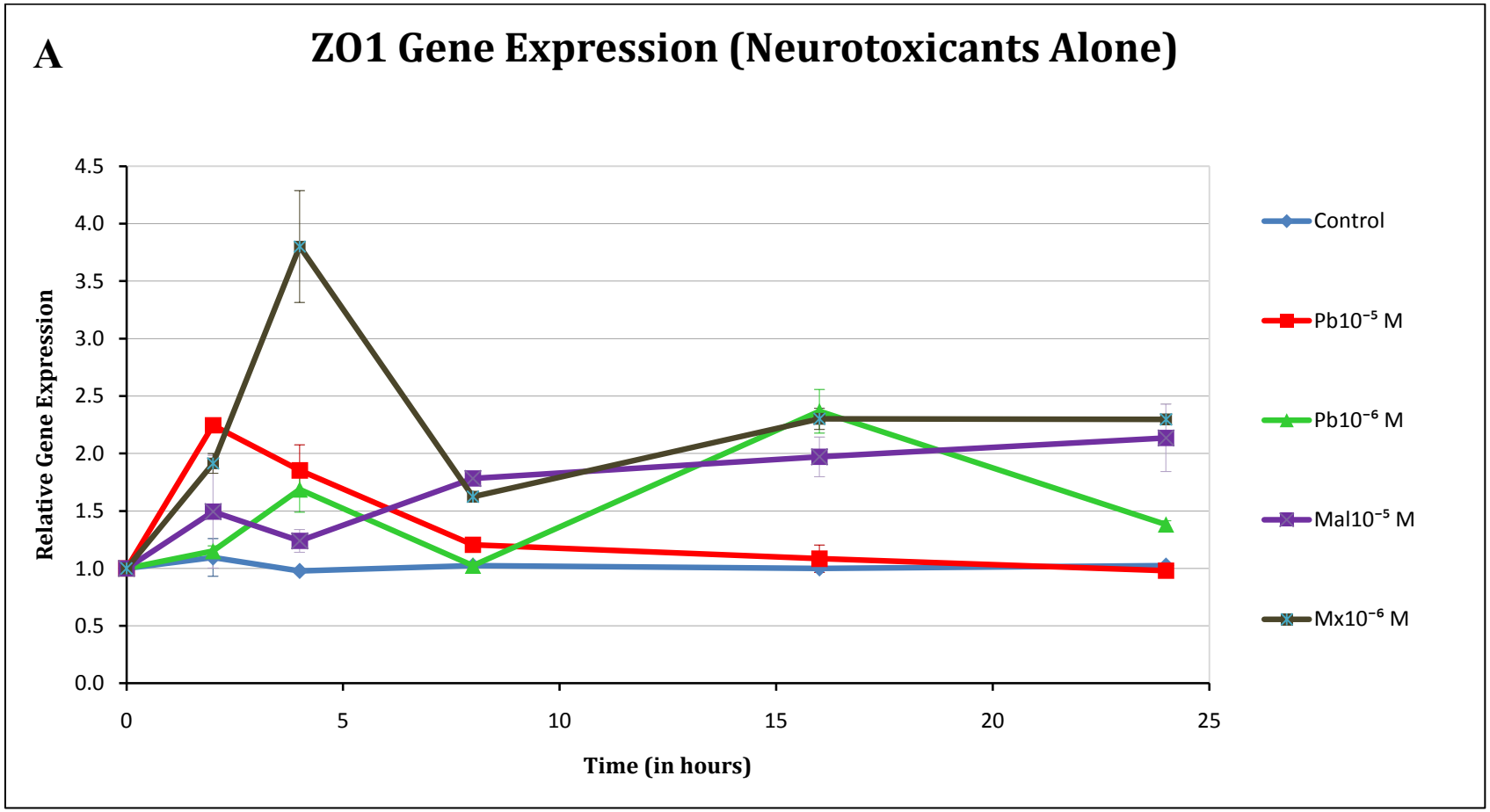

Figure 7a. RBE4 cells ZO1 gene expression in response to treatments with the neurotoxicants lead (Pb), malathion (Mal) and malaoxon (Mx) alone. Gene expression was increased dramatically by Mx 10^{-6} M at 4 hr ($p<0.001$), and by all the compounds at 16 hr and 24 hr with the exception of Pb 10^{-5} M ($p<0.05$).

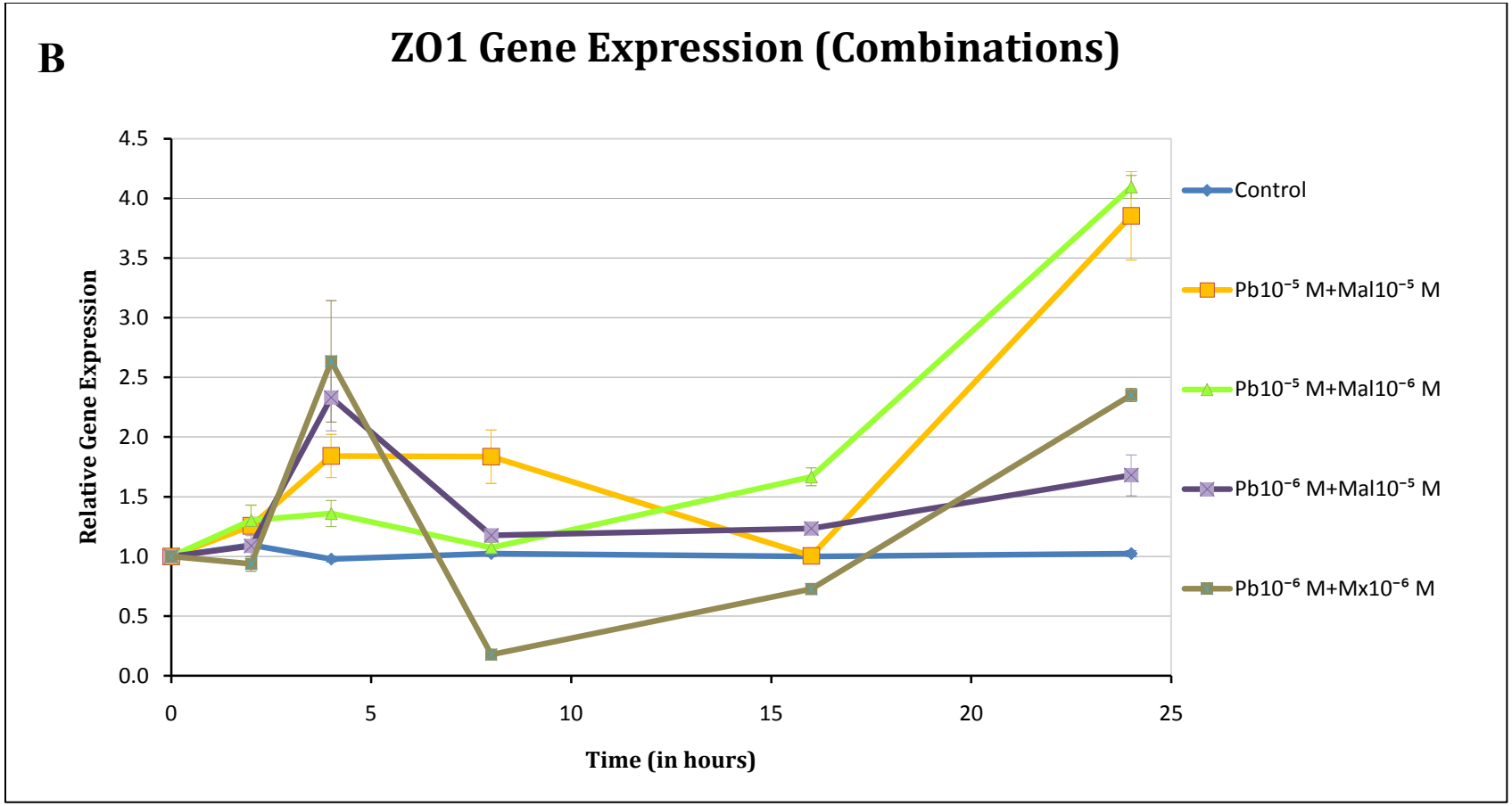

Figure 7b. RBE4 cells ZO1 gene expression responses to combinations of neurotoxicants. All combinations increased expression of ZO1 gene at 4 hr (p<0.05), with Pb 10^{-6} M combined with both malathion and malaoxon increasing it almost 2.5-fold. All combinations increased expression of the gene at 24 hr, but the combinations of lead 10^{-5} M with malathion or malaoxon increased ZO1 expression to almost 4-fold (p<0.01).

FIGURE 8

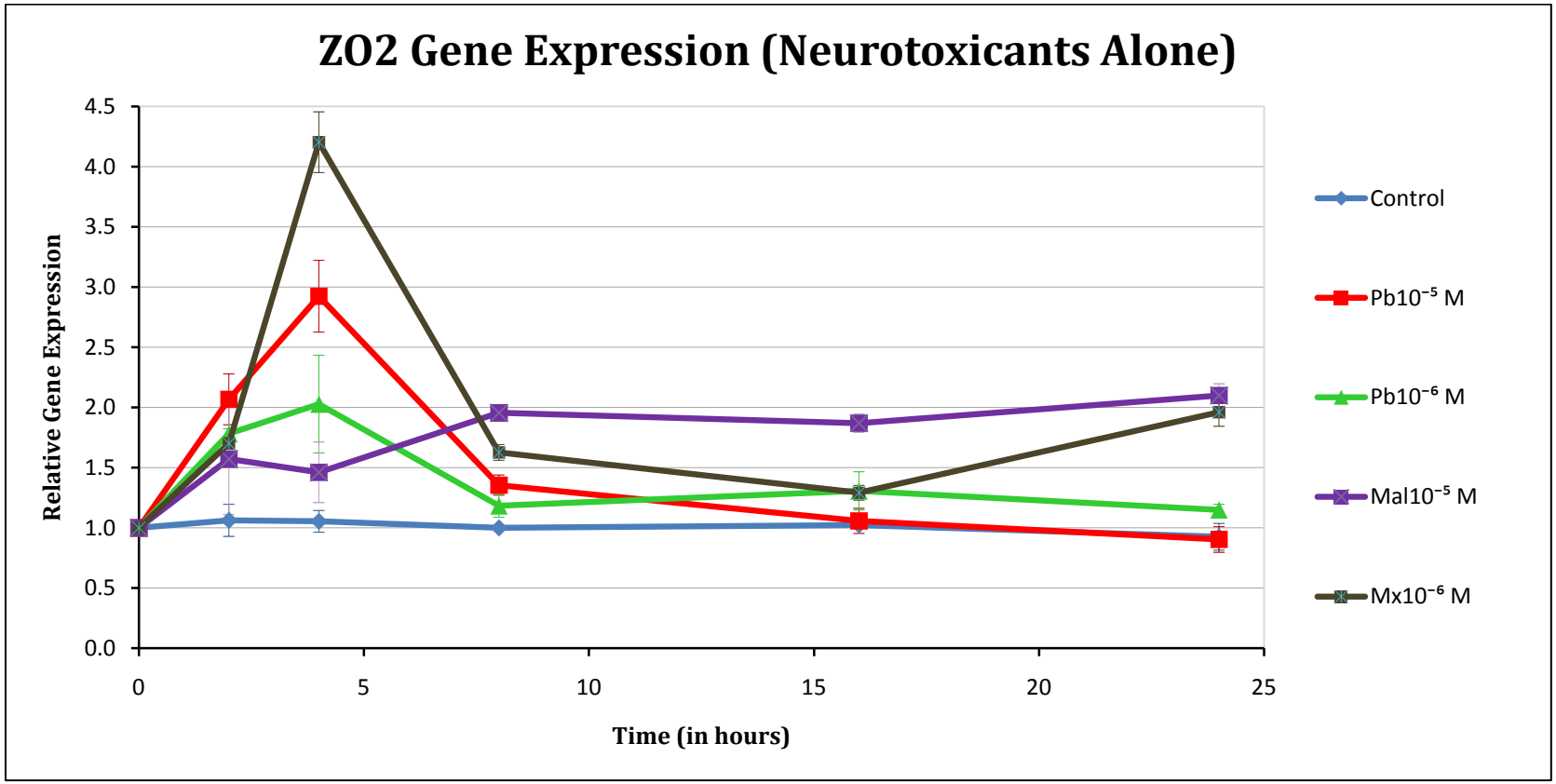

Figure 8a. Gene expression of ZO2 in RBE4 cells with treatments of neurotoxicants alone. Significant increases in gene expression were noted for all compounds at 4 hr ($p<0.05$); with gene expression for Pb 10^{-5} M increasing 3-fold ($p<0.01$), and expression in response to Mx 10^{-6} M increasing 4-fold ($p<0.01$). Gene expression was increased at all other times as well ($p<0.05$), except 8-24 hr after exposure to Pb 10^{-5} M.

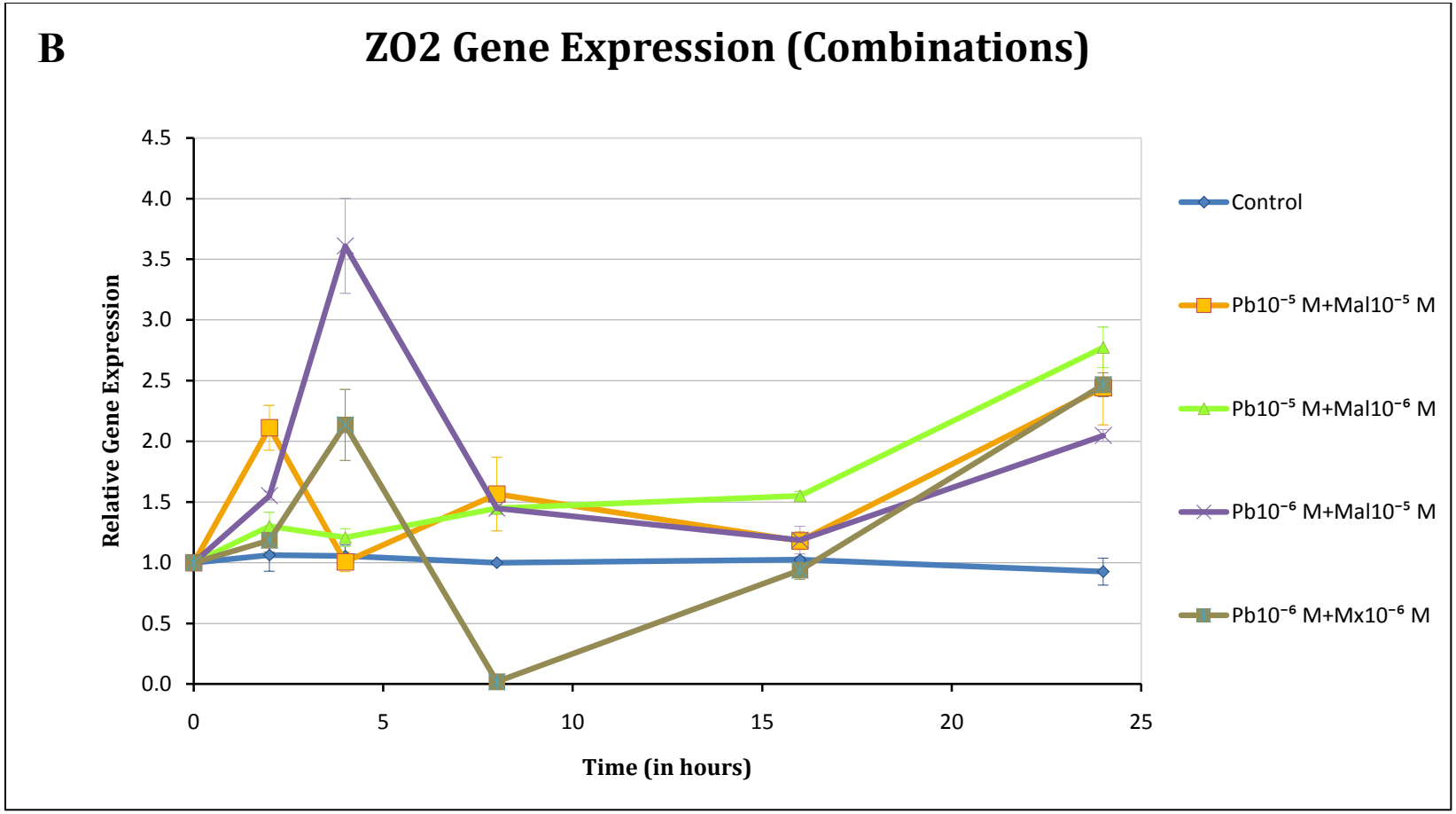

Figure 8b. ZO2 gene expression responses to treatments with combinations of neurotoxicants in RBE4 cells. $Pb10^{-5}$ M+$Mal10^{-5}$ significantly increased gene expression at 2 hr (2-fold, $p<0.05$) and $Pb10^{-6}$ M+$Mx10^{-6}$ M increased it to the same level for the 4 hr period. $Pb10^{-6}$ M+$Mal10^{-5}$ M increased ZO2 expression 3.5-fold at 4 hr ($p<0.01$). All combinations increase the expression of ZO2 gene at 24 hr ($p<0.05$).

Chapter 5:

MALATHION/OXON AND LEAD ACETATE INCREASE GENE EXPRESSION AND PROTEIN LEVELS OF TRANSIENT RECEPTOR POTENTIAL CANONICAL CHANNEL SUBUNITS TRPC1 AND TRPC4 IN RAT ENDOTHELIAL CELLS OF THE BLOOD-BRAIN BARRIER

Pergentino Balbuena[1], Wen Li[1], and Marion Ehrich[1]

[1]Virginia-Maryland Regional College of Veterinary Medicine, Virginia Tech, Blacksburg, VA,

Corresponding author: Marion Ehrich, Virginia-Maryland Regional College of Veterinary Medicine, 1 Duck Pond Drive, Virginia Tech, Blacksburg VA 24061.

Telephone (540) 231-6033; e-mail marion@vt.edu

ABSTRACT

Endothelial cells of the vasculature in the blood-brain barrier (BBB) regulate paracellular and transcellular transport by forming tight junctions between cells. Disruption of tight junctions increases permeability. Permeability disruption may also result in increases in intracellular calcium, which can be caused by opening of TRPC channels.

This study examined malathion and lead effects on store-operated calcium channels TRPC1/TRPC4 in rat brain endothelial cells (RBE4s). Lead 10^{-5} M and 10^{-6} M, malathion 10^{-5} M, malaoxon 10^{-6} M, and combinations of these four concentrations were assessed for protein levels by immunoblotting assessments, and then, analyzed for gene expression by real time PCR. Measurements included time periods of 2 hr, 4 hr, 8 hr, 16 hr, and 24 hr.

Both lead and malathion and their combinations increased TRPC1 and TRPC4 protein levels as well as gene expression within 4 hr after exposure. Since increases in gene and protein expression can be associated with an increase in numbers of TRPC channels, this increase may be a mechanism by which these neurotoxicants affect permeability.

Key words: BBB, TRPC1, TRPC4, permeability, lead, malathion.

INTRODUCTION

Microvascular endothelial cells of the blood–brain barrier (BBB) are structured to maintain a tightly regulated control on paracellular and intracellular molecular transport between the brain and the blood systemic circulation (Abbott 2002). This transport regulation is critical for homeostasis in the central nervous system (CNS) and is responsible for the total restriction of paracellular ion transport in the BBB (de Boer et al., 2003; Hawkins and Davis, 2005). Endothelial cells of the BBB implement this function by way of tight junction structures present between adjacent cells of the brain microvasculature that restrict the passage of molecules through the paracellular space (Balda and Matter, 2000; Gonzalez-Mariscal *et al*., 2003; Kniesel and Wolburg, 2000; Liebner *et al*.,2000; Wolburg *et al*., 2006). Occludin and the claudin family are the most important membranous components of the tight junctions (Ando-Akatsuka *et al*., 1996; Furuse *et al*., 1993; Furuse *et al*., 1998; Tsukita and Furuse, 2000), and claudin 5 is expressed specifically in tight junctions of the BBB (Morita et al., 1999; Nitta et al., 2003) suggesting a specific role in BBB function. Disruption of tight junction structures results in increases in permeability which is associated with several pathological conditions such as ischemic stroke (Brouns and De Deyn, 2009; Kidwell *et al*., 2008; Takenaga *et al*., 2009), traumatic brain injury (Ballabh *et al*., 2004; Lotocki *et al*., 2009), multiple sclerosis (Hawkins and Davis, 2005; Kirk *et al*., 2003; McQuaid *et al*., 2009), and Alzheimer's disease (Starr *et al*., 2009).

Increases in intracellular calcium are associated with increases in permeability in endothelial cells by inducing gap formation between cells (Tiruppathi *et al*., 2003). Increases of the cytoplasmic Ca^{2+} by depletion of intracellular stores through the store-operated calcium (SOC) entry pathway are associated with increases in permeability (Tiruppathi *et al*., 2006;

Cioffi and Stevens, 2006; Parekh and Putney Jr., 2005). Disruption in BBB permeability has also been associated with increases in intracellular calcium in endothelial cells initiated by transient receptor potential canonical (TPRC) channel activity (Antoniotti *et al*., 2006; Brown and Davis, 2002; Cioffi and Stevens, 2006; Gias and Asrar, 2005; Tiruppathi *et al*., 2003; Tiruppathi *et al*., 2006).

The present study examined the effects of two neurotoxic substances, lead and malathion, on TRPC channels activity in rat brain endothelial cells (RBE4s) of the BBB. Lead is a recognized neurotoxicant that can disrupt the cerebral capillary endothelial cells forming the BBB causing cerebral hemorrhage and the leakage of proteins (Goldstein *et al.* 1974, Kerper and Hinkle 1997b, Shi and Zheng 2007). Lead is capable of entering cells through store-operated calcium channels (Kerper and Hinkle 1997a, Kerper and Hinkle 1997b) which are in fact TRPC channels (Malarkey and Parpura 2008; Zhu et al., 1996). Lead has also been associated with interfering with several intracellular calcium-related pathways (Goldstein, 1993; Sun and Suszkiw, 1995). Previous work in our lab established that lead decreases transendothelial electrical resistance in the BBB *in vitro* (Balbuena *et al*., 2010) and also disrupts BBB permeability by reducing tight junction protein levels (Chapter 4), but the mechanism (or mechanisms) by which it induces this damage is still to be elucidated.

Organophosphorus (OP) compounds are best known for their use as insecticides in pest control of crops and households with malathion the insecticide of choice in many cases (Environmental Protection Agency, 2000-2001 pesticide market estimates). The efficacy of OP compounds as insecticides resides in their capability to inhibit degradation of the neurotransmitter acetylcholine via acetylcholinesterase (AChE). This is the same mechanism associated with OP toxicities in humans and animals. OP compounds can disrupt BBB

permeability *in vitro* (Balbuena *et al*., 2010; Parran 2005), and malathion decreased levels of tight junction proteins in endothelial cells of the BBB (Chapter 4). Furthermore, chlorpyrifos (another OP compound) has also been associated with altered phosphorylation of calcium/cAMP response element binding protein in neurons (Schuh *et al*., 2002). However, mechanisms by which OPs disrupt tight junction proteins and therefore increase BBB permeability were not described.

TRPC1 and TRPC4 are subunits of TRPC store operated calcium channels composed of up to seven isoforms, TRPC1 to TRPC7 (Pedersen et al., 2005; Nilius and Droogmans, 2001). The structure of the channel is arranged into six putative transmembrane subunits or domains that can assemble into both homomeric and heteromeric complexes (Pedersen et al., 2005). TRPC1 channels show similarity to voltage-gated calcium channels in the region called S3 through S6, which include the S5-S6 linker that forms the ion selective pore (Montell and Rubin, 1989; Zhu *et al*., 1996). The only exception is localized in the fourth transmembrane segment S4, where TRPCs lack the complete set of positively charged residues that confer voltage sensitivity (voltage sensor) to most voltage-gated ion channels (Catterall, 2000; Montell and Rubin, 1989). TRPC1 are phospholipase C (PLC)-operated nonselective cation channels that demonstrate variable Ca^{2+}/ Na^{+} permeability ratios ranging from 1 to 9 (Montell, 2001).

We assessed TRPC1/TRPC4 channels in endothelial cells of the BBB following exposure to neurotoxic agents lead and malathion. Since lead and organophosphates are associated with variations in intracellular calcium concentrations in different cell systems (Marcovac and Goldsetein, 1988; Schanne *et al*., 1997; Long *et al*., 1994; Goldstein, 1993; Schuh *et al*., 2002), the TRPC channels are good candidates to explore as contributors to disruption of the BBB.

MATERIALS AND METHODS

Chemicals: Malathion of 94% purity was donated by the American Cyanamid Company, agricultural division (Princeton, NJ). Malaoxon 98.2% pure was obtained from Chem Services Inc. (West Chester, PA); it was used to determine the need for having an active esterase inhibitor in order to observe changes in levels of tight junction and scaffold proteins. Lead acetate, Na_2HPO_4, KH_2PO_4, NaCl, trizma base, triton X-100, glycine, SDS, tween-20, and deoxycholate were purchased from Sigma-Aldrich, Inc. (St. Louis, MO). Blocking buffer was purchased from LI-COR Biotechnology (Lincoln, Nebraska).

Cell culture: The rat brain microvascular endothelial cell line RBE4 was donated by the laboratory of Dr. M. Aschner, Vanderbilt University. Cells were cultured in 100 mm x 20 mm polystyrene tissue-culture treated dishes (Sigma-Aldrich) at a concentration of 1.5×10^5 cells per culture dish and were left to reach 100% confluency. RBE4 cultures were cultured in 44.5% minimum essential medium (MEM), 44.5% Ham's F10 with glycine, 10% fetal bovine serum (FBS), and 1% of a penicillin/streptomycin/amphotericin B solution and kept at 37°C with 5% CO_2. All the cell culture media and reagents utilized in cell culture procedures were obtained from Mediatech Inc. (Manassas, VA), unless otherwise noted. After 3-4 days cells were incubated for an additional 2 days with astrocyte conditioned medium (ACM) in order to induce the presence of tight junctions on the endothelial cells. ACM has been associated with induction of blood-brain barrier specific characteristics such as tight junctions in several cell lines (Abbott,

2002; Omidi et al., 2008). After the incubation with the ACM, cells were treated with neurotoxicants lead acetate and malathion/oxon.

Treatments: Cells were treated with combinations and compounds alone at different times and concentrations. Treatments groups include lead acetate at 10^{-5} M ($Pb10^{-5}$ M) and 10^{-6} M, malathion 10^{-5} M ($Mal10^{-5}$ M), malaoxon 10^{-6} M ($Mx10^{-6}$ M), and combinations of both neurotoxicants ($Pb10^{-5}$ M+$Mal10^{-5}$ M, $Pb10^{-5}$ M+$Mx10^{-6}$ M, $Pb10^{-6}$ M+$Mal10^{-5}$ M, and $Pb10^{-6}$ M+$Mx10^{-5}$ M). Cells were incubated with treatments for 2 hr, 4 hr, 8 hr, 16 hr, and 24 hr periods. Viability was unaffected after exposure of BBB cells to these concentrations for these periods of time (Balbuena *et al*., 2010).

Western blot assessment: RBE4 cells were washed in 5 ml ice-cold phosphate buffered saline (PBS) pH 7.4 and then lysed for 10 minutes with an ice-cold lysis buffer solution containing 150 mM NaCl, 10 mM trizma base, 0.5% v/v triton X-100, and 0.5% w/v deoxycholate. Lysates were centrifugated at 16,000g for 5 minutes and resuspended in 700 µl of ice-cold PBS. Lysates were processed immediately for protein determination; sample concentrations were adjusted to 1 mg/ml and stored at -20°C. Proteins were separated by electrophoresis in 4%-15% Tris-HCl 1.0 mm pre-casted gels (Bio-Rad Laboratories, Hercules CA), and then transferred to a 0.45 µm pure nitrocellulose membrane by electroblotting. Membranes were blocked for 1 hr at room temperature with Odyssey blocking buffer (LI-COR Biotechnology) and then incubated for one hour with polyclonal antibodies (Santa Cruz Biotechnology, Santa Cruz, CA) for TRPC1, TRPC4, and anti-β-actin (as a normalizing control) at 1:200 dilutions. Membranes were washed 5 times (5 minutes each) with a solution of PBS pH 7.4 and 0.1 % tween-20 and then incubated

for one hour with IRDye™ 700DX conjugated affinity purified anti-rabbit IgG (donkey) and IRDye™ 800CW conjugated affinity purified anti-goat IgG (donkey) secondary antibodies (Rockland, Gilbertsville PA) at 1:5000 dilutions. Membranes were washed and then analyzed by near-infrared (NIR) fluorescence detection methods with the Odyssey® Infrared Imaging System. Results were expressed as relative band fluorescence in pixels.

Total RNA extraction and reverse transcription/cDNA synthesis: Total RNA was extracted utilizing the Total RNA purification RNeasy kit from Qiagen (Valencia, CA). Briefly, cells were lysed with lysis buffer applied directly on the cell culture dishes after washing them with ice-cold PBS; lysates were then homogenized with 70% ethanol utilizing a blunt 20-gauge needle (0.9 mm diameter), and pipetted into RNeasy spin columns and centrifugated. Samples were treated with DNase I in order to digest any genomic DNA that may have been present in the samples and then washed again in the columns. RNA was then eluted directly from the columns with 30 µl of RNase-free water. Concentrations of total RNA were determined for samples with an Eppendorf UV/Vis bioPhotometer analysis system (Hamburg, Germany), and then RNAs were stored at -80°C. Reverse transcription synthesis was carried out utilizing the reverse transcription system from Promega (Madison, WI) processing 1 µg of total RNA per reaction. Briefly, total RNA was incubated at 70°C for 10 minutes and placed on ice. Reactions were prepared at the following concentrations: 50 ng/µl of total RNA, 50 mM $MgCl_2$, 10X reverse transcription buffer (100 mM Tris-HCl[pH 9.0 at 25°C]; 500 mM KCl; 1% Triton®X-100), 1 mM each dNTP mixture, 1unit/µl recombinant RNasin® ribonuclease inhibitor, 50units/µg AMV reverse transcriptase (high concentration), and 0.5 µg of random primers per microgram RNA with Nuclease-free water to a total volume of 20 µl per reaction. Reactions were incubated at

room temperature for 10 minutes and then at 42°C for 15 minutes before they were heated at 95°C for 5 minutes. After cooling off, cDNA reactions were stored at -20°C until used.

Quantitative real time polymerase chain reaction: Rattus norvegicus real time oligonucleotide primers for TRPC1 and TRPC4, and β-actin (as an internal normalizing control) were designed with the Beacon Designer™ 7.6 software (Premier Biosoft International, Palo Alto, CA) as shown in Table 1. Primers were designed to be compatible with the SYBR® Green PCR assays avoiding significant cross homologies and preventing secondary structures that can interfere with SYBR® Green primer extension. Primers were synthesized by Invitrogen and then concentrations of each primer were standardized to 30 µM concentrations. Quantitative real time PCR (qPCR) amplifications were carried out utilizing an iCycler iQ™ optical system (Bio-Rad). The PCR reaction mix was generated by adding 12.5 µl of SYBR® Green Supermix® (Bio-Rad) with 0.25 µl of each primer (forward/reverse), 1 µl of cDNA template, and RNA-free water to a total of 25 µl per reaction. The relative quantification of gene expression was attained utilizing the comparative C_T method (Livak and Schmittgen, 2001).

Statistical analysis: All results are expressed as means ± SEM of three or more individual assays. Multiple comparisons were performed by utilizing one-way analysis of variance (ANOVA), followed by Dunnett's test. Data were analyzed by GraphPad Prism 4 (GraphPad software, San Diego, CA); *p* values less than 0.05 were considered to be significant.

RESULTS

Levels of TRPC1 protein increased considerably ($p<0.05$) at the 4 hr period (Fig 1), especially for the combinations of neurotoxicants ($p<0.01$). Levels of protein were still high at 8 hr after exposure to the combinations and after exposure to the organophosphates. At 16 hr, protein levels were still above those of controls only for the $Pb10^{-6}M$+$Mal10^{-5}M$ combination (Fig 1). In general, combinations induced higher levels of TRPC1 protein for the 4 hr and 8 hr periods ($p<0.01$) suggesting the production of more TRPC1 channels in the membrane of cells since more protein is available. The results for experiments determining TRPC4 protein levels showed time related differences when compared with levels of TRPC1 protein. For example, TRPC4 protein levels increased at 2 hr for all treatments, with the exception of $Pb10^{-6}M$ and its combination with Mx $10^{-6}M$ ($p<0.01$) (Fig 2). At 4 hr, only treatments with $Pb10^{-5}M$ and malathion/malaoxon increased levels of protein (Fig 2).

When gene expression for TRPC1 was assessed, an increase in gene expression at 4 hr was noted following exposure to both organophosphates and for the higher concentration of lead ($p<0.05$). At 8 hr however, only the organophosphates were still increasing TPRC1 gene expression (Fig 3A). Combinations of neurotoxicants significantly increased TRPC1 gene expression at 4 hr ($p<0.01$) (Fig 3B). At 24 hr, gene expression was still upregulated except for the $Pb10^{-6}$ M+$Mal10^{-5}$ M combination. The pattern of TRPC4 gene expression differed from that of TRPC1. For example, the response to treatments with neurotoxicants alone was increased significantly ($p<0.01$) earlier, with effects seen at 2 hr and 4 hr (Fig 4A) with the exception of the lower concentration of lead. Increases in gene expression occurred after exposure to both concentrations of lead at 24 hr. In contrast to gene expression in cells that were exposed to single

neurotoxicants, all combinations of compounds decreased TRPC4 gene expression significantly at 16 and 24 hr (Fig 4B).

DISCUSSION

TRPC channels are associated with permeability in endothelial cells of the BBB (Tiruppathi et al., 2003; Montell et al., 2002). These channels are activated by increases in intracellular calcium caused by depletion of calcium from stores of the endoplasmic reticulum (Tiruppathi et al., 2006; Cioffi and Stevens, 2006; Parekh and Putney Jr., 2005). Increases in intracellular calcium are associated with endothelial cell permeability (Tiruppathi et al., 2003), which may cause BBB disruption. The results presented in this work established a marked increase in protein levels of TPRC1 measured by Western blot, which are in accord with the increases in TRPC1 gene expression measured by real time PCR. The increase in TRPC1 protein and gene expression denotes increased presence of TRPC channels in the cell membranes especially at the 4 hr period. Activation of these channels may be followed by increases of intracellular calcium that can activate several calcium dependant pathways. For example, increases in calcium can activate proteases such as metalloproteinases that are associated with tight junction proteolysis (Wachtel *et al*., 1999, Chen *et al*., 2009; Fujimura *et al*., 1999), inducing in the process increases in permeability of the BBB. The results indicate that neurotoxicants lead and malathion considerably increase TRPC1 levels, which may be one of the mechanisms by which these compounds increase BBB permeability.

TRPC4 protein levels were increased by the treatments with the neurotoxicants alone; however, combinations did not appeared to have any synergistic effect on levels of proteins. This trend was confirmed with the measurements of gene expression by real time PCR. Decreases in TRPC4 levels would indicate smaller quantity of TRPC channels in the membrane of RBE4 cells if the TRPC4 subunit could form homomeric channels; however, in most cases TRPC4 subunits are associated with TRPC1 subunits to form functional heteromeric channels (Pedersen et al., 2005). The percentage of each subunit present in heteromeric channels, however, has not yet been reported. TRPC1 also has been known to form homomeric channels, but its functionality is decreased (Zhang et al., 2009). Identification of number of subunits in each channel in a mixed population of TRPC1/TRPC4 heteromeric channels would allow us to assess if variation of protein levels for both subunits could modify increases in permeability on the BBB. These variations may contribute to the damage in protein levels and gene expression noted after exposure to the neurotoxicants lead and malathion in this study. Nevertheless, the increases in gene expression and protein levels of the TRPC subunits indicate that these increases may be a mechanism by which lead and malathion contribute to changes in BBB permeability and, therefore, damage to the tight junction structures.

REFERENCES

Abbott NJ. Astrocyte-endothelial interactions and blood-brain barrier permeability. J Anat. 200: 629-638, 2002.

Ando-Akatsuka Y, Saitou M, Hirase T, Kishi M, Sakaqkibara A, Itoh M, Yonemura S, Furuse M, Tsukita S. Interspecies diversity of the occludin sequence: cDNA cloning of human, mouse, dog, and rat-kangaroo homologues. J Cell Biol 1996; 133:43–48.

Antoniotti S, Pla AF, Barral S, Scalabrino O, Munaron L, Lovisolo D. Interaction between TRPC channel subunits in endothelial cells. Journal of Receptors and Signal Transduction. 26: 225-240, 2006.

Balbuena P, Li W, Magnin-Bissel G, Meldrum B, Ehrich M. Comparison of two blood-brain barrier *in vitro* systems: Cytotoxicity and transfer assessments of malathion/oxon and lead acetate. Toxicol Sci 2010, 114:260-271.

Balda SM, Matter K. Transmembrane proteins of the tight junctions. Cell Dev Biol. 11: 281-289, 2000.

Ballabh P, Braun A, Nedergaard M. The blood-brain barrier: an overview structure, regulation, and clinical implications. Neurobiol Dis. 16: 1-13, 2004.

Brouns R, De Dyen PP. The complexity of neurobiological processes in acute schemic stroke. Clin Neurol Neurosurg. 111: 482-495, 2009

Brown RC, Davis TP. Calcium modulation of adherens and tight junction function: a potential mechanism for blood-brain barrier disruption after stroke. Stroke. 33: 1706-1711, 2002.

Catterall WA. From ionic currents to molecular mechanisms: the structure and function of voltage-gated sodium channels. Neuron. 26: 13-25, 2000.

Cioffi DL, Stevens T. Regulation of endothelial cell barrier function by store-operated calcium entry. Microcirculation. 13: 709-723, 2006.

de Boer AG, van der Sandt ICG, Gaillard PJ. The role of drug transporters at the blood-brain barrier. Annu Rev Pharmacol Toxicol. 43:629–56, 2003.

Environmental Protection Agency. 2000-2001 Pesticide market estimates. Pesticide industry sales webpage. Available at http://www.epa.gov/oppbead1/pestsales/01pestsales/usage2001_3.htm#3_8. Accessed May 13, 2010.

Furuse M, Fujita K, Hiragi T, Fujimoto K, Tsukita S. Claudin-1 and -2: novel integral membrane proteins localizing at tight junctions with no sequence similarity to occludin. J Cell Biol. 141: 1539–1550, 1998.

Furuse M, Hirase T, Itoh M, Nagafuchi A, Yonemura S, Tsukita S. Occludin: a novel integral membrane protein localizing at tight junctions. J Cell Biol. 123: 1777–1788, 1993.

Gias UA, Asrar BM. Functional role of TRPC channels in the regulation of endothelial permeability. Arch-Eur J Physiol. 451: 131-142. 2005.

Goldstein GW, Asbury A K, Diamond I. Pathogenesis of lead encephalopathy: uptake of lead and reaction of brain capillaries. Archives of Neurology. 31: 382-383, 1974.

Goldstein GW. Evidence that lead acts as a calcium substitute in second messenger metabolism. Neurotoxicol. 14 (2-3): 97-101, 1993.

Gonzalez-Mariscal L, Betanzos A, Nava P, Jaramillo BE. Tight junction proteins. Prog Biophys Mol Biol. 81: 1-44, 2003.

Hawkins BT, Davis TP. The blood-brain barrier/neurovascular unit in health and disease. Pharmacol. Rev. 57: 173-185, 2005.

Kerper LE, Hinkle PM. Cellular uptake of lead is activated by depletion of intracellular calcium stores. The Journal of Biological Chemistry. 272: 8346-8352, 1997a.

Kerper LE, Hinkle PM. Lead uptake in brain capillary endothelial cells: activation by calcium store depletion. Toxicology and Applied Pharmacology. 146: 127-133, 1997b.

Kidwel CS, Latour L, Saver JL, Alger JR, Starkman S, Duckwiler G, Jahan R, Vinuela F, Kang DW, Warach S. Thrombolytic toxicity: blood-brain barrier disruption in human ischemic stroke. Cerebrovasc Dis. 25: 338-343, 2008.

Kirk J, Plumb J, Mirakhur M, McQuaid S. Tight junctional abnormality in multiple sclerosis white matter affects all calibers of vessel and is associated with blood-brain barrier leakage and active demyelination. J Pathol. 2001: 319-327, 2003.

Kniesel U, Wolburg H. Tight junctions of the blood-brain barrier. Cell Mol Neurobiol. 20(1): 57-76, 2000.

Liebner S, Kniesel U, Kalbacher H, Wolburg H. Correlation of tight junction morphology with the expression of tight junction proteins in blood-brain barrier endothelial cells. Eur J Cell Biol.79: 707-717, 2000.

Livak KJ, Schmittgen TD. Analysis of relative gene expression data using real-time quantitative PCR and the C_T method. Methods. 25: 402-408, 2001.

Long GJ, Rosen JF, Schanne FAX. Lead activation of protein kinase C from rat brain. J Biol Chem. 14: 834-837, 1994.

Lotocki G, Vaccari JP de R, Perez ER, Sanchez-Molano J, Furones-Alonso O, Bramlett HM, Dietrich WD. Alterations in blood-brain barrier permeability to large molecules and leukocyte accumulation after traumatic brain injury: effects of post-traumatic hypothermia. J Neurotrauma. 26: 1123-1134, 2009.

Malarkey EB, Ni Y, Parpura V. Ca2+ entry through TRPC1 channels contributes to intracellular Ca2+ dynamics and consequent glutamate release from rat astrocytes. Glia. 56(8): 21-35, 2008.

Marcovac J, Goldstein GW. Picomolar concentrations of lead stimulate brain protein kinase C. Nature. 334: 71-73, 1988.

McQuaid S, Cunnea P, McMahon J, Fitzgerald U. The effects of blood-brain barrier on glial cell function in multiple sclerosis. Biochem Soc Trans. 37: 329-331, 2009.

Montel C, Bimbaumer L, Flockerzi V. The TRP channels, a remarkable functional family. Cell. 108: 595-598, 2002.

Montell C, Rubin GM. Molecular Characterization of the Drosophila *trp* Locus: A putative integral membrane protein required for phototransduction. Neuron. 2: 1313-1323,1989.

Montell C. Physiology, phylogeny, and functions of the TRP superfamily of cation channels. Sci. STKE. Re1. 90: 2-17, 2001.

Morita K, Sasaki H, Furose M, Tsukita S. Endothelial claudin: claudin-5/TMVCF constitutes tight junction strands in endothelial cells. J Cell Biol. 147: 185-194, 1999.

Nilius B, Droogmans G. Ion channels and their role in vascular endothelium. Physiol Rev. 81: 1415-1459, 2001.

Nitta T, Hata M, Gotoh S, Seo Y, Sasaki H, Hashimoto N, Furuse M, Tsukita S. Size-selective loosening of the blood-brain barrier in claudin-5-deficient mice. J Cell Biol. 161: 653-660, 2003.

Parekh AB, Putney Jr. JW. Store-operated calcium channels. Physiol Rev. 85: 757-810, 2005.

Parran DK, Magnin G, Li W, Jortner BS, Ehrich M. Chlorpyrifos alters functional integrity and structure of an *in vitro* model: co-cultures of bovine endothelial cells and neonatal rat astrocytes. Neurotoxicology. 2005; 26: 77-88, 291.

Pedersen SF, Owsianik G, Nilius B. TRP channels: an overview. Cell Calcium. 38: 233-252, 2005.

Schanne FA X, Long GJ, Rosen JF. Lead-induced rise in intracellular free calcium is mediated trough activation of protein kinase C in osteoblastic bone cells. Biochim Biophys Acta. 1360: 247-254, 1997.

Schuh RA, Lein PJ, Beckles RA, Jett DA. Non-cholinesterase mechanisms of chlorpyrifos neurotoxicity: altered phosphorylation of CA^{2+}/ cAMP response element binding protein in cultured neurons. Toxicol Appl Pharmacol. 182: 176-185, 2002.

Shi LZ, Zheng W. Early lead exposure increases the leakage of the blood-cerebrospinal fluid barrier *in-vitro*. Human & Experimental Toxicology. 26: 159-167, 2007.

Starr JM, Farral AJ, Armitage P, McGurn B, Wardlaw J. Blood-brain barrier permeability in Alzheimer's disease: a case-control MRI study. Psychiatry Res. 171: 232-241, 2009.

Sun LR, Suszkiw JB. Extracellular inhibition and intracellular enhancement of Ca2 currents by Pb2 in bovine adrenal chromaffin cells. J Neurophysiol. 74: 574-581, 1995.

Takenaga Y, Takagi N, Murotoni K, Tanonaka K, Takeo S. Inhibition of Src activity decreases tyrosine phosphorylation of occludin in brain capillaries and attenuates increase in permeability of the blood-brain barrier after transient focal cerebral schemia. J Cereb Blood Flow Metab. 29: 1099-1108, 2009.

Tiruppathi C, Ahmmed GU, Vogel SM, Malik AB. Calcium signaling, TRP channels, and endothelial permeability. Micro Inf Health.13: 692-708, 2006.

Tiruppathi C, Minshall RD, Paria BC, Vogel SM, Malik AB. Role of Ca2+ signaling in the regulation of endothelial permeability. Vascul Pharmacol. 39: 173-185, 2003.

Tsukita S, Furose M. Pores in the wall: claudins constitute tight junction strands containing aqueous pores. J Cell Biol 2000; 149:13-16.

Wachtel M., Frei K., Ehler E., Fontana A., Winterhalter K., and Gloor S. M. Occludin proteolysis and increased permeability in endothelial cells through tyrosine phosphatase inhibition. J Cell Sci. 112: 4347-4356, 1999.

Wolburg H, Lippoldt A, Ebnet K. Tight junctions and the blood-brain barrier. In: Tight Junctions (L.Gonzalez-Mariscal ed.), Landes Bioscience, Georgetown Texas; Springer Science+Business Media, New York NY. pp. 175-195, 2006.

Zhang P, Luo Y, Chasan B, Gonzalez-Perrett S, Montalbetti N, Timpanaro GA, Cantero MR, Ramos AJ, Goldmann WH, Zhou J, Cantiello HF. The multimeric structure of polycystin-2 (TRPP2): structural-functional correlates of homo- and hetero-multimers with TRPC1. Hum Mol Genet. 18: 1238-1251, 2009.

Zhu X, Jiang M, Peyton M, Boulay G, Hurst R, Stefani E, Birnbaumer L. TRP, a novel mammalian agonist-activated capacitative Ca^{2+} entry. Cell. 85: 661-671, 1996.

Tables and Figures:

Table 1 *Rattus norvegicus* oligonucleotide primer sequences used in the real time PCR assessments. All the primers were synthesized by Invitrogen (Carlsbad, CA)

Gene	Accession Number	Primer/Forward	Primer/Reverse	Product Length (bp)
TRPC1	NM_053558	5'-AGGTGAAGGAGGAGAACACCTTG-3'	5'-CCATAAGTTTCTGACAACCGTAGTCC-3'	101
TRPC4	AF421364	5'-AATTACTCGTCAACAGGCGGC-3'	5'-CACCACCACCTTCTCCGACTT-3'	179
B-actin	NM_053558	5'-TATCGGCAATGAGCGGTTCC-3'	5'-GTGTTGGCATAGAGGTCTTTACG-3'	144

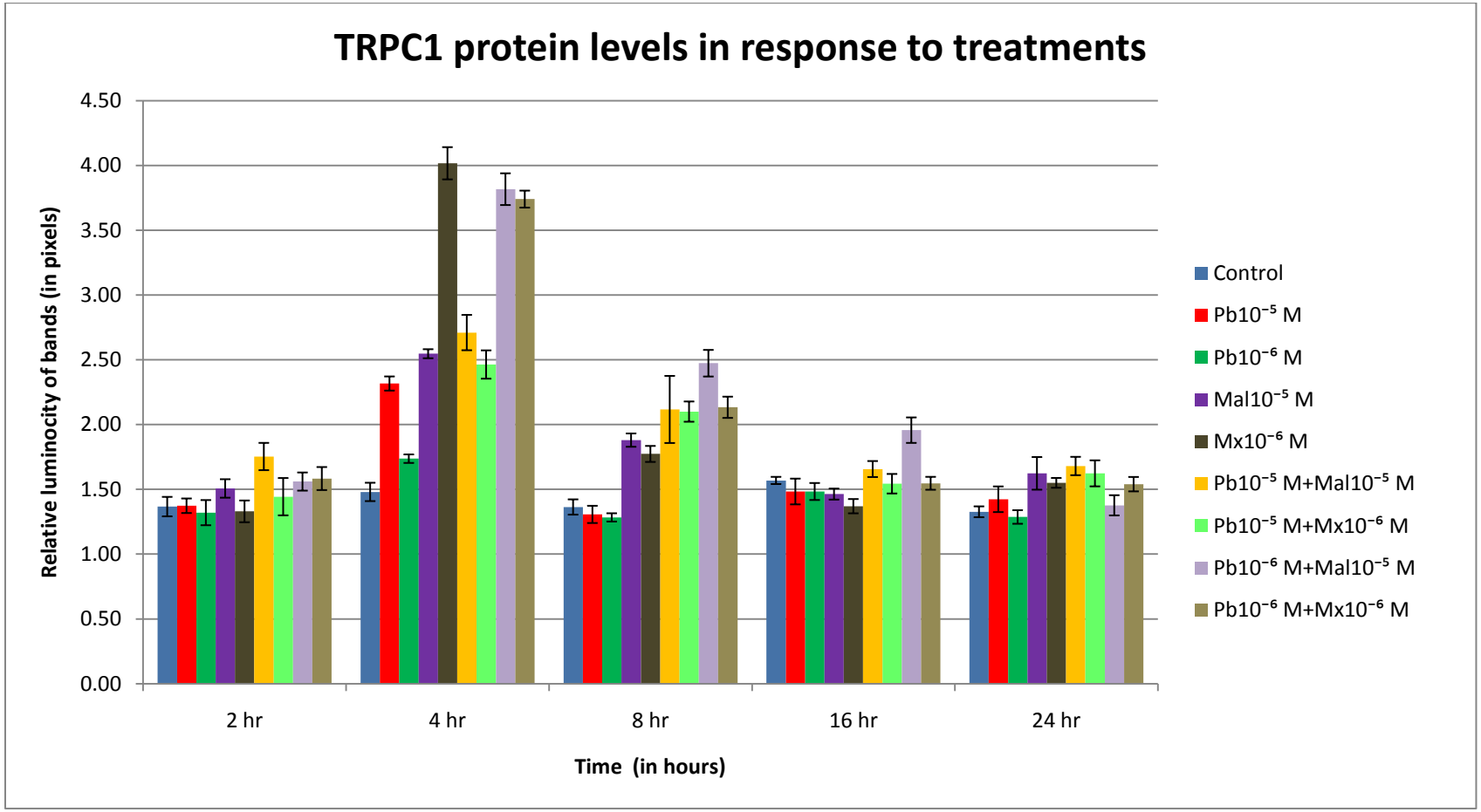

Figure 1. TRPC1 protein levels in response to treatment. Levels increased for the 4 hr period, with the combinations elevating the levels of TRPC1 protein more than the compounds alone ($p<0.01$). At 8 hr, only the combinations and the organophosphates maintain the increased levels of protein ($p<0.05$).

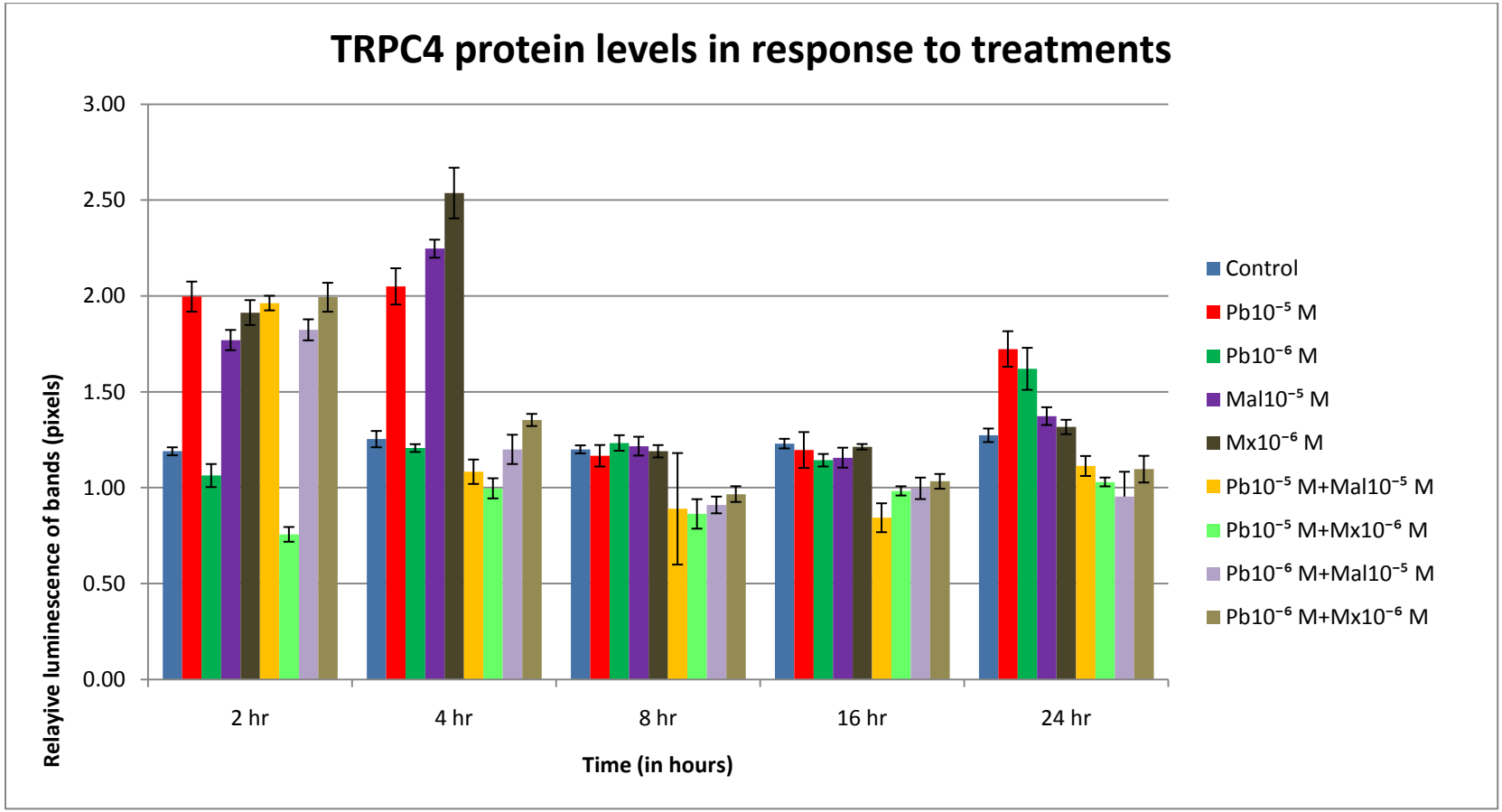

Figure 2. TRPC4 protein levels in response to treatment. Protein levels increased at the 2 hr period for both compounds alone and combinations ($p<0.01$), with the exception of the lowest concentration of lead and the $Pb10^{-5}$ M+$Mx10^{-6}$ M combination. At 8 hr and 16 hr combinations decreased protein levels ($p<0.05$), a trend that continued to the 24 hr period.

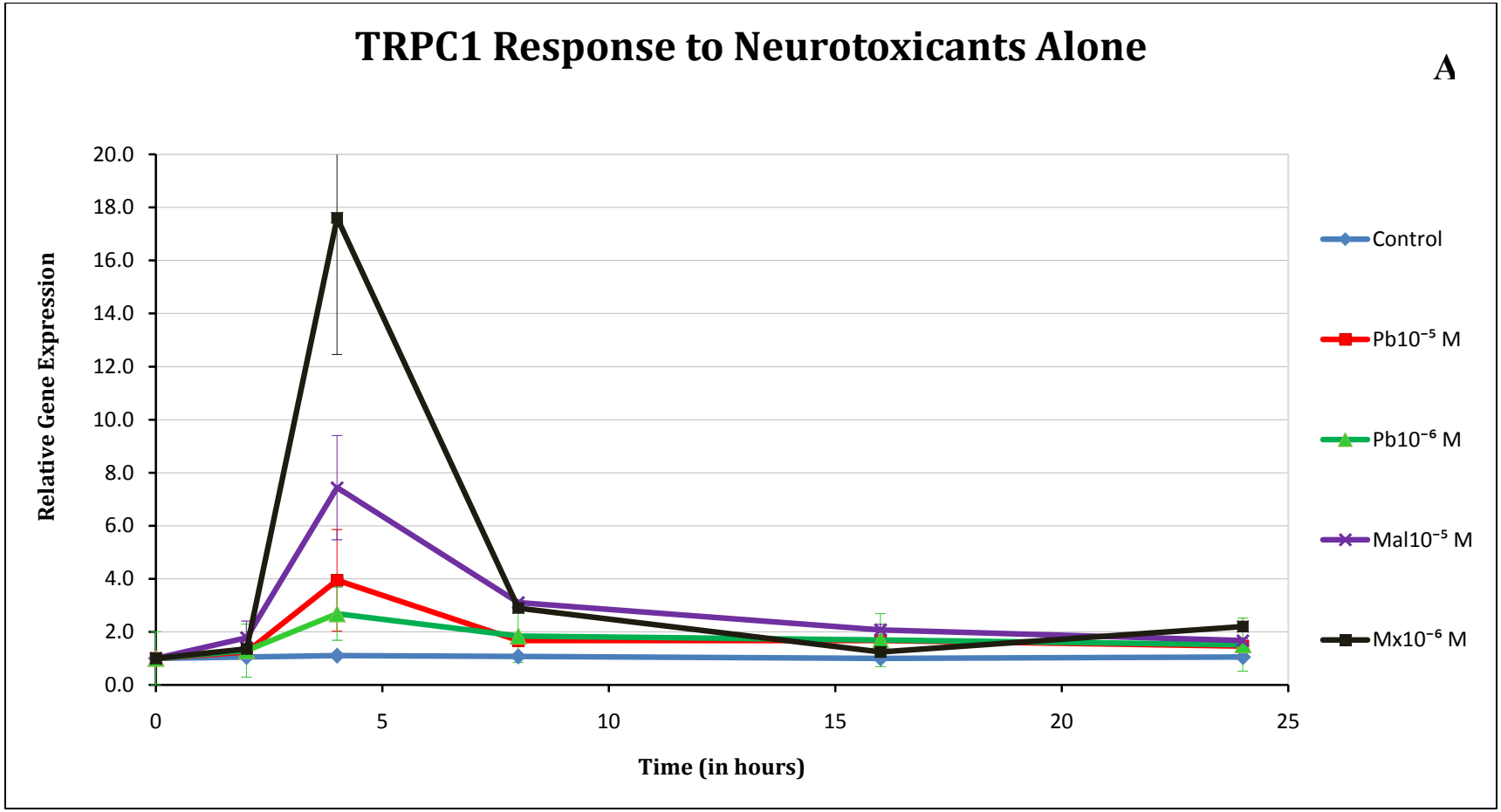

Figure 3A. TRPC1response to neurotoxicants alone. Gene expression was increased significantly for all the compounds at the 4 hr period ($p<0.05$), especially for malaoxon ($Mx10^{-6}$ M) ($p<0.01$).

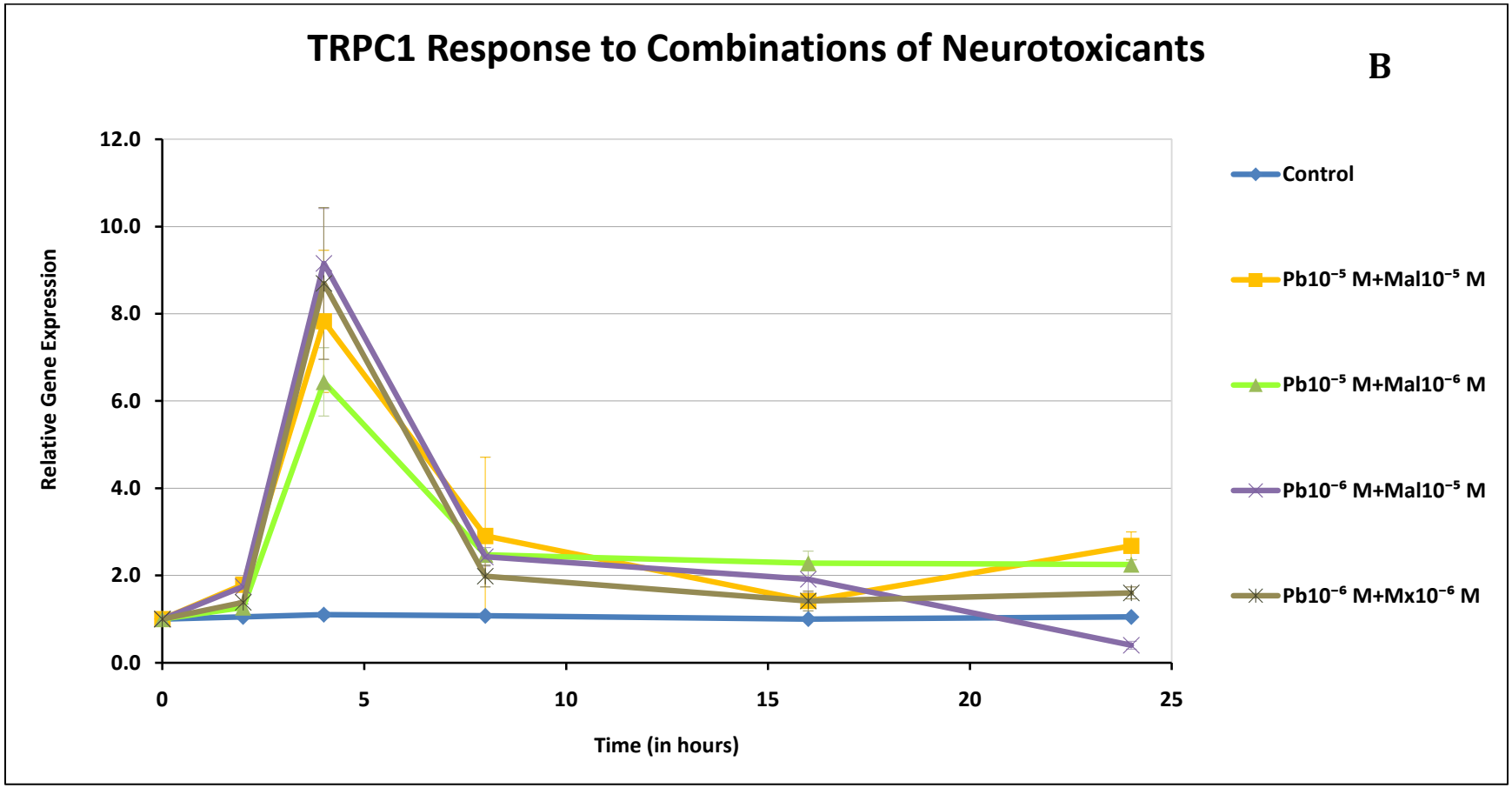

Figure 3B. TRPC1response to combinations of neurotoxicants. Gene expression significantly increased at the at 4 hr period for all the combinations ($p<0.01$).The expression of the gene was still above control levels at 24 hr ($p<0.05$) with the exception of the $Pb10^{-6}$ M+$Mx10^{-6}$ M
+.

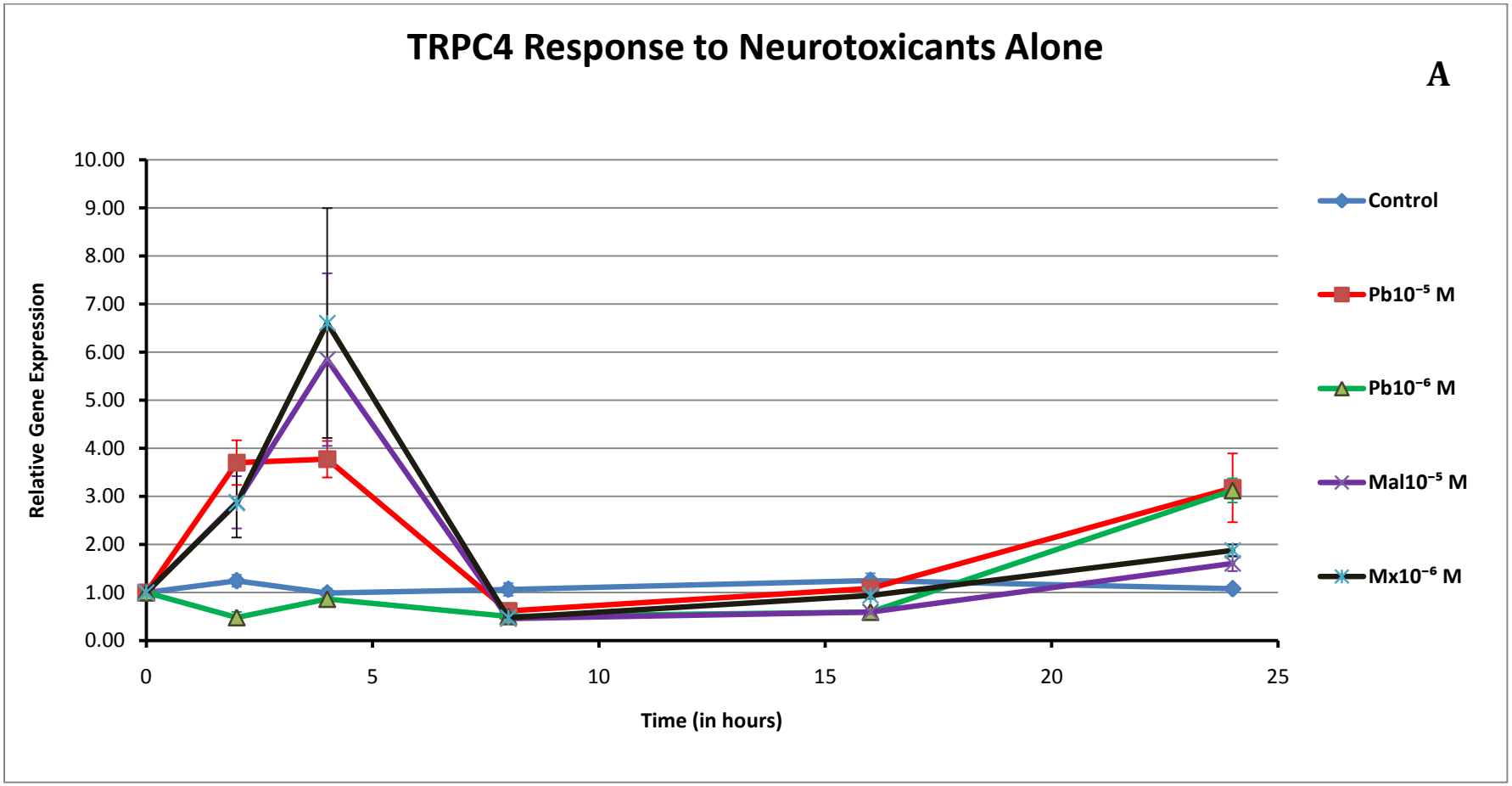

Figure 4A. TRPC4 response to neurotoxicants alone. Gene expression was increased by all the compounds alone at 2 hr and especially at 4 hr ($p<0.01$). The exception was $Pb10^{-6}$ M which decreased gene expression at 2 hr ($p<0.05$). At 24 hr however, all compounds were noted to increase TRPC4 expression when compared to controls ($p<0.05$).

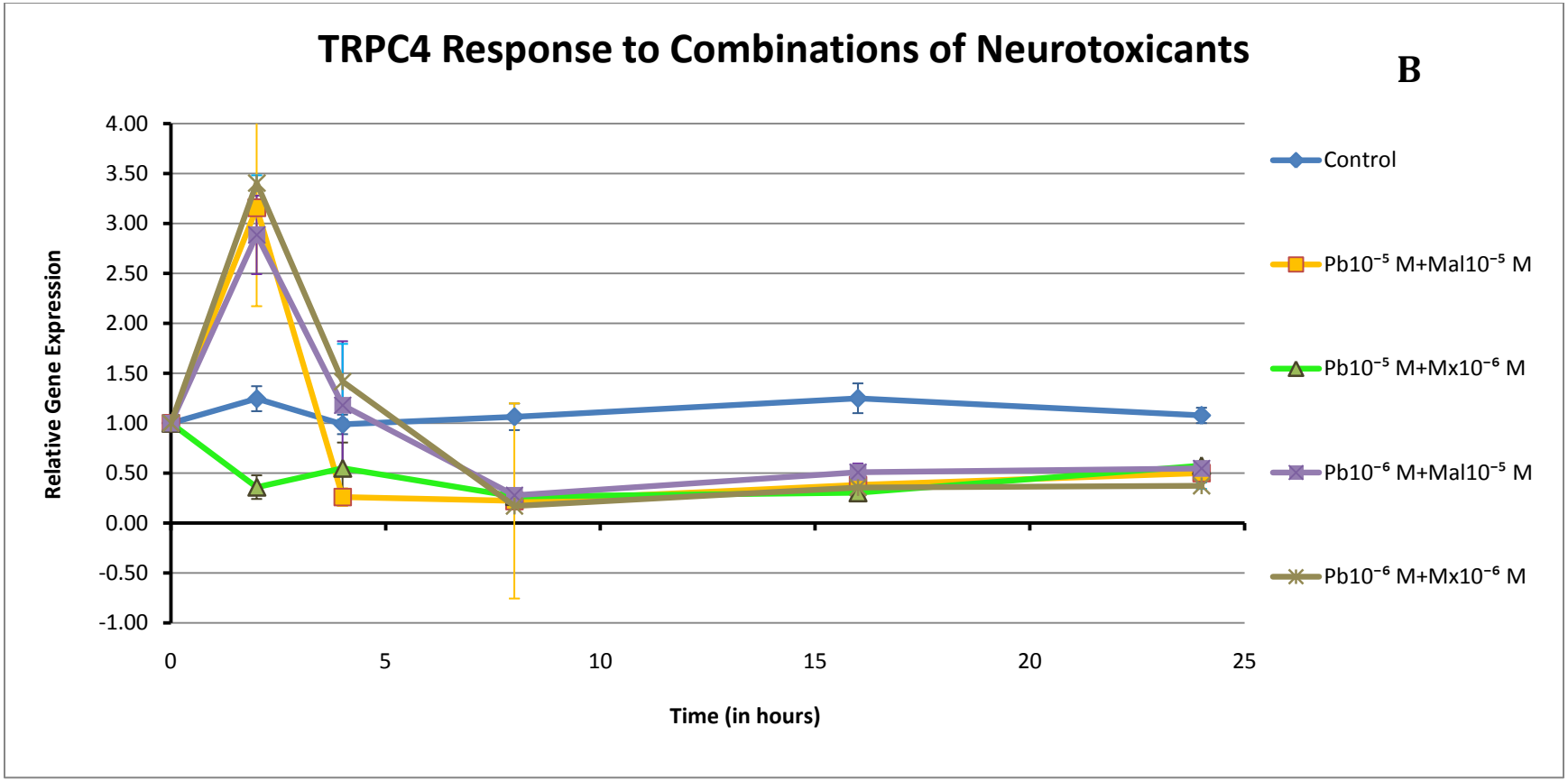

Figure 4A. TRPC4 response to combinations of neurotoxicants. Combinations of neurotoxicants increased TRPC4 gene expression at 2 hr ($p<0.01$), with the exception of $Pb10^{-5}$ M+$Mx10^{-6}$ M. At 16 hr and 24 hr however, combinations significantly decreased TRPC4 gene expression ($p<0.05$). $Pb10^{-5}$ M+$Mx10^{-6}$ M decreased gene expression at all times ($p<0.05$).

Chapter 6

DISCUSSION

The development of BBB *in vitro* systems to assess experimental conditions in different settings is an ongoing process with various ramifications that impact basic science research. Utilization of BBB models is relevant to pharmacology where models are utilized to assess molecular transport and permeability rates of new chemical compounds (Audus and Borchardt, 1986; Joost *et al*., 1988). *In vitro* BBB models are also important in molecular biology to assess the presence of specific molecular transporters (Audus and Borchardt, 1986; de Boer *et al*., 2003), and neurotoxicology to assess tight junction disruptive effects in response to cytotoxic insult (Balbuena *et al*., 2010, Zheng *et al*., 2003).

The present work examined BBB models constructed with different types of endothelial cells in order to establish the best *in vitro* BBB system to analyze neurotoxic effects of lead and malathion and its active metabolite malaoxon, alone and in combinations. The two models constructed presented two variations in their assembly and differences were noted when assessments of neurotoxicant insult were performed. For the resistance assessments, the model constructed with rat astrocytes and a line of rat brain microvessel endothelial cells (RBE4) achieved a higher transendothelial electrical resistance (TEER) than the model constructed with rat astrocytes and a primary cell culture of bovine brain microvascular endothelial cells (BMECs). Both models also responded differently to transport of neurotoxicants through the barrier. Therefore, although both models incorporate brain microvascular endothelial cells with similar characteristics, the origin of the cells dictated a different response from both endothelial cell types, not only to development of TEER on the endothelial cell layers, but also to metabolic

activity, quantities of neurotoxicants transferred through the barrier, and sensitivity to the tested compounds.

For these assessments involving transfer of neurotoxicants through the barrier, decreases in TEER were associated with increases in permeability. This was true in both models exposed to malathion/oxon and lead. These results corroborate *in vivo* assessments that associate lead and malathion treatments with increases in BBB permeability in rats (Bradbury and Deane, 1993). However, the differences in the transfer of both neurotoxicants, as indicated by differences in the concentrations of these compounds in the luminal and abluminal sides of the systems, and the dissimilarity in metabolic activity related to the conversion of malathion into malaoxon, indicated that endothelial cells from different species respond differently under the same experimental conditions. This can alter the results and, therefore, compromise any comparison to *in vivo* assessments.

From our results, we suggest that the origin of endothelial cells utilized in the construction of BBB models has an important influence on the results of experiments involving barrier permeability and metabolism. Considering the vast amount of literature on BBB *in vitro* systems, and the many different cell types utilized in their construction (Reinhart and Gloor, 1997), the predictable variation in results is an important factor influencing the interpretation of data. This factor needs to be considered when comparing results that assessed the same endpoints in different BBB *in vitro* systems. This is also a very important consideration when *in vitro* systems are used to predict *in vivo* responses to the same compounds.

The differences noted in our experiments were a big factor when choosing the model that was more viable to assess the endpoints that would test our hypothesis, and we choose the system constructed with rat astrocytes and RBE4 cells since most BBB work cited in literature

was performed in rodents. We hypothesized that proteins involved in BBB structure stability were lost in response to neurotoxicant insult with the consequent increase in permeability. Therefore, this model was assessed, first, for the presence of tight junction proteins occludin and claudin 5, and scaffold proteins ZO1 and ZO2; and then for changes in these protein levels in response to neurotoxicant insult. These proteins were present in the rat RBE4 endothelial cells, therefore assessments of their levels in response to lead and malathion/oxon combinations were performed.

The results indicated that lead and malathion/oxon in concentrations that affected BBB permeability affected tight junction and scaffold protein levels in the endothelial cells of our BBB *in vitro* system. These results confirmed our first hypothesis, that neurotoxicants malathion and lead acetate disrupt BBB function by decreasing TEER and increasing permeability. They achieve these actions by reducing tight junction protein levels in the paracellular spaces of adjacent endothelial cells and by reducing scaffold protein levels that support tight junctions in the cytoplasmic side of cell membranes. Since changes in protein levels are usually associated with gene expression of that particular gene, assessments of gene expression by real time PCR (qPCR) were investigated as a potential mechanism for the reduction of tight junction proteins occludin and claudin 5, and scaffold proteins ZO1 and ZO2.

Although gene expression was increased for most proteins, especially at the early times assessed, in general there was no relationship between gene expression and decreases in protein levels. Two separate approaches may be taken in considering these results, including identification of factors other than gene expression involved in tight junction protein changes, and detection of alternative mechanisms associated with scaffold protein changes. Decreases in occludin protein levels occurred even though qPCR indicated early increases in gene expression,

suggesting that the upregulation of the gene was the result of the decrease of protein levels rather than a neurotoxic effect on the expression of its gene. The protein reduction mechanism may be explained by a different hypothesis. Occludin proteolysis in endothelial cells has been associated with increases in permeability and this suggests the activation of proteases in the paracellular space (Chen *et al*., 2009). Metalloproteinases mediate numerous proteolytic reactions involving cellular surface elements, including adhesion molecules and tight junction proteins, and at least MMP-9 has been associated with disruption of occludin and claudin 5 in brain endothelial cells *in vitro* (Chen *et al*., 2009; Fujimura *et al*., 1999). Since calcium influx is known to activate metalloproteinases (Barbosa *et al*., 2006), and at least lead is associated with rises in intracellular calcium (Goldstein, 1993), this mechanism is a good candidate to explain decreases in tight junction protein levels not associated with gene expression. However, further assessments are necessary in order to elucidate the connection between activation of metalloproteinases by intracellular calcium increases and the decreases in occludin and claudin 5 protein levels observed in the present experiments when treatments with malathion/oxon and lead were performed.

The decreases in ZO1 and ZO2 protein levels cannot be explained by the mechanism cited for the tight junction proteins because ZO1 and ZO2 are intracellular proteins, therefore, they are not affected by metalloproteinases activation. However, lead and organophosphates have been associated with increases in intracellular calcium levels, and calcium increases are associated with increases in BBB permeability (Kerper and Hinkle, 1997; Brown and Davis, 2002; Tiruppathi *et al.*, 2003; Wang et al., 2006). These increases in permeability are mostly associated with re-adjustment of scaffold proteins and their cytoskeleton support. Therefore, a separate mechanism in which neurotoxicants activate intracellular calcium pathways and re-

arrange scaffold proteins and cytoskeleton structures is a good candidate to explain the decreases in scaffold protein levels observed in the present experiments.

Both mechanisms proposed to explain the reduction in tight junction and scaffold protein levels observed in our results involve increases in calcium concentrations in the cytosol of endothelial cells of the BBB. If these two neurotoxicants affect calcium concentrations intracellularly, a mechanism associated with increases in intracellular calcium may explain the effects noted in tight junction and scaffold protein levels reduction. Since increases in calcium are usually associated with activation of specific calcium channels, and membrane regulation of calcium ion transport, we proposed that a calcium channel may be involved in the proposed calcium increases that could explain the effects caused on protein levels of tight junction and scaffold proteins of the BBB.

Transient receptor potential canonical (TRPC) channels form heteromeric structures between subunits 1 and 4 (TRPC1/TRPC4) in endothelial cells of the BBB. They are calcium ion channels that display overwhelming ion selectivity for this cation (Montell, 2005; Alexander *et al.*, 2008; Gaudet, 2008), and seem to be involved in the regulation of endothelial cell permeability (Tiruppathi *et al*., 2006). TRPCs in endothelial cells have been implicated in the response from store-operated calcium pathways that deplete calcium from the endoplasmic reticulum into the intracellular space (Tiruppathi *et al*., 2003) by phospholipase C (PLC)-catalyzed formation of inositol 1, 4, 5-triphosphate or IP3 (Montell *et al*., 2002). Since lead and OP compounds are associated with variations in intracellular calcium concentrations in different cell systems (Goldstein, 1993; Long *et al*., 1994; Marcovac and Goldstein, 1998, Schanne *et al*., 1997; Schuh *et al*., 2002), and given the fact that TRPC activation is affected by calcium dependant mechanisms, and both lead and malathion can be associated with effects on calcium

dependant intracellular pathways, the TRPC channels are good candidates to explain the increases of intracellular calcium induced by lead-OP neurotoxicity.

The results obtained from analysis of TRPC1/TRPC4 protein levels by western blot demonstrated that the neurotoxicants induced an increase in protein levels in RBE4 cells shortly after exposure. Analysis of gene expression of both TRPC1 and TRPC4 by qPCR revealed a connection between these increases of protein levels and expression of the genes associated with the protein assembly. These results support the second part of our hypothesis, that at least one mechanism utilized by neurotoxicants lead and malathion to induce changes in tight junction and scaffold proteins and hence, induce BBB permeability, is by increasing production of TRPC channels in the membrane of endothelial cells of the BBB. These increases induce raises in intracellular calcium (separate measurements of intracellular calcium confirmed calcium increases in response to lead-malathion/oxon insult) that could modify BBB structure. This BBB modification induced by rises of cytosolic calcium could in turn affect by different mechanisms, scaffold proteins in the cytosolic portion of endothelial cell membranes and tight junctions proteins in the paracellular space between adjacent endothelial cells.

Although the hypotheses proposed in this dissertation were well supported by our findings, many areas in this study need to be analyzed further. Indeed, assessments of metalloproteinases activation, measurements of calcium levels in response to malathion and lead insult, and analyses of intracellular calcium pathways need to be addressed and resolved. Nevertheless, in endothelial cells of the BBB, activation of TRPC channels seems to play an important role in initiating the mechanism or mechanisms that disrupt tight junction and scaffold proteins inducing BBB damage.

General References

Abbott N. J. Astrocyte-Endothelial Interactions and Blood-Brain Barrier Permeability. *J Anat*. 200: 629-638, 2002.

Abbott N.J., Ronnback L., Hansson E. Astrocyte-Endothelial Interactions at the Blood-Brain Barrier. *Nat Rev Neurosci*. 7:41-53, 2006.

Abou-Donia M. B. Organophosphorus Ester-Induced Chronic Neurotoxicity. *Arch Environ Health*. 58(8): 484-498, 2003.

Agency for Toxic Substances and Disease Registry. Interaction Profile for Chlorpyrifos, Lead, Mercury, and Methyl Mercury. *U. S. Department of Health and Human Services*, 2006.

Alavijeh M. S., Chishty M., Qaiser M. Z., Palmer A. M. Drug Metabolism and Pharmacokinetics, the Blood-Brain-Barrier, and Central Nervous System Drug Discovery. *NeuroRx*. 2: 554-571, 2005.

Aldridge W. N. Organophosphorus Compounds and Carbamates. In: *Mechanisms and Concepts in Toxicology.* Taylor & Francis, London. 1996.

Alexander S. P. H., Mathie A., Peters J. A. Guide to Receptors and Channels (GRAC). *Br J Pharmacol.* 153(2): S1–S209, 2008.

Ando-Akatsuka Y., Saitou M., Hirase T., Kishi M., Sakaqkibara A., Itoh M., Yonemura S., Furuse M., Tsukita S. Interspecies Diversity of the Occludin Sequence: cDNA Cloning of Human, Mouse, Dog, and Rat-Kangaroo Homologues. *J Cell Biol.* 133:43–48, 1996.

Andreeva A. Y., Krause E., Muller E. C., Blasig I. E., Utepbergenov D. I. Protein kinase C Regulates the Phosphorylation and Cellular Localization of Occludin. *J Biol Chem*. 276: 38480–38486, 2001.

Antoniotti S., Pla A. F., Barral S., Scalabrino O., Munaron L., Lovisolo D. Interaction Between TRPC Channel Subunits in Endothelial Cells. *Journal of Receptors and Signal Transduction*. 26: 225-240, 2006.

Audus K. L., Borchardt R. T. Characterization of an *In vitro* Model for Studying Drug Transport and Metabolism. *Pharma Res.* 3: 81-87, 1986a.

Audus K. L., Borchardt R. T. Characterization of the Large Neutral Amino Acid Transport of Bovine Brain Microvessel Endothelial Cell Monolayers. *J Neurochem.* 47: 484-488, 1986b.

Avazeri N., Denys A., Lefẽvre B. Lead Cations Affect the Control of Both Meiosis Arrest and Meiosis resumption of the Mouse Oocyte In vitro at Least Via the PKC Pathway. *Biochimie.* 88(11): 1823-1829, 2006.

Balbuena P., Li W., Magnin-Bissel G., Meldrum B., Ehrich M. Comparison of Two Blood-Brain Barrier *In vitro* Systems: Cytotoxicity and Transfer Assessments of Malathion/Oxon and Lead Acetate. *Toxicol Sci.*114(2): 260-271. 2010.

Balbuena P., Meldrum B., Fuhrman K., Wise B., Ehrich M. Transfer of Neurotoxicants (Malathion and Lead Acetate) in Combination Through *In vitro* Blood-Brain Barrier Systems. The Toxicologist, supplement for Toxicological Sciences. 102: 469, 2008.

Balda M. S., Anderson J. M. Two Classes of Tight Junctions are Revealed by ZO1 Isoforms. *Am J Physiol.* 264: C918–C924, 1993.

Balda M. S., Anderson J. M., Matter K. The SH3 Domain of the Tight Junction Protein ZO1 Binds to A Serine Protein Kinase that Phosphorylates a Region C-terminal to This Domain. *FEBS Lett.* 399:326-332, 1996.

Balda M. S., Gonzalez-Mariscal L., Matter K., Cereijido M., Anderson J. M. Assembly of the Tight Junction: The Role of Diacylglycerol. *J Cell Biol.* 123: 293-302, 1993.

Balda M. S., Matter K. The tight Junction Protein ZO1 and an Interacting Transcription Factor Regulate ErbB-2 Expression. *EMBO J.* 19: 2024-2033, 2000.

Balda M. S., Whitney J. A., Flores C., Gonzales S., Cereijido M., Matter K. Functional Dissociation of Paracellular Permeability and Transepithelial Electrical Resistance and

Disruption of the Apical-Basolateral Intramembrane Diffusion Barrier by Expression of Mutant Tight Junction Membrane Protein. *J Cell Biol.* 134: 1031-1049. 1996.

Balda S. M., Matter K. Biogenesis of Tight Junctions: The C-Terminal Domain of Occludin Mediates Basolateral Targeting. *J Cell Sci.* 111: 511-519, 1998a.

Balda S. M., Matter K. Tight Junctions. *J Cell Sci.* 111: 541-547, 1998b.

Balda S. M., Matter K. Transmembrane Proteins of the Tight Junctions. *Cell Dev Biol.* 11: 281-289, 2000.

Ballabh P., Braun A., Nedergaard M. The Blood-Brain Barrier: an Overview Structure, Regulation, and Clinical Implications. *Neurobiol Dis*. 16: 1-13, 2004.

Banerjee S., Bhat M.A. Neuron-Glial Interactions in Blood-Brain Barrier Formation. *Ann Rev Neurosci*. 30:235-258, 2007.

Beatch M., Jesaitis L. A., Gallin W. J., Goodenough D. A., Stevenson B. R. The Tight Junction Protein ZO-2 Contains Three PDZ (PSD-95/Discs-Large/ZO1) Domains and an Alternatively Spliced Region. *J Biol Chem.* 271: 25723-25726, 1996.

Bevilagua L. R., Medina J. H., Izquierdo I., Camarota M. Memory consolidation induces N-methyl-D-aspartic acid-receptor- and Ca2+/calmodulin-dependent protein kinase II-dependent

modifications in alpha-amino-3-hydroxy-5-methylisoxazole-4-propionic acid receptor properties. *Neuroscience*. 136(2): 397-403, 2005.

Biegel D., Spencer D.D., Patcher J. S. Isolation and Culture of Human Brain Microvessel Endothelial Cells for the Study of Blood-Brain Barrier Properties *In vitro*. *Brain Res.* 692: 183-189, 1995.

Bondy S. C. The Neurotoxicity of Organic and Inorganic Lead. In: *Metal Neurotoxicity.* S. C. Bondy, K. N. Prasad eds. CRC Press, Boca Raton Florida. pp 96, 1988.

Boulding T. W., Mushak P., O'tuama L. A., Krigman M. R. Blood-Brain Barrier Dysfunction in Acute Lead Encephalopathy: A Reappraisal. *Env Health Perspect.*12: 81-88, 1975.

Bowman P. D., Betz A. L., Ar D., Wolinsky J. S., Penney J. B., Shivers R. R., Goldstein G. W. Primary Culture of Capillary Endothelium from Rat Brain. *In vitro*. 17: 353-362, 1981.

Bressler J., Kim K., Chakraborti T., Goldstein G. Molecular Mechanisms of Lead Neurotoxicity. *Neurochem Res.* 24(4): 595-600, 1999.

Brightman M. W., Reese T. S. Junctions Between Intimately Apposed Cell Membranes in the Vertebrate Brain. *J Cell Biol.* 40:648–677, 1969.

Buratti F. M., D'aniello A., Volpe M. T., Meneguz A., Testai E. Malathion Bioactivation in the Human Liver: The Contribution of Different Cytochrome P450 Isoforms. *Drug Metabol Disp.* 33: 295-302, 2005.

Calderon-Salinas J. V., Quintanar-Escorcia M. A., Gonzales-Martinez M. T., Luna C. E. Lead and Calcium Transport in Human Erythrocyte. *Hum Exp Toxicol.* 18: 327-332, 1999.

Carlson K., Ehrich M. Human Neuroblastoma Cell Viability and Growth are Affected by Altered Culture Conditions. *In vitro and Molec Toxicol.* 13(4): 249-262, 2000.

Casida J. E., Quistad G. B. Serine Hydrolase Targets of Organophosphorus Toxicants. *Chem Biol Interac.* 157-157: 277-283, 2005.

Catterall W. A. From Ionic Currents to Molecular Mechanisms: The Structure and Function of Voltage-Gated Sodiun Channels. *Neuron.* 26: 13-25, 2000.

Chen Y. H., Lu Q., Goodenough D. A., Jeansonne B. Nonreceptor Tyrosine Kinase C-Yes Interacts with Occludin During Tight Junction Formation in Canine Kidney Epithelial Cells. *Mol Biol Cell.* 13: 1227–1237, 2002.

Choudhary S., Verma S. K., Raheja G., Kaur P., Joshi K., Dip-Gill K. The L-Type Calcium Channel Blocker Nimodipine Mitigates Cytoskeletal Proteins Phosphorylation in Dichlorvos-Induced Delayed Neurotoxicity in Rats. *Basic Clin Pharmacol Toxicol*. 98: 447–455, 2006.

Cioffi D.L., Stevens T. Regulation of Endothelial Cell Barrier Function by Store-Operated Calcium Entry. *Microcirculation*. 13: 709-723, 2006.

Citi S. The Cytoplasm Plaque Protein of the Tight Junction. In: *Tight Junctions 2nd. Edition.* M. Cereijido, J. Anderson eds. CRC Press LLC, Boca Raton Florida. pp. 231-264, 2001.

Citi S., Sabanay H., Jakes R., Geiger B., Kedrick-Jones J. Cingulin: a New Peripheral Component of Tight Junctions. *Nature.* 333: 272-276, 1988.

Citi S., Sabanay H., Kedrick-Jones J., Geiger B. Cingulin: Characterization and Localization. *J Cell Sci.* 93: 107-122, 1989.

Clark E. A., Leach K. L., Trojanowski J. Q., Lee V. M. Characterization and Differential Distribution of the Three Major Human Protein Kinase C Isozymes (PKC-alpha, PKC-beta, and PKC-gamma) of the Central Nervous System in Normal and Alzheimer's Disease Brain. *Lab Invest.* 64(1): 35-44, 1991.

Coisne C., Dehouck L., Faveeuw C., Delplace Y., Miller F., Landry C., Morissette C., Fenart L., Cecchelli R., Tremblay P., Dehouck B. Mouse Syngenic *In vitro* Blood-Brain Barrier Model: a New Tool to Examine Inflammatory Events in Cerebral Endothelium. *Lab Invest.* 85: 734-746, 2005.

Colomer J., Means A. R. Physiological Roles of the Ca2+/CaM-Dependent Protein Kinase Cascade in Health and Disease. *Subcell Biochem.* 45: 169-214, 2007.

Cordenonsi M., Mazzon E., De Rigo L., Baraldo S., Meggio F., Citi S. Occludin Dephosphorylation in Early Development of Xenopus laevis. *J Cell Sci.* 110: 3131–3139, 1997.

Cordenonsi M., Turco F., D'Atri F., Hammar E., Martinucci G., Meggio F., Citi S. Xenopus Laevis Occludin: Identification of *In vitro* Phosphorylation Sites by Protein Kinase CK2 and Association with Cingulin. *Eur J Biochem*. 264: 374–384, 1999.

de Boer A. G., van der Sandt I. C. G., Gaillard P. J. The Role of Drug Transporters at the Blood-Brain Barrier. *Annu Rev Pharmacol Toxicol*. 43:629–56, 2003.

DeMaio L., Chang Y. S., Gardner T. W., Tarbell J. M, Antonetti D. A. Shear Stress Regulates Occludin Content and Phosphorylation. *Am J Physiol Heart Circ Physiol.* 281: H105–H113, 2001.

Diglio C. A., Grammas P., Giacomelli F., Wiener J. Primary Culture of Rat Cerebral Microvascular Endothelial Cells: Isolation, Growth and Characterization. *Lab Invest*. 46: 554-563, 1982.

Dyer K., Jortner B. S., Shell L. G., Ehrich M. Comparative Dose-Response Studies of Organophosphorus Ester-Induced Delayed Neuropathy in Rats and Hens. *Neurotoxicol.* 13: 745-756, 1992.

Eaton D. L. , Stacey N. H., Wong K. L., Klaassen C. D. Dose-Response Effects of Various Metal Ions on Rat Liver Metallothionein, Glutathione, Heme Oxygenase, and Cytochrome P-450. *Toxicol App Pharmacol.* 55(2): 393-402, 1980.

Ebnet K., Aurrand-Lions M., Kuhn A., Kiefer F, Butz S., Zander K., Meyer zu Brickwedde M., Suzuki A., Imhof B. A., Vestweber D. The Junctional Adhesion Molecule (JAM) Family Members JAM-2 and JAM-3 Associate with the Cell Polarity Protein PAR-3: a Possible Role for JAMs in Endothelial Cell Polarity. *J Cell Sci.* 116 (19): 3879-3891, 2003.

Ecobichon D. J. Toxic Effects of Pesticides. In: *Casarett & Doull's Toxicology, The Basic Science of Poisons 6th edition.* C. D. Klaassen, ed. McGraw-Hill, NY. pp 763-810, 2001.

Ehrich M. Bridging the Gap Between In vitro and In vivo Toxicology Testing. *ATLA.* 31, 267-271, 2003.

Ehrich M. Organophosphates. In: *Encyclopedia of Toxicology Vol. 2* (P. Wexler, ed.), Academic Press, San Diego, pp 308-311, 2005.

Ehrich M., Correll L. Inhibition of Carboxylesterases in SH-SY5Y Human and NB41A3 Mouse Neuroblastoma Cells by Organophosphorus Esters. *J Toxicol Environ Health*. 53: 385-399, 1998.

Ehrich M., Gross W. B. Modification of TOTP Toxicity in Chickens by Stress. *Toxicol. Appl. Pharmacol.* 70: 249-254, 1983.

Ehrich M., Hancock S., Ward D., Holladay S., Pung T., Floyd L., Hinckley J., Jortner B. S. Neurologic and Immunologic Effect of Exposure to Corticosterone, Chlorpyrifos, and Multiple Doses of Tri-Ortho-Tolyl Phosphate Over 28-Day Period in Rats. *J Toxicol Environ Health.*67(A): 431-457, 2004.

Ehrich M., Jortner B. S., Padilla S. Comparison of the Relative Inhibition of Acetylcholinesterase and Neuropathy Target Esterase in Rats and Hens Given Cholinesterase Inhibitors. *Fundam App Toxicol.* 24: 94-101, 1995.

Ehrich M., Veronesi B. *In vitro* Neurotoxicology. In: *Target Organ Toxicity Neurotoxicology* (H. Tilson, J. Harris, eds.), Taylor and Francis, Washington DC. pp 37-51, 1999.

Ehrich M., Wu X., Were S. R., Major M. A., McCain W. C., Reddy G. Calcium Signaling in Neuronal Cells Exposed to the Munitions Compound Cyclotrimethylenetrinitramine (RDX). *Int J Toxicol.* 28(5):425-435, 2009.

Ehrlich P. About the Relationship Between Chemical Constitution and Effective Distribution of Phamacological Dyes. In: *Collected Works on Immunological Research*. pp 574, 1904.

El-Fawal H. A. N., Correll L., Gay L., Ehrich M. Protease Activity in Brain, Nerve, and Muscle of Hens Given Neuropathy-Inducing Organophosphates and a Calcium Channel Blocker. *Toxicol App Pharmacol*. 103: 132-142, 1990.

El-Fawal H. A. N., Jortner B.S., Ehrich M. Effect of Verapamil on Organophosphorus-Induced Delayed Neuropathy in Hens. *Toxicol Appl Pharmacol*. 97: 500-511, 1989.

El-Fawal H. A. N., Jortner B.S., Ehrich M. Modification of Phenyl Saligenin Phosphate-Induced Delayed Effects by Calcium Channel Blockers: *In vivo* and *In vitro* Electrophysiological Assessment. *Neurotoxicol*. 11: 573-592, 1990.

Eng L. F., Ghirnikar R. S. GFAP and Astrogliosis. *Brain Pathol.* 4(3): 229-237. 1994.

Eng L. F., Ghirnikar R. S., Lee Y. L. Glial Fibrillary Acidic Protein: GFAP-Thirty-One Years (1969-2000). *Neurochem Res.* 25(9-10): 1439-1451, 2000.

Environmental Protection Agency. (2000-2001). Pesticide Market Estimates. Pesticide Industry Sales webpage. Retrieved August 10, 2009, from http://www.epa.gov/oppbead1/pestsales/01pestsales/usage2001_3.htm#3_8

Fanning A. S. ZO Proteins and Tight Junction Assembly. In: *Tight Junctions* (L.Gonzalez-Mariscal ed.), Landes Bioscience, Georgetown Texas; Springer Science+Business Media, New York NY, pp 64-75, 2006.

Fanning A. S., Jameson B. J., Jesaitis L. A., Anderson J. M. The Tight Junction Protein Z0-1 Establishes a Link Between the Transmembrane Protein Occludin and the Actin Cytoskeleton. *J Biol Chem.* 273: 29745-29753, 1998.

Filippelli G. M., Laidlaw M. A. The Elephant in the Playground: Confronting Lead-Contaminated Soils as an Important Source of Lead Burdens to Urban Populations. *Perspect Biol Med*. 53: 31-45, 2009.

Fullmer C. S., Edelstin S., Waserman R. H. Lead-Binding Properties of Intestinal Calcium-Binding Proteins. *J Biol Chem.* 260: 6816-6819, 1985.

Furuse M., Fujita K., Hiragi T., Fujimoto K., Tsukita S. Claudin-1 and -2: Novel Integral Membrane Proteins Localizing at Tight Junctions with no Sequence Similarity to Occludin. *J Cell Biol.* 141:1539–1550, 1998.

Furuse M., Hirase T., Itoh M., Nagafuchi A., Yonemura S., Tsukita S. Occludin: a Novel Integral Membrane Protein Localizing at Tight Junctions. *J Cell Biol.* 123:1777–1788, 1993.

Furuse M., Itoh M., Hirase T., Nagafuchi A., Yonemura S., Tsukita S. Direct Association of Occludin with ZO1 and Its Possible Involvement in the Localization of Occludin at Tight Junctions. *J Cell Biol*. 127: 1617–1626, 1994.

Furuse M., Tsukita S. Claudins in Occluding Junctions of Humans and Flies. *Trends Cell Biol.* 16: 181-188, 2006.

Gallo M. A., Lawryk N. J. Organic phosphorus pesticides. In: *Handbook of Pesticide Toxicology*. W. J. Hayes, E. R. Laws, Eds. Academic Press, pp 263, New York, NY, 1991.

Gao L., Joberty G., Macara I. G. Assembly of Epithelial Tight Junctions Is Negatively Regulated by PAR-6. *Curr Biol.* 12 (3): 221-225, 2002.

Gaudet R. TRP Channels Entering the Structural Era. *J Physiol.*586 (15): 3565-3575, 2008

Gias U. A., Asrar B. M. Functional Role of TRPC Channels in the Regulation of Endothelial Permeability. *Arch-Eur J Physiol.* 451: 131-142. 2005.

Giepmans B. N., Moolenaar W. H. The Gap Junction Protein Conexin-43 Interacts with the Second PDZ Domain of the Zona Occludens-1 Protein. *Curr Biol.*8: 931-934, 1998.

Gilbert M. E., Lasley S. M. Developmental Lead(Pb) Exposure Reduces the Ability of the NMDA Antagonist MK-801 to Suppress Long Term Potentiation (LTP) in the Rat Dentate Gyrus *In vivo*. *Neurotoxicol Teratol.* 29(3): 385-393, 2007.

Gilbert M. E., Mack C. M. Chronic Lead Exposure Accelerates Decay of Long Term Potentiation in Rat Dentate Gyrus *In vivo*. *Brain Res.* 789(1): 139-149, 1998.

Gilbert M. E., Mack C. M., Lasley S. M. Chronic Developmental Lead Exposure Increases the Threshold for Long Term Potentiation in Rat Dentate Gyrus *In vivo*. *Brain Res.* 736(1-2): 118-124, 1996.

Goldmann E. E. Fundamentals of Staining in Central Nervous System. *Treaties of the Royal Prussian Academy of the Sciences.* 1:1–60, 1913.

Goldstein G. W. Evidence that Lead Acts As a Calcium Substitute in Second Messenger Metabolism. *Neurotoxicol.* 14: 97-102, 1993.

Goldstein G. W. Lead Poisoning and Brain Cell Function. *Env Health Perspect.* 89: 91-94, 1990.

Goldstein G. W., Asbury A. K., Diamond I. Pathogenesis of Lead Encephalopathy: Uptake of Lead and Reaction of Brain Capillaries. *Arch Neurol.* 31: 382-389, 1974.

Gonzalez-Mariscal L., Betanzos A., Nava P., Jaramillo B. E. Tight Junction Proteins. *Prog Biophys Mol Biol.* 81: 1-44, 2003.

Goyer R. A. Lead Toxicity: Current Concerns. *Environ Health Perspect*. 100: 177-187, 1993.

Goyer R. A., Clarkson T. W. Toxic Effects of Metals. In: *Casarett & Doull's Toxicology, The Basic Science of Poisons 6th edition.* C. D. Klaassen, ed. McGraw-Hill, NY. pp 811-867, 2001.

Grebenkämper K., Galla H. J. Translational Diffusion Measurements of a Fluorescent Phospholipid Between MDCK-1 Cells Support the Lipid Model of the Tight Junctions. *Chem Phys Lipid.* 71: 133-143, 1994.

Greenblatt H. M., Dvir H., Silman I., Sussman J. L. Acetylcholinesterase: a Multifaceted Target for Structure-Based Drug Design of Anticholinesterase Agents for the Treatment of Alzheimer's Disease. *J Mol Neurosci.* 20: 369-383, 2003.

Gumbiner B., Lowenkopf T, Apatira D. Identification of a 160kDa Polypeptide that Binds to the Tight Junction Protein ZO1. *Proc Natl Acad Sci.* 88: 3460-3464, 1991.

Habermann H. C., Crowell K., Janicki P. Lead and Other Metals Can Substitute for Ca2+ in Calmodulin. *Arch Toxicol.* 54: 61-70, 1983.

Harel M., Kryger G., Rosenberry T. L., Mallender W. D., Lewis T., Fletcher R. J., Guss J. M., Silman I., Sussman J. L. Three-Dimentional Structures of *Drosophila melanogater* Acetylcholinesterase and of Its Complexes with Two Potent Inhibitors. *Protein Sci.* 9:1063-1072, 2000.

Haskins J., Gu L., Wittchen E. S., Hibbard J., Stevenson B. R. ZO-3, A Novel Member of the MAGUK Protein Family Found at the Tight Junction, Interacts With ZO1 and Occludin. *J Cell Biol.* 141:199–208, 1998.

Hawkins B. T., Davis T. P. The Blood-Brain Barrier/Neurovascular Unit in Health and Disease. *Pharmacol. Rev*. 57: 173-185, 2005.

He L., Poblenz A. T., Medrano C. J., Fox D. A. Lead and Calcium Produce Rod Photoreceptor Cell Apoptosis by Opening the Mitochondrial Permeability Transition Pore. *J Biol Chem.* 275: 12175-12184, 2000.

Hein M., Madefessel C., Haag B., Teichmann K., Post A., Galla H. J. Implications of a Non-Lamellar Lipid Phase for the Tight Junction Stability. Part II: Reversible Modulation of Transepithelial Resistance in High and Low Resistance MDCK-Cells by Basic Amino Acids, Ca+, Protoamine and Protons. *Chem Phys Lipid.* 63(3): 223-233, 1992.

Heo Y., Lee W. T., Lawrence D. A. Differential Effects of Lead and cAMP on Development and Activities of TH-1 and TH2- Lymphocytes. *Toxicol Sci.* 43: 172-185, 1998.

Hernberg S. Lead Poisoning in a Historical Perspective. *Am J Ind Med.* 38: 244-254, 2000.

Hirase T., Staddon J. M., Saitou M., Ando-Akatsuka Y., Itoh M., Furuse M., Fujimoto K., Tsukita S., Rubin L. Occludin as a Possible Determinant of Tight Junction permeability in Endothelial Cells. *J Cell Sci.* 110: 1603-1613, 1997.

Hirose T., Izumi Y., Nagashima Y., Tamai-Nagai Y., Kurihara H., Sakai T., Suzuki Y., Yamanaka T., Suzuki A., Mizuno K., Ohno S. Involvement of ASIP/PAR-3 in the Promotion of Epithelial Tight Junction Formation. *J Cell Sci.* 115 (12): 2485-2495, 2002.

Holash J. A., Noden D. M., Stewart P. A. Re- Evaluating the Role of Astrocytes in Blood-Brain Barrier Induction. *Dev Dyn*. 197: 14-25, 1993.

Hong M. S., Hong S. J., Barhoumi R., Burghardt R. C., Donnelly K.C., Wild J. R., Venkatraj V., Castiglionib E. Neurotoxicity Induced in Differentiated SK-N-SH-SY5Y Human Neuroblastoma Cells by Organophosphorus Compounds. *Toxicol Appl Pharmacol.* 186: 110–118, 2003.

Ide N., Hata Y., Nishioka H., Hirao K., Yao I., Deguchi M., Mizoguchi A., Nishimori H., Tokino T., Nakamura Y., Takai Y. Localization of Membrane-Associated Guanylate Kinase (MAGI)-1/BAI-Associated Protein (BAP) 1 at Tight Junctions of Epithelial Cells. *Oncogene.* 18: 7810-7815, 1999.

Isobe I., Watanabe T., Yotsuyanagi T., Hazemoto N., Yamagata K., Ueki T., Nakanishi K., Asai K., Kato T. Astrocytic Contributions to Blood-Brain Barrier Formation by Endothelial Cells: A possible Use of Aortic Endothelial Cell for In vitro BBB Model. *Neurochem Int.* 28: 523-533, 1996.

Itoh M., Furuse M., Morita K., Kubota K., Saitou M., Tsukita S. Direct Binding of Three Tight Junction-Associated MAGUKs, ZO1, ZO-2, and ZO-3 with the COOH Termini of Claudins. *J Cell Biol.*147(6): 1351-1363, 1999a.

Itoh M., Morita K., Tsukita S. Characterization of ZO-2 as a MAGUK Family Member Associated with Tight ss well as Adherens Junctions with a Binding Affinity to Occludin and Alpha Catenin. *J Biol Chem.* 274:5981-5986, 1999b.

Itoh M., Nagafuchi A., Moroi S., Tsukita S. Involvement of ZO1 in Cadherin-Based Cell Adhesion Through Its Direct Binding to Alpha Catenin and Actin Filaments. *J Cell Biol.*138: 181-192, 1997.

Itoh M., Nagafuchi A., Yonemura S., Kitani-Yasuda T., Tsukita S. The 220-kD Protein Colocalizing With Cadherins in Non-Epithelial Cells is Identical to ZO1, a Tight Junction-Associated Protein in Epithelial Cells: cDNA Cloning and Immunoelectron Microscopy. *J Cell Biol.* 121: 491–502, 1993.

Jason K. M, Kellogg C. K. Neonatal Lead Exposure: Effects of Lead on Development of Behavior and Striatal Dopamine Neurons. *Biochem Behav.* 15: 641-649, 1981.

Jesaitis L. A., Goodenough D. A. Molecular Characterization and Tissue Distribution of ZO-2, a Tight Junction Protein Homologous to ZO1 and the Drosophila Discs-Large Tumor Suppressor Protein. *J Cell Biol.* 124:949–962, 1994.

Jett D. A., Guilarte T. R. Developmental Lead Exposure Alters N-Methyl-D-Aspartate and Muscarinic Cholinergic Receptors in the Hippocampus: An Autoradiography Study. *Neurotoxicol.* 16(1): 7-18, 1995.

Joo F. The Cerebral Microvessels in Culture: An Update. *J Neurochem.* 58: 1-17, 1992.

Joost B. M. M. van Bree, Albertus G. de Boer, Danhof M., Ginsel L. A., Breimer D. D. Characterization of an "*in vitro*" blood-brain barrier: effects of molecular size and lipophilicity on cerebrovascular endothelial transport rates of drugs. *J Pharmacol and Exper Therap*. 247: 1233-1239, 1988.

Jortner B. S., Hancock S. K., Hinckley J., Floyd L., Colby L., Tobias L., Williams L., Ehrich M. Neuropathological Studies of Rats Following Multiple Exposure to Tri-Ortho-Tolyl Phosphate, Chlorpyrifos and Stress. *Toxicol Pathol*. 33: 378-385, 2005.

Jortner B., Ehrich M. Neurophatological Effects of Phenyl Saligenin Phosphate in Chickens. *Neurotoxicol.* 8: 97-108, 1987.

Kamanyire R., Karalliedde L. Organophosphate Toxicity and Occupational Exposure. *Occup Med*. 54: 69-75, 2004.

Kerper L. E., Hinkle P. M. Cellular Uptake of Lead is Activated by Depletion of Intracellular Calcium Stores. *J Biol Chem.* 272(13): 8346-8352, 1997a.

Kerper L. E., Hinkle P. M. Lead Uptake in Brain Capillary Endothelial Cells: Activation by Calcium Store Depletion. *Toxicol App Pharmacol.* 146: 127-133, 1997b.

Kidd S. K., Anderson D. W., Schneider J. S. Postnatal Lead Exposure Alters Expression of Forebrain p75 and TrkA Nerve Growth Factor Receptors. *Brain Res.* 1195: 113-119, 2007.

Kiuchi-Saishin Y., Gotoh S., Furuse M., Takasuga A., Tano Y., Tsukita S. Differential Expression Patterns of Claudins, Tight Junction Membrane Proteins, in Mouse Nephron Segments. *J Am Soc Nephrol.* 13: 875-886, 2002.

Kniesel U., Wolburg H. Tight Junctions of the Blood-Brain Barrier. *Cell Mol Neurobiol*. 20(1): 57-76, 2000.

Kohout S. C., Corbalan-Garcia S., Torrecillas A., Gomez-Fernandez J. C., Falke J. J. C2 Domains of Protein Kinase C Isoforms alpha, beta, and gamma: Activation Parameters and Calcium Stoichiometries of the Membrane-bound State. *Biochemistry.* 41(38): 11411-11424, 2002.

Kurihara H., Anderson J. M., Farquhar M. G. Diversity Among tight Junctions in Rat Kidney: Glomerular Slit Diaphragms and Endothelial Junctions Express Only One Isoform of the Tight Junction Protein ZO1. *Proc Natl Acad Sci.* 89: 7075-7079, 1992.

Kursula P., Majava V. A Structural Insight Into Lead Neurotoxicity and Calmodulin Activation by Heavy Metals. *Acta Crystallogr Sect F Struct Biol Cryst Commun*. 63(8): 653-656, 2007.

Lai C. H., Kuo K. H. The Critical Component to Establish In vitro BBB Model: Pericyte. *Brain Res Rev*. 40: 258-265, 2005.

Lasley S. M., Gilbert M. E. Glutamatergic Components Underlying Lead-Induced Impairments in Hippocampal Synaptic Plasticity. *Neurotoxicol.* 21(6): 1057-1068, 2000.

Lasley S. M., Lane J. D. Diminished Regulation of Mesolimbic Dopaminergic Activity in Rat After Chronic Inorganic Lead Exposure. *Toxicol Appl Pharmacol.* 95(3): 474-483, 1988.

Lee H. S., Han J., Bai H., Kim K. Brain Angiogenesis in Developmental and Pathological Processes: Regulation, Molecular and Cellular Communication at the Neurovascular Interface. *FEBS J*. 276 (17): 4622-4635. 2009.

Legare M. E., Barhoumi R., Hebert E., Bratton G. R., Burghardt R. C., Tiffany-Castiglioni E. Analysis of Pb^{2+} Entry Into Cultured Astroglia. *Toxicol Sci.* 46: 90-100, 1998.

Li W. Y., Huey C. L., Yu A. S. L. Expression of Claudin-7 and -8 Along the Mouse Nephron. *Am J Physiol Renal Physiol.* 286: F1063-F1071, 2004.

Liebner S., Kniesel U., Kalbacher H., Wolburg H. Correlation of Tight Junction Morphology with the Expression of Tight Junction proteins in Blood-Brain Barrier Endothelial Cells. *Eur J Cell Biol.*79: 707-717, 2000.

Long G. J., Rosen J. F., Schanne F. A. X. Lead Activation of Protein Kinase C from Rat Brain. *J Biol Chem.* 14: 834-837, 1994.

Lundin A., Hasenson M., Persen J., Pousette A. Estimation of Biomass in Growing Cell lines by Adenosine Triphosphate Assay. *Methods Enzymol*. 133: 27-42, 1986.

Ma T., Chen H. H., Hume A. S., Ho I. K. Excitatory Amino Acids and Lead-Induced Neurotoxicity. *J Toxicol Sci.* 2: 181-183, 1998.

Macian F., Lopez-Rodriguez C., Rao A. Partners in Transcription: NFAT and AP-1. *Oncogene.* 20(19): 2476-2489, 2001.

Malarkey E.B., Ni Y., Parpura V. Ca2+ Entry Through TRPC1 Channels Contributes to Intracellular Ca2+ Dynamics and Consequent Glutamate Release From Rat Astrocytes. *Glia*. 56(8): 21-35, 2008.

Manabi T. Molecular Mechanisms for Memory Formation. *Brain Nerve.* 60(7): 701-715, 2008.

Manalis R. S., Cooper G. P., Pomeroy S. L. Effects of Lead on Neuromuscular Transmission in the Frog. *Brain Res.* 294(1): 95-109, 1984.

Mañay N., Cousillas A. Z., Alvarez C., Heller T. Lead Contamination in Uruguay: "La Teja" Neighborhood Case. *Rev Environ Contam Toxicol*. 195: 93-115, 2008

Marchetti C. Molecular Targets of Lead in Brain Neurotoxicity. *Neurotox Res.* 5(3): 221-236, 2003.

Marcovac J., Goldstein G. W. Picomolar Concentrations of Lead Stimulate Brain Protein Kinase C. *Nature.* 334: 71-73, 1988.

Marrs T. C., Ballantyne B. Part I Insecticides. In: *Pesticide Toxicology and International Regulation*. T. C. Marrs, B. Ballantyne Eds. John Wiley and Sons. pp 89-128, 2004.

Massiah M. A., Viragh C., Reddy P. M., Kovac I. M., Johnson J., Rosenberry T. L., Mildvan A. S. Short, Strong Hydrogen Bonds at the Active Site of Human Acetylcholinesterase: Proton NMR Studies. *Biochem.* 40: 5682-5690, 2001.

Meldrum B., Balbuena P., Fuhrman K., Wise B., Hirani A., Lee Y., Ehrich M. Transfer Lead Acetate Through an *In Vitro* Blood-Brain Barrier System. The Toxicologist, supplement to Toxicological Sciences. 96: 145, 2007.

Mellström B., Savignac M., Gomez-Villafuertes R., Naranjo J. R. Ca2+-Operated Transcriptional Networks: Molecular Mechanisms and In vivo Models. *Physiol Rev.* 88: 421-449, 2008.

Montel C., Bimbaumer L., Flockerzi V. The TRP Channels, a Remarkable Functional Family. *Cell.* 108: 595-598, 2002.

Montell C. Physiology, Phylogeny, and Functions of the TRP Superfamily of Cation Channels. *Sci. STKE.* Re1. 90: 2-17, 2001.

Montell C. The TRP Superfamily of Cation Channels. *Sci STKE.* Re3, 1-25, 2005.

Montell C., Rubin G. M. Molecular Characterization of the Drosophila *trp* Locus: A Putative Integral Membrane Protein Required for Phototransduction. *Neuron.* 2: 1313-1323, 1989.

Morita K., Furuse M., Fujimoto K., Tsukita S. Claudin Multigene Family Encoding Four Transmembrane Domain Protein Components of Tight Junction Strands. *Proc Natl Acad Sci.* 96: 511-516, 1999.

Morita K., Sasaki H., Furuse M., Tsukita S. Endothelial Claudin: Claudin-5/TMVCF Constitutes Tight Junction Strands in Endothelial Cells. *J Cell Biol.* 147: 185-194, 1999.

Moriwaki K., Tsukita S., Furuse M. Tight Junctions Containing Claudin 4 and 6 are Essential for Blastocyst Formation in Preimplantation Mouse Embryos. *Dev Biol.* 312: 509-522, 2007.

Mosior M., Epand R. M. Protein Kinase C: An Example of a Calcium-Regulated Protein Binding to Membranes. *Mol Membr Biol.* 14(2): 65-70, 1997.

Nagy Z., Peters H., Hüttner I. Fracture Faces of Cell Junctions in Cerebral Endothelium During Normal and Hyperosmotic Conditions. *Lab Invest*. 50: 313–322, 1984.

Nalefski E. A., Newton A. C. Membrane Binding Kinetics of Protein Kinase C βII Mediated by the C2 Domain. *Biochemistry.* 40(44): 13216-13229, 2001.

Nihei M. K., McGlothan J. L., Toscano C. D., Guilarte T. R. Low Level Pb (2+) Exposure Affects Hippocampal Protein Kinase C Gamma Gene and Protein Expression in Rats. *Neurosci Lett.* 298(3): 212-216, 2001.

Nilius B., Droogmans G. Ion Channels and Their Role in Vascular Endothelium. *Physiol Rev.* 81: 1415-1459, 2001.

Nitta T., Hata M., Gotoh S., Seo Y., Sasaki H., Hashimoto N., Furuse M., Tsukita S. Size-Selective Loosening of the Blood-Brain Barrier in Claudin-5-Deficient Mice. *J Cell Biol.* 161: 653-660, 2003.

Nostrandt A. C., Ehrich M. Development of a Model Cell Culture System in Which to Study Early Effects of Neuropathy-Inducing Organophosphorus Esters. *Toxicol Letts.* 60: 107-114, 1992.

Nostrandt A. C., Rowles T. K., Ehrich M. Cytotoxic Effects of Organophosphorus Esters and Other Neurotoxic Chemicals on Cultured Cells. *In vitro Toxicol.* 5: 127-136, 1992.

Oortgiesen M., van Kleef R. G., Vijverberg H. P. Dual, Non-Competitive Interactions of Lead with Neuronal Nicotinic Acetylcholine Receptors in N1E-115 Neuroblastoma Cells. *Brain Res.* 747(1): 1-8, 1997.

Parekh A. B., Putney Jr. J. W. Store-Operated Calcium Channels. *Physiol Rev.* 85: 757-810, 2005.

Parran D. K., Magnin G., Li W., Jortner B.S., Ehrich M. Chlorpyrifos Alters Functional Integrity and Structure of an *In vitro* Model: Co-Cultures of Bovine Endothelial Cells and Neonatal Rat Astrocytes. *Neurotoxicol.* 26: 77-88, 291, 2005.

Patel M. M., Goyal B. R., Bhadada S. V., Bhatt J. S., Amin A. F. Getting Into the Brain: Approaches to Enhance Brain Drug Delivery. *CNS Drugs*. 23(1): 35-58, 2009.

Pedersen S. F., Owsianik G., Nilius B. TRP Channels: An Overview. *Cell Calcium.* 38: 233-252, 2005.

Pelletier J. G., Lacaille J. C. Long-Term Synaptic Hippocampal Feedback Inhibitory Networks. *Prog Brain Res.* 169: 241-250, 2008.

Peralta O. A., Eyestone W. H. Quantitative and Qualitative Analysis of Cellular Prion Protein (PrPC) Expression in Bovine Somatic Tissues. *Prion*. 3 (3): 161-170,

Petroianu G. A., Lorke D. E., Hasa M. Y., Adem A., Sheen R.. Nurulain S. M., Kalasz H. Paraoxon Has a Minimal Effect on Pralidoxime Brain Concentration in Rats. *J Appl Toxicol.* 27(4): 350-357, 2007.

Platt B., Busselberg D. Combined Actions of Pb2, Zc2, and Al3 on Voltage-Activated Calcium Channel Currents. *Vell Mol Neurobiol.* 14: 831-840, 1994.

Pocock S. J., Smith M., Baghurst P. Environmental Lead and Children's Intelligence: A Systematic Review of the epidemiological Evidence. *BMJ*. 5: 1189-1197, 1994.

Pope C., diLorenzo K., Ehrich M. Possible Involvement of a Neurotrophic Factor During the Early Stages of Organophosphate-Induced Delayed Neurotoxicity. *Toxicol Lett.* 75: 111-117, 1995.

Rahner C., Mitic L. L., Anderson J. M. Heterogeneity in Expression and Subcellular Localization of Claudins 2, 3, 4, and 5 in the Rat Liver, Pancreas, and Gut. *Gastroenterology.* 120: 411-422, 2001.

Reese T.S., Karnovsky M.J. Fine Structural Localization of a Blood– Brain Barrier to Exogenous Peroxidase. *J Cell Biol*. 34: 207– 217, 1967.

Reinhart C. A., Gloor S. M. Co-Cultured Blood-Brain Barrier Models and Their Use for Pharmatoxicological Screening. *Toxicol Vitro*. 11: 513-518, 1997.

Reyes J. L., Lamas M., Martin D., Namorado M. C., Islas S., Tauc M., Gonzales-Mariscal L. The Renal Segmental Distribution of Claudins Changes with Development. *Kidney Int.* 62: 476-487, 2002.

Rowles T., Song X., Ehrich M. Identification of Endpoints Affected by Exposure of Human Neuroblastoma Cells to Neurotoxicants at Concentrations Below Those that Affect Cell Viability. *In vitro Toxicol*. 8: 3-13, 1995.

S. Hernberg. Lead Poisoning in a Historical Perspective. *Am J Ind Med*. 38:244-254, 2000.

Saitou M., Furuse M., Sasaki H., Schulzke J. D., Fromm M., Takano H., Noda T., Tsukita S. Complex Phenotype of Mice Lacking Occludin, a Component of Tight Junction Strands. *Mol Biol Cell.*11: 4131-4142, 2000.

Sakakibara A., Furuse M., Saitou M., Ando-Akatsuka Y., Tsukita S. Possible Involvement of Phosphorylation of Occludin in Tight Junction Formation. *J Cell Biol.* 137: 1393–1401, 1997.

Schanne F. A. X., Long G. J., Rosen J. F. Lead-Induced Rise in Intracellular Free Calcium is Mediated Trough Activation of Protein Kinase C in Osteoblastic Bone Cells. *Biochim Biophys Acta.* 1360: 247-254, 1997.

Schock M. R., Hyland R. N., Welch M. M. Occurrence of Contaminant Accumulation in lead Pipe Scales from Domestic Drinking-Water Distribution Systems. *Environ Sci Technol.* 42: 4285–4291, 2008.

Schuh R. A., Lein P. J., Beckles R. A., Jett D. A. Non-Cholinesterase Mechanisms of Chlorpyrifos Neurotoxicity: Altered Phosphorylation of Ca^{2+}/ cAMP Response Element Binding Protein in Cultured Neurons. *Toxicol Appl Pharmacol.* 182: 176-185, 2002.

Shi L. Z., Zheng W. Early Lead Exposure Increases the Leakage of the Blood-Cerebrospinal Fluid Barrier In vitro. *Hum Exp Toxicol.* 26: 159-167, 2007.

Shirai Y., Saito N. Protein Kinase C Isotypes and Their Specific Function, Activation Mechanisms of PKC: Maturation, Activation, and Targeting. *J Biochem.* 132: 663-668, 2002.

Si M. L., Lee T. J. Pb2+ Inhibition of Sympathetic 7-Nicotinic Acetylcholine receptor-mediated Nitrergic Neurogenic Dialtion in Porcine Basilar Arteries. *J Pharmacol Exp Ther. 305(3):* 1124-1131, 2003.

Siddharthan V., Kim Y. V., Liu S., Kim K. S. Human Astrocytes/Astrocyte-Conditioned Medium and Shear Stress Enhance the Barrier Properties of Human Brain Microvascular Endothelial Cells. *Brain Res.* 1147: 39-50, 2007.

Silbergeld E. K. Mechanisms of Lead Neurotoxicity, or Looking Beyond the Lamppost. *FASEB J.* 6: 3201-3206, 1992.

Silman I., Sussman J. L. Acetylcholinesterase: "Classical" and "Non-classical" Functions and Pharmacology. *Curr Opin Pharmacol*. 5: 293-302, 2005.

Silman I., Sussman J. L. Acetylcholinesterase: How Structure Is Related to Function? *Chem Biol Interac.* 175: 3-10, 2008.

Steinber S. F. Structural Basis of Protein Kinase C Isoform Function. *Physiol Rev.* 88(4): 1341-1378, 2008.

Stevenson B. R., Siliciano J. D., Mooseker M. S., Goodenough D. A. Identification of ZO1: a Higher Molecular Weight Polypeptide Associated With the Tight Junction (Zonula Occludens) in a Variety of Epithelia. *J Cell Biol.* 103:755–766, 1986.

Sun L. R., Suszkiw J. B. Extracellular Inhibition and Intracellular Enhancement of Ca2 Currents by Pb2 in Bovine Adrenal Chromaffin Cells. *J Neurophysiol.* 74: 574-581, 1995.

Suzkiw J. B. Presynaptic Disruption of Transmitter Release by Lead. *Neurotoxicol.* 25: 599-604, 2004.

Takai Y., Nakanishi H. Nectin and Afadin: Novel Organizers of Intercellular Junctions. *J Cell Sci.* 116 (1): 17-27, 2003.

Tiruppathi C., Ahmmed G. U., Vogel S. M., Malik A. B. $Ca2^{+}$ Signaling, TRP Channels, and Endothelial Permeability. *Microcirculation*. 13: 693–708, 2006.

Tiruppathi C., Minshall R. D., Paria B. C., Vogel S. M., Malik A. B. Role of Ca2+ Signaling in the Regulation of Endothelial Permeability. *Vascul Pharmacol.* 39: 173-185, 2003.

Toscano C. D., Guilarte T. Lead Neurotoxicity: From Exposure to Molecular Effects. *Brain Res Rev.*49: 529 – 554, 2005.

Tsukita S., Furuse M. Pores in the Wall: Claudins Constitute Tight Junction Strands Containing Aqueous Pores. *J Cell Biol.* 149: 13-16, 2000.

Turksen K., Troy T. C. Barriers Built on Claudins. *J Cell Sci.* 117: 2435-2447, 2004

Turksen K., Troy T. C. Claudin-6: A Novel Tight Junction Molecule is Developmentally Regulated in Mouse Embryonic Epithelium. *Dev Dyn.* 222: 292-300, 2001.

van Bree J. B. M. M., de Boer A. G., Danhof M. M., Ginsel L. A., Breimer D. D. Characterization of an *In vitro* Blood-Brain Barrier: Effects of Molecular Size and Lipophilicity on Cerebrovascular Endothelial Transport Rates of Drugs. *J Pharmacol Exp Ther.* 247(3): 1233-1239, 1988.

Veronesi B., Ehrich M., Blusztajn J. K., Oortgiesen M, Durham H. Cell Culture Models of Interspecies Selectivity to Organophosphorus Insecticides. *Neurotoxicol.* 18(1): 283-298, 1997.

Volterra A., Meldolesi J. Astrocytes, From Brain Glue to Communication Elements: The Revolution Continues. *Nat Rev Neurosci*. 6 (8): 626-640. 2005.

Waalkes M. P., Klaassen C. D. Concentration of Metallothionein in Major Organs of Rats After Administration of Various Metals. *Fund App Toxicol.* 5(3): 473-477, 1985.

Wang L., Chen D., Wang H., Liu Z. Effects of Lead and/or Cadmium on the Expression of Metallothionein in the kidney Rat. *Biol Trace Elem Res.* 129: 190-199, 2009.

Wang L., Luo L., Luo Y. Y., Gu Y., Ruan D. Y. Effects of Pb2+ on Muscarinic Modulation of Glutamatergic Synaptic Transmission in Rat Hippocampal CA1 Area. *Neurotoxicol.* 28(3): 449-507, 2007.

Wang W,, Duan B., Xu H., Xu L., Xu T. Calcium-Permeable Acid-Sending Ion Channel Is a Molecular Target of the Neurotoxic Metal Ion Lead. *J Biol Chem*. 281(5): 2497-2505, 2006.

Watts S. W., Chai S., Webb R. C. Lead Acetate-Induced Contraction in Rabbit Mesenteric Artery: Interactions with Calcium and Protein Kinase C. *Toxicol.* 99: 55-65, 1995.

Wayman G. A., Lee Y. S., Tokumitsu H., Silva A., Soldering T. R. Calmodulin-Kinases: Modulators of Neuronal Development and Plasticity. *Neuron.* 59(6): 914-931, 2008.

White L. D., Cory-Slechta D. A., Gilbert M. E., Tiffany-Castiglioni E., Zawia N. H., Virgolini M., Rossi-George A., Lasley S. M., Qian Y. C., Basha R. New and Evolving Concepts in the Neurotoxicology of Lead. *Toxicol App Pharmacol.* 225: 1-27, 2007.

Wilcox E. R., Burton Q. L., Naz S., Riazuddin S., Smith T. N., Ploplis B., Belyantseva I., Ben-Yosef T., Liburd N. A., Morell R. J., Kachar B., Wu D. K., Griffith A. J., Riazuddin S., Friedman T. B. Mutation in the Gene Encoding Tight Junction Claudin-14 Cause Autosomal Recessive Deafness DFNB29. *Cell.* 104: 165-172, 2001.

Willott E., Balda M. S., Fanning A. S., Jameson B., Van Itallie C., Anderson J. M. The Tight Junction Protein ZO1 is Homologous to the *Drosophila* Disc-Large Tumor Suppressor Protein of Septate Junctions. *Proc Natl Acad Sci.* 90: 7834–7838, 1993.

Wittchen E. S., Haskins J., Stevenson B. R. Protein Interactions at the Tight Junction. Actin Has Multiple Binding Partners, and ZO1 Forms Independent Complexes with ZO-2 and ZO-3. *J Biol Chem.* 274: 35179-35185, 1999.

Wolburg H., Liebner S., Lippoldt A. Freeze-Fracture Studies of Cerebral Endothelial Tight Junctions. *Meth Mol Med.* 89: 51-66, 2003.

Wolburg H., Lippoldt A. Tight Junctions of the Blood-Brain Barrier: Development, Composition and Regulation. *Vascul Pharmacol.* 38: 323-337, 2002.

Wolburg H., Lippoldt A., Ebnet K. Tight Junctions and the Blood-Brain Barrier. In: *Tight Junctions* (L.Gonzalez-Mariscal ed.), Landes Bioscience, Georgetown Texas; Springer Science+Business Media, New York NY. pp. 175-195, 2006.

Wolburg H., Noell S., Mack A., Wolburg-Buchholz K., Fallier-Becker P. Brain Endothelial Cells and the Glio-Vascular Complex. *Cell Tissue Res*. 335(1): 75-96, 2009.

Wong V. Phosphorylation of Occludin Correlates with Occludin Localization and Function at the Tight Junction. *Am J Physiol*. 273: 1859–1867, 1997.

Wong V., Gumbiner B. M. A Synthetic Peptide Corresponding to the Extracellular Domain of Occludin Perturbs the Tight Junction Permeability Barrier. *J Cell Biol.* 136: 399–409, 1997.

Xu S. Z., Bullock L., Shan C. J., Cornelius K., Rajanna B. PKC Isoforms Were Reduced in the Developing Rat Brain. *Int J Dev Neurosci.* 23: 53-64, 2005.

Xu S. Z., Shan C. J., Bullock L., Baker L., Rajanna B. Pb2+ Reduces PKCs and NF-κB In vitro. *Cell Biol Toxicol.* 22: 189-198, 2006.

Yamamoto T., Harada N., Kano K., Taya S., Canaani E., Matsuura Y., Mizoguchi A., Ide C., Kaibuchi K. The Ras Target AF-1 Interacts with ZO1 and Serves as a Peripheral Component of Tight Junctions in Epithelial Cells. *J Cell Biol.* 139 (3): 785-795, 1997.

Yang J., Aschner M. Developmental Aspects of Blood-Brain Barrier (BBB) and Rat Brain Endothelial (RBE4) Cells as *In vitro* Models for Studies on Chlorpyrifos Transport. *Neurotoxicol.* 24: 741-745, 2003.

Yu A. S. L., Enck A. H., Lencer W. I., Schneeberger E. E. Claudin-8 Expression in MDCK Cells Augments the Paracellular Barrier to Cation Permeation. *J Biol Chem.* 278: 17350-17359, 2003.

Zheng W. Neurotoxicology of the Brain Barrier Systems: New Implications. *Clin Toxicol.* 39(7): 711-719, 2001.

Zheng W., Aschner M., Ghersi-Egeac J. Brain Barrier Systems: a New Frontier in Metal Neurotoxicological Research. *Toxicol Appl Pharmacol*. 192: 1–11, 2003.

Zhu X., Jiang M., Peyton M., Boulay G., Hurst R., Stefani E., Birnbaumer L. TRP, A Novel Mammalian Agonist-activated Capacitative Ca^{2+} Entry. *Cell.* 85: 661-671, 1996.

Appendix A

License agreement for reproduction of material from

Toxicological Sciences (Oxford University Press)

OXFORD UNIVERSITY PRESS LICENSE

TERMS AND CONDITIONS

May 24, 2010

This is a License Agreement between Marion Ehrich ("You") and Oxford University Press ("Oxford University Press") provided by Copyright Clearance Center ("CCC"). The license consists of your order details, the terms and conditions provided by Oxford University Press, and the payment terms and conditions.

All payments must be made in full to CCC. For payment instructions, please see information listed at the bottom of this form.

License Number

2395390035540

License date

Mar 24, 2010

Licensed content publisher

Oxford University Press

Licensed content publication

Toxicological Sciences

Licensed content title

Comparison of Two Blood-Brain Barrier In Vitro Systems: Cytotoxicity and Transfer Assessments of Malathion/Oxon and Lead Acetate

Licensed content author

Pergentino Balbuena, et. al.

Licensed content date

April 2010

Type of Use

Thesis/Dissertation

Institution name

Title of your work

Neurotoxic Effects of Malathion and Lead Acetate on the Blood-Brain Barrier

Publisher of your work

n/a

Expected publication date

Jun 2010

Permissions cost

0.00 USD

Value added tax

0.00 USD

Total

0.00 USD

Total

0.00 USD

Terms and Conditions

STANDARD TERMS AND CONDITIONS FOR REPRODUCTION OF MATERIAL FROM AN OXFORD UNIVERSITY PRESS JOURNAL

1. Use of the material is restricted to the type of use specified in your order details.

2. This permission covers the use of the material in the English language in the following territory: world. If you have requested additional permission to translate this material, the terms and conditions of this reuse will be set out in clause 12.

3. This permission is limited to the particular use authorized in (1) above and does not allow you to sanction its use elsewhere in any other format other than specified above, nor does it apply to quotations, images, artistic works etc that have been reproduced from other sources which may be part of the material to be used.

4. No alteration, omission or addition is made to the material without our written consent. Permission must be re-cleared with Oxford University Press if/when you decide to reprint.

5. The following credit line appears wherever the material is used: author, title, journal, year, volume, issue number, pagination, by permission of Oxford University Press or the sponsoring society if the journal is a society journal. Where a journal is being published on behalf of a learned society, the details of that society must be included in the credit line.

6. For the reproduction of a full article from an Oxford University Press journal for whatever purpose, the corresponding author of the material concerned should be informed of the proposed use. Contact details for the corresponding authors of all Oxford University Press journal contact can be found alongside either the abstract or full text of the article concerned, accessible from www.oxfordjournals.org Should there be a problem clearing these rights, please contact journals.permissions@oxfordjournals.org

7. If the credit line or acknowledgement in our publication indicates that any of the figures, images or photos was reproduced, drawn or modified from an earlier source it will be necessary

for you to clear this permission with the original publisher as well. If this permission has not been obtained, please note that this material cannot be included in your publication/photocopies.

8. While you may exercise the rights licensed immediately upon issuance of the license at the end of the licensing process for the transaction, provided that you have disclosed complete and accurate details of your proposed use, no license is finally effective unless and until full payment is received from you (either by Oxford University Press or by Copyright Clearance Center (CCC)) as provided in CCC's Billing and Payment terms and conditions. If full payment is not received on a timely basis, then any license preliminarily granted shall be deemed automatically revoked and shall be void as if never granted. Further, in the event that you breach any of these terms and conditions or any of CCC's Billing and Payment terms and conditions, the license is automatically revoked and shall be void as if never granted. Use of materials as described in a revoked license, as well as any use of the materials beyond the scope of an unrevoked license, may constitute copyright infringement and Oxford University Press reserves the right to take any and all action to protect its copyright in the materials.

9. This license is personal to you and may not be sublicensed, assigned or transferred by you to any other person without Oxford University Press's written permission.

10. Oxford University Press reserves all rights not specifically granted in the combination of (i) the license details provided by you and accepted in the course of this licensing transaction, (ii) these terms and conditions and (iii) CCC's Billing and Payment terms and conditions.

11. You hereby indemnify and agree to hold harmless Oxford University Press and CCC, and their respective officers, directors, employs and agents, from and against any and all claims

arising out of your use of the licensed material other than as specifically authorized pursuant to this license.

12. Other Terms and Conditions:

v1.4

Gratis licenses (referencing $0 in the Total field) are free. Please retain this printable license for your reference. No payment is required.

If you would like to pay for this license now, please remit this license along with your payment made payable to "COPYRIGHT CLEARANCE CENTER" otherwise you will be invoiced within 48 hours of the license date. Payment should be in the form of a check or money order referencing your account number and this invoice number RLNK10756516. Once you receive your invoice for this order, you may pay your invoice by credit card. Please follow instructions provided at that time.

Make Payment To:
Copyright Clearance Center
Dept 001
P.O. Box 843006
Boston, MA 02284-3006

If you find copyrighted material related to this license will not be used and wish to cancel, please contact us referencing this license number 2395390035540 and noting the reason for

cancellation.

Questions? customercare@copyright.com or +1-877-622-5543 (toll free in the US) or +1-978-646-2777.

Appendix B

GC-MS Analysis of malathion and malaoxon

ANALYSIS OF MALATHION FROM CELL MEDIA

A. SAMPLE EXTRACTION

- **Standards**

Malathion, Malaoxon and malathion-d10 (internal standard) were purchased from ChemServices. The stock solutions (0.1M) were prepared in acetonitrile. The working solutions of malathion and malaoxon ($2.5x10^{-8}$M to 10^{-6}M) were prepared in acetone and each concentration contained 10^{-7}M of malathion-d10 (internal standard).

The calibration curve was submitted to the solid phase extraction process in an identical way to the samples. To 1 ml of media and 1 ml of HPLC grade water was added 100 µl of each standard in acetone. The mixture was cleaned-up through a solid phase extraction (SPE) cartridge.

- **Samples**

To X ml of sample (media) was added 1 ml of HPLC grade water and 100 µl of Malathion-d10 10^{-7}M in acetone. The mixture was then ready for SPE.

- **Solid phase extraction procedure**

The standards and samples were purified and concentrated through a solid phase extraction cartridge Waters Oasis® HLB, 1cc (30 mg), part#186001879.

The cartridge was conditioned with 1 ml of methanol and 1 ml of water

The sample was loaded on the cartridge

The cartridge was washed with 2 x 1 ml of water

The organophosphates were eluted with 1.5 ml of ethyl acetate

The upper layer (ethyl acetate) was transferred to a 1 dram glass vial and the solvent was evaporated under a stream of nitrogen.

Note: the lower layer is water and it was discarded.

The residue was reconstituted in 100 µl of ethyl acetate and it was analyzed by GC-MS.

B. GAS-CHROMATOGRAPHY-MASS SPECTROMETRY (GC-MS)

- **Gas Chromatograph parameters**

  - Gas Chromatograph Agilent Technologies 6890
  - Column: HP-5MS (5% Phenyl Methyl Siloxane), length 30 m, Nominal diameter 250.00 µm, film thickness 0.25 µm
  - Injection port: split/splitless, in splitless mode
  - Injection port temperature: 220 °C
  - Oven parameters

Initial T (°C)	Initial T (°C)	Rate (°C/min)	Hold time (min)
60			2
60	200	3	
200	300	15	3

  - Carrier gas: Helium at a constant flow rate of 1.2 ml/min
  - Transfer line temperature: 250 °C
  - Injection volume: 2 µl

- **Mass spectrometer parameters**

  - Mass Spectrometer : Agilent Technologies 5973 inert
  - Ion source: Negative chemical ionization (NCI)

- Source temperature: 150 °C
- Quadrupole temperature: 150 °C
- EM Voltage: 1623.529
- Gain factor: 10
- Resulting EM Voltage: 2176
- Tune file: ncich4.u
- Solvent delay: 14 min
- Acquisition mode: single ion monitoring (SIM), low resolution

Group	Start time (min)	m/z	Dwell time (ms)	Compounds monitored
Malaoxon	14.00	141.0	100	Malaoxon
		172.0	100	Malaoxon
Malathion	16.50	156.9	100	Malathion and Malathion-d10
		172.0	100	Malathion
		182.1	100	Malathion-d10

The malathion concentration was calculated by summing the intensities of the two ions m/z *156.90* and *172.0*.

The malaoxon concentration was calculated by summing the intensities of the two ions m/z *141.0* and *172.0*.

The malathion-d10 (internal standard) concentration was calculated by summing the intensities of the two ions m/z *156.90* and *182.10*.

C. RESULTS

- **STANDARDS**

  - Calibration curves (average between 3 different preparations)

Concentration	Intensity ratios
2.5E-08	1.09
5.0E-08	1.34
7.5E-08	1.67
1.0E-07	1.97
2.5E-07	3.72
5.0E-07	7.19
7.5E-07	10.00
1.0E-06	13.08

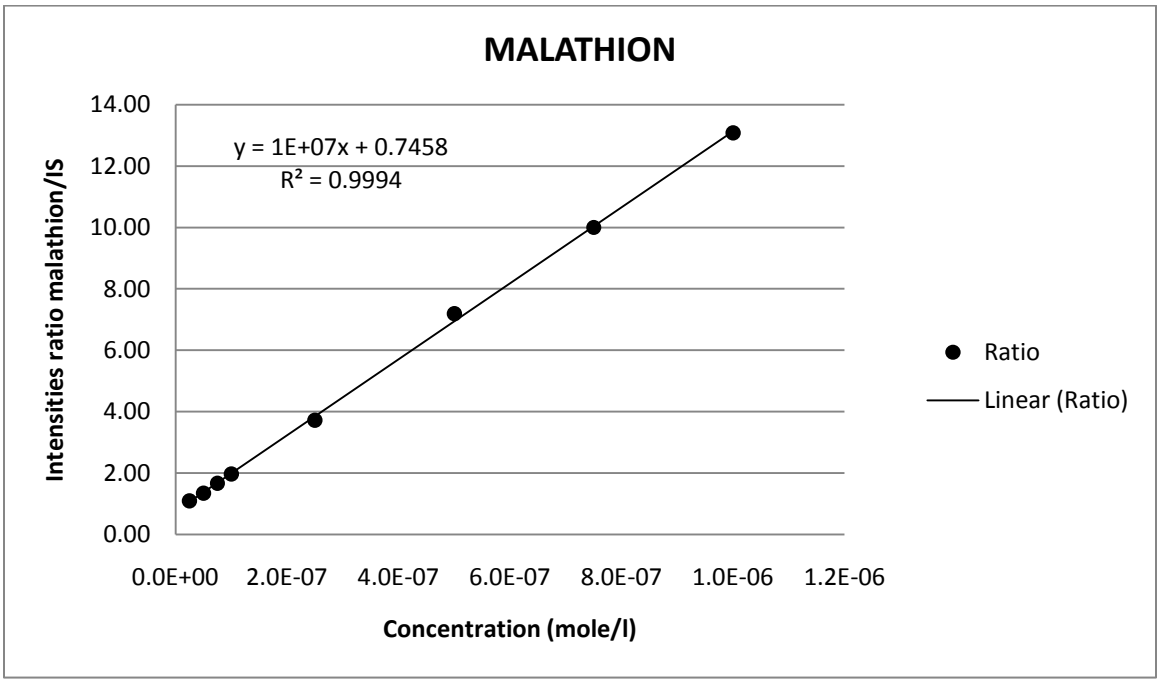

- Detection limit**:** 0.05 pmole

- Variability between preparation

The variability between preparation was calculated by injecting 3 times (n=3) 3 different standard preparations (through SPE) at different concentrations.

Concentration (mole/l)	AVE Ratio (n=3)	STDEV	CV (%)
2.5E-08	1.09	0.5711	52
5.0E-08	1.34	0.4471	33
7.5E-08	1.67	0.3476	21
1.0E-07	1.97	0.3724	19
2.5E-07	3.72	0.2841	8
5.0E-07	7.19	0.5917	8
7.5E-07	10.00	0.5537	6
1.0E-06	13.08	1.4833	11

- **Samples**

No malaoxon or malathion was detected in the submitted samples.

- **Recoveries:** 53-91%

Table 1. Malathion results

ID	TUBE ID	CELL	DESCRIPTION	MALATHION INTENSITY*	IS INTENSITY**	Ratio MALATHION/IS	AVE RATIO	STDEV	CV(%)	[Malathion] mole/l
1	**#1 in**	BMEC	Control	7,961	6,562	1.21	**1.13**	0.12	11%	ND
				10,320	9,924	1.04				
2	**#2 in**	BMEC	Lead 10-5M	9,626	10,015	0.96	**0.95**	0.02	2%	ND
				10,908	11,721	0.93				
3	**#3 in**	BMEC	Malathion 10-5M	3,259	25,533	0.13	**0.12**	0.00	3%	ND
				689	5,661	0.12				
4	**#4 in**	BMEC	Malathion 10-5M and lead 10-5M	4,326	33,129	0.13	**0.12**	0.01	12%	ND
				3,949	36,060	0.11				
5	**#5 in**	BMEC	Malaoxon 10-6M	3,826	34,383	0.11	**0.11**	0.00	4%	ND
				8,184	69,481	0.12				
6	**#6 in**	BMEC	Malaoxon 10-6M and lead 10-5M	8,993	64,476	0.14	**0.15**	0.01	6%	ND
				6,222	40,854	0.15				
10	**#10 in**	BMEC	Malathion 10-5M and lead 10-6M	2,419	13,218	0.18	**0.19**	0.01	6%	ND
				2,581	12,914	0.20				
12	**#12 in**	BMEC	Malaoxon 10-6 and lead 10-6M	2,007	8,141	0.25	**0.23**	0.02	7%	ND
				2,248	10,063	0.22				
13	**#1 out**	BMEC	Control	2,914	15,729	0.19	**0.17**	0.02	15%	ND
				5,270	35,141	0.15				
14	**#2 out**	BMEC	Lead 10-5M	4,543	34,046	0.13	**0.14**	0.01	5%	ND
				5,020	34,885	0.14				
15	**#3 out**	BMEC	Malathion 10-5M	1,441	5,971	0.24	**0.25**	0.01	6%	ND
				1,598	6,087	0.26				
16	**#4 out**	BMEC	Malathion 10-5M and lead 10-5M	1,303	5,978	0.22	**0.22**	0.00	2%	ND
				1,953	8,698	0.22				
17	**#5 out**	BMEC	Malaoxon 10-6M	1,555	6,185	0.25	**0.26**	0.01	4%	ND
				1,796	6,763	0.27				
18	**#6 out**	BMEC	Malaoxon 10-6M and lead 10-5M	1,668	6,842	0.24	**0.25**	0.00	1%	ND
				1,860	7,530	0.25				
22	**#10 out**	BMEC	Malathion 10-5M and lead 10-6M	2,131	7,106	0.30	**0.30**	0.00	1%	ND
				2,224	7,312	0.30				

ID	TUBE ID	CELL	DESCRIPTION	MALATHION INTENSITY*	IS INTENSITY**	Ratio MALATHION/IS	AVE RATIO	STDEV	CV(%)	[Malathion] mole/l
24	**#12 out**	BMEC	Malaoxon 10-6 and lead 10-6M	2,129	7,117	0.30	**0.30**	0.00	0%	ND
				2,410	8,113	0.30				
25	**#1 inside**	RBE4	Control	1,921	10,311	0.19	**0.16**	0.03	19%	ND
				3,875	27,376	0.14				
27	**#3 inside**	RBE4	Malathion 10-5M	1,229	4,625	0.27	**0.25**	0.02	7%	ND
				872	3,643	0.24				
28	**#4 inside**	RBE4	Malathion 10-5M and lead 10-5M	1,098	4,748	0.23	**0.21**	0.02	11%	ND
				1,010	5,105	0.20				
29	**#5 inside**	RBE4	Malaoxon 10-6M	1,015	3,555	0.29	**0.27**	0.02	7%	ND
	(Plate 1)			904	3,490	0.26				
30	**#6 inside**	RBE4	Malaoxon 10-6M and lead 10-5M	823	3,552	0.23	**0.24**	0.02	7%	ND
	(Plate 1)			951	3,711	0.26				
31	**#7 outside**	RBE4	Control	2,944	16,911	0.17	**0.18**	0.01	4%	ND
	(Plate 1)			2,858	15,568	0.18				
33	**#9 outside**	RBE4	Malathion 10-5M	989	2,957	0.33	**0.30**	0.04	15%	ND
	(Plate 1)			1,078	3,968	0.27				
34	**#10 outside**	RBE4	Malathion 10-5M and lead 10-5M	1,173	4,499	0.26	**0.27**	0.01	4%	ND
	(Plate 1)			1,200	4,343	0.28				
35	**#11 outside**	RBE4	Malaoxon 10-6M	1,439	4,641	0.31	**0.27**	0.06	22%	ND
	(Plate 1)			1,597	7,070	0.23				
36	**#12 outside**	RBE4	Malaoxon 10-6M and lead 10-5M	1,527	4,868	0.31	**0.28**	0.05	19%	ND
	(Plate 1)			1,940	8,080	0.24				
39	**#3 inside**	RBE4	Malathion 10-5M	1,019	4,438	0.23	**0.24**	0.01	6%	ND
	(Plate 2)			939	3,761	0.25				
40	**#4 inside**	RBE4	Malathion 10-5M and lead 10-5M	947	3,784	0.25	**0.24**	0.01	5%	ND
	(Plate 2)			1,028	4,409	0.23				
41	**#5 inside**	RBE4	Malaoxon 10-6M	1,034	4,038	0.26	**0.26**	0.01	3%	ND
	(Plate 2)			1,020	3,795	0.27				

ID	TUBE ID	CELL	DESCRIPTION	MALATHION INTENSITY*	IS INTENSITY**	Ratio MALATHION/IS	AVE RATIO	STDEV	CV(%)	[Malathion] mole/l
42	**#6 inside**	RBE4	Malaoxon 10-6M and lead 10-5M	919	3,830	0.24	**0.23**	0.01	5%	ND
	(Plate 2)			1,309	5,820	0.22				
45	**#9 outside**	RBE4	Malathion 10-5M	1,244	4,666	0.27	**0.28**	0.01	5%	ND
	(Plate 2)			1,444	5,082	0.28				
46	**#10 outside**	RBE4	Malathion 10-5M and lead 10-5M	948	3,775	0.25	**0.26**	0.01	3%	ND
	(Plate 2)			1,308	5,020	0.26				
47	**#11 outside**	RBE4	Malaoxon 10-6M	1,045	5,042	0.21	**0.21**	0.01	4%	ND
	(Plate 2)			1,132	5,168	0.22				
48	**#12 outside**	RBE4	Malaoxon 10-6M and lead 10-5M	1,007	6,941	0.15	**0.07**	0.10	141%	ND
	(Plate 2)			0	6,553	0.00				

*Sum of intensities @ *m/z* 156.9 and *m/z* 172.0
** Intensity @ *m/z* 156.9

Table 2. Malaoxon results

ID	TUBE ID	CELL	DESCRIPTION	MALAOXON INTENSITY*	IS INTENSITY**	Ratio MALATHION/IS	AVE RATIO	STDEV	CV(%)	[Malaoxon] mole/l
1	**#1 in**	BMEC	Control	1,468	6,562	0.22	**0.20**	0.03	16%	ND
				1,761	9,924	0.18				
2	**#2 in**	BMEC	Lead 10-5M	1,887	10,015	0.19	**0.18**	0.02	10%	ND
				1,908	11,721	0.16				
3	**#3 in**	BMEC	Malathion 10-5M	1,864	14,747	0.13	**0.13**	0.00	3%	ND
				2,002	15,271	0.13				
4	**#4 in**	BMEC	Malathion 10-5M and lead 10-5M	0	33,129	0.00	**0.00**	0.00	NA	ND
				0	36,060	0.00				
5	**#5 in**	BMEC	Malaoxon 10-6M	0	34,383	0.00	**0.00**	0.00	NA	ND
				0	69,481	0.00				

ID	TUBE ID	CELL	DESCRIPTION	MALAOXON INTENSITY*	IS INTENSITY**	Ratio MALATHION/IS	AVE RATIO	STDEV	CV(%)	[Malaoxon] mole/l
6	**#6 in**	BMEC	Malaoxon 10-6M and lead 10-5M	1,340	64,476	0.02	**0.01**	0.01	141%	ND
				0	40,854	0.00				
10	**#10 in**	BMEC	Malathion 10-5M and lead 10-6M	0	13,218	0.00	**0.00**	0.00	NA	ND
				0	12,914	0.00				
12	**#12 in**	BMEC	Malaoxon 10-6 and lead 10-6M	0	8,141	0.00	**0.00**	0.00	NA	ND
				0	10,063	0.00				
13	**#1 out**	BMEC	Control	0	15,729	0.00	**0.00**	0.00	NA	ND
				0	35,141	0.00				
14	**#2 out**	BMEC	Lead 10-5M	0	34,046	0.00	**0.00**	0.00	NA	ND
				0	34,885	0.00				
15	**#3 out**	BMEC	Malathion 10-5M	0	5,971	0.00	**0.00**	0.00	NA	ND
				0	6,087	0.00				
16	**#4 out**	BMEC	Malathion 10-5M and lead 10-5M	0	5,978	0.00	**0.00**	0.00	NA	ND
				0	8,698	0.00				
17	**#5 out**	BMEC	Malaoxon 10-6M	0	6,185	0.00	**0.00**	0.00	NA	ND
				0	6,763	0.00				
18	**#6 out**	BMEC	Malaoxon 10-6M and lead 10-5M	0	6,842	0.00	**0.00**	0.00	NA	ND
				0	7,530	0.00				
22	**#10 out**	BMEC	Malathion 10-5M and lead 10-6M	0	7,106	0.00	**0.00**	0.00	NA	ND
				0	7,312	0.00				
24	**#12 out**	BMEC	Malaoxon 10-6 and lead 10-6M	0	7,117	0.00	**0.00**	0.00	NA	ND
				0	8,113	0.00				
25	**#1 inside**	RBE4	Control	0	10,311	0.00	**0.00**	0.00	NA	ND
				0	27,376	0.00				
27	**#3 inside**	RBE4	Malathion 10-5M	0	4,625	0.00	**0.00**	0.00	NA	ND
				0	3,643	0.00				
28	**#4 inside**	RBE4	Malathion 10-5M and lead 10-5M	0	4,748	0.00	**0.00**	0.00	NA	ND
				0	5,105	0.00				
29	**#5 inside** (Plate 1)	RBE4	Malaoxon 10-6M	0	3,555	0.00	**0.00**	0.00	NA	ND
				0	3,490	0.00				
30	**#6 inside** (Plate 1)	RBE4	Malaoxon 10-6M and lead 10-5M	0	3,552	0.00	**0.00**	0.00	NA	ND
				0	3,711	0.00				

ID	TUBE ID	CELL	DESCRIPTION	MALAOXON INTENSITY*	IS INTENSITY**	Ratio MALATHION/IS	AVE RATIO	STDEV	CV(%)	[Malaoxon] mole/l
33	**#9 outside**	RBE4	Malathion 10-5M	0	2,957	0.00	**0.00**	0.00	NA	ND
	(Plate 1)			0	3,968	0.00				
34	**#10 outside**	RBE4	Malathion 10-5M and lead 10-5M	0	4,499	0.00	**0.00**	0.00	NA	ND
	(Plate 1)			0	4,343	0.00				
35	**#11 outside**	RBE4	Malaoxon 10-6M	0	4,641	0.00	**0.00**	0.00	NA	ND
	(Plate 1)			0	7,070	0.00				
36	**#12 outside**	RBE4	Malaoxon 10-6M and lead 10-5M	0	4,868	0.00	**0.00**	0.00	NA	ND
	(Plate 1)			0	8,080	0.00				
39	**#3 inside**	RBE4	Malathion 10-5M	0	4,438	0.00	**0.00**	0.00	NA	ND
	(Plate 2)			0	3,761	0.00				
40	**#4 inside**	RBE4	Malathion 10-5M and lead 10-5M	0	3,784	0.00	**0.00**	0.00	NA	ND
	(Plate 2)			0	4,409	0.00				
41	**#5 inside**	RBE4	Malaoxon 10-6M	0	4,038	0.00	**0.00**	0.00	NA	ND
	(Plate 2)			0	3,795	0.00				
42	**#6 inside**	RBE4	Malaoxon 10-6M and lead 10-5M	0	3,830	0.00	**0.00**	0.00	NA	ND
	(Plate 2)			0	5,820	0.00				
45	**#9 outside**	RBE4	Malathion 10-5M	0	4,666	0.00	**0.00**	0.00	NA	ND
	(Plate 2)			0	5,082	0.00				
46	**#10 outside**	RBE4	Malathion 10-5M and lead 10-5M	0	3,775	0.00	**0.00**	0.00	NA	ND
	(Plate 2)			0	5,020	0.00				
47	**#11 outside**	RBE4	Malaoxon 10-6M	0	5,042	0.00	**0.00**	0.00	NA	ND
	(Plate 2)			0	5,168	0.00				
48	**#12 outside**	RBE4	Malaoxon 10-6M and lead 10-5M	0	6,941	0.00	**0.00**	0.00	NA	ND
	(Plate 2)			0	6,553	0.00				

*Sum of intensities @ *m/z* 141.0 and *m/z* 172.0
** Intensity @ *m/z* 156.9

Figure 1. Extracted chromatogram for a standard mixture: malathion (*m/z* 156.9, 172.0), malaoxon (*m/z* 141.0, 172.0) and IS (*m/z* 156.9) @ 1.0 x10-7M.

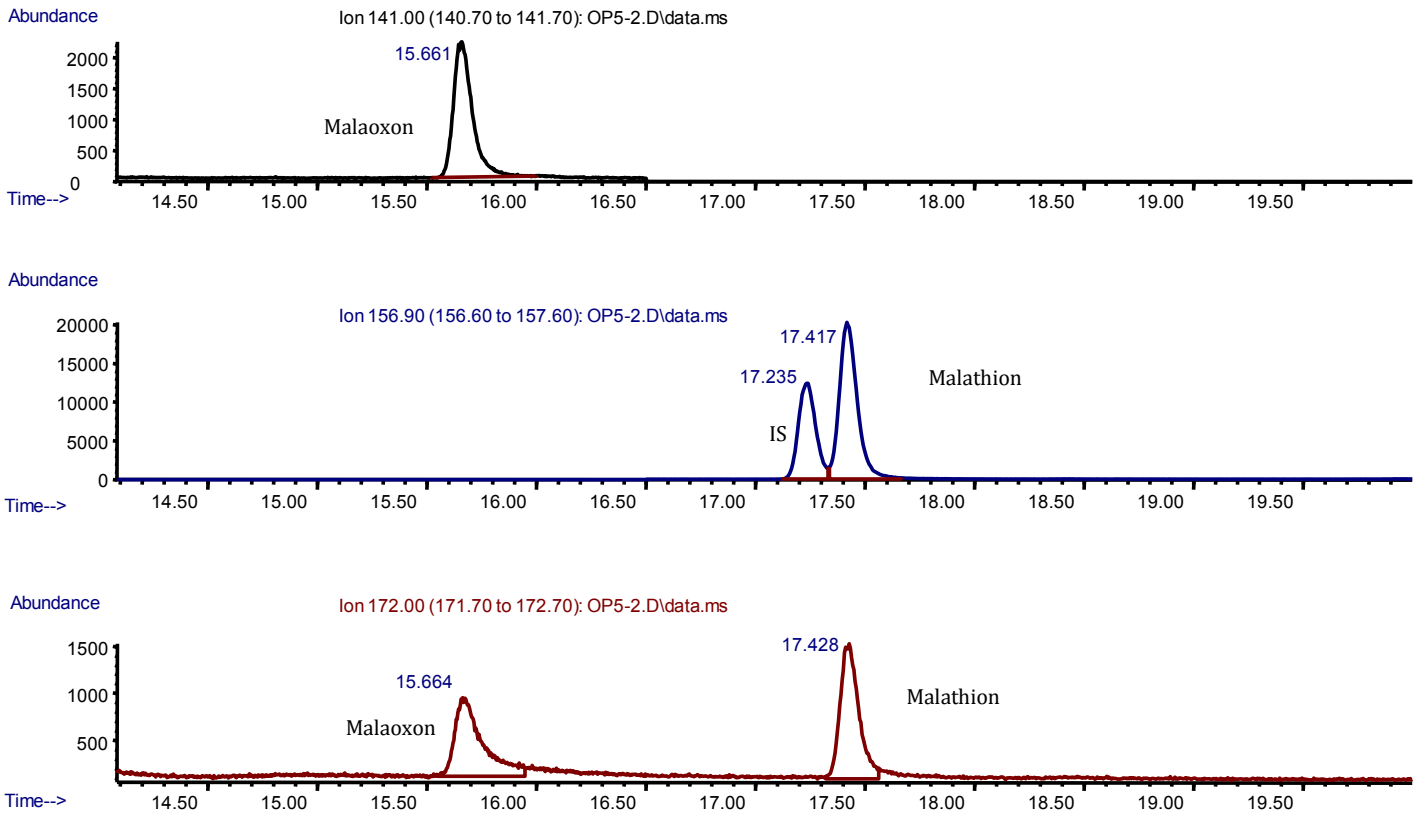

Figure 2: Malathion standard @ 2.5 x10-8M (upper chromatogram) and sample 33 (bottom chromatogram).

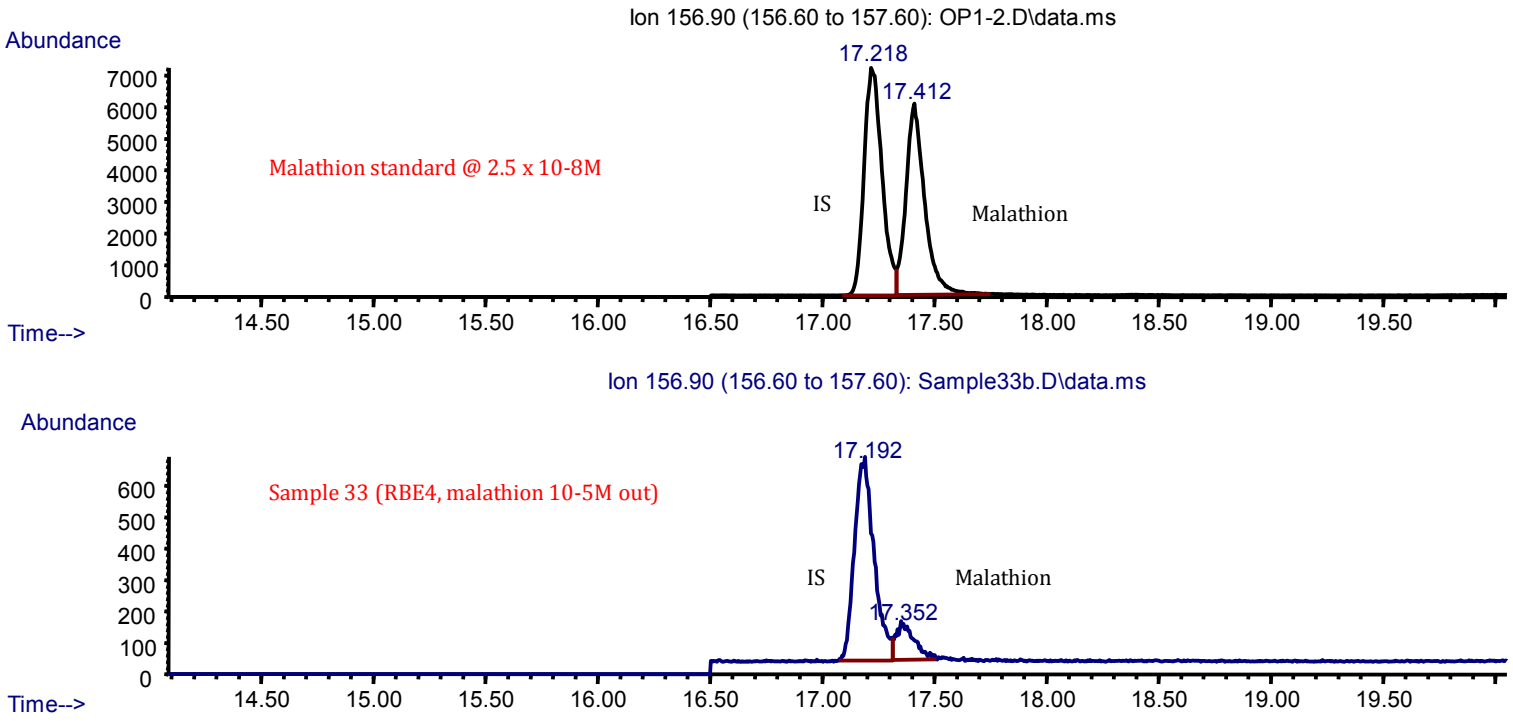

Figure 3: Malaoxon standard @ 2.5 x10-8M (upper chromatogram) and sample 33 (bottom chromatogram).